

DISSERTATION

MICROALGAE TO BIOFUELS EVALUATION THROUGH EXPERIMENTALLY VALIDATED MODELS

Submitted by

Jason Quinn

Department of Mechanical Engineering

In partial fulfillment of the requirements

For the Degree of Doctor of Philosophy

Colorado State University

Fort Collins, Colorado

Summer 2011

Doctoral Committee:

Advisor: Thomas H. Bradley

Anthony J. Marchese

Bryan D. Willson

Thomas J. Siller

Copyright by Jason Charles Quinn 2011

All right Reserved

## ABSTRACT

### MICROALGAE TO BIOFUELS EVALUATION THROUGH EXPERIMENTALLY VALIDATED MODELS

Microalgae have been of interest as a feedstock for biofuels but until recently have not been economically feasible. Recent energy uncertainties coupled with technological advancements have made microalgae more appealing as an alternative feedstock for transportation fuel. Algae characteristically have many advantages over traditional terrestrial based biofuel feedstocks. Prior to commercialization of the microalgae to biofuels process there are technological challenges that need to be overcome.

The work presented can be divided into three primary modeling efforts, a process level analysis, bulk growth evaluation, and a diffuse versus direct light evaluation. All models presented are experimentally validated and used to assess the near term realizable impact of microalgae. Results from this work are intended to accurately represent the current state of the field by more accurately representing the current potential and technologies being explored.

Biofuels derived from microalgae have the potential to replace petroleum fuel and first-generation biofuel, but the efficacy with which sustainability goals can be achieved is dependent on the lifecycle impacts of the microalgae-to-biofuel process. This work proposes a detailed, industrial-scale engineering model of the growth, dewater, extraction, conversion, and transportation and distribution stages of the microalgae to biofuels process for the species *Nannochloropsis* using a photobioreactor architecture. This process level model is integrated with a lifecycle energy and greenhouse gas emissions analysis compatible with the methods and boundaries of the Argonne National Laboratory GREET model, thereby ensuring comparability to preexisting fuel-cycle assessments. Results are used to evaluate the net energy ratio (NER) and net greenhouse gas emissions (GHGs) of microalgae biodiesel in comparison to petroleum diesel and soybean-based biodiesel with a boundary equivalent to “well-to-pump”. The resulting NER of the microalgae biodiesel process is 0.93 MJ of energy consumed per MJ of energy produced. In terms of net GHGs, microalgae-based biofuels avoids 75 g of CO<sub>2</sub>-equivalent emissions per MJ of energy produced. The scalability of the consumables and products of the proposed microalgae-to-biofuels processes are assessed in the context of 150 billion liters (40 billion gallons) of annual production.

A more detailed bulk growth model has been assembled to more accurately represent the growth of microalgae. To date, there is little published data on the productivity of microalgae in growth systems that are scalable to commercially viable footprints. To inform the development of more detailed assessments of industrial-scale microalgae biofuel processes, this paper presents the construction and validation of a

model of microalgae biomass and lipid accumulation in an outdoor, industrial-scale photobioreactor. The model incorporates a time-resolved simulation of microalgae growth and lipid accumulation based on solar irradiation, species specific characteristics, and photobioreactor geometry. The model is validated with 9 weeks of growth data from an industrially-scaled outdoor photobioreactor. A sensitivity of the model input parameters is presented.

The model presented was used to more accurately represent the current US productivity potential. Current calculations for the large-scale productivity potential of microalgae are based on growth data from small-scale non-industrially representative systems. To accurately assess the near-term large-scale microalgae potential, a thermal basin model is presented and combined with a bulk growth model previously validated with industrial-scale outdoor photobioreactor growth data. The combined models require meteorological data to accurately predict microalgae growth and lipid production. This study integrates 15 years of hourly historical weather data from 864 locations in the US to accurately assess the current productivity potential of microalgae in the US. Geospatial information system (GIS) land availability and slope data are used to generate a set of dynamic maps of the current feasible locations and productivity potential of microalgae in the US based on a variety of geographic characteristics and restrictions. A comparison of model results based on optimal location with current productivity potentials reported in literature shows the need for more realistic estimation of microalgae growth potential for future LCA.

The bulk growth model does not differentiate between diffuse and direct light growth. The microalgae growth as a function of diffuse versus direct light with the application to reactor design evaluation was evaluated for *Nannochloropsis salina* experimentally with modeling applications. For the application to large scale cultivation modeling and evaluation, a small scale reactor representative test apparatus was constructed to investigate the growth response of *Nannochloropsis salina* under a variety of real world relevant light intensities and temperatures on a batch growth time scale with the intention of modeling growth in larger scale devices. Growth data was also collected from two geometrically different large scale indoor photobioreactors under a variety of light intensities for model evaluation. The application of small scale data to accurately predict growth at large scale enables the evaluation of photobioreactor geometry. Temperature experimentation illustrates the detrimental effect that temperatures above 30 °C and below 7 °C have on microalgae batch growth. Discussion focuses on the application of the data set to reactor design and evaluation and modeling efforts and evaluation of photic volume data reduction. Results show a significant difference in growth from direct light compared to diffuse light and the difficulty of photic volume growth modeling.

The work presented uses the results of a high level environmental assessment of microalgae biofuels to guide further research in growth modeling and process evaluation based on pilot plant experience. A more detailed bulk growth model incorporating 21 species and reactor specific characteristics with primary inputs of light and temperature was developed from literature and validated with real world large-

scale photobioreactor data. This model was used to illustrate the current microalgae productivity potential in the US. This modeling effort illustrated the need for a more fundamental understanding of diffuse versus direct light utilization in microalgae cultivation. Experimental setup was designed and operated to generate a photosynthesis irradiance curve. This curve was used to inform a model validated with growth data from large scale photobioreactors. This data was directly used in the evaluation of photobioreactor geometry and used to investigate optimum geometry based on the metric of areal productivity.

The experimentally validated models presented are used to critically evaluate the current state of the microalgae to biofuels process. Previous efforts have made unrealistic assumptions leading to the mis-representation of the environmental impact and productivity potential of microalgae.

## **Acknowledgments**

I gratefully acknowledge financial support provided by Solix Biosystems, Inc., and the Colorado Center for Biorefining and Biofuels. I also want to express sincere gratitude to Thomas Bradley, Anthony Marchese, Thomas Siller, Bryan Willson, Chris Turner, Liaw Batan, Nick Wagner, Kimberly Catton, Kelly Fagerstone, Joel Bulter, Pete Hentges, and most importantly Danna and Max Olbright, and Mike, Jo, Ben, and Lucy Quinn.

# TABLE OF CONTENTS

<b>ABSTRACT .....</b>	<b>ii</b>
<b>Acknowledgments.....</b>	<b>vii</b>
<b>TABLE OF CONTENTS.....</b>	<b>viii</b>
<b>LIST OF TABLES.....</b>	<b>xiv</b>
<b>LIST OF FIGURES.....</b>	<b>xvii</b>
<b>LIST OF SYMBOLS .....</b>	<b>xxiv</b>
<b>Chapter 1-Introduction to Microalgae Biofuels .....</b>	<b>1</b>
1.1 Research motivation.....	1
1.2 Microalgae overview .....	4
1.2.1 What are microalgae?.....	4
1.2.2 Microalgae advantages.....	5
1.2.3 Cultivation technologies .....	8
<b>Chapter 2-Research Challenges .....</b>	<b>11</b>
2.1 Current challenges.....	11
2.1.1 Growth modeling.....	11
2.1.2 LCA.....	12
2.2 Research questions, tasks, and plan.....	14
2.2.1 Research Question 1:.....	15
2.2.2 Research Question 2:.....	18

2.2.3 Research Question 3:.....	20
2.2.4 Research Plan .....	23
<b>Chapter 3-Net Energy and Greenhouse Gas Emissions Evaluation of Biodiesel Derived from Microalgae</b> .....	<b>25</b>
3. Abstract.....	25
3.1. Introduction .....	26
3.2. Methods.....	28
3.2.1. Detailed Engineering Process Model .....	30
3.2.1.1. Growth Model .....	32
3.2.1.2. Dewater Model.....	36
3.2.1.3. Extraction Model .....	37
3.2.1.4. Conversion Model.....	38
3.2.1.5. Transportation and Distribution Model .....	38
3.2.2. Lifecycle Assessment Model.....	39
3.2.2.1. Lifecycle Energy Model .....	44
3.2.2.2. GHG Emission Model .....	45
3.2.2.3. Co-Product Allocation Methods .....	46
3.3. Results.....	47
3.3.1. Materials and Energy Consumption of the Microalgae-to-Biofuel Process .....	48
3.3.2. Net Energy Results.....	49
3.3.3. GHG Emissions Results.....	51
3.3.4. Scalability .....	58
3.3.5 Sensitivity to Co-Product Allocation .....	60
3.3.6 Sensitivity to Electricity Sources .....	64
3.3.7 Sensitivity to Process Parameters.....	65
3.4. Conclusion.....	72

<b>Chapter 4-Microalgae Bulk Growth Model with Application to Industrial Scale Systems .....</b>	<b>74</b>
4. Abstract.....	74
4.1. Introduction .....	75
4.2. Materials and Methods.....	76
4.2.1 Modeling Equations Overview .....	76
4.2.1.1 Light distribution modeling.....	77
4.2.1.2 Photosynthetic rate modeling .....	79
4.2.1.3 Respiration rate modeling .....	81
4.2.1.4 Growth rate modeling .....	81
4.2.1.5 Temperature rate dependence modeling.....	82
4.2.1.6 Nitrogen dependence modeling .....	84
4.2.1.7 Lipid accumulation modeling.....	87
4.2.2 Model Parameters Summary.....	88
4.2.2.1 Light saturation level .....	91
4.2.2.2 Absorption coefficient .....	91
4.2.2.3 Maximum growth rate.....	91
4.2.2.4 Maintenance respiration rate.....	92
4.2.2.5 Biosynthetic efficiency.....	92
4.2.2.6 Optimum temperature.....	92
4.2.2.7 Activation energy.....	92
4.2.2.8 Maximum cell quota of nitrogen .....	93
4.2.2.9 Minimum cell quota of nitrogen.....	93
4.2.2.10 Cell quota of nitrogen in inocula.....	93
4.2.2.11 Half Saturation constant for nitrogen uptake.....	94
4.2.2.12 Maximum specific uptake rate of nitrogen .....	94
4.2.2.13 Maximum photosynthetic rate.....	96
4.2.2.14 Photon efficiency.....	96

4.2.3 Experimental Materials and Methods .....	97
4.2.3.1 Organism, culture media, and inoculation .....	97
4.2.3.2 Outdoor culture system .....	97
4.2.3.3 Growth monitoring .....	100
4.2.3.4 Lipid assay .....	101
4.3. Results and Discussion .....	102
4.3.1 Sample Growth Results .....	102
4.3.2 Growth Model Validation .....	106
4.3.3 Lipid Model Validation .....	112
4.3.4 Sensitivity Analysis .....	114
4.3.6 Life Cycle Assessment (LCA) Modeling .....	120
4.4. Conclusion .....	123
<b>Chapter 5- Current US Biofuel Potential from Microalgae Cultivated in Large-Scale Photobioreactors</b>	<b>124</b>
5. Abstract .....	124
5.1 Introduction .....	125
5.2 Materials and Methods .....	126
5.2.1 Validated bulk growth model .....	126
5.2.2 Thermal basin model .....	128
5.2.3 Geospatial information system (GIS) .....	129
5.2.4 Historical weather data .....	130
5.3 Results .....	131
5.3.1 Dynamic map .....	131
5.4 Discussion .....	137
5.4.1 Current practical production potential of microalgae compared to literature .....	137
5.5 Conclusion .....	140

<b>Chapter 6- Scale-Up of Flat Plate Photobioreactors Considering Diffuse and Direct Light Characteristics</b>	<b>142</b>
.....	
Abstract .....	142
6.1 Introduction .....	143
6.2 Experimental Materials and Methods .....	146
6.2.1 Small Scale System.....	147
6.2.2 Large Scale System .....	152
6.2.3 Culture and Growth Media .....	158
6.2.4 Light Measurement Device and Technique.....	158
6.2.5 Comparison of Small Scale and Large Scale Growth Systems .....	159
6.3 Results .....	159
6.3.1 Small Scale Reactor Growth Data .....	160
6.3.2 Large Scale Reactor Growth Data .....	162
6.3.3 Modeling- Large Scale Growth Based on Small Scale PI Data.....	164
6.4 Discussion .....	168
6.4.1 Application of Data to Modeling and Evaluation of Photobioreactors.....	168
6.4.2 Photic Reduction .....	173
6.5 Conclusions .....	183
<b>Chapter 7-Conclusions.....</b>	<b>185</b>
7.1 Engineering Process Model and LCA.....	186
7.2 Bulk Growth Modeling.....	187
7.3 Diffuse Versus Direct Light Evaluation .....	188
7.4 Dissertation impact.....	189
<b>Chapter 8- Future Work in Feasibility of Large Scale Production .....</b>	<b>190</b>
8.1 The Potential Productivity and Feasibility of Large Scale Microalgae Production in the US .....	191
8.2 Net Energy and Greenhouse Gas Emissions Evaluation of Biodiesel Derived from Microalgae.....	195

8.3 Direct versus Diffuse Light Utilization-Design Optimization through Experimentally Validated Models	197
8.4 Research Proposal-Integration of Microalgae Growth Utilizing Commercial CO <sub>2</sub> and Nutrient Sources	200
8.4.1 Background	200
8.4.2 Engineering Growth Model	201
8.4.3 Research Question	204
8.4.4 Research Tasks	205
8.4.5 Research Impact	206
8.4.6 Summary	207
8.5 Research Proposal-Net Energy and Life Cycle Assessment of Current Microalgae Cultivation Systems	208
8.5.1 Background	208
8.5.2 Research Question	211
8.5.3 Research Tasks	211
8.5.4 Research Impact	211
8.5.5 Summary	212
8.6 Research Proposal-Optimization of Light Utilization in Outdoor Photobioreactors	213
8.6.1 Background	213
8.6.2 Diffuse versus Direct Light Utilization	214
8.6.3 Research Question	216
8.6.4 Research Tasks	217
8.6.5 Research Impact	217
8.6.6 Summary	218
<b>References</b>	<b>219</b>

## LIST OF TABLES

Table 1. Summary material and energy inputs and outputs for the baseline microalgae to biofuel process for a period of 1 year .....	49
Table 2. Net Energy Ratio (NER) in MJ/MJ of Conventional Diesel, Soybean Biodiesel and Microalgae Biodiesel Processes with the Energy Consumption for Each Feedstock Processing Stage .....	52
Table 3. Net GHG Emissions of Conventional Diesel, Soybean Biodiesel and Microalgae Biodiesel Processes with the Contribution of CO <sub>2</sub> , CH <sub>4</sub> , and N <sub>2</sub> O gases per unit of MJ of energy produced .....	53
Table 4. Net GHG Emissions of Conventional Diesel, Soybean Biodiesel and Microalgae Biodiesel Processes with the Contribution of CO <sub>2</sub> , CH <sub>4</sub> , and N <sub>2</sub> O gases per unit of MJ of energy produced .....	57
Table 5. Scalability metrics derived from the baseline microalgae to biofuels process model scaled to a production of 40 billion gallons per year of microalgae biodiesel .....	59
Table 6. Comparison of the net GHG Emissions of the microalgae to biodiesel process as a function of method of co-product allocation .....	63

Table 7. Net Energy Ratio per Electricity Source and Mix with a LCA boundary of “strain-to-pump” for the baseline scenario.....	64
Table 8. Analysis of Net GHG per source of Electricity with a LCA boundary of “strain-to-pump” for the baseline scenario .....	66
Table 9. Summary of input of material and energy for sensitivity analysis for a period of 1 year.....	68
Table 10. Summary of model parameters .....	90
Table 11. Summary of analysis of <i>Nannochloropsis oculata</i> cultivated Solix photobioreactor analyzed by MSU and Dairyland. Data used with published literature data for model input parameters.....	95
Table 12. Summary of total change in biomass as predicted by the model and measured by the sensor for 8 batches, (6 high light and 2 low light) including total time of the batch.....	111
Table 13. Summary of biomass output of model for increasing and decreasing input parameters by 20%. The baseline model density at 100 hr is 2.54 g·L <sup>-1</sup> under cloud free irradiation with optimum thermal basin component. ....	116
Table 14. Table comparing reported productivity potentials (some calculations performed for comparison purposes) from various sources. Some authors reported a range of productivity potential, consequently the high (††) and low (†) values are repeated. ....	121
Table 15. Table of the land availability and total US production for slope criteria of 1%, 2%, and 5%. ....	137

Table 16. Table comparing reported productivity potentials (some calculations performed for comparison purposes) from various sources. Some authors reported a range of productivity potential, consequently the high (††) and low (†) values are repeated. ....138

Table 17. 24 hr average productivity of three 4 day batches is presented for the 0.28 m deep and 0.14 m deep reactors for the two different light intensities tested. .163

Table 18. Summary material and energy inputs and outputs for the baseline microalgae growth process for a period of 1 year.....203

Table 19. Scalability metrics derived from the baseline microalgae to biofuels process model scaled to a production of 40 billion gallons per year of microalgae biodiesel .....205

## LIST OF FIGURES

Figure 1. Historical cost of oil in 2008 US dollars illustrating the current volatility and renewed interest in alternative fuels (Energy Information Administration, 2010). .....	2
Figure 2. Comparison of different feedstocks for biofuels. For this comparison the value reported for microalgae represents the near term realizable potential not the optimistic long term potential reported in literature. <sup>†</sup> (Chisti, 2007) <sup>††</sup> (Quinn et al., 2011) .....	7
Figure 3. Open raceway pond architecture for the cultivation of microalgae, picture courtesy of Ami Ben-Amotz (top). Closed photobioreactor architecture for microalgae cultivation, picture courtesy of Solix Biosystems (bottom). .....	9
Figure 4. Microalgae Biodiesel Processing and Lifecycle Analysis Model Overview .....	29
Figure 5. Detailed engineering process model illustrating the mass and energy flow to and from each of the processing stages .....	31
Figure 6. Illustration and photograph of the pilot facility modeled for this study .....	33
Figure 7. General fuel production pathways (Wang, 2005) .....	40

Figure 8. Illustration of “Well-to-Pump” and “Well-to-wheel” boundaries (Wang, 2005)	41
Figure 9. System Boundaries for Life cycle Analysis of Petroleum Diesel, Soybean Biodiesel and Microalgae Biodiesel (Wang, 2005)	43
Figure 10. Cumulative Net Energy Ratio of the microalgae to biodiesel process as a function of feedstock processing parameters	70
Figure 11. Net GHG emissions of the microalgae to biodiesel process as a function of feedstock processing parameters	71
Figure 12. Graph of photosynthetic rate for three different temperature and nitrogen efficiencies. Photo-saturation illustrated in red.	83
Figure 13. Plot of cell composition for ideal light conditions in June at a location of Fort Collins, Colorado	89
Figure 14. Diagram and Photograph of the generation 3 Solix photobioreactor used to validate bulk growth model. Reactors are evenly spaced in a structural/thermal water basin in Fort Collins, Colorado, USA.	99
Figure 15. Solid blue line represents results from summer-time simulation and dashed black line represents winter-time simulation. All simulations assumed ideal basin temperatures and clear sky ideal light conditions based on a geographical location of Fort Collins, Colorado using the Rest2 solar model. Top Left: Model prediction of overall culture density with harvesting at 3 g·L <sup>-1</sup> over a 30 day period. Top Right: Model results for bio-available nitrogen in media over a 5 day growth period. Bottom Left: Model results for lipid accumulation over a 5 day	

growth period. Bottom Right: Model results for growth rate for a 5 day growth period. ....	104
Figure 16. Approximately one week of raw summer (blue) and winter (red) time PAR data (top) used as primary input for validation of model. Approximately one week of raw thermal basin temperature data used as primary input for model validation (bottom). ....	108
Figure 17. Plot of model output (Model), institute OD sensor (Senor), and manual samples performed daily (Manual Sample) for two reactors A and B are presented. Approximately one week of high light (June 13-18) for reactor A and approximately one week of low light (November 11- 16) for reactor B raw growth data from the sensor and manual OD and model simulated growth are presented. ....	109
Figure 18. Plot of predicted versus actual daily change in density on a minute time scale for 6 weeks of growth during high light conditions, summer (top) and 3 weeks of growth during low light conditions, winter (bottom).....	110
Figure 19. Plot of lipid percentage in biomass for 3 weeks of continual monitoring over 11 day period overlaid on top of predicted lipid percentage from model. ....	113
Figure 20. Growth of baseline bulk model with the max photosynthetic rate increased and decreased by 20% for sensitivity analysis. ....	115
Figure 21. Sensitivity of model inputs presented in tornado plot format. Model inputs were altered by +/- 20% with total predicted biomass production after 100 hours	

compared to baseline scenario. Vertical lines represent 95% confidence interval.

.....118

Figure 22. Image of cultivation system modeled courtesy of Solix Biosystems.

Photobioreactors are structurally and thermally supported in a water basin. ...127

Figure 23. Lipid productivity Potential of microalgae in the US based on 15 years of

hourly meteorological data. ....133

Figure 24. Dynamic map of near-term realizable large scale microalgae oil production in

$m^3 \cdot ha^{-1} \cdot yr^{-1}$ . Areas that do not meet the land availability and slope criteria

defined for the baseline scenario have been grayed out. ....134

Figure 25. Dynamic map of near-term realizable large scale microalgae oil production in

$m^3 \cdot ha^{-1} \cdot yr^{-1}$ . Areas that do not meet the land availability and 2% slope criteria

have been grayed out. ....135

Figure 26 Dynamic map of near-term realizable large scale microalgae oil production in

$m^3 \cdot ha^{-1} \cdot yr^{-1}$ . Areas that do not meet the land availability and 1% slope criteria

have been grayed out. ....136

Figure 27 Schematic of core sample technique relating the geometry of the small scale

system to the large scale system. ....147

Figure 28 CAD representation of one test apparatus consisting of 6 test reactors (left).

Two of the apparatus (left) were constructed with each one attached to a

Polyscience 28 L shaking thermal basin and illuminated with a Sun Systems, Yield

Master II classic with a 1000 watt metal halide grow lamp (right). ....149

Figure 29. Picture of one of two small scale units used for data collection (left). Picture of two test apparatuses (right).....150

Figure 30 Geometry of large scale photobioreactors based on Solix generation 3 technology, 0.28m deep reactors-left and 0.14 m deep reactors-right. The primary difference between the two geometries is the culture height and volume is halved. Support structure is not detailed. ....153

Figure 31. Photograph with light bank removed of large scale reactors (left). Photograph of large scale growth system with lights turned on (right). ....156

Figure 32. Raw growth data collected for 4 different light intensities. The percentages reported in the figure are light intensity with respect to  $1500 \mu\text{moles}\cdot\text{m}^{-2}\cdot\text{s}^{-1}$ . .160

Figure 33 Batch averaged growth data from small scale test reactor. Growth reported in average 24 hour productivity in grams per liter of culture based on a 4 day batch versus light intensity for the two volumes tested, 150 mL and 75 mL.....161

Figure 34. Light measurements for the high light scenario for the 0.28 m and 0.14 m deep reactors with the water surface being zero and down into the basin being positive. ....165

Figure 35. Light intensity on the 0.14 m deep reactors (left) and the 0.28 m reactors (right) for the low light scenario. ....166

Figure 36 Predicted 24 hour productivity in large reactors by PI growth model based small scale data versus measured 24 hour productivity in large scale reactors. 167

Figure 37 Measured average 24 hour productivity in grams per square meter for the 0.14 m and 0.28 m deep reactors compared to the predicted productivity for 0.56 m and 0,84 m reactors based on the PI growth model presented.....172

Figure 38. Schematic for attenuation experimentation.....176

Figure 39. Results from absorption characterization experimentation. Data is from three densities all tested in three different beaker sizes.....177

Figure 40. Plot of baseline (150 mL) and half volume (75 mL) small scale growth data reduced based on attributing the growth to a photic-volume defined by the surface area of the reactors and a light penetration depth. The average productivity based on a 4 day batch is presented in grams of microalgae per cubic meter of photic-volume. ....178

Figure 41. Predicted 24 hour productivity in large scale reactors based on natural logarithmic model of small scale growth data (Figure 40) versus measured 24 hour productivity in large scale. ....179

Figure 42. . ½x reactor photic growth data with a natural logarithmic curve fit. Photic growth data is 24 hr batch averaged growth based on a 4 day batch plotted against average light intensity on the surface of the reactors.....180

Figure 43. Predicted 24 hour photic growth in 1x reactors by ½x photic data versus measured 24 hour photic growth in 1x reactors.....181

Figure 44. ½x reactor growth data with a natural logarithmic curve fit. Growth data is 24 hr batch averaged growth based on a 4 day batch plotted against average light intensity on the surface of the reactors.....182

Figure 45. Predicted 24 hour productivity in 1x reactors by ½x data versus measured 24 hour productivity in 1x reactors. ....183

Figure 46. Plot of model output (Model), institute OD sensor (Sensor), and manual sample performed daily (Manual Sample) in reactor A at high light (June 13-18) and in reactor B at low light (November 11- 16). Some sensor data has been removed due to sensor maintenance. ....192

Figure 47. Biomass productivity potential of the US generated using validated bulk growth model including thermal effects. Plot generated using 15 years of historical weather information from 788 Continental US location. ....193

Figure 48. Experimental growth data at two different culture volumes normalized to active photic volume and logarithmically curve fit. Data presented is batch averaged growth collected over a 5 day period in biological triplicate. ....198

Figure 49. Modeling results of direct, diffuse and total productivity in a photobioreactor. Two geometries are presented, 1x, photobioreactor depth of 0.3 m and 2x, photobioreactor depth of 0.6 m. ....215

Figure 50. PI curve for *Nannochloropsis Salina* cultivated in a 5 day batch fit with Smith model using  $\alpha = 0.778 \text{ g}\cdot\text{s}\cdot\text{m}^{-2}\cdot\mu\text{mol}^{-1}$ ,  $P_m = 0.50 \text{ g}\cdot\text{L}^{-1}$ ,  $R_d = -0.05 \text{ g}\cdot\text{L}^{-1}$ . ....216

## LIST OF SYMBOLS

Symbol	Description	Unit
AGS	algae growth system	-
B	reactor thickness	m
Biomass	biomass composition	-
CHO	percent carbohydrate in biomass	-
Lipid	percent lipid in biomass	-
cC,X	carbon content of biomass in reactor	$\text{g}\cdot\text{L}^{-1}$
cC,X <sub>0</sub>	carbon content of biomass at previous time step in reactor	$\text{g}\cdot\text{L}^{-1}$
cN <sub>medium</sub>	nitrogen concentration in media	$\text{g}\cdot\text{L}^{-1}$
PRO	percent protein in biomass	-
cX <sub>dw</sub>	biomass concentration in reactor	$\text{g}\cdot\text{L}^{-1}$
E (L)	light intensity at distance L	$\mu\text{mol}\cdot\text{m}^{-2}\cdot\text{s}^{-1}$
E <sub>0</sub>	light intensity incident on reactor wall	$\mu\text{mol}\cdot\text{m}^{-2}\cdot\text{s}^{-1}$
E <sub>a</sub>	activation energy carboxylation Rubisco	$\text{J}\cdot\text{mol}^{-1}$
E <sub>av</sub>	average light intensity in photobioreactor	$\mu\text{mol}\cdot\text{m}^{-2}\cdot\text{s}^{-1}$
E <sub>k</sub>	light saturation level	$\mu\text{mol}\cdot\text{m}^{-2}\cdot\text{s}^{-1}$
f(T)	temperature function	-
G	24 hr growth	$\text{g}\cdot\text{L}^{-1}$
I	light intensity	$\mu\text{mol}\cdot\text{m}^{-2}\cdot\text{s}^{-1}$
K <sub>N</sub>	half saturation constant for nitrogen uptake	$\text{g}\cdot\text{L}^{-1}$
L	distance from reactor wall into culture	m
OD	optical density	-
PAR	photosynthetic active radiation	$\mu\text{mol}\cdot\text{m}^{-2}\cdot\text{s}^{-1}$
P <sub>c</sub>	photosynthetic rate (carbon)	$\text{h}^{-1}$
P <sub>c_calc</sub>	calculated maximum photosynthetic rate (carbon)	$\text{h}^{-1}$
P <sub>c_max</sub>	maximum photosynthetic rate (carbon)	$\text{h}^{-1}$

PI	photosynthetic irradiance	-
$P_{\text{total}}$	24 hour productivity	$\text{g}\cdot\text{L}^{-1}$
$q_{\text{N},X}$	cell quota of nitrogen in biomass	$\text{g}\cdot\text{g}^{-1}$
$q_{\text{N},X_0}$	amount of nitrogen present at previous time step in biomass	$\text{g}\cdot\text{g}^{-1}$
$q_{\text{N},X_{\text{max}}}$	maximum cell quota for nitrogen in biomass	$\text{g}\cdot\text{g}^{-1}$
$q_{\text{N},X_{\text{min}}}$	minimum amount of nitrogen in biomass	$\text{g}\cdot\text{g}^{-1}$
R	universal gas constant	$\text{J}\cdot\text{K}^{-1}\cdot\text{mol}^{-1}$
$rR_{\text{C}}$	maintenance respiration rate (carbon)	$\text{h}^{-1}$
$rR_{\text{N}}$	respiration constant for nitrogen	$\text{h}^{-1}$
$r_{\text{N}}$	specific uptake rate of nitrogen	$\text{h}^{-1}$
$r_{\text{N}_{\text{calc}}}$	calculated specific uptake rate of nitrogen	$\text{g}\cdot\text{g}^{-1}\cdot\text{h}^{-1}$
$r_{\text{N}_{\text{max}}}$	maximum specific uptake rate of nitrogen	$\text{g}\cdot\text{g}^{-1}\cdot\text{h}^{-1}$
SCFH	standard cubic feet per hour	$\text{ft}^3\cdot\text{h}^{-1}$
t	time	seconds
T	bath temperature	$^{\circ}\text{C}$
$T_{\text{opt}}$	optimum growth temperature	$^{\circ}\text{C}$
x	depth	m
$\alpha$	absorption coefficient	$\text{m}^2\cdot\text{g}^{-1}$
$\zeta$	biosynthetic efficiency	$\text{g}\cdot\text{g}^{-1}$
$\mu$	carbon specific growth rate	$\text{h}^{-1}$
$\mu_{\text{max}}$	Maximum carbon specific growth rate	$\text{h}^{-1}$
$\phi_{\text{m}}$	photon efficiency	$\text{g}\cdot(\mu\text{mol photons})^{-1}$
$\phi_{q_{\text{N ext}}}$	uptake of external nitrogen concentration efficiency	-
$\phi_{q_{\text{N},X \text{ int}}}$	uptake of internal nitrogen concentration efficiency	-
$\phi_{\text{T}}$	temperature efficiency factor	-

---

## **Chapter 1-Introduction to Microalgae Biofuels**

### **1.1 Research motivation**

The current instability in domestic oil prices has researchers and entrepreneurs searching for alternative answers to transportation fuel and energy needs Figure 1 (Energy Information Administration, 2010). This coupled with the current rising global temperature due to green house gas emissions has renewed interest in alternative or green fuels for use in transportation vehicles (Doney, 2011; Kerr and Kintisch, 2010; Trenberth, 2010). It is expected with the development of new growing economies, such as China and India, the global demand for transportation fuel and energy will raise leading to more volatility in energy prices and environmental damage (Adams and Shachmurove, 2008; Hang and Tu, 2007; Lutz et al., 2010).

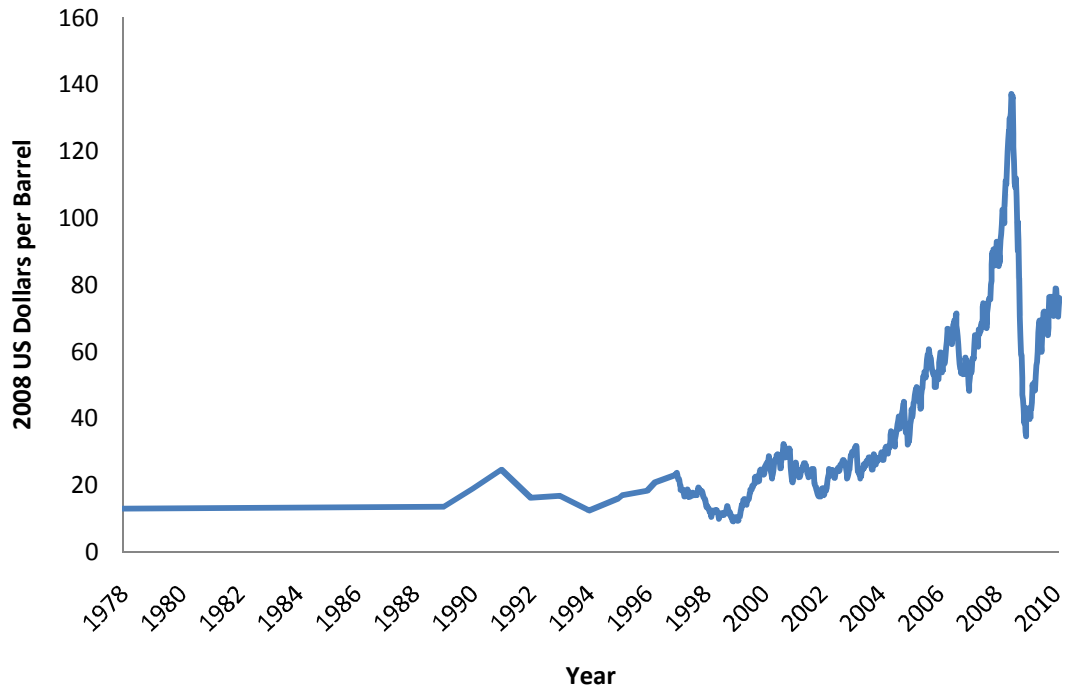


**Figure 1. Historical cost of oil in 2008 US dollars illustrating the current volatility and renewed interest in alternative fuels (Energy Information Administration, 2010).**

GHG emissions have more of an effect on the environment than just increasing global temperatures. Currently the ocean absorbs approximately one third of the CO<sub>2</sub> emitted every year. As the CO<sub>2</sub> concentration in the atmosphere increases the pH in the ocean gradually becomes more acidic. The decrease in pH can lead to the destruction of marine habitat such as coral reefs causing a change in the marine ecosystem which will inevitably affect surface life.

The solution to global warming is a multidisciplinary task with a host of solutions required including alternative fuels and energy. Clean and renewable fuels and energy are currently taking a front runner in answering the increased global demand and reduction of GHG emissions. In the energy sector, nations around the world have set

renewable energy goals and are moving forward with projects to meet those goals. Renewable energy is defined here as energy that comes from natural resources. Currently Germany is leading the way in the European Union with 16.1% renewable energy with a goal of 35% by 2020. Renewable energy is currently being generated around the world using thermal and photovoltaic solar cells, geothermal, wind turbines, and hydro-electric generation; however it is still at relatively small levels. Each of the alternatives has advantages and disadvantages depending on the location of implementation some are more successful than others but all are commercially viable for energy production. Biofuels production is expected to offer a similar answer for liquid transportation fuels in GHG reductions, develop long term replacement of petroleum fuels, increase energy security, and diversify fuel sources.

Biodiesel and bio-ethanol are currently the most common biofuels and are commercially available in the continental US. Current biodiesels are considered drop in fuels requiring no modification to vehicles for the use of the alternative fuel. These biofuels are currently being produced and represent a safe replacement due to already existing transportation and distribution infrastructure as compared to other options such as hydrogen. Currently biofuels are more expensive than traditional petroleum fuels; production continues to increase in countries around the world with a current production of over 35 billion liters.

Currently in the US, the primary feedstock for bio-ethanol is corn (Pimentel and Patzek, 2005). Bio-ethanol derived from a food crops or first generation feedstocks lead to instability in food availability and prices but more importantly do not scale to DOE

2030 alternative goals (Chisti, 2007; Department of Energy, 2007). Biodiesel is currently derived from variety of feedstocks with a primary source being soybeans. The scalability of biodiesel production in the US is similar to bio-ethanol when considering the use of first generation feedstocks, coupled with the ethical issue of utilizing a food based crop for fuel has lead the search for an alternative second generation feedstock, which include but are not limited to miscanthus, cellulosic ethanol, palm, and jatropha. Currently microalgae are considered a third generation feedstock based on the immaturity of the technology. Of the second and third generation feedstocks currently being investigated, microalgae have some distinct advantages which have lead to an increase in research and development around the microalgae to biodiesel process.

The work presented here looks at the environmental impact of microalgae biofuels, the current US productivity potential considering geographic impacts, and presents experimentally validated growth models used for reactor design evaluation and optimization.

## **1.2 Microalgae overview**

### ***1.2.1 What are microalgae?***

Microalgae are prokaryotic or eukaryotic photosynthetic microorganisms that can grow rapidly and live in diverse environments due to their unicellular or simple multi-cellular structure. Their size range from a few micrometers ( $\mu\text{m}$ ) to a few hundreds of micrometers. Examples of some typical microalgae currently being looked at as feedstocks for biofuels are: *Nannochloropsis salina*, *Chlorella*, *Tetraselmis sueica*,

*Chlorella vulgaris*, *Botryococcus braunii* based on high productivities and high neutral lipid content (Raja et al., 2008). A more in depth description of microalgae is presented in Richmond (2004).

Microalgae represent a diverse organism that currently lives in all earth ecosystems, aquatic and terrestrial. There are estimated 50,000 different species with 30,000 strains researched or currently being studied. There are a variety of collections that have been assembled through the world, the largest being at the University of Coimbra (Portugal) with 4000 strains and 1000 species. The biodiversity of microalgae is far superior to any other feedstock currently being investigated (Richmond, 2004).

Due to their simple cellular structure, microalgae are very efficient photosynthetic organisms (6-20%) compared to terrestrial plants (0.5-2.2%) (Aresta et al., 2005; Li et al., 2008). Microalgae are typically grown in an aqueous environment which provides them ready access to key growth constituents. Algae have naturally adapted to a range of ecosystems and can be grown in freshwater, brackish, marine and hyper-saline habitats with a range of pH and nutrients (Harwood and Guschina, 2009; Hu et al., 2008).

### ***1.2.2 Microalgae advantages***

There are many reports on the advantages of microalgae as a feedstock for biofuels production (Chisti, 2007; Hossain et al., 2008; Hu et al., 2008; Li et al., 2008; Li et al., 2008; Rodolfi et al., 2009; Rosenberg et al., 2008; Schenk et al., 2008; Sheehan et al., 1998; Tsukahara and Sawayama, 2005). Compared to other biofuel feedstocks, microalgae are characterized by higher solar energy yield, year-round cultivation, the

use of lower quality or brackish water, the ability to sequester CO<sub>2</sub>, and the use of less- and lower-quality land (Batan et al., 2010; Brown and Zeiler, 1993; Dismukes et al., 2008; Li et al., 2008; Mata et al., 2010; Posten and Schaub, 2009; Raja et al., 2008; 2008; Wijffels and Barbosa, 2010; Williams et al., 2009).

Microalgae compared to traditional terrestrial crops have significantly higher growth rates and high lipid percentages thus high productivity potentials. The theoretical maximum production of oil from microalgae has been calculated at 354,000 L·ha<sup>-1</sup>·a<sup>-1</sup> (38,000 gal·acre<sup>-1</sup>·a<sup>-1</sup>) (Weyer et al., 2009), but scalable experimental data have shown a near term realizable production of 46,000 liters·hectare<sup>-1</sup>·a<sup>-1</sup> (5000 gal·acre<sup>-1</sup>·a<sup>-1</sup>), compared to 2,533 liters·hectare<sup>-1</sup>·a<sup>-1</sup> (271 gal·acre<sup>-1</sup>·a<sup>-1</sup>) of ethanol from corn or 584 liters·hectare<sup>-1</sup>·a<sup>-1</sup> (62.5 gal·acre<sup>-1</sup>·a<sup>-1</sup>) of biodiesel from soybeans (Ahmed et al., 1994; Chisti, 2007; Pimentel, 2005; Pradhan et al., 2008; Yeang, 2008) Figure 2. Current research has shown under typical conditions of commercial scale reactor systems, *Nannochloropsis salina* can achieve a lipid content of 50% by weight (Emdadi and Berland, 1989; Fabregas et al., 2004; Suen et al., 1987), and an average annual growth rate of 25 g·m<sup>-2</sup>·day<sup>-1</sup> (Boussiba et al., 1987; Gudín and Chaumont, 1991; Suen et al., 1987). In laboratory conditions, *Nannochloropsis* can attain lipid percentages of 60% by weight and growth rates of 260 mg·L<sup>-1</sup>·hr<sup>-1</sup> or 150 g·m<sup>-2</sup>·day<sup>-1</sup> (Richmond et al., 2003; Rodolfi et al., 2009). The values reported in Figure 2 represent the current near term large scale production potential from microalgae based on this dissertation work and are not a scale up of small scale laboratory data.

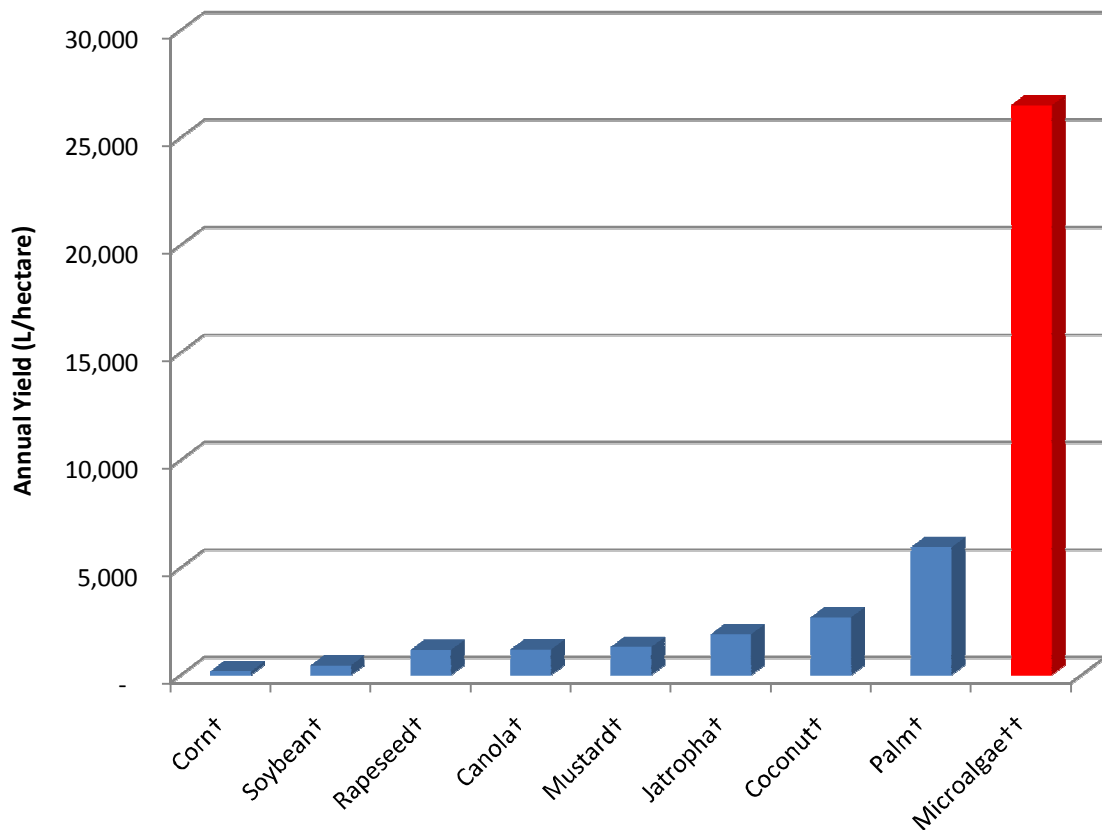


**Figure 2. Comparison of different feedstocks for biofuels. For this comparison the value reported for microalgae represents the near term realizable potential not the optimistic long term potential reported in literature. <sup>†</sup>(Chisti, 2007) <sup>††</sup>(Quinn et al., 2011)**

Different microalgae species can adapt to environmental conditions. This makes it possible to geographically optimize productivity potentials by cultivating specific species. This is not possible with first generation feedstocks. Traditional terrestrial crops have high tolerances to soil, water, and other uncontrollable environmental factors.

Microalgae have the potential to integrate with waste streams. Inherent in microalgae growth is the absorption of carbon. Microalgae are typically cultivated with

supplemental CO<sub>2</sub> in order to improve growth rates. Researchers have shown that microalgae feedstock cultivation can be coupled with coal fired power plants, natural gas aiming plants, and other CO<sub>2</sub> sources to sequester CO<sub>2</sub>. Microalgae do not require potable water and has the potential to utilize nutrients from wastewater treatment plants (Chisti, 2008; Li et al., 2008; Schenk et al., 2008; Wijffels and Barbosa, 2010).

Microalgae do not compete for valuable agricultural land and represent a non-food based bio-feedstock. The diversity of microalgae and their ability to grow in any environment enable cultivation locations where traditional feedstocks are not feasible.

The advantages presented have lead to an increased interest in the microalgae biofuels process.

### ***1.2.3 Cultivation technologies***

Two primary architectures for mass-culture of algae have been proposed: open ponds and photobioreactors (PBR). The traditional method is open pond cultivation with some selected illustrations presented in Figure 3.

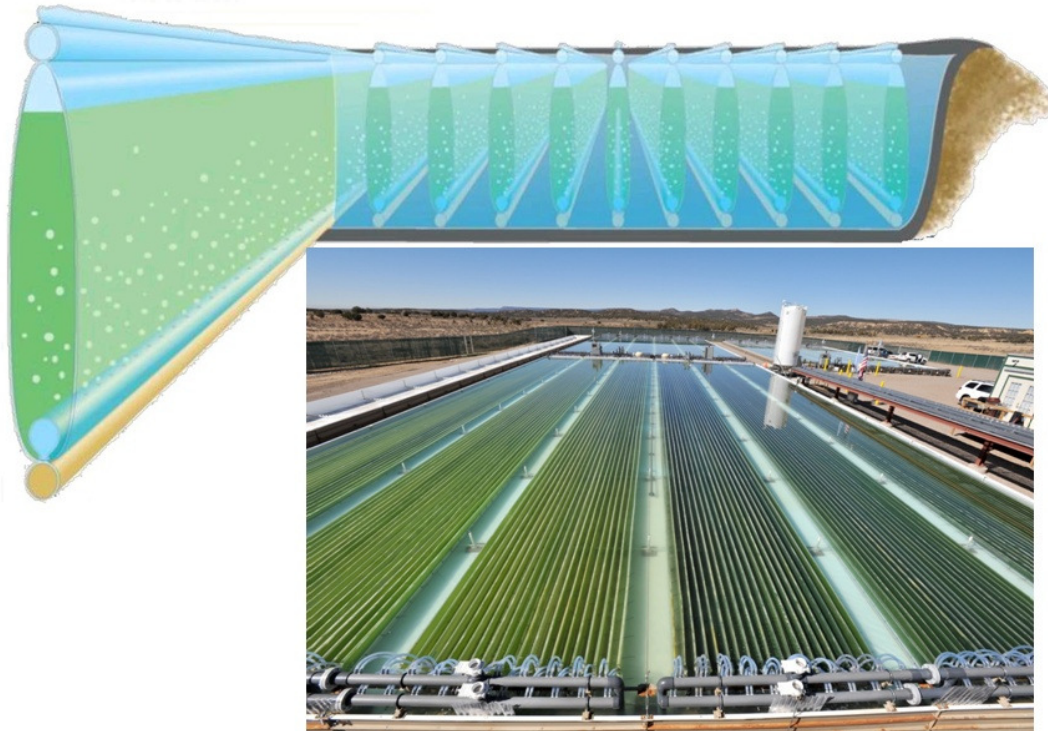


**Figure 3. Open raceway pond architecture for the cultivation of microalgae, picture courtesy of Ami Ben-Amotz (top). Closed photobioreactor architecture for microalgae cultivation, picture courtesy of Solix Biosystems (bottom).**

Open pond cultivation is characterized by low algae density, the potential for contamination by non desirable species, a thermal regulation requirement, and high

evaporative water losses. Closed photobioreactor cultivation has advantages over open raceway ponds (ORP) in they can achieve higher algae densities, higher productivity, can mitigate contamination, and capture direct and diffuse light, however have a higher capital and operating cost (Li et al., 2008; Pulz, 2001; Richmond, 2004). Current technological advances have reduced the capital and operating costs of PBRs making them more appealing as a commercially viable system (Richmond, 2004).

## **Chapter 2-Research Challenges**

### **2.1 Current challenges**

The utilization of microalgae as a potential feedstock was initially evaluated by NREL in the Aquatic Species Program. The research effort was in response to the energy crisis of the 1970's but was abandoned for economic reasons (Sheehan et al., July 1998). Renewed interest in microalgae as a potential alternative feedstock for biofuels has emerged again due to the volatility of crude oil markets, interest in energy independence, and carbon sequestration. This renewed enthusiasm has reenergized microalgae research communities.

#### ***2.1.1 Growth modeling***

The mechanisms defining growth are conceptually understood and 1<sup>st</sup> order models that are reactor specific have been developed. These models are typically based on light, temperature, and nutrients (Fernandez et al., 1998; Fuentes et al., 1999; Qiang et al., 1998; Rossignol et al., 2000). Most of the models generated are based on laboratory scale growth systems with constant optimized light (Benson et al., 2007). Mixing assumptions are assumed and in turn light interactions with algae are generalized including microalgae growth kinetics which ignore complex fluid dynamics and strictly focus on biological light utilization and absorption. The understanding,

modeling, and optimizing of such a complex growth system is extremely difficult. The CFD of air mixed reactor systems is computationally difficult based on two phase flow dynamics. Few have taken on the challenge of understanding the fundamental kinetics of mixing, let alone incorporating light dynamics (Posten, 2009). To get a first order understanding of light intensity, the effect on productivity mixing must initially be ignored. There is evidence to support that at low cell densities that light utilization is more important than mixing when the mixing is not extremely high or low (Hu et al., 1996; Qiang and Richmond, 1996; Qiang et al., 1998).

Current modeling efforts have focused on the utilization of indoor artificially illuminated data for validations. This type of validation does not facilitate the use of the models to outdoor systems. Models have been generated that represent large outdoor systems, however archaic reactor scaling factors limit the application of the models (Molina et al., 2000).

Due to the inherent complexity in growth modeling of microalgae cultures there has been limited work on the effects of diffuse light (Hu et al., 1996; Richmond, 2004). Diffuse light capture is fundamentally what extended photobioreactors depend on being significant to increasing productivity compared to open raceway ponds and offset higher operational and capital costs.

### ***2.1.2 LCA***

The life-cycle energy consumption of the microalgae to biofuel process is consumed predominantly in three places, mixing during growth, de-water, and

extraction. There is little published data about the effect of mixing less than 1 VVM on productivity. Experimental setups operate with mixing energies that are orders of magnitude higher than what is commercially used in pilot plant facilities such that mixing is not a primary variable in the experimentation (Barbosa et al., 2003; Chisti, 1998 ; Hu et al., 1996; Lehr and Posten, 2009; Qiang and Richmond, 1996).

Life cycle assessment (LCA) has been the fundamental tool to evaluate the sustainability of biofuels. The LCA literature makes use of the metrics of net energy ratio (NER, defined here as the ratio of energy consumed to fuel energy produced) and GHG emissions per unit of energy produced as the functional units for comparison purposes. Although LCA is a well recognized method, published standards are few and not widely adhered to (Delucchi, 2004). As a result, there are many different approaches and thus many conflicting results among authors (Aresta et al., 2005; Batan et al., 2010; Campbell et al., 2011; Clarens et al., 2010; Davis et al., 2009; Farrell et al., 2006; Hill et al., 2006; Hirano et al., 1998; Jorquera et al., 2010; Lardon et al., 2009; Minowa and Sawayama, 1999; Pimentel and Patzek, 2005; Stephenson et al., 2010). The conflicting results can partially be attributed to LCA results being highly sensitive to definitions of system boundaries, life-cycle inventories, process efficiencies, and functional units. Other factors differ among studies, including definitions of NER, key parameter values, sources of fossil energy, and co-product allocation and displacement methods make comparison among studies difficult (Davis et al., 2009; Farrell et al., 2006; Hill et al., 2006; Kim and Dale, 2002; Pimentel, 2005; Sheehan et al., 1998) As

such, LCA is best used to compare technologies, policies, and scenarios within sets of consistent assumptions.

LCAs of the microalgae-based biodiesel process exist in the literature but consensus on the inputs and methods appropriate for microalgae-based biofuels is lacking. Hirano (1998) considered the production of algae-derived methanol and derived a NER of 1.1. Minowa and Sawayama (1999) studied different algae strains with some strains achieving promising results with NERs greater than 1. Studies that include models of the feedstock processing stages of the microalgae-to-biofuel process (growth, dewater, and extraction) are less common. Minowa and Sawayama (1999) perform a net energy analysis of algae gasification with nitrogen recovery but do not incorporate a detailed process model. Campbell (2008) performs a net energy analysis based on review of previous studies, however the combination of data from different microalgae strains presents a problem of consistency. Lardon (2009) provides a thorough life cycle assessment of an open raceway pond system for the production of algae biodiesel, but does not address co-product allocation, making comparison to other studies more difficult.

## **2.2 Research questions, tasks, and plan**

Based on these Challenges, a primary research thrust can be posed:

**PRIMARY RESEARCH Charge: *RESEARCHERS HAVE SHOWN THAT THE SYSTEM SCALE ECONOMIC AND SUSTAINABILITY PERFORMANCE OF MICROALGAE BIOFUELS IS***

***DEPENDANT ON THE CONSUMPTIONS AND PRODUCTS OF THE ALGAE DURING THE FEEDSTOCK STAGES. IN ORDER TO QUANTIFY THE SENSITIVITY OF ALGAE FEEDSTOCK GROWTH AND PROCESSING ON SYSTEM-SCALE PERFORMANCE METRICS WE MUST CONNECT LOW-LEVEL MODELS OF ALGAE GROWTH AND PROCESSING TO THESE SYSTEM-SCALE PERFORMANCE METRICS.***

To address this challenge a system of models must be developed and individually validated. The validated models can then be integrated into a system where high level questions can be proposed and answered.

The primary research challenge can be broken down into three fundamental questions. Each of the following fundamental research questions can be used to help answer the primary research challenge.

### ***2.2.1 Research Question 1:***

***WHAT IS THE STRUCTURE AND COMPONENTS OF A VALIDATED AND EXTENSIBLE MODEL OF THE GROWTH STAGE OF NANNOCHLOROPSIS SP.?***

Previous work has developed models of the algae growth that uses a bulk growth model incorporating light absorption within the algae reactor. This has limitations in terms of the understandings that can be gained and also in terms of the applicability of these models to the engineering challenges that are in reactor design today. By developing a more detailed model of the light utilization by microalgae, reactor geometry can be evaluated and optimized based on a closed PBR geometry.

### 2.2.1.1 Hypotheses 1.1

A detailed model of incident and diffuse light is required in order to enable a more fundamental understanding of growth kinetics. This model overlaid with a high level economic analysis enables the validated design of optimized PBR reactor geometries.

### 2.2.1.2 Task 1.1 – Generate light model based on diffuse versus direct light

Develop a model based on literature data to evaluate the impact of diffuse light on algal productivity.

### 2.2.1.3 Task 1.2 - Experimentally generate small scale growth model

Design and build an experiment to evaluate the productivity of *Nannochloropsis sp.* under different intensities of light while maintaining thermal regulation and constant mixing.

### 2.2.1.4 Task 1.3 – Experimentally generate large scale growth data

Design and build a large scale (3 m x 1.5 m x 1.5 m) indoor growth system that can accommodate discreetly different reactor geometry.

### 2.2.1.5 Task 1.4 – Validate the scalability of small scale growth reactor

Use light and growth measurements from large scale system to critically evaluate the scalability of the small scale Pi growth model generated.

#### 2.2.1.6 Task 1.5 - Evaluate the impact of the proposed model

Evaluating the diffuse versus direct light utilization of microalgae is important in establishing economic feasibility of extended area photobioreactors. To date the primary means for mass cultivation of microalgae is in open raceway ponds. There are distinct differences between photobioreactors and open raceway ponds. Economically speaking open raceway ponds are significantly cheaper to build, maintain, and operate, however they are susceptible to contamination crashes, have a lower areal productivity, operate at a lower density which impacts dewatering economics, among other things. Extended area photobioreactors utilize not only direct light but a large amount of diffuse light. Understanding the productivity due to diffuse light will shed light on the feasibility of large scale microalgae production in photobioreactors.

#### 2.2.1.7

Evaluate the reduction of the data based on attributing the growth in the system to the active photic volume. Experimentation must be performed to evaluate the attenuation coefficient of light into the culture such that the data collected in the small and large scale system can be reduced on a photic volume metric. The scalability of the data reduction can then be evaluated.

## ***2.2.2 Research Question 2:***

### ***What is the potential productivity and feasibility of large scale algae production in the US?***

Dynamic maps have been generated by NREL illustrating potential wind and solar resources in the US. Utilizing a validated bulk growth model, historical hourly average PAR, ambient temperatures, wind speeds, land, water, and CO<sub>2</sub> availability a microalgae biomass potential map can be generated.

#### **2.2.2.1 Hypotheses 2.1**

The economic value and environmental sustainability of algae production for biofuels in the US will be highly dependent on environmental compatibility of the geography to the algae production process. Utilizing historical average weather data collected at various places throughout the US, a map of the summer, winter, and annual algae productivity can be developed. Year round cultivation will be limited to the milder climates of the southern US.

#### **2.2.2.2 Task 2.1 – Develop macro scale growth model**

Develop and validate a microalgae growth model based on a large scale outdoor photobioreactor geometry and operating conditions. The macro model is designed to capture the first order effects of light, temperature,

and nutrients on microalgae growth. This model will include biomass output along with lipid productivity potential.

#### 2.2.2.3 Task 2.2 – Develop a thermal bath model

Develop and integrate a thermal bath model based on ambient average measured temperatures and incident solar radiation with a validated biological growth model specific to the Solix photobioreactor configuration growing *Nannochloropsis oculata*.

#### 2.2.2.4 Task 2.3 – Generate productivity feasibility maps

Develop the following regional maps:

1. Primary map of potential year round locations based on growth.
2. Secondary map of summer vs. winter production
3. Integrate land, water, and CO<sub>2</sub> availability

#### 2.2.2.5 Task 2.3 – Evaluate impact of microalgae based on proposed model

The Energy Policy Act of 1992 directed the US Department of Energy to evaluate the goal of replacing 30% (~40 billion gallons) of the transportation fuel consumed in the US by 2010 with replacement fuels. In March of 2007 this goal was deemed unreachable and the deadline for fuel replacement was changed to 2030 (Department of Energy, 2007). Algae-based biofuels are purported to be the most scalable of the biofuel processes currently available (Chisti, 2007). Evaluating microalgae potential in the US will enable feasibility to be taken to the next level.

Even though algae scale better than terrestrial crops, year round cultivation is limited to temperate climates. Integrating resource availability such as water and land will again narrow the possible locations for mass production.

### ***2.2.3 Research Question 3:***

***What is the potential environmental impact of the microalgae to biofuel process?***

A detailed engineering model based on material consumption and energy use in the microalgae to biofuel process linked with a lifecycle assessment (LCA) model will enable the evaluation of the environmental impact of the microalgae of biofuels process. Maintaining a consistent LCA boundary, this process can be compared to soy based biofuels as well as conventional diesel in terms of net energy ratio (NER) and greenhouse gas (GHG) emissions. The engineering model should be constructed based on large scale near term realizable production in order to evaluate the scalability of the process.

#### **2.2.3.1 Hypotheses 3.1**

Currently there is a lack of a comprehensive systems level model of the microalgae to biofuel process incorporating near term realizable growth, dewater, and extraction technologies. Developing a detailed engineering model will enable a more fundamental understanding of where the process is most energy intensive and how changes to the fundamental stages of the process affect the overall GHG footprint. A

modular format enables the evaluation of different growth, dewater, and extraction technologies.

#### 2.2.3.2 Task 3.1 – Develop integrated engineering model based on internal knowledge

Develop an integrated engineering model for the growth, dewater, and extraction technologies currently being investigated by Solix. This requires a high level understanding of the key constituents (energy and materials) in all of the technologies in each of the different processes.

#### 2.2.3.3 Task 3.2 – Develop integrated engineering model based on current literature

Develop an integrated engineering model of growth, dewater, and extraction technologies currently attainable in the near future. The data for these phases is based on current research.

#### 2.2.3.4 Task 3.3 – Integrate engineering model with GHG model

Integrate the individual models into a systems level model that produces outputs that can be inputted into a life cycle assessment model, specifically Argon National Labs GREET (Wang, 2005).

#### 2.2.3.5 Task 3.4 – Evaluate process variable sensitivity

Evaluate the sensitivity of net energy ratio (NER) and GHGs to primary system inputs such as growth rate, culture density, sparge rate, solvent ratios, ect.

#### 2.2.3.6 Task 3.5 – Evaluate scalability of proposed system

Evaluate the scalability of the proposed microalgae to biofuel system at 40 billion gallons per year which represents the DOE 2030 alternative fuel goals with respect to energy and material consumption (Department of Energy, 2007).

#### 2.2.3.7 Task 3.5 – Impact of Life Cycle Assessment

The next generation of biofuel feedstocks must be critically analyzed to determine their energetic and GHG impact while considering scalability to a level of tens of billions of gallons per year. Microalgae have many sustainability and scalability advantages compared to terrestrial crops. Compared to first-generation biofuel feedstocks, microalgae are characterized by higher solar energy yield, year-round cultivation, the use of lower quality or brackish water, the use of less- and lower-quality land (Brown and Zeiler, 1993; Dismukes et al., 2008; Li et al., 2008; Posten and Schaub, 2009; Raja et al., 2008; Williams et al., 2009). Algae have experimentally been shown to produce biodiesel at 46,769 liters/hectare/yr (5000 gal/acre/yr) compared to 2,533 liters/hectare/yr (271 gal/acre/yr) of ethanol from corn or 584 liters/hectare/yr (62.5 gal/acre/yr) of biodiesel from soybeans (Ahmed et al., 1994; Chisti, 2007; Pimentel, 2005; Pradhan et al., 2008; Weyer, 2009; Yeang, 2008).

### **2.2.4 Research Plan**

A three stage research plan has been implemented to answer the three primary research questions previously presented. The independent stages all add to a collective knowledge but do not directly build on each other and can be worked on concurrently.

#### 2.2.4.1 Stage 1:

Develop a full understanding of the entire life cycle of microalgae biofuels. Utilizing appropriate tools to develop systems models for all technologies realistically being considered for the following stages: growth, dewater, extraction, conversion, and transportation and distribution. The model requires detail such that fundamental questions can be evaluated in terms of energy and material consumption at large scale.

#### 2.2.4.2 Stage 2:

Develop and validate (based on Solix data) a bulk growth model that incorporates current Solix geometry, light, temperature, and nutrients. Develop a thermal model and incorporate it into bulk biological model that can then be utilized to develop a dynamic map of microalgae biomass and lipid potential in the US.

#### 2.2.4.3 Stage 3:

Develop a productivity model that differentiates between direct and diffuse light utilization. This model is validated through two independent experiments to determine the potential impact of an extended surface area reactor. Optimization of PBR geometry as a function of reactor depth is based on light intensity.

## Chapter 3-Net Energy and Greenhouse Gas Emissions Evaluation of Biodiesel Derived from Microalgae<sup>1</sup>

### 3. Abstract

Biofuels derived from microalgae have the potential to replace petroleum fuel and first-generation biofuel, but the efficacy with which sustainability goals can be achieved is dependent on the lifecycle impacts of the microalgae-to-biofuel process. This study develops a detailed, industrial-scale engineering model for the species *Nannochloropsis* using a photobioreactor architecture. This process level model is integrated with a lifecycle energy and greenhouse gas emissions analysis compatible with the methods and boundaries of the Argonne National Laboratory GREET model, thereby ensuring comparability to preexisting fuel-cycle assessments. Results are used to evaluate the net energy ratio (NER) and net greenhouse gas emissions (GHGs) of microalgae biodiesel in comparison to petroleum diesel and soybean-based biodiesel with a boundary equivalent to “well-to-pump”. The resulting NER of the microalgae biodiesel process is 0.93 MJ of energy consumed per MJ of energy produced. In terms of net GHGs, microalgae-based biofuels avoids 75 g of CO<sub>2</sub>-equivalent emissions per MJ of energy produced. The scalability of the consumables and products of the proposed

---

<sup>1</sup> The work presented in this chapter is based on the publication Batan, L, Quinn, J, Willson, B, Bradley, T, 2010. Net energy and greenhouse gas emission evaluation of biodiesel derived from microalgae. *Environ. Sci. Technol.*, 44, 7975-7980. Co-authored by Batan and Quinn.

microalgae-to-biofuels processes are assessed in the context of 150 billion liters (40 billion gallons) of annual production.

### 3.1. Introduction

The next generation of biofuel feedstocks must be critically analyzed to determine their energetic and greenhouse gas (GHG) emissions impact while considering scalability to a significant level of production. Compared to first-generation biofuel feedstocks, microalgae are characterized by higher solar energy yield, year-round cultivation, the use of lower quality or brackish water, and the use of less- and lower-quality land (Brown and Zeiler, 1993; Dismukes et al., 2008; Li et al., 2008; Posten and Schaub, 2009; Raja et al., 2008; Williams et al., 2009). Researchers have shown that microalgae feedstock cultivation can be coupled with combustion power plants or other CO<sub>2</sub> sources to sequester GHG emissions and has the potential to utilize nutrients from wastewater treatment plants (Li et al., 2008). The theoretical maximum production of oil from microalgae has been calculated at 354,000 L·ha<sup>-1</sup>·a<sup>-1</sup> (38,000 gal·acre<sup>-1</sup>·a<sup>-1</sup>) (Weyer et al., 2009), but pilot plant facilities and scalable experimental data have shown a near term realizable production of 46,000 liters·hectare<sup>-1</sup>·a<sup>-1</sup> (5000 gal·acre<sup>-1</sup>·a<sup>-1</sup>), compared to 2,533 liters·hectare<sup>-1</sup>·a<sup>-1</sup> (271 gal·acre<sup>-1</sup>·a<sup>-1</sup>) of ethanol from corn or 584 liters·hectare<sup>-1</sup>·a<sup>-1</sup> (62.5 gal·acre<sup>-1</sup>·a<sup>-1</sup>) of biodiesel from soybeans (Ahmed et al., 1994; Chisti, 2007; Pimentel, 2005; Pradhan et al., 2008; Yeang, 2008).

Life cycle assessment (LCA) is the fundamental tool that has been used to evaluate the sustainability of biofuels. Although LCA is a well recognized method, published standards are incomplete and are not widely adhered to (Delucchi, 2004). The LCA literature makes use of the metrics of net energy ratio (NER, defined here as the ratio of energy consumed to fuel energy produced) and GHG emissions per unit of energy produced as the functional units for comparison purposes. The results from LCA are highly sensitive to definitions of system boundaries, life-cycle inventories, process efficiencies, and functional units (Farrell et al., 2006; Hill et al., 2006; Pimentel, 2005). LCA studies often include various NER definitions, key parameter values, sources of fossil energy, and co-product allocation and displacement methods, complicating comparisons among studies and policy synthesis (Davis et al., 2009; Farrell et al., 2006; Hill et al., 2006; Kim and Dale, 2002; Pimentel, 2005; Sheehan et al., 1998).

LCAs of the microalgae-based biodiesel process exist in the literature but consensus on the inputs and methods appropriate for microalgae-based biofuels is lacking. Hirano (1998) considered the production of microalgae-derived methanol and derived a NER of 1.1 (Hirano et al., 1998). Minowa and Sawayama (1999) perform a net energy analysis of microalgae gasification with nitrogen recovery which increases the NER (>1) but do not incorporate a detailed process model (Chisti, 2008; Minowa and Sawayama, 1999). Campbell et al. (2008) perform a net energy analysis based on review of previous studies, but the combination of data from different microalgae strains presents a problem of consistency (Campbell et al., 2010). Lardon et al. (2009) provides a thorough life cycle assessment of an open raceway pond system for the production of

microalgae biodiesel. Lardon et al. extrapolates laboratory-scale results to assign the energy burdens due to cultivation and allocates energy consumption to co-products without using co-product displacements (Lardon et al., 2009). Clarens et al. 2010 does not incorporate energy and materials for conversion of microalgae oil to fuel, but does include energy for the procurement of CO<sub>2</sub> (Clarens et al., 2010). Performing a coherent LCA of the microalgae to biodiesel process requires detailed models of each of the feedstock processing stages (growth, dewater, extraction, conversion, and distribution) combined with a standard and consistent set of LCA boundary conditions.

Based on the state of the field, there exists a need to quantify the sustainability effects of the microalgae-to-biofuel process. This study builds on academic literature, industrial consultation, and pilot plant experience of microalgae feedstock processing to generate a model of net energy and GHG emissions of the microalgae-to-biofuel process. This baseline LCA will be used to compare and contrast the net energy and GHGs of microalgae to that of conventional petroleum-based diesel and soybean-based biodiesel. For clarity and comparability, these comparisons are made using the same assumptions and LCA boundaries as GREET 1.8c (Wang, 2005).

### **3.2. Methods**

In order to describe the net energy and GHG impacts of microalgae biodiesel, we must develop a valid, extensible, and internally consistent model of the materials inputs, energy use, and products for the process. The simulation architecture is shown in Figure 4.

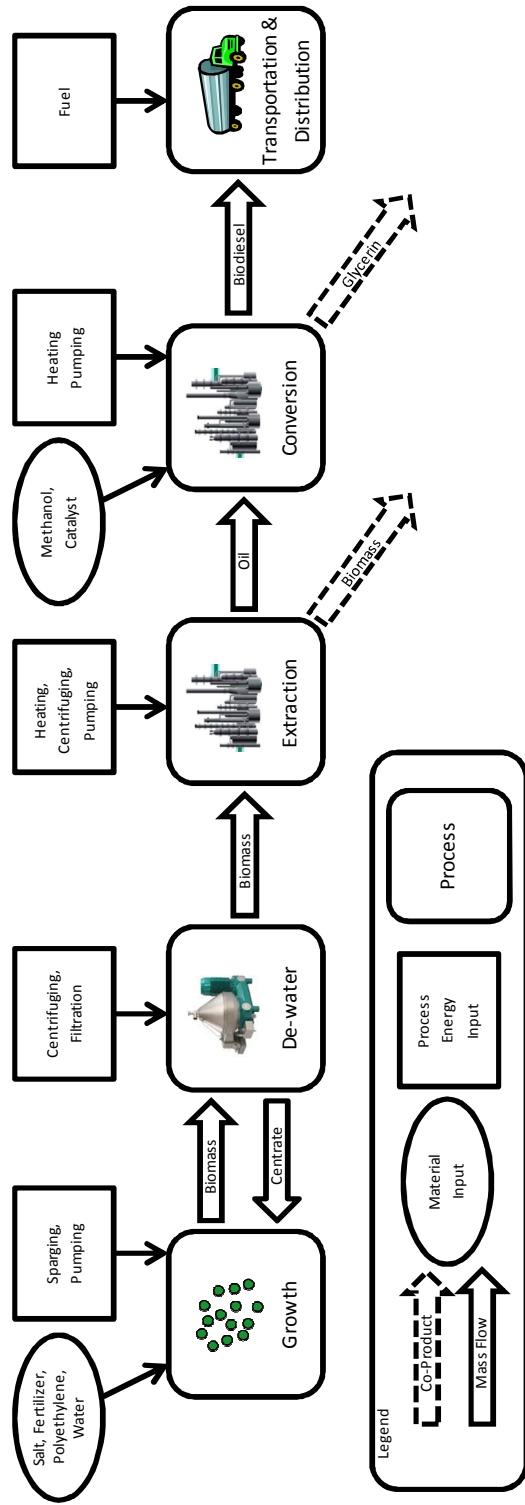


Figure 4. Microalgae Biodiesel Processing and Lifecycle Analysis Model Overview

The three primary components of this model are: a detailed engineering process simulation of microalgae from growth through extraction, a more generalized model of microalgae from conversion to end use, and an integrated calculation of net energy and GHG emissions due to impacts from the inputs, outputs, processes, and co-product allocation for the microalgae biodiesel production. A more detailed representation of the modular nature of the engineering model is presented in Figure 5.

The engineering model is constructed to be a modular such that a variety of technologies can easily be evaluated.

### ***3.2.1. Detailed Engineering Process Model***

The purpose of the detailed engineering process model of the microalgae growth, harvest, and extraction phases is to describe the material inputs, material outputs, and types and amounts of energy consumed in the microalgae feedstock processing stages. The baseline model of microalgae to biodiesel process is based on a 315 hectares (776 acres) facility, which includes photosynthetically active and built areas. The temporal unit for evaluation of the process is 1 year. The model incorporates the recycling of growth media but does not recover nitrogen from extracted biomass (Chisti, 2008). Additional material recycling will affect the results of the LCA, but a lack of data regarding the energy and material costs preclude its inclusion in this study.

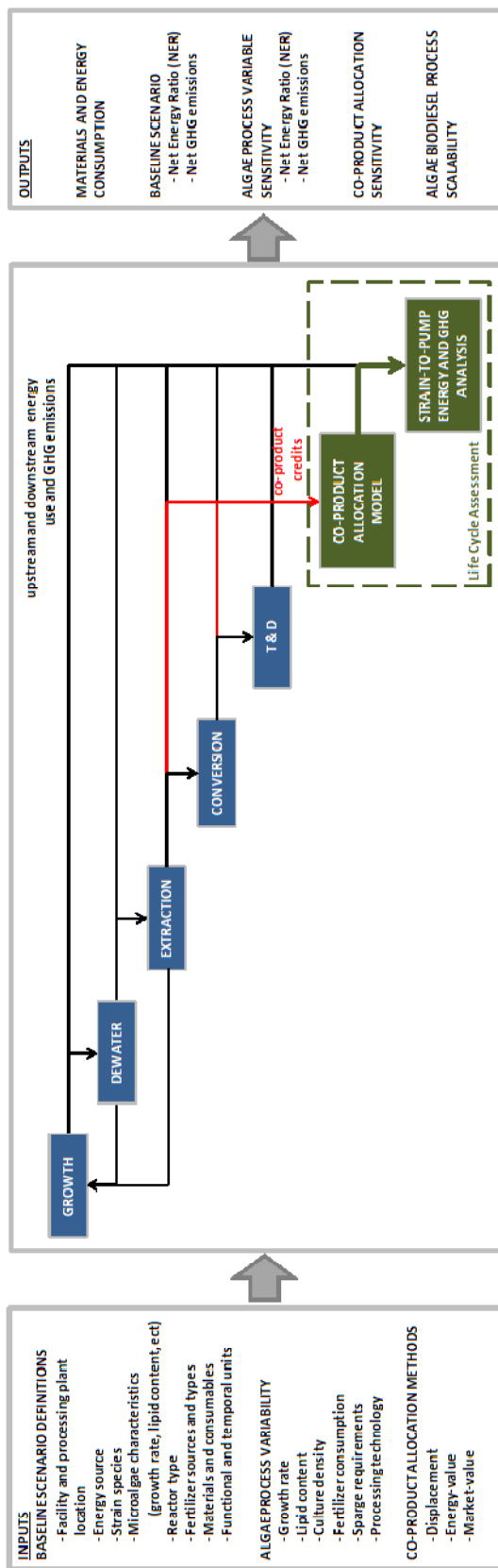


Figure 5. Detailed engineering process model illustrating the mass and energy flow to and from each of the processing stages

### **3.2.1.1. Growth Model**

Two primary architectures for mass-culture of microalgae have been proposed: open ponds (ORP) and photobioreactors (PBR). PBR cultivation has advantages over ORP in they can achieve higher microalgae densities, higher productivity, and mitigate contamination. Current technological advances have reduced the capital and operating costs of PBRs making them more appealing as a commercially viable system (Richmond, 2004).

The microalgae strain *Nannochloropsis salina* was selected and modeled because of its high lipid content and high growth rate. Under the conditions of the Colorado State University pilot plant scale reactor system, *Nannochloropsis salina* can achieve a lipid content of 50% by weight (Emdadi and Berland, 1989; Fabregas et al., 2004; Suen et al., 1987), and an average annual growth rate of  $25 \text{ g}\cdot\text{m}^{-2}\cdot\text{day}^{-1}$  (Boussiba et al., 1987; Gudín and Chaumont, 1991; Suen et al., 1987). The use of these validated data for this study is conservative and proper, considering that under laboratory conditions, *Nannochloropsis* can attain lipid percentages of 60% by weight and growth rates of  $260 \text{ mg}\cdot\text{L}^{-1}\cdot\text{hr}^{-1}$  or  $150 \text{ g}\cdot\text{m}^{-2}\cdot\text{day}^{-1}$  extrapolated to the system modeled (Richmond et al., 2003; Rodolfi et al., 2009). The nitrogen and phosphate content of the microalgae are defined as 15% and 2% by mass according to biological growth requirements and lipid productivity research (Arrigo, 2005; Redfield, 1958; Rodolfi et al., 2009). The salinity of the system is set at  $20 \text{ g}\cdot\text{L}^{-1}$  (Abu-Rezq et al., 1999).  $\text{CO}_2$  enriched air (2%  $\text{CO}_2$ ) is sparged through the bioreactor to provide carbon and active mixing of the culture. The energy required for sparge is based on an experimentally validated specific power requirement

of  $0.4 \text{ W}\cdot\text{m}^{-2}$  (Weissman et al., 1988). Mixing by sparge is performed during periods of photosynthetically active growth and when bio-available nitrogen is present in the media. The facility is assumed to be located in a temperate region of the US where the amount of energy required for thermal regulation is assumed negligible due to the availability of very low power thermal regulation resources (including ground and pond loop heat exchangers). The difference between precipitation and evaporation results in water losses of  $2.5 \text{ cm}\cdot\text{day}^{-1}$  ( $1 \text{ in}\cdot\text{day}^{-1}$ ) from the water bath that supports the reactors (Smith et al., 1994). The life cycle costs of the polyethylene PBR bags are include and assumed to be replaced at 5 year intervals.

The biological growth facility modeled for this work is illustrated in Figure 6.

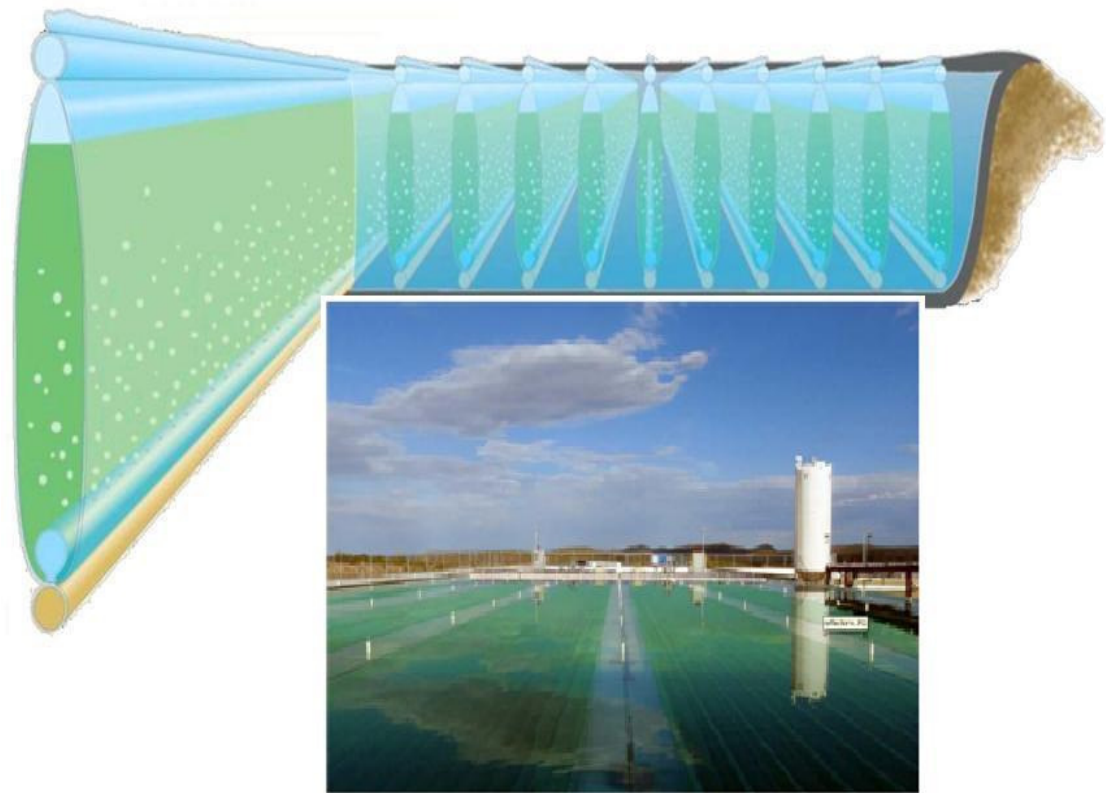


**Figure 6. Illustration and photograph of the pilot facility modeled for this study**

The modeled photosynthetic facility is composed of a number of 36 meter (120 ft) long and 0.12 millimeter thick clear polyethylene photobioreactors supported in a thermal bath, as shown in Figure 6. The reactors incorporate an air sparge system designed to provide CO<sub>2</sub> and turbulent mixing. The reactors are assumed to have a lifetime of 5 years based on biofouling and other material failures. The bags are subdivided into three different reactor sets: incubation reactors, growth/stress reactor set 1, and growth/stress reactor set 2.

The growth process as modeled is a batch system comprised of one set of incubation reactors and 2 sets of growth/stressing reactors. The incubation reactors are used to provide microalgae inoculum for the growth/stress reactor systems. The growth/stress reactors are used to grow and stress the culture in a procedure to maximize lipid yield, while minimizing energy consumption.

The growth process begins with the inoculation of microalgae into nutrient-rich medium in the incubator reactors. All bioavailable nutrients are absorbed in the first 2 days of growth. The culture is then cultivated until it transitions from linear growth stage (nutrient-rich growth) to a stationary growth stage (nutrient-depleted) after approximately 5 days. The stationary growth stage represents a growth stage with lower biomass productivity rate (approximately 15 g m<sup>-2</sup> day<sup>-1</sup>), but with increased lipid production. On the 5<sup>th</sup> day, all of the culture in the incubation reactors is harvested, and mixed with nutrient-rich media. Part of the culture is injected into the incubation reactors, the remainder is injected into the growth/stress reactors. This incubation,

growth, and inoculation process is repeated every 5 days within the incubation reactors.

In the growth/stress reactors, the inoculum from the incubation reactors will grow for 5 days and will then transition from the linear growth phase into the stationary growth phase. For the next 5 days, the culture is cultivated under nutrient-deprived stationary growth conditions. Lipid content increases to 50% of cell weight during the stationary stress growth (Emdadi and Berland, 1989). At the end of a 10 day growth cycle, the culture is harvested and the reactors are re-inoculated with culture from the incubation reactors. This inoculation, linear growth, stationary growth, harvest cycle is repeated every 10 days with each set of growth/stress reactors. Two sets of growth/stress reactors with their 10 day cycle time are required to match the 5 day cycle of the incubation reactors. The facility is assumed to operate year round and does not require annual repopulation.

It has been shown that increasing sparge rates can improve yields, however the level of sparge typically utilized in laboratory experimentation is economically disadvantageous for a product such as biodiesel. It has also been shown in low density cultures that the sparge rate does not have a major effect on growth (Qiang and Richmond, 1996).

Electricity is used to power pumping and sparging. Diesel is used to fuel transportation on the facility for maintenance and inspection. The microalgae facility is assumed to be located next to a pure CO<sub>2</sub> source, such as a natural gas amine plant, which implies no transportation costs, preprocessing costs, or energy requirements to

deliver CO<sub>2</sub>. This assumption is based on the current abundance of pure CO<sub>2</sub>. The material inputs, material outputs, and energetic inputs for the growth model are detailed in Table 1.

### ***3.2.1.2. Dewater Model***

The removal of free water from the harvested microalgae is required and can be achieved through flocculation, centrifugation, vacuum belt dryers, or solar driers. Centrifugation is modeled for this study because it is currently commercially used and represents a mature technology (Grima et al., 2003).

The energy consumption for transport of the microalgae medium from the PBR to a centralized processing unit is based on losses from pumping through a 13 cm (5 in) PVC pipe over a distance of 500 m with a pump efficiency of 70% (Glover, 2000; White, 1999). The energy consumption required for centrifugation is modeled based on the performance of a continuous clarifier that consumes 45 kW steady state with a throughput of 45,000 liters·hour<sup>-1</sup> (based on the particle size of *Nannochloropsis*) (Yanovsky, 2009). The centrate (free water) from the clarifier is recycled with a 0.1 micron polypropylene filtration system (Keystone\_Division, 2002). The microalgae paste is then conveyed from the clarifier output to the extraction stage requiring 19.4 J·kg<sup>-1</sup> m<sup>-1</sup> (Herum, 1960).

Energy consumption for these processes is derived entirely from electricity as summarized in Table 1.

### ***3.2.1.3. Extraction Model***

The lipid extraction and recovery model is designed from literature to represent a scalable and near-term realizable and commercially viable extraction process. The process is based off of the process for recovery of lipids from soybeans due to the lack of large scale oil recovery systems for microalgae. The process incorporates a shear mixer, centrifuge, decant tank, solvent recovery, and two distillation units for the recovery of solvents.

The extraction system uses a hexane to ethanol solvent mixture of 9:1, at a solvent to oil ratio of 22:1, which recovers 90% of the lipids present in the microalgae. The parameters of this process are assumed to be identical to the extraction process used for other oil crops (Conkerton et al., 1995; Dominguez et al., 1995; Gandhi et al., 2003; Zhang and Liu, 2005). Counter flow heat exchangers with an effectiveness of 0.90 are used to recover process heat (Shah, 2003). Evaporator-condenser systems with 80% energy recovery are used for solvent recovery and oil separation. The energy required to move and centrifuge is modeled based on 500 m length, 13 cm (5 in) diameter PVC transfer pipe with a pump efficiency of 70% and a centrifugal separator respectively (Glover, 2000; Yanovsky, 2009).

Energy consumption for these processes is derived from electricity for pumping, shear mixing, and centrifugation and natural gas for heating, with all solvents being recycled as summarized in Table 1.

#### ***3.2.1.4. Conversion Model***

The conversion stage consists of the chemical and industrial processes required to convert the extracted microalgae lipids into biodiesel through transesterification. The process requires the reaction of lipids (triacylglycerols) with methanol in the presence of a catalyst, producing fatty acid methyl esters (biodiesel) and glycerin. Microalgae lipids and soybean lipids are composed of similar triacylglycerols but at slightly different composition percentages (Reske et al., 1997; Tonon et al., 2002). For this study, the types and quantities of energy and material inputs to the conversion processes are assumed identical and are derived from the GREET 1.8c soy-oil conversion model.

Natural gas is used for process heating at a rate of  $2.10 \text{ MJ}\cdot\text{kg}^{-1}$  of microalgae biodiesel and electricity is used for mixing and transport at a rate of  $0.03 \text{ KWh}\cdot\text{kg}^{-1}$  of biodiesel. The methanol, catalyst (sodium methoxide), and neutralizer (hydrochloric acid) are consumed in proportion to the quantity of biodiesel produced, as summarized in Table 1.

#### ***3.2.1.5. Transportation and Distribution Model***

The microalgae production facility modeled includes facilities for growth, dewater, extraction, and conversion stages, enabling the transportation of the feedstock to the processing plant to be performed by conveyor. The distances and means of transportation and distribution (barge, rail, and truck) are assumed to be the same as

soybean-based biofuel. Energy consumption for the transportation and distribution stage is summarized in Table 1.

### ***3.2.2. Lifecycle Assessment Model***

The Center for Transportation Research at Argonne National Labs was funded by the U.S. department of Energy's Office of Energy Efficiency and Renewable Energy (EERE), to develop a full life cycle model for the evaluation of various fuel and vehicle combinations. The project generated the GREET (Greenhouse gases, Regulated Emissions, and Energy use in Transportation) model (Wang, 2005), which evaluates the energy and material consumption and the corresponding emissions of a full fuel-cycle. GREET incorporates more than 100 fuel production pathways with the general fuel pathways illustrated in Figure 7. The LCA boundary of GREET can be defined by either "well-to-pump" or "well-to-wheel" as illustrated in Figure 8.

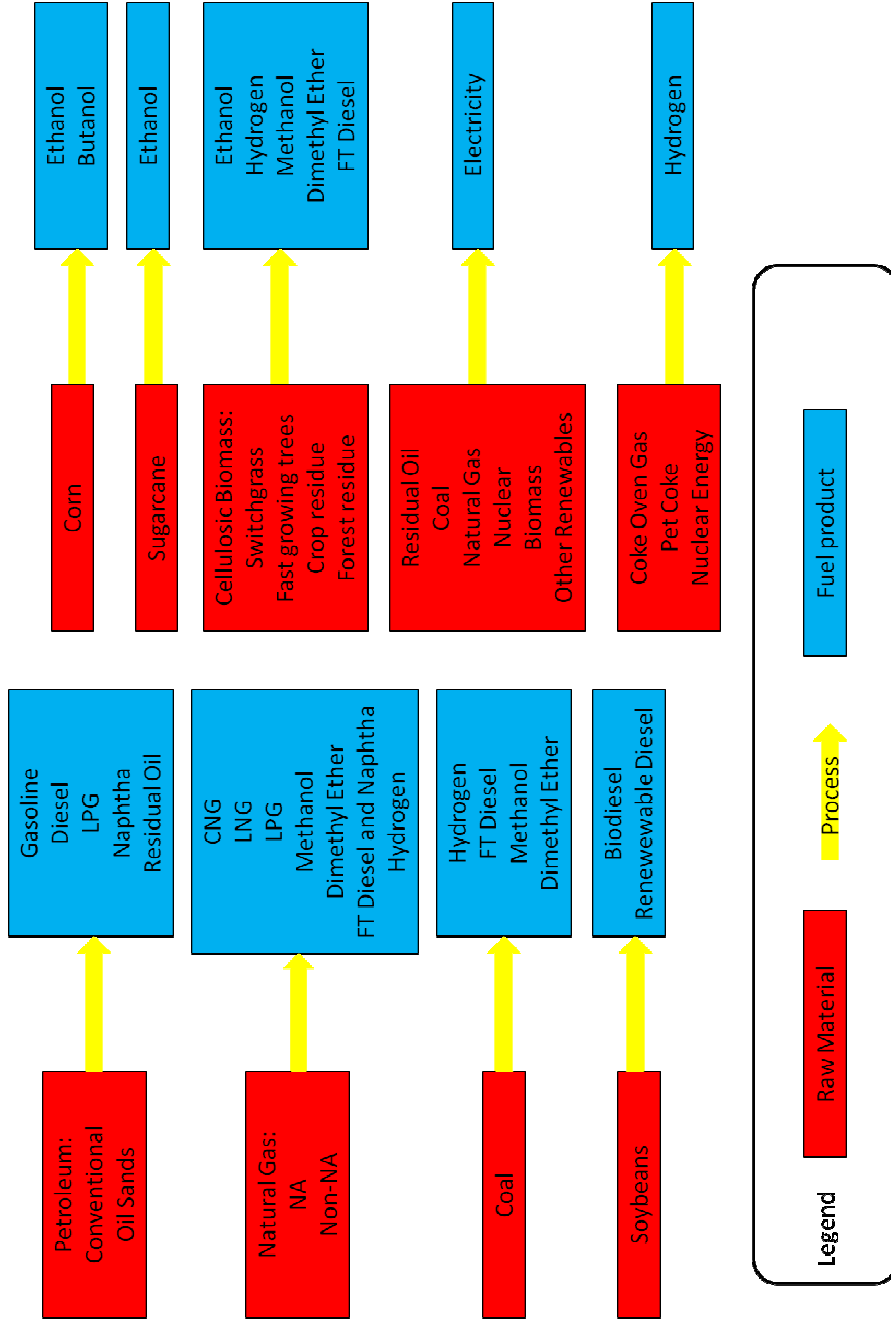


Figure 7. General fuel production pathways (Wang, 2005)

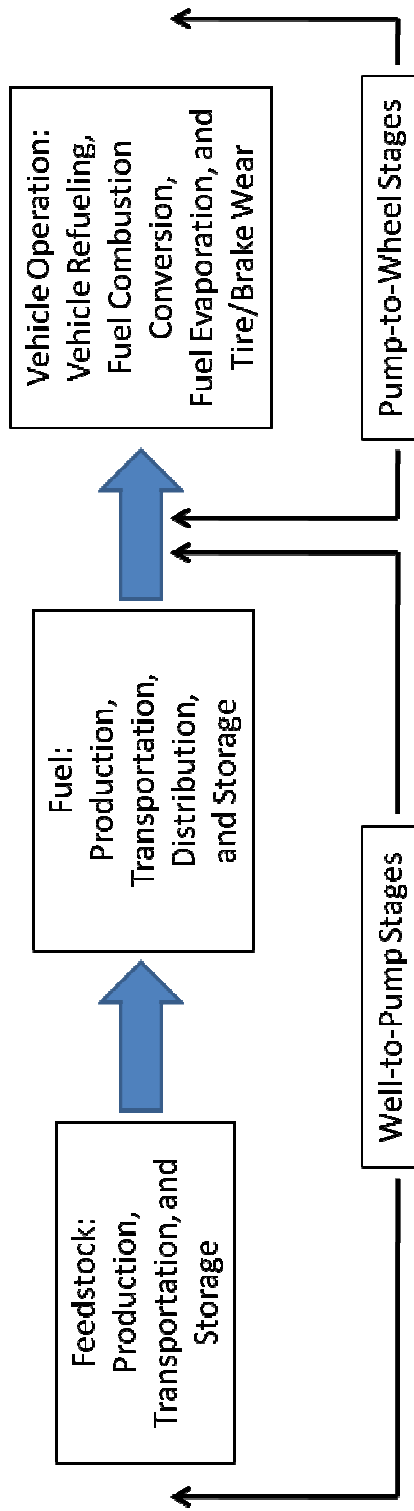


Figure 8. Illustration of “Well-to-Pump” and “Pump-to-Wheel” boundaries (Wang, 2005)

GREET separates the energy use by type (petroleum, coal, natural gas, nuclear, etc) to more accurately evaluate environmental impacts. GREET evaluates the type of energy consumed to calculate upstream energy and GHG emissions implicit in materials and energy flows. GREET draws on open literature, engineering analysis, and stakeholder inputs to generate an accurate data base of energy and material requirements for specific processes. The major assumptions in GREET on “well-to-pump” study are the energy efficiencies of the fuel production activities, GHG emissions of the fuel production activities and the emission factors of fuel combustion technologies. In this study, the GREET model was utilized to evaluate the microalgae life cycle with a boundary defined as “strain-to-pump” (cultivation stage of microalgae, dewatering microalgae, microalgae oil extraction, microalgae oil conversion and microalgae biodiesel transportation and distribution) which is analogous to “well-to-pump” for conventional diesel. The system boundaries for the analysis performed are presented in Figure 9.

The GREET model utilizes data from Energy Information Administration (EIA) and US Department of Agriculture (USDA) for all energy and material inputs in the process of recovery and refinery of petroleum based diesel, and the production and process of soybean based biodiesel, including the stages of agricultural farming, harvesting, transportation of feedstock, soybean oil extraction, conversion and biodiesel transportation and distribution to the pump stations.

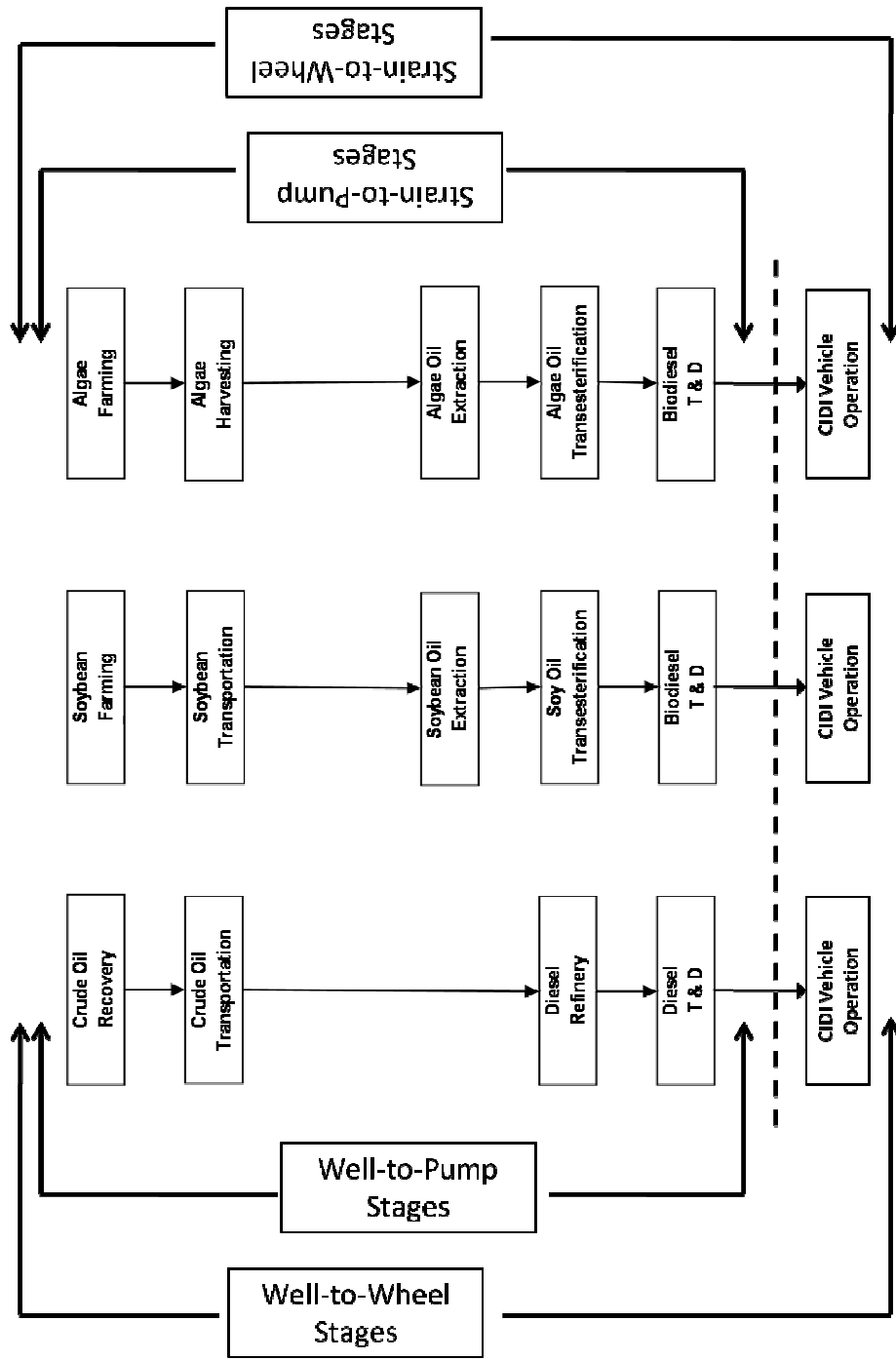


Figure 9. System Boundaries for Life cycle Analysis of Petroleum Diesel, Soybean Biodiesel and Microalgae Biodiesel (Wang, 2005)

The GREET 1.8c model was used to simulate the material consumption, net energy use, and GHG emissions for the life cycle of the microalgae-to-biofuel process. The boundaries of the life-cycle considered for this study start with the growth stage of the microalgae and end at the point of distribution of biodiesel to consumer pumping stations. This LCA boundary is called “strain-to-pump” and is analogous to the “well-to-pump” boundary for conventional crude oil.

GREET 1.8c was modified to represent the microalgae-to-biodiesel process, with no changes in methodology inherent in the original model. To allow a direct comparison of these results to previous GREET LCAs on soybean-based and conventional petroleum fuels, this study applies the same lifecycle boundaries as does GREET. For example, GREET 1.8c excludes the energy required to construct agricultural facilities, processing facilities and refineries. Similarly, this study excludes the energy required to construct the microalgae bioreactors.

### ***3.2.2.1. Lifecycle Energy Model***

The modified GREET model is used to calculate both direct and upstream energy consumption throughout the microalgae-to-biofuel process and to calculate energy credits due to co-products. The total energy consumption can be represented as a NER with units of MJ of energy consumed per MJ of energy produced. The modifications required to the GREET model for the evaluation of microalgae based biofuel were the inclusion of life cycle energy and emissions of salt (NaCl) and high density polyethylene (HDPE) bags (material for construction of the photobioreactors) to the database.

### ***3.2.2.2. GHG Emission Model***

REET is used for the evaluation of the lifecycle GHG emissions associated with the microalgae-to-biofuel process. REET accounts for CO<sub>2</sub>, CH<sub>4</sub> and N<sub>2</sub>O emissions originated from specific sources of energy and materials consumed and their respective upstream emissions. IPCC global warming potentials are applied to CH<sub>4</sub> and N<sub>2</sub>O emissions to calculate the CO<sub>2</sub> equivalent (CO<sub>2</sub>-eq) emissions of the microalgae-to-biofuel process (Ipcc, **2006**). REET also accounts the avoidance of CO<sub>2</sub> emissions due to allocation of co-products, i.e. replacement of conventional products by microalgae-to-biofuel co-products.

REET also calculates the emissions of six criteria air pollutants: non-methane volatile organic compounds (NMVOCs), carbon monoxide (CO), nitrogen oxides (NO<sub>x</sub>), particulate matter with a diameter of 10 micrometers or less (PM10) and 2.5 micrometers or less (PM2.5), and sulfur oxides (SO<sub>x</sub>). Both this study and REET assign an indirect GHG emissions equivalency to NMVOC and CO emissions. This indirect GHG emissions equivalency considers that NMVOC and CO emissions are converted into CO<sub>2</sub> in the atmosphere (Seinfeld and Pandis, 1998). Molecular weight ratios are used to convert NMVOC and CO emissions to CO<sub>2</sub>-eq emissions. This method for assessing environmental burden from CO and NMVOC has been the subject of debate and revision at IPCC. Although IPCC methods do not define a global warming potential associated with CO or NMVOC emissions, IPCC assessment reports do quantify an indirect global

warming potential for CO and NMVOCs (Forster, 2007). Inclusion of indirect emissions is methodologically defensible (Gillenwater, 2008), and the methods used in GREET and in this paper have been used in peer-reviewed publication (Huo et al., 2009). The inclusion of the indirect emissions of CO and NMVOCs using the molecular weight method allows for direct comparison to GREET's conventional and biofuel models.

GREET contains a database of the GHG emissions for many types of energy sources, fertilizers, and other relevant materials used in this assessment. Only the upstream GHG emissions and energy consumption due to the production of NaCl (required for replacing salt lost in media recycling) had to be added to the GREET inventory.

The GHG emissions model totals the CO<sub>2</sub> captured during microalgae growth with the CO<sub>2</sub> credits due to co-products and combines the CO<sub>2</sub> and CO<sub>2-eq</sub> emissions due to the energy and materials consumed for a final result.

### ***3.2.2.3. Co-Product Allocation Methods***

In evaluating the life cycle energy consumption of the microalgae-to-biofuel process, the biomass that is not converted to fuel can be considered as a co-product. For this study, the microalgae co-product credits are allocated using the displacement method. The displacement method assumes that the co-product displaces a preexisting conventional product. The displacement co-product credits represent the lifecycle energy and GHG emissions that would be required to produce the displaced product.

Co-product credits are subtracted from the overall energy and GHG emissions of the microalgae-to-biofuel process.

The two primary co-products of the microalgae to biofuels process are extracted microalgae biomass (generated from the extraction stage) and glycerin (generated from the conversion stage). For the displacement method, the extracted microalgae biomass is used to displace conventional microalgae biomass, which is an ingredient in aquacultural fish feed. The displaced microalgae biomass is cultivated using conventional, industrial-scale processes (Aresta et al., 2005; Carraretto et al., 2004; Markovits et al., 1992; Reboloso-Fuentes et al., 2001; Renaud et al., 1991; Sukenik et al., 1993). The microalgae extract mass to microalgae mass displacement ratio is 1.3:1 due to the higher content of protein in microalgae extract. Microalgae-derived glycerin is assumed to directly displace petroleum-derived glycerin (Wang, 2005). Sensitivity to co-product allocation is also presented based on an energy value, and market value co-product methods.

### **3.3. Results**

The process parameters presented above and the displacement co-product allocation method define the baseline scenario designed to represent a near-term realizable, industrially relevant microalgae-to-biofuel production process based on a PBR configuration. A sensitivity analysis to co-product credit allocation method, energy sources, and process parameters are also presented.

### ***3.3.1. Materials and Energy Consumption of the Microalgae-to-Biofuel***

#### ***Process***

The first results of the microalgae-to-biofuel process model are a tabulation of the consumables and energy consumption of each process stage, presented in Table 1.

The quantities and types of these direct consumables are the inputs to the NER and GHG calculation models which translate these consumptions into lifecycle energy consumption and GHG emission rates.

There are a few steps of the microalgae-to-biofuel process that make up a large proportion of the primary energy consumption. 99% of the electrical energy consumed in the growth phase is consumed to compress air for sparge. 76% of the energy consumed during extraction is required for solvent recovery. Some other steps of the process are energetically negligible (moving the microalgae and recycling media consume less than 1% of the total electrical energy).

**Table 1. Summary material and energy inputs and outputs for the baseline microalgae to biofuel process for a period of 1 year**

<b>STAGE/Inputs</b>	<b>VALUE</b>	<b>UNITS</b>
<b>GROWTH STAGE</b>		
Photosynthetic area per facility area	0.80	ha·ha <sup>-1</sup>
Salt consumption	134	g·(kg dry algae) <sup>-1</sup>
Nitrogen fertilizer consumption	147	g·(kg dry algae) <sup>-1</sup>
Phosphorus fertilizer consumption	20	g·(kg dry algae) <sup>-1</sup>
Polyethylene consumption	1.17	m <sup>3</sup> ·ha <sup>-1</sup>
Diesel fuel consumption	10	L·ha <sup>-1</sup>
Electricity consumption	41,404	kWh·ha <sup>-1</sup>
Microalgae biomass yield	91,000	kg·ha <sup>-1</sup>
<b>DEWATER STAGE</b>		
Electricity use	30,788	kWh·ha <sup>-1</sup>
<b>EXTRACTION STAGE</b>		
Natural gas consumption	141,994	MJ·ha <sup>-1</sup>
Electricity consumption	12,706	kWh·ha <sup>-1</sup>
Extracted oil yield	43,009	L·ha <sup>-1</sup>
<b>CONVERSION STAGE</b>		
Natural Gas consumption	2.10	MJ·(kg biodiesel) <sup>-1</sup>
Electricity consumption	0.03	kWh·(kg biodiesel) <sup>-1</sup>
Methanol consumption	0.10	kg·(kg biodiesel) <sup>-1</sup>
Sodium hydroxide consumption	0.005	kg·(kg biodiesel) <sup>-1</sup>
Sodium methoxide consumption	0.0125	kg·(kg biodiesel) <sup>-1</sup>
Hydrochloric acid consumption	0.0071	kg·(kg biodiesel) <sup>-1</sup>
<b>TRANSPORTATION &amp; DISTRIBUTION</b>		
Diesel consumption	0.0094	L·(kg biodiesel) <sup>-1</sup>

### ***3.3.2. Net Energy Results***

The second result of this analyses is a comparison of the net energy of the microalgae-to-biofuel process to the soybean-to-biofuel process and to a conventional petroleum-to-diesel process (both obtained from U.S. average data of GREET 1.8c), illustrated in Table 2. It is notable that both soybean-based biodiesel and microalgae-biodiesel take advantage of co-product credits to reduce the net energy consumed.

Since refineries produce multiple products, the energy use and emission of petroleum-based fuel are calculated by allocating total refinery energy use into individual refinery products at the aggregate refinery level (Wang, 2008). The microalgae biofuel has 30% less input energy per unit of product (before co-product allocation) than conventional soybean-based biofuel.

Table 2 shows that the energy required to support the growth stage during microalgae cultivation is 2.1 times higher than the energy required to support the growth stage for soy cultivation. Microalgae oil extraction uses less energy than soy oil extraction, however, the microalgae-to-biofuels process requires an energy intense dewatering stage that is not present in the soybean-to-biofuels process. The primary energetic advantage of the microalgae process, relative to soy, is related to the energy embedded in the feedstock. Soybeans contain 18% lipid by dry weight, whereas *Nannochloropsis salina* contains 50%. This means that less microalgae is required to produce 1 unit of biofuel energy than is required of soybeans. GREET quantifies this relationship as a conversion ratio, defined as the ratio of the lower heating value (LHV) of biodiesel to the LHV of the feedstock. For soybeans, the ratio of the energy of the feedstock to the energy of the fuel output is 40% compared to 70% for microalgae. A higher conversion ratio means that a lower fraction of the LHV of the feedstock input to the conversion process is lost to co-products. In summary, although algae cultivation is more energy intensive, as has been asserted in previous studies (Hirano et al., 1998; Nash and Frankel, 1986; Posten, 2009; Reijnders, 2008; Richmond, 2004; Sawayama et

al., 1999; Spolaore et al., 2006), lifecycle analysis shows that the microalgae-to-biofuels process is less energy intensive per unit of energy output.

### ***3.3.3. GHG Emissions Results***

Total GHGs can provide a more holistic comparison of the environmental impact of the production of these fuels. Table 3 presents the comparison of the GHG components and net emissions for production of petroleum diesel, biodiesel from soybean and microalgae feedstocks.

These results show that soybean and microalgae based biofuels processes can realize GHG reductions relative to a petroleum diesel baseline. Both biofuels result in a net negative CO<sub>2</sub> output due to CO<sub>2</sub> capture intrinsic in the production of biomass during photosynthesis, the displacement of petroleum, and the displacement of co-products. The microalgae biodiesel process has a 5% better performance in terms of net GHGs compared to soybean based biodiesel in the boundary “strain-to-pump”. A notable component of the microalgae GHG emissions reduction is the net avoidance of N<sub>2</sub>O that is achieved. Although the microalgae growth stage uses a higher mass of N-fertilizer than the soy growth stage, the aerobic conditions of microalgae cultures suppress the direct emission of N<sub>2</sub>O. For microalgae, no biomass is left in the field where it can be subject to de-nitrification and the closed PBRs do not experience loss of fertilizer through runoff (Bothe, 2007; Flynn et al., 1993; Golterman, 1985; Jannasch, 1960; Sacks and Barker, 1949; Skerman and Macrae, 1957).

**Table 2. Net Energy Ratio (NER) in MJ/MJ of Conventional Diesel, Soybean Biodiesel and Microalgae Biodiesel Processes with the Energy Consumption for Each Feedstock Processing Stage**

Stage	Conventional Diesel	Soybean Biodiesel	Microalgae Biodiesel
Crude oil recovery*	0.053	-	-
Growth*	-	0.32	0.73
Dewater*	-	-	0.17
Oil extraction*	-	0.46	0.21
Fuel conversion*	0.13	0.17	0.17
Feedstock input*	-	1.50	0.43
Transportation & Distribution*	1.8E-7	0.01	0.01
Co-product credits*	-	(0.83)	(0.79)
Total NER**	0.19	1.64	0.93

\*Stage MJ consumed·(MJ produced)<sup>-1</sup>

\*\*Total MJ consumed·(MJ produced)<sup>-1</sup>

**Table 3. Net GHG Emissions of Conventional Diesel, Soybean Biodiesel and Microalgae Biodiesel Processes with the Contribution of CO<sub>2</sub>, CH<sub>4</sub>, and N<sub>2</sub>O gases per unit of MJ of energy produced**

Conventional Diesel	Soybean Biodiesel	Microalgae Biodiesel
CO <sub>2</sub> (g·MJ <sup>-1</sup> )	14.69	-72.73
CH <sub>4</sub> (g·MJ <sup>-1</sup> )	2.48	0.42
N <sub>2</sub> O (g·MJ <sup>-1</sup> )	0.07	0.58
Net "strain to pump" GHG (gCO <sub>2-eq</sub> ·MJ <sup>-1</sup> )	17.24	-71.73
		-59.49
		0.74
		-16.54
		-75.29

Due to their high global warming potential value, N<sub>2</sub>O emissions can have a significant impact in the total GHG emissions. For terrestrial crops, N<sub>2</sub>O emissions are produced in 3 distinct ways,

- From upstream N<sub>2</sub>O emissions during manufacture of nitrogen-based fertilizer,
- From direct emissions from the fertilizer applied to the field,
- From residual biomass left in the field after harvesting.

For microalgae biofuels, these upstream, direct, and residual biomass sources of N<sub>2</sub>O emissions must be reconsidered for their applicability to the microalgae growth system.

For the upstream emissions, the default GREET 1.8c N<sub>2</sub>O emissions from the manufacturing of nitrogen-based (urea) fertilizer are used.

For the direct and residual biomass sources of N<sub>2</sub>O, the microalgae growth system is fundamentally different than a traditional terrestrial crop system. This study proposes that the direct and residual biomass N<sub>2</sub>O emissions for the microalgae-to-biofuel are negligible due to the processes and controls used to cultivate microalgae. In terrestrial crop N<sub>2</sub>O emissions, the guideline for calculating the emissions assumes that 1% of the total nitrogen applied is converted to N<sub>2</sub>O (Ipcc, **2006**). This percentage includes:

- fertilizer converted into N<sub>2</sub>O by denitrifying bacteria in the soil,
- biomass left in the field which is afterward converted into N<sub>2</sub>O,
- fertilizer carried away by runoff and then converted into N<sub>2</sub>O in the watershed.

The mechanism for the generation of N<sub>2</sub>O in terrestrial crop fields is the anaerobic de-nitrification of nitrogen based fertilizer by bacteria found in the soil (Bothe, 2007; Delwiche, 1981; Golterman, 1985). Despite the presence of bio-available nitrogen within microalgae reactors, de-nitrification (and direct N<sub>2</sub>O emissions) will not occur within the reactors because the system is a closed system where denitrifying bacteria is not present, and because the reactors are an aerobic environment. In the microalgae growth stage, nitrogen is supplied in the form of dissolved fertilizer at the beginning of the batch growth process. The uptake rate of the nitrogen by the microalgae is a light-dependent process and the bio-available nitrogen is depleted in 36 hours (Flynn et al., 1993; Takagi et al., 2000; Yamaberi et al., 1998). During photosynthetically active periods, the microalgae produce oxygen and therefore are growing in an aerobic environment (Jannasch, 1960; Skerman and Macrae, 1957). At night, an oxygen level of 8 ppm can be achieved by sparging air through the culture. Maintaining an oxygen level greater than 0.2 ppm will inhibit the reduction of nitrogen by denitrifying bacteria (Skerman and Macrae, 1957). Denitrifying bacteria that are grown in a high oxygen environment will not synthesize the nitrogen-reducing enzyme, thereby inhibiting the potential for N<sub>2</sub>O emission (Sacks and Barker, 1949). For this study, the system is sparged 24 hours per day during periods of bio-available nitrogen to generate an aerobic environment, eliminating de-nitrification and direct N<sub>2</sub>O emissions.

For this study, the microalgae reactor is a self-contained closed photobioreactor (PBR) and thus does not have any loss of fertilizer through runoff with the assumption that all bio-available nitrogen is utilized by the microalgae.

Co-product displacement provides additional net-negative N<sub>2</sub>O emissions. The net N<sub>2</sub>O emission avoidance that can be realized through the microalgae-to-biofuels process represents a significant difference between the GHG emissions profiles of microalgae compared to other agricultural bioenergy processes, which often have N<sub>2</sub>O emissions as the largest source of positive GHG emissions (Adler et al., 2007). The sensitivity of these results to energy source assumptions is provided in section 3.3.6.

In addition to the “strain-to-pump” analysis, this study has also run simulations using the “strain-to-wheel” LCA boundary, which includes all stages of “strain-to-pump” as well as the combustion of fuel in transportation vehicles. Results are presented in Table 4. GREET assumes that soybean-derived and microalgae-based diesel fuels are used in 100% pure form in compression-ignition, direct-injection (CIDI) engine vehicles. Due to the lack of emissions data from the combustion of microalgae based biofuel, it was assumed that the fuel economy and emissions from soy- and microalgae-based biofuels in CIDI vehicles are the same. These simulations result in 93.08 g CO<sub>2</sub>-eq/MJ for petroleum-based diesel, 5.01 g CO<sub>2</sub>-eq/MJ for soy-based biodiesel, and the avoidance of 1.31 g CO<sub>2</sub>-eq/MJ for microalgae-based biodiesel.

**Table 4. Net GHG Emissions of Conventional Diesel, Soybean Biodiesel and Microalgae Biodiesel Processes with the Contribution of CO<sub>2</sub>, CH<sub>4</sub>, and N<sub>2</sub>O gases per unit of MJ of energy produced**

	Conventional Diesel	Soybean Biodiesel	Microalgae
Biodiesel			
CO <sub>2</sub> (g/MJ)	14.69	-72.73	-59.49
CH <sub>4</sub> (g/MJ)	2.48	0.42	0.74
N <sub>2</sub> O (g/MJ)	0.07	0.58	-16.54
Net "strain to pump" GHG (gCO <sub>2-eq</sub> /MJ)	17.24	-71.73	-75.29
Net "strain to wheel" GHG (gCO <sub>2-eq</sub> /MJ)	93.08	5.01	-1.31

### ***3.3.4. Scalability***

The Energy Policy Act of 1992 directed the US Department of Energy to evaluate the goal of replacing 30% (~150 billion liters) of the transportation fuel consumed in the US by 2010 with replacement fuels. In March of 2007 this goal was deemed unreachable and the deadline for fuel replacement was changed to 2030 (Department of Energy, 2007). Algae-based biofuels are purported to be the most scalable of the biofuel processes currently available (Chisti, 2007). In order to understand the scalability of the proposed processes, material inputs and material outputs, the baseline engineering process model was scaled so as to produce 150 billion liters per year with the corresponding consumables and products presented in Table 4.

Limits on water availability, nitrogen availability, and the constraints of the glycerin co-product market will limit the scale to which this type of microalgae biofuels production model can be extrapolated, which are not considered in this study. Alternative sources of nitrogen and water, including perhaps from wastewater (Yun et al., 1997) or anaerobic digestion for nitrogen recovery from the extracted biomass (Chisti, 2008), and other uses for the glycerin co-product (Yazdani and Gonzalez, 2007) must be considered to achieve long-term process scalability.

**Table 5. Scalability metrics derived from the baseline microalgae to biofuels process model scaled to a production of 40 billion gallons per year of microalgae biodiesel**

<b>Scalability Metric</b>	<b>Value</b>	<b>Notes</b>
Land Required	4.41x10 <sup>6</sup> hectares	16% of Colorado Land Area (0.45% of US Land Area) (U.S. Census Bureau, 2009)
CO <sub>2</sub> Consumption	8.17 x10 <sup>11</sup> kg·a <sup>-1</sup>	32% of CO <sub>2</sub> from US power generation (Energy Information Administration, 2007)
Natural Gas Consumption	1.39 x10 <sup>11</sup> kWh·a <sup>-1</sup>	2% of US production (Energy Information Administration, 2009)
Electricity Consumption	2.77 x10 <sup>11</sup> kWh·a <sup>-1</sup>	7% of US production (Energy Information Administration, 2007)
Water Consumption	5.07 x10 <sup>12</sup> L·a <sup>-1</sup>	27% of Colorado river annual flow (Reisner, 1993)
Nitrogen Consumption	4.71 x10 <sup>10</sup> kg·a <sup>-1</sup>	1900% of US urea production (U.S. Census Bureau, 2009)
Algae Biodiesel Production	150 x10 <sup>9</sup> L·a <sup>-1</sup>	18% of US Transportation Energy Sector (Energy Information Administration, 2009)
Glycerin Co-product Production	2.1 x10 <sup>10</sup> kg·a <sup>-1</sup>	7500% of North American production (Energy Information Administration, 2007)
Algae Extract Co-Product	6.3x10 <sup>8</sup> kg·a <sup>-1</sup>	11% of protein required for NOAA US Aquaculture Production Outlook for 2025 (Kim and Kaushik, 1992; U. S. Department of Commerce, 2009)

The results of this study are limited to assessment of the scenarios proposed and investigated, but this work has shown that a microalgae biodiesel process using currently available technologies can show significant improvement in lifecycle GHG emissions and NER. Technology and biofuels system-level improvements which are currently under investigation by a variety of researchers will improve the environmental performance and scalability of the microalgae-to-biofuels process. This study suggests that near-term algae biofuels production can be environmentally beneficial compared to petroleum-based diesel, and that the proposed microalgae to biofuel process exhibits significant NER and GHG advantages over soybean-based biodiesel.

### ***3.3.5 Sensitivity to Co-Product Allocation***

This section presents an analysis of the sensitivity of the LCA results to variation in the co-product allocation methods. The production of microalgae-based biofuel has not been performed at industrial scale, the uses and values of the microalgae co-products are highly uncertain. To test the sensitivity of the results of this study to co-product end-uses, allocations of co-product credits are considered in three different ways: displacement, energy-value allocation, and market-value allocation.

With the displacement method, it is assumed that a conventional product is displaced by a co-product generated in the biofuel process. The life cycle energy that would have been used and the emissions that would have been generated during production of the displaced product are counted as credits for the co-product generated

by the biofuel pathway. These credits are subtracted from the total energy use and emissions associated with the fuel pathway under evaluation. The allocation method allocates the feedstock use, energy use, and emissions between the primary product and co-products on the basis of mass, energy content, or economic revenue. In this study, glycerin and extracted biomass are produced as co-products during the production of algae-based fuel.

The displacement method is based on the displacement of microalgae used as fish and rotifer feed in aquaculture by the microalgal extract produced in the microalgae-to-fuel process. An averaged value for the energy dedicated to cultivation of microalgae for fish feed in aquaculture of  $7.6 \text{ MJ kg}^{-1}$  of dry microalgae (3,250 Btu (lb of dry algae)<sup>-1</sup>) was used (Aresta et al., 2005; Kadam, 2002). For GHG emissions allocation, the energy used during the microalgae cultivation was assumed to be primarily electricity from coal and natural gas powered plants.

The energy-value allocation method bases the value of the co-product credits on the heating value of the co-product. This study assumes that the extracted biomass can be used as co-firing material with a heating value of  $14.2 \text{ MJ kg}^{-1}$  (Kadam, 2002).

Glycerin is allocated at its lower heating value.

The market value method bases the value of the co-product credits on the economic revenue potential of the co-product. The value of extracted biomass as an economic commodity has not been fully investigated due to the immaturity of the technology. At present, a large-scale use of microalgae biomass is as a component of the feed used for the cultivation of fish fry in aquaculture. The current commercial

(Kost, 2010) market value of fish feed for aquaculture, is US \$2.65 kg<sup>-1</sup>. This feed is composed of a minimum of 50% protein and of 20% oil content. The extracted biomass can be used to construct a feed of similar composition. The extracted biomass is 36.7% protein and 5% oil on a dry weight basis. Canola oil at \$0.93 kg<sup>-1</sup> (20) is added to the extracted biomass to produce a product with the same ratio of protein to oil. To create an equivalency between the algae-canola feed and the conventional feed, a mass displacement of 1.5 is applied, where 1.5 lb of algae-canola feed can replace 1 lb of fish feed (De Pauw et al., 1984; Lubzens et al., 1995; Metting, 1996; Pulz and Gross, 2004; Richmond, 2004). A market value for the original microalgae extract (before oil addition) is then estimated is \$1.87 kg<sup>-1</sup>. Costs relating to oil mixing and transportation are not included. The market value of glycerin applied in the simulation is \$0.81 kg<sup>-1</sup>, which is the average of the range of \$0.62-\$0.99 kg<sup>-1</sup> (21)

The NER obtained using the displacement method is 0.93 MJ of energy consumed per MJ of fuel energy produced, which is lower than the NER of 1.29 MJ MJ<sup>-1</sup> and 0.83 MJ MJ<sup>-1</sup>, obtained by energy- and market-value methods, respectively. In terms of NER, the displacement and market-value methods find that the proposed microalgae-to-biofuels process realizes more energy than it consumes. The CO<sub>2</sub> equivalent discounts as calculated using the displacement method are higher than those calculated using the energy-value or the market-value method. For the metric of net GHG emissions, the sustainability benefits of the proposed process are shown to be sensitive to these three methods of co-product allocation as presented in Table 6.

**Table 6. Comparison of the net GHG Emissions of the microalgae to biodiesel process as a function of method of co-product allocation**

<b>Microalgae Biodiesel Emissions</b>	<b>Displacement Method</b>	<b>Energy-Value Method</b>	<b>Market-value Method</b>
CO <sub>2</sub> (g MJ <sup>-1</sup> )	-59.49	-29.80	-55.92
CH <sub>4</sub> (g MJ <sup>-1</sup> )	0.74	2.22	0.98
N <sub>2</sub> O (g MJ <sup>-1</sup> )	-16.54	0.21	0.09
Net "strain to pump" GHG (gCO <sub>2-eq</sub> MJ <sup>-1</sup> )	-75.29	-27.37	-54.85
Net "strain to wheel" GHG (gCO <sub>2-eq</sub> MJ <sup>-1</sup> )	-1.44	49.35	21.88

### 3.3.6 Sensitivity to Electricity Sources

This section presents an analysis of the sensitivity of the LCA results to variation modeled source of electricity. A major component of the energy used in the microalgae to biofuels process is electricity, as shown in Table 1.

As such, the composition of the electricity will have an effect on the process NER and GHG emissions. Average US electricity mix, the Northeast electricity mix, and the California electricity mix are compared to understand the sensitivity of this analysis to electricity sources.

The average US electricity mix is composed of 50.4% coal, 20% Nuclear power, 18.3% natural gas, and 11.3% biomass, residual oil and others. Northeast (NE) mix is composed of 33.9% nuclear, 29.9% coal, 21.7% natural gas, 14.5% biomass, residual oil and others. The California mix is composed of 36.6% natural gas, 28.3% variety of renewable sources, 20.5% nuclear, 13.3% coal and 1.3% biomass (Wang, 2005). The NER and GHG emissions for the different power sources are presented in Table 7 and Table 8, respectively.

**Table 7. Net Energy Ratio per Electricity Source and Mix with a LCA boundary of “strain-to-pump” for the baseline scenario**

<b>Electricity Source</b>	<b>NER</b>
US Average Mix	0.93 MJ MJ <sup>-1</sup>
North-east Mix	0.86 MJ MJ <sup>-1</sup>
California Mix	0.82 MJ MJ <sup>-1</sup>

The small variation in NER and GHG emissions shown in Table 7 and Table 8 are due to the different efficiencies and sources for electricity generation. The California mix as electricity source presents the best net GHG emission and NER compared to Northeast and US average mix.

This analysis shows that the NER and GHG performance of the proposed microalgae-to-biofuels process is robust to assumptions regarding electricity sources.

### ***3.3.7 Sensitivity to Process Parameters***

This section presents an analysis of the sensitivity of the LCA results to variation in the process model. The parameters of the detailed microalgae-to-biofuels process model were used to evaluate some of the alternative biological growth systems and alternative extraction techniques that have been proposed to improve the productivity, economics, and sustainability of microalgae-based biofuels. For each stage of the process, we seek to understand how effective the proposed changes are at improving the NER and GHG emissions of microalgae-based biofuels. Six potential improvements to the baseline process scenario are proposed.

**Table 8. Analysis of Net GHG per source of Electricity with a LCA boundary of “strain-to-pump” for the baseline scenario**

	Conventional Diesel		Soybean Biodiesel		Microalgae Biodiesel	
	U.S. Electricity	Mix	U.S. Electricity	Mix	California State Electricity	Northeast Electricity Mix
CO <sub>2</sub> (g MJ <sup>-1</sup> )	14.69	14.69	-72.73	-80.36	-72.34	-59.49
CH <sub>4</sub> (g MJ <sup>-1</sup> )	2.48	2.48	0.42	0.45	0.45	0.74
N <sub>2</sub> O (g MJ <sup>-1</sup> )	0.07	0.07	0.58	-16.56	-16.54	-16.54
Net GHG (g CO <sub>2</sub> -eq MJ <sup>-1</sup> )	17.24	17.24	-71.73	-96.47	-88.43	-75.29

The high lipid case represents a scenario where the lipid content of the microalgae has been improved to 70% by weight. The 2x growth rate case represents a scenario where the growth rate of the microalgae has been doubled to  $50 \text{ g m}^{-2} \text{ day}^{-1}$ . The  $\frac{1}{2}$  nutrient case represents a scenario where the nutrients required for microalgae growth are halved. The 2x density case represents a scenario where the microalgae culture is grown at double the currently realizable density. These changes to the growth parameters of the microalgae have been proposed as possible results from genetic engineering, bio-prospecting, or integration of microalgae/wastewater facilities (Beer et al., 2009; Ghirardi et al., 2000; Hu et al., 2008). These results are achieved without changes in reactor size, mixing rates, extraction efficiency, or other process parameters. The sparge  $\text{CO}_2$  case represents a scenario where the sparge of an air/ $\text{CO}_2$  mixture in the baseline scenario is replaced with purely  $\text{CO}_2$ . The energy consumption of the sparge  $\text{CO}_2$  case is based on a uptake of 50% accomplished by 10 passes with an average uptake of 5% per pass (Sheehan et al., 1998). The  $\frac{1}{2}$  solvent case represents the scenario where the ratio of microalgae to solvent can be halved in the extraction stage (Zhang and Liu, 2005). This scenario might represent the commercialization of new extraction processes, or catalysts.

**Table 9. Summary of input of material and energy for sensitivity analysis for a period of 1 year**

<b>STAGE/INPUTS</b>	<b>1/2 nutrient</b>	<b>Sparge CO<sub>2</sub></b>	<b>2X growth</b>	<b>2X density</b>	<b>1/2 solvent</b>	<b>high lipid</b>	<b>Base-line</b>	<b>UNITS</b>
<b>GROWTH STAGE</b>								
P-synthetic area per facility	0.8	0.8	0.8	0.8	0.8	0.8	0.8	ha·ha <sup>-1</sup>
Polyethylene bags	1.17	1.17	1.17	1.17	1.17	1.17	1.17	m <sup>3</sup> ·ha <sup>-1</sup>
Salt	134	134	134	134	134	134	134	g·(kg dry algae) <sup>-1</sup>
Nitrogen fertilizer	73	147	147	147	147	147	147	g·(kg dry algae) <sup>-1</sup>
Phosphorus fertilizer	10	20	20	20	20	20	20	g·(kg dry algae) <sup>-1</sup>
Diesel fuel use	580	580	580	580	580	580	10	L·ha <sup>-1</sup>
Electricity use	41,404	5,801	41,404	41,404	41,404	41,404	41,404	kWh·ha <sup>-1</sup>
Algae biomass yield	91,000	91,000	182,000	91,000	91,000	91,000	91,000	kg·ha <sup>-1</sup>
<b>DEWATER STAGE</b>								
Electricity use	30,788	30,788	61,564	15,398	30,788	30,788	30,788	kWh·ha <sup>-1</sup>
<b>EXTRACTION STAGE</b>								
Natural gas use	3,878	3,878	7,755	3,878	2,264	5,662	141,994	MJ·ha <sup>-1</sup>
Electricity use	12,706	12,706	25,412	11,817	12,171	13,232	12,706	kWh·ha <sup>-1</sup>
Extracted oil yield	43,009	43,009	86,018	43,009	43,009	68,815	43,009	L·ha <sup>-1</sup>
<b>CONVERSION STAGE</b>								
Natural Gas use (kg biodiesel) <sup>-1</sup>	2.1	2.1	2.1	2.1	2.1	2.1	2.1	MJ·
Electricity use (kg biodiesel) <sup>-1</sup>	0.03	0.03	0.03	0.03	0.03	0.03	0.03	kWh·
Methanol	0.1	0.1	0.1	0.1	0.1	0.1	0.1	kg·(kg biodiesel) <sup>-1</sup>
Sodium hydroxide	0.005	0.005	0.005	0.005	0.005	0.005	0.005	kg·(kg biodiesel) <sup>-1</sup>
Sodium methoxide	0.0125	0.0125	0.0125	0.0125	0.0125	0.0125	0.0125	kg·(kg biodiesel) <sup>-1</sup>
Hydrochloric acid	0.0071	0.0071	0.0071	0.0071	0.0071	0.0071	0.0071	kg·(kg biodiesel) <sup>-1</sup>
<b>TRANSPORTATION &amp; DISTRIBUTION</b>								
Diesel use	0.0094	0.0094	0.0094	0.0094	0.0094	0.0094	0.0094	L·(kg biodiesel) <sup>-1</sup>

The results of these sensitivity analyses are presented in Figure 10 and Figure 11 in order of NER reduction efficacy. It is notable that the proposed improvements in the microalgae lipid content, growth rates, and culture density are only marginally effective at reducing the energy consumption and GHG emissions of the microalgae-to-biofuels process. The scenarios most effective at reducing energy consumption and GHG emissions are the reduced nutrient and reduced sparge cases. These cases have the additive effect of reducing energy and material consumption. In general, these results show that some of the improvements to microalgae feedstocks that have been proposed are relatively ineffective at improving the NER and GHG emissions of the microalgae-to-biofuels process. For example, although improving the lipid content of microalgae has been suggested to reduce the cost of microalgae-based biofuels, it is less effective at improving sustainability metrics than other process improvements, such as optimization of the sparge system.

The sensitivity analysis presented illustrates the importance of a more detailed understanding of the growth system. Nutrients, mixing energy, and growth rate have the largest impact on the process based on environmental impact.

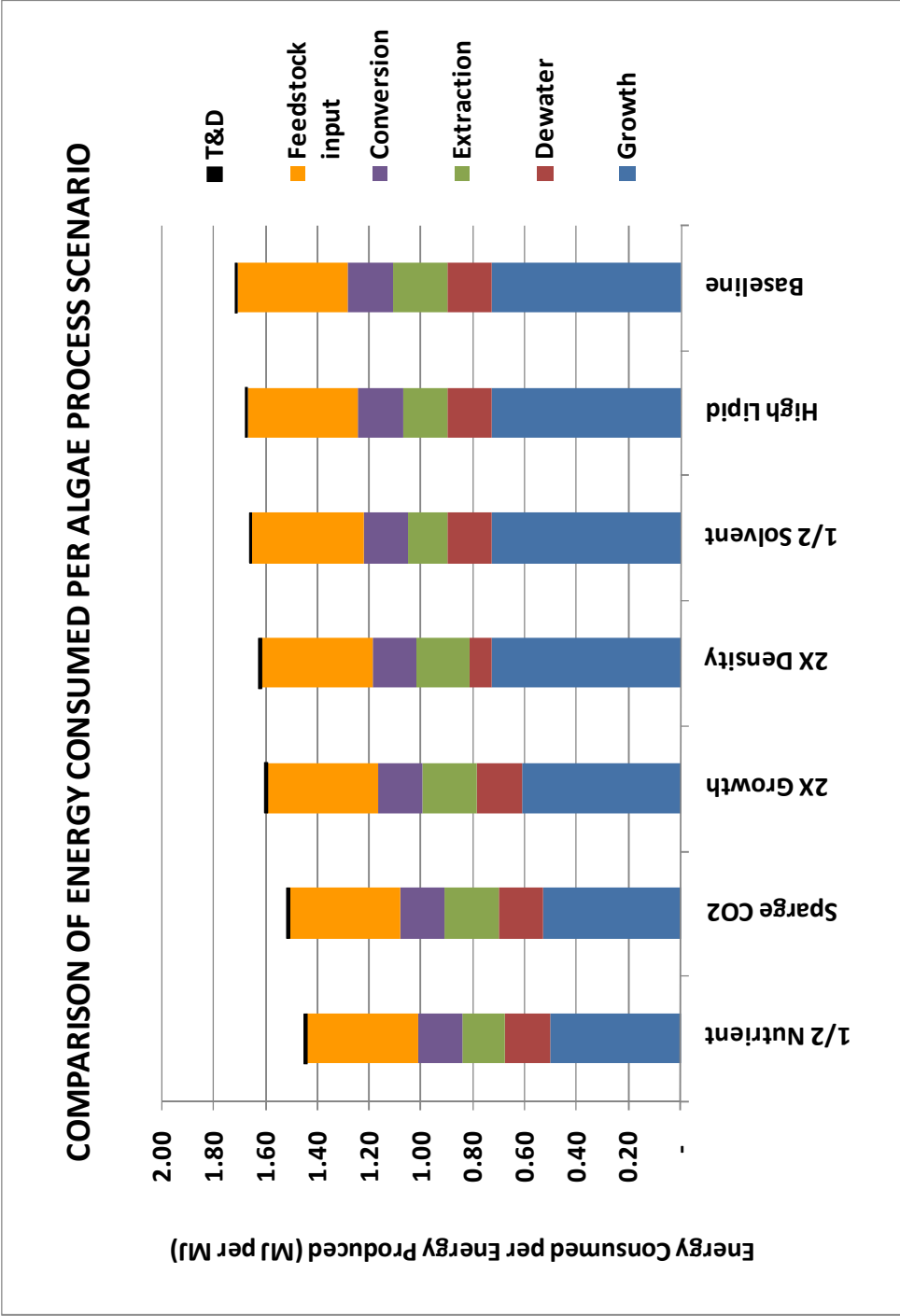
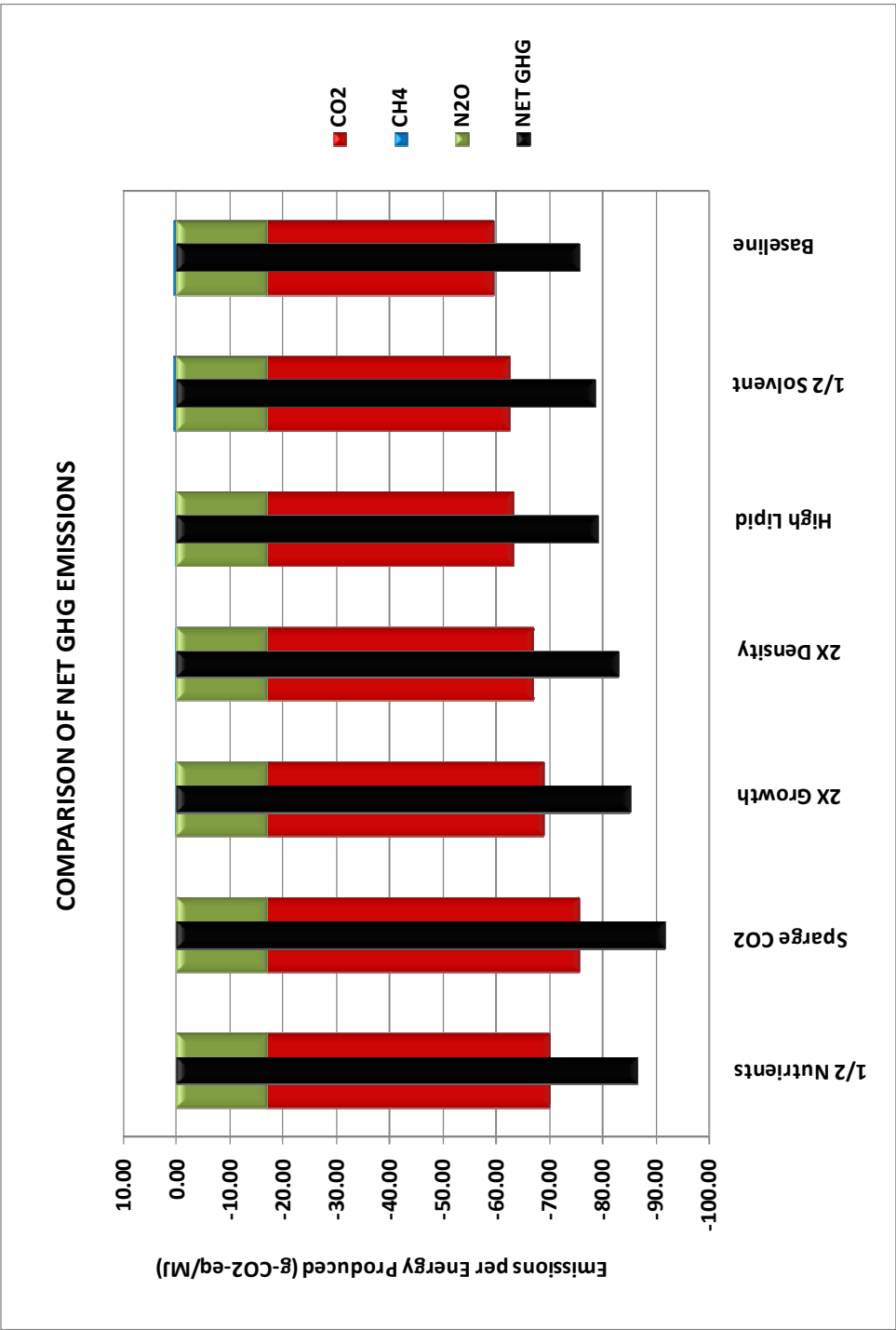


Figure 10. Cumulative Net Energy Ratio of the microalgae to biodiesel process as a function of feedstock processing parameters



**Figure 11. Net GHG emissions of the microalgae to biodiesel process as a function of feedstock processing parameters**

### 3.4. Conclusion

Biofuels derived from microalgae have the potential to replace petroleum fuel and first-generation biofuel, but the efficacy with which sustainability goals can be achieved is dependent on the lifecycle impacts of the microalgae-to-biofuel process. A detailed, industrial-scale engineering model for the species *Nannochloropsis* using a photobioreactor architecture has been constructed to accurately represent the biofuels process from growth to transportation and distribution of fuel. The purpose of the detailed engineering process model of the microalgae growth, harvest, and extraction phases is to describe the material inputs, material outputs, and types and amounts of energy consumed in the microalgae feedstock processing stages. The baseline model of microalgae to biodiesel process is based on a 315 hectares (776 acres) facility, which includes photosynthetically active and built areas. The temporal unit for evaluation of the process is 1 year. The model incorporates the recycling of growth media but does not recover nitrogen from extracted biomass. Additional material recycling will affect the results of the LCA, but a lack of data regarding the energy and material costs preclude its inclusion in this study. This process level model is integrated with a lifecycle energy and greenhouse gas emissions analysis compatible with the methods and boundaries of the Argonne National Laboratory GREET model, thereby ensuring comparability to preexisting fuel-cycle assessments. Results are used to evaluate the net energy ratio (NER) and net greenhouse gas emissions (GHGs) of microalgae biodiesel in comparison to petroleum diesel and soybean-based biodiesel with a boundary equivalent to “well-to-pump”. The resulting NER of the microalgae biodiesel process is

0.93 MJ of energy consumed per MJ of energy produced. In terms of net GHGs, microalgae-based biofuels avoids 75 g of CO<sub>2</sub>-equivalent emissions per MJ of energy produced. The scalability of the consumables and products of the proposed microalgae-to-biofuels processes are assessed in the context of 150 billion liters (40 billion gallons) of annual production.

## **Chapter 4-Microalgae Bulk Growth Model with Application to Industrial Scale Systems<sup>2</sup>**

### **4. Abstract**

The scalability of microalgae growth systems is a primary research topic in anticipation of the commercialization of microalgae-based biofuels. To date, there is little published data on the productivity of microalgae in growth systems that are scalable to commercially viable footprints. To inform the development of more detailed assessments of industrial-scale microalgae biofuel processes, this dissertation presents the construction and validation of a model of microalgae biomass and lipid accumulation in an outdoor, industrial-scale photobioreactor. The model incorporates a time-resolved simulation of microalgae growth and lipid accumulation based on solar irradiation, species specific characteristics, and photobioreactor geometry. The model is validated with 9 weeks of growth data from an industrially-scaled outdoor photobioreactor. Discussion focuses on the sensitivity of the model input parameters, a comparison of predicted microalgae productivity to the literature, and an analysis of the implications of this more detailed growth model on microalgae biofuels lifecycle assessment studies.

---

<sup>2</sup> The work presented in this chapter is based on the publication Quinn, J, Dewinter, L, Bradley, T, 2011. Microalgae bulk growth model with application to industrial scale systems Bioresour. Technol.

## 4.1. Introduction

Microalgae-based biofuels have several sustainability, economic, and environmental benefits over more conventional biofuels. When compared to first-generation biofuel feedstocks, microalgae are characterized by higher solar energy yield, year-round cultivation, the use of lower quality or brackish water, and the use of less- and lower-quality land. Microalgae feedstock cultivation can be coupled with combustion power plants or other CO<sub>2</sub> sources to sequester GHG emissions and it has the potential to utilize nutrients from wastewater treatment facilities (Batan et al., 2010; Schenk et al., 2008; Wijffels and Barbosa, 2010). These advantages have led to an increased interest in microalgae as a second generation feedstock for biofuels.

Analyses that have attempted to model the productivity, economics, and lifecycle environmental impacts of the latest generation of microalgae cultivation systems have relied on scale-up of laboratory data to model microalgae growth at industrial scale. Previous modeling efforts have undertaken the specific challenge of modeling growth and lipid accumulation in nutrient limited algal systems, however validation was done utilizing small-scale laboratory data (Mairet et al., 2011; Packer et al., 2010). The scaling of laboratory data has been justified due to the immaturity of the microalgae-to-biofuels process and lack of peer reviewed, published, scalable growth data. It is well-understood that these laboratory-scale processes do not accurately represent industrial-scale facilities (Chisti, 2007; Wijffels and Barbosa, 2010). To fully understand the productivity potential of microalgae-based biofuels, models must be constructed, and validated to predict the productivity of the microalgae in a realizable

configuration and at industrial scale while incorporating real locational characteristics (James and Boriah, 2010).

This study presents a literature-based bulk growth model incorporating the primary factors that affect microalgae growth and lipid accumulation. This article then describes the experimental methods including the Solix research and development microalgae growth facility located at Colorado State University, and presents a direct comparison and validation of the model using actual *Nannochloropsis oculata* growth data from outdoor Solix Generation 3 photobioreactors. The discussion focuses on a sensitivity analysis and some potential applications of the model. Specifically, the model results are applied to illustrate the sensitivity of scalability calculations and life-cycle assessment (LCA) studies to the increased fidelity available from this model of microalgae growth and lipid productivity.

## **4.2. Materials and Methods**

### **4.2.1 Modeling Equations Overview**

The following sections detail the governing equations and parameters of the microalgae bulk growth and lipid production model. The purpose of the model is to accurately represent microalgae growth and lipid accumulation of an outdoor photobioreactor. The primary factors that have been experimentally and theoretically shown to effect the productivity of microalgae are: light intensity, photosynthetic rate, respiration rate, temperature, nutrient availability, and lipid production (Richmond, 2004; Sheehan et al., 1998). The bulk model presented here takes into account all of

these factors. The model incorporates 7 sub-systems defined by 16 species-specific modeling parameters. The model requires inputs of light and reactor temperature, and has outputs of biomass growth and lipid accumulation for the reactor system modeled. The origins and application of the subsystems and species parameters are detailed.

The bulk model equations and microalgae characteristics are developed from literature, coded in MatLab<sup>®</sup>, and validated with growth data of *Nannochloropsis oculata* cultivated at Solix in outdoor photobioreactors.

#### ***4.2.1.1 Light distribution modeling***

In this model, a primary input is light which is represented as a volumetric average light intensity calculated based on light intensity at reactor surface. Mixing microalgae cultures has an effect on growth by increasing the frequency of light to dark cycling of the cells. In systems that operate at a relative low cell density, in short optical path reactors, at relatively low sparge rates, mixing dynamics will not dramatically affect the microalgae culture growth rates (Qiang and Richmond, 1996). This model therefore assumes that the culture is adapted to the average light intensity (Richmond, 2004). The alternative is to simultaneously model time-resolved microalgae growth kinetics, fluid dynamics, and light penetration, but the increase in computational cost and validation effort for this alternative is currently not justified.

At low densities within the reactor, the intensity of light will fall off exponentially according to the Lambert-Beer Law (Richmond, 2004):

$$\mathbf{E(L)} = \mathbf{E_0} \cdot \mathbf{e^{-\alpha \cdot q_{dw} \cdot L}} \quad (1)$$

At higher densities scattering can become an important consideration for determining local light intensities. This model uses an average light intensity and uses Lambert-Beer for a 1<sup>st</sup> order approximation to conservatively estimate the amount of light that passes completely through the reactor, which for the reactor system modeled would only occur at low cell densities where Lambert-Beer law is applicable. The average light intensity in the plate reactor modeled can then be calculated as:

$$E_{av} = E_0 \cdot \frac{1 - e^{-\alpha \cdot X_{dw} \cdot B}}{\alpha \cdot X_{dw} \cdot B} \quad (2)$$

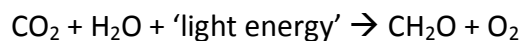
It is well accepted that light modeling in algal cultures increases in complexity with increasing densities due to the potential effects of light scattering from microalgae. A variety of modeling efforts have made different assumptions regarding the overall impact of scattering with a variety of models developed to accurately capture the penetration depth of light into dense cultures (Fernández et al., 1997; Gitelson et al., 1996; Janssen et al., 2003; Kim et al., 2002; Packer et al., 2010). The literature agrees that at ultra high densities Lambert-Beer assumptions are not valid; however there is no agreement on what constitutes ultra high density. Packer et al. (2010) use the same Lambert-Beer assumption used in this modeling effort to calculate average light intensities for a modeling effort validated with culture densities of greater than 7 g·L<sup>-1</sup>. Fernandez et al. (1997) did experimental hyperbolic model (absorption and scattering) validation of light penetration and compared the results with Lambert-Beer (absorption) and a model proposed by Cornet et al. (1992) (absorption and scattering). The results of this study illustrate that all three models capture the holistic trends with the proposed hyperbolic model more accurate (average coefficient of determination 0.998)

then Lambert-Beer (average coefficient of determination 0.981) but not dramatically more accurate than the model proposed by Cornet et al. (1992) (average coefficient of determination 0.998). The results also indicate that Lambert-Beer can accurately capture penetration depths for densities close to  $3 \text{ g}\cdot\text{L}^{-1}$  depending on the metabolic state of the microalgae.

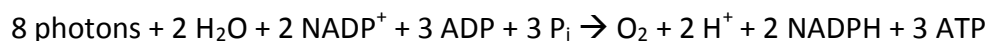
There currently lacks sufficient data for light penetration effects as a function of density for *Nannochloropsis oculata*. The majority of the articles surveyed integrate or directly use Lambert-Beer assumptions regarding light penetration. The modeling effort presented in this work uses Lambert-Beer to conservatively estimate the amount of light that directly passes through the reactor and to calculate an average light intensity as detailed in the main document.

#### ***4.2.1.2 Photosynthetic rate modeling***

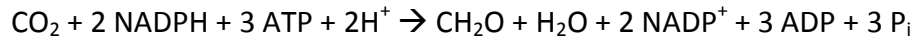
A chemical reaction analogy overview of the photosynthetic process is provided by



Photosynthesis occurs in the chloroplasts in two stages, typically referred to as light reactions and dark reactions. The light reactions can be further broken down according to:



for an idealized system. The ATP and NADPH produced by the light reactions are used to fix carbon via the action of the enzyme ribulose-biphosphate carboxylase (Rubisco) in the Calvin cycle, regenerating the substrates NADP, ADP and P<sub>i</sub>:



The combination of the later two chemical formulas forms the overall equation of photosynthesis. Thus the carbon specific rate of photosynthesis ( $P_c$ ) is dependent on the light intensity, light absorption, and the efficiency of using photons as illustrated by (3) (Geider and Osborne, 1992; Williams et al., 2002)

For this model, biomass growth is calculated based on an energy balance incorporating photosynthetic, respiration, and energy required for the uptake of nitrogen. Photosynthesis involves a series of reactions that start with light absorption, involve synthesis of NADPH and ATP as intermediate energy-conserving compounds, and lead to carbon fixation in the Calvin cycle. The carbon specific rate of this reaction ( $P_c$ ) is dependent on the light intensity, light absorption, and the efficiency of using photons (Geider and Osborne, 1992; Williams et al., 2002):

$$P_c = P_{c\_calc} \cdot \left( 1 - \exp \left[ \frac{-\alpha \cdot \phi_m \cdot E_{av}}{P_{c\_calc}} \right] \right) \quad (3)$$

$P_{c\_max}$  is affected by two efficiency factors (see 2.1.5 and 2.1.6 for definitions of  $\phi_T$  and  $\phi_{qN,Xint}$ ) Figure 12:

$$P_{c\_calc} = P_{c\_max} \cdot \phi_T \cdot \phi_{qN,Xint} \quad (4)$$

The final expression (3) balances energy flow with carbon fixation including, respiration losses, and energy loss requirements for nitrogen uptake when bioavailable nitrogen is present (more details on nitrogen effects are presented in 2.1.6)

#### ***4.2.1.3 Respiration rate modeling***

This model incorporates respiration losses from metabolic costs of biosynthesis and the costs of cell maintenance. Metabolic costs such as the reduction of nitrate to ammonium and incorporation of ammonium into biomass is incorporated as a function of the specific uptake rate of nitrogen and biosynthetic efficiency which is not incorporated into the respiration portion of the model (Geider et al., 1998).

Researchers in the past have shown that respiration rates during the night are the same as respiration rates during the day, indicating that maintenance respiration is neither stimulated nor inhibited by growth (Geider and Osborne, 1992). For this model maintenance respiration ( $rR_c$ ) is defined as a constant.

The respiration rates observed in the field are the combination of bacterial and microalgae respiration. This model assumes that contamination levels of bacteria are insignificant; however, as described below, the respiration of the culture modeled is based on growth data that would include the effects of respiration from bacteria, if present.

#### ***4.2.1.4 Growth rate modeling***

The model presented defines the carbon specific growth rate as a function of the photosynthetic rate, the respiration rate, and specific uptake rate of nitrogen:

$$\frac{1}{cC,X} \cdot \frac{dcC,X}{dt} = \mu = P_c - rR_c - \zeta \cdot rN \quad (5)$$

The dry weight (DW) of the biomass in the reactor ( $cX_{dw}$ ) can be calculated for each time step based on the assumption that the biomass is 50% carbon. The specific growth rate,  $\mu$ , is calculated at each time step and is assumed to be constant for the duration of the time step:

$$cX_{dw} = 2 \cdot cC, X_0 \cdot e^{\mu \cdot t} \quad (6)$$

#### ***4.2.1.5 Temperature rate dependence modeling***

In this model the temperature dependence of photosynthesis is described by the effect of temperature on ribulose-biphosphate carboxylase (Rubisco) activity. When considering a seasonal cycle, temperature is the environmental factor that consistently accounts for the largest part of the variance in growth (Geider and Osborne, 1992). This model assumes that temperature only affects the light-saturated photosynthesis rate, and not the initial slope of the photosynthesis-irradiance curve, Figure 12 (Geider et al., 1997). It is assumed that the reactor temperature affects the culture photosynthetic rate and respiration rate equally.

Photosynthetic light response is typically classified into three primary zones, 1) limiting photon flux density (PFD) where the photosynthetic rate increases linearly with increasing light intensity, 2) light saturation photosynthetic rate characterized by constant photosynthetic rate with increasing PFD, and 3) photo-inhibition characterized by a decrease in photosynthetic rate with increasing PFD (Henley, 1993; Macintyre et al., 2002; Richmond, 2000). The modeling effort here captures the first two regimes as illustrated by Figure 12.

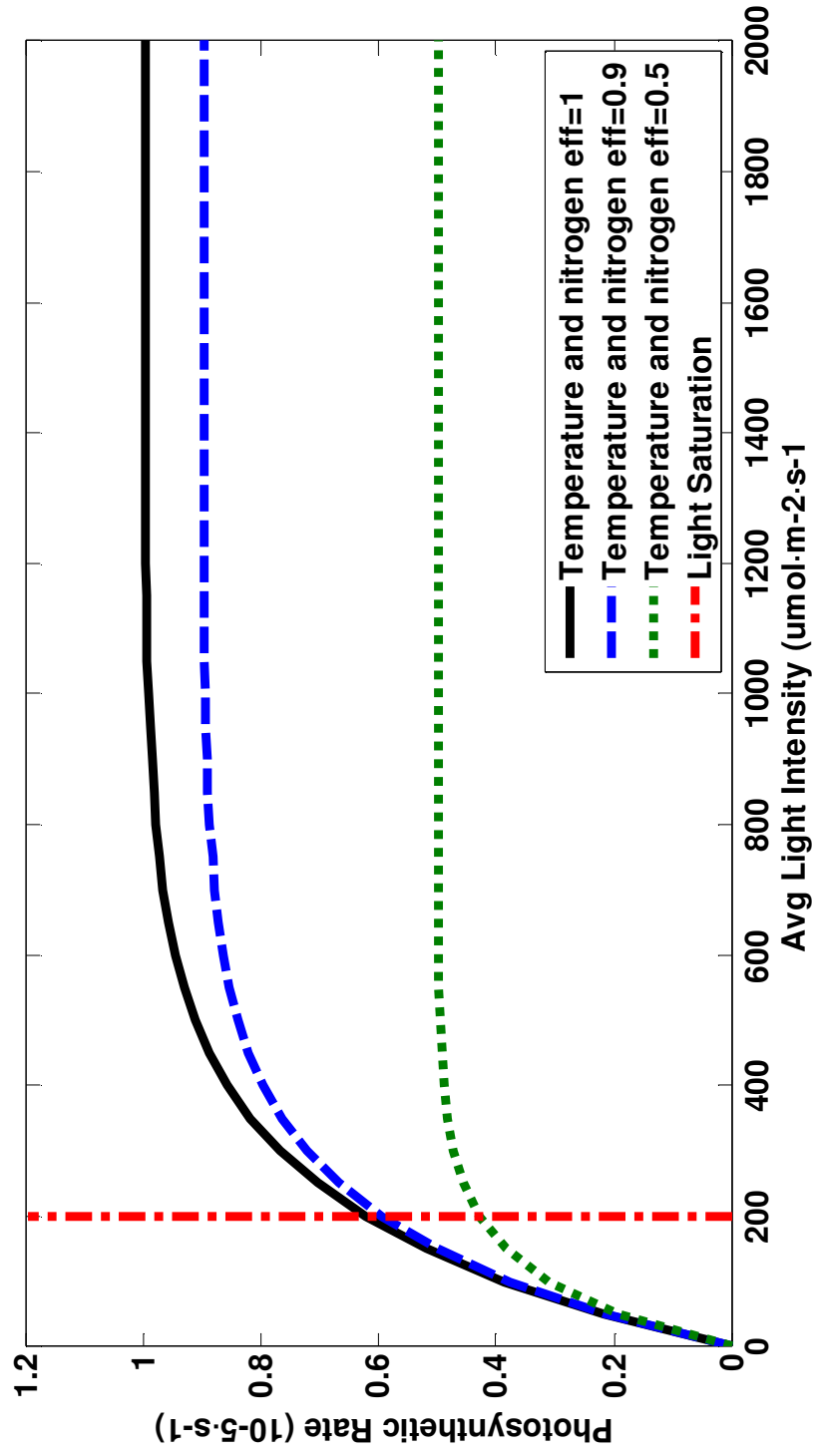


Figure 12. Graph of photosynthetic rate for three different temperature and nitrogen efficiencies. Photosaturation illustrated in red.

Figure 12 illustrates that the initial slope of the photosynthetic curve is not affected by the temperature or nitrogen efficiency, just the overall maximum photosynthetic rate is affected.

For this modeling effort photo-inhibition is not incorporated due to the nature of the system being modeled. Photo-inhibition typically occurs at high light intensities which are not achieved in the system modeled (Goldman, 1979; Henley, 1993).

The model presented by Alexandrov and Yamagata (2007) relating thermodynamic concepts, such as activation energy, to the typical bell shape of the enzyme activity temperature curve illustrated in (7) and (8) have been adapted to this model.

$$\varphi_T = \frac{2 \cdot f(T)}{(1 + f^2(T))} \quad (7)$$

$$f(T) = e^{\frac{Ea}{R \cdot T_{opt}} - \frac{Ea}{R \cdot T}} \quad (8)$$

The efficiency factor for temperature ( $\varphi_T$ ), is a dimensionless number between 0 and 1. At the optimum growth temperature  $\varphi_T = 1$ , and for temperatures higher or lower than the optimum temperature,  $0 < \varphi_T < 1$  according to (7).

#### ***4.2.1.6 Nitrogen dependence modeling***

For the model presented, it is assumed that microalgae growth is limited by nitrogen availability and not by phosphorus availability based on the relative required amounts from the Redfield ratio and the lipid accumulation modeling used in this study (Redfield, 1958). The model presented incorporates nitrogen dependence modeling to accurately capture the growth and lipid production. The components of the cellular

photosynthetic apparatus account for a large fraction of the total nitrogen in microalgae. Therefore, microalgae respond to a reduction in nitrogen availability by reducing the size of the photosynthetic apparatus. A linear dependence of maximum photosynthesis rates on nutrient-limited growth has been observed. Correlated with this reduction in maximum photosynthesis rate is a decrease in the proportion of cell nitrogen, which is associated with a decrease in Rubisco. In general, the light-limited photosynthesis rates are less affected by nutrient limitation than the light-saturated rates (Geider and Osborne, 1992). Geider et al. (1997) assumed in their model that nutrient-limitation affects growth rate only by imposing a limit on the light-saturated photosynthesis rate. Nutrient limitation will be modeled by multiplying maximum photosynthesis rate with an efficiency factor for nutrient-limitation ( $\phi_{qN,Xint}$ ) according to the Droop model (4).

The Droop model assumes that microalgal growth rate is dependent on intracellular nitrogen concentration (Lemesle and Maillet, 2008):

$$\mu = \mu_{max} \cdot \left[ 1 - \frac{qN,X_{min}}{qN,X} \right] \quad (9)$$

The cell quota ( $qN,X$ ) is defined as the mass of internal nitrogen per total mass of biomass. This quota can be experimentally measured and is time varying. The minimum cell quota ( $qN,X_{min}$ ) is the internal nitrogen level where cells cease to grow. The dimensionless efficiency factor for intercellular nitrogen will therefore be described by:

$$\phi_{qN,Xint} = 1 - \frac{qN,X_{min}}{qN,X} \quad (10)$$

The efficiency factor for the specific uptake rate of nitrogen considering external nitrogen concentration is treated as a Michaelis-Menten function (Geider et al., 1998; Legovic and Cruzado, 1997):

$$\varphi_{qN_{ext}} = \frac{cN_{medium}}{cN_{medium} + K_N} \quad (11)$$

When the extracellular concentration of nitrogen is low or the intercellular concentration of nitrogen is high, specific uptake rate is low.

When nitrogen is present in the medium in the form of nitrate, uptake is an energy-linked process and happens mostly during daylight (Richmond, 2004). The maximum specific uptake rate of nitrogen is a function of maximum photosynthetic rate. The calculated specific uptake rate of nitrogen ( $rN_{calc}$ ) is calculated by multiplying the maximum specific uptake rate of nitrogen with three efficiency factors: intracellular concentration of nitrogen efficiency (10), extracellular concentration of nitrogen efficiency (11), and temperature efficiency (7) (Geider et al., 1998):

$$rN_{calc} = rN_{max} \cdot \varphi_{qN,X_{int}} \cdot \varphi_{qN_{ext}} \cdot \varphi_T \quad (12)$$

The specific uptake rate of nitrogen can now be defined by (13).

Integration of (13) yields the total nitrogen in the biomass, (14).

$$\frac{1}{qN,X} \cdot \frac{dqN,X}{dt} = rN = \frac{rN_{calc}}{qN,X} - rR_N \quad (13)$$

$$qN,X = qN,X_0 \cdot e^{rN \cdot t} \quad (14)$$

The total remaining nitrogen in the growth media can now be calculated through mass balance.

#### ***4.2.1.7 Lipid accumulation modeling***

The model incorporates a lipid accumulation model that has been developed to predict the lipid production of the microalgae based on a mass balance due to the effects of nitrogen. Once nitrogen is depleted, microalgae metabolism switches from protein synthesis to lipid or carbohydrate synthesis causing a change in the biomass composition (Richmond, 2004). Suen et al. (1987) reported lipid concentrations of 55% under nitrogen limited growth of *Nannochloropsis sp.* Hu and Gao (2006) found that lipid content upon nitrogen depletion increased from 9 to 62% of dry weight, while protein content decreased from 59% to 23% of dry weight in *Nannochloropsis sp.* grown under low nitrogen concentration with carbohydrate content only increased by 10% upon nitrogen depletion. These results suggest that in *Nannochloropsis sp.* metabolism almost entirely shifts from protein synthesis to lipid synthesis.

The model presented is a mass balance model based on the carbohydrate, protein, and lipid content of the cell. The protein content of the cell is calculated based on the internal nitrogen content of the cell,  $P = q \cdot 4.78$ .

The conversion factor of 4.78 was obtained from Diagnostic Center for Population and Animal Health Michigan State University (Diagnostic Center for Population and Animal Health Michigan State University, 2008).

For this model it is assumed that the microalgae metabolism is primarily protein synthesis to lipid and the protein molar percentage, the carbohydrate molar percentage, and the lipid molar percentage in the biomass stays constant:

$$Biomass = Lipid + CHO + PRO \quad (15)$$

It is assumed that the overall carbohydrate percentage of the cell remains constant at 40% based on previous cell characterization. A plot of the carbohydrate, protein, and lipid percentages in the cell for two weeks of ideal radiation as predicted by the REST2 model are presented in Figure 13.

As illustrated in Figure 13 the composition of the cell drastically changes throughout the growth of the culture from 1 to 3 g·L<sup>-1</sup>. The culture is turned at 3 g·L<sup>-1</sup> after just over 5 days of growth and nutrients are added thus causing a change in the intercellular composition.

It should be noted that other environmental factors, like salinity and temperature, can also have an influence on lipid production (Richmond, 2004). Although (13) represents a 1<sup>st</sup> order relationship between lipid content and nitrogen content, validation data (presented in 4.3.3) illustrates its effectiveness.

#### **4.2.2 Model Parameters Summary**

**The following section presents an overview of the inputs to the model with the specific assumptions explained. The model is based off of the cultivation of *Nannochloropsis oculata* grown in an outdoor Solix photobioreactor. Model inputs and parameters are summarized in Table 10 with ideal model outputs shown in**

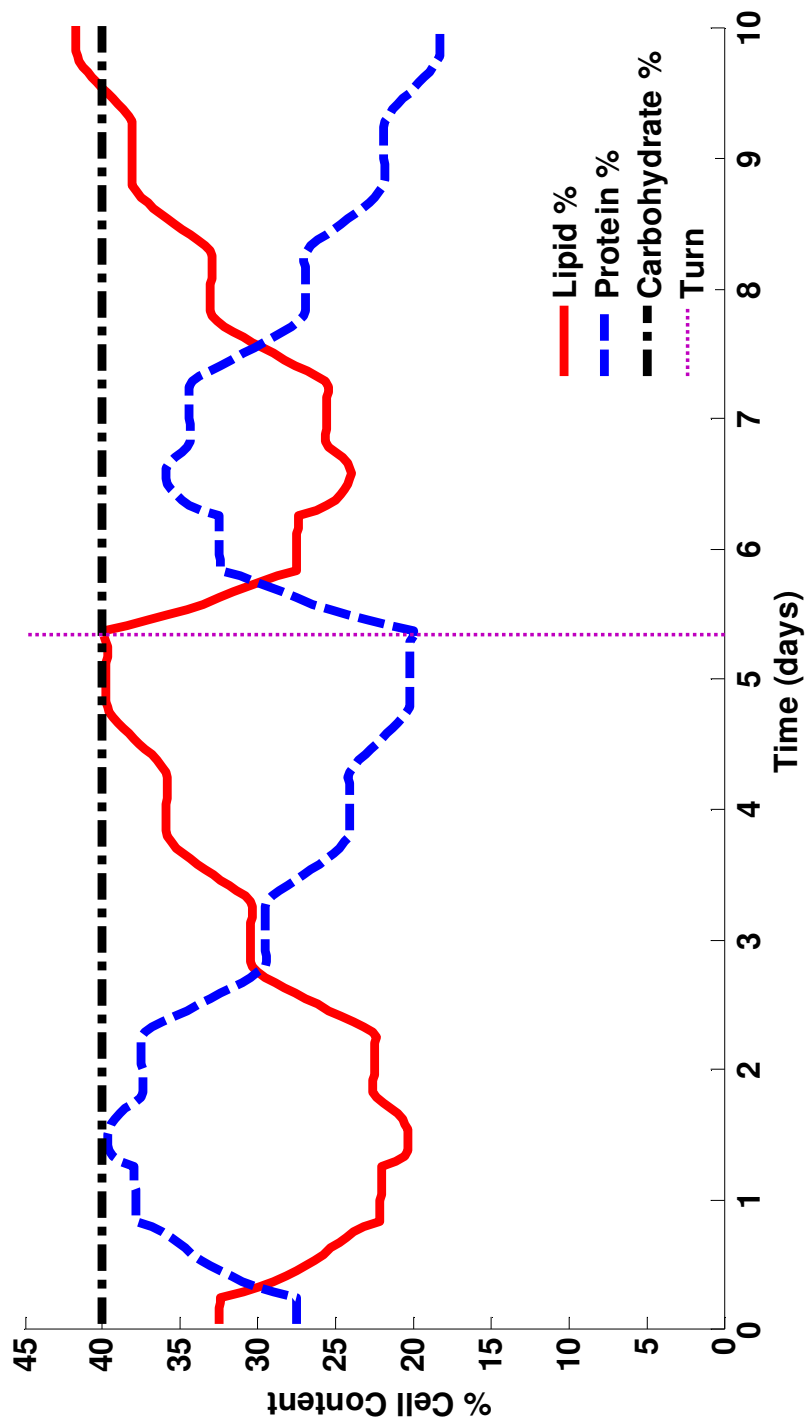


Figure 13. Plot of cell composition for ideal light conditions in June at a location of Fort Collins, Colorado

**Table 10. Summary of model parameters**

Parameter	Abbreviation	Value	Unit
Light saturation level	$E_k$	200	$\mu\text{mol}\cdot\text{m}^{-2}\cdot\text{s}^{-1}$
Absorption coefficient	$\alpha$	0.0752	$\text{m}^2\cdot\text{g}^{-1}$
Maximum growth rate	$\mu_{\text{max}}$	$2.5\cdot 10^{-2}$	$\text{h}^{-1}$
Maintenance respiration rate	$rR_c$	$4.32\cdot 10^{-4}$	$\text{h}^{-1}$
Biosynthetic efficiency	$\zeta$	4	$\text{g}\cdot\text{g}^{-1}$
Optimum Temperature	$T_{\text{opt}}$	23	$^{\circ}\text{C}$
Activation energy	$E_a$	63	$\text{kJ}\cdot\text{mol}^{-1}$
Maximum cell quota of nitrogen	$qN, X_{\text{max}}$	0.150	$\text{g}\cdot\text{g}^{-1}$
Minimum cell quota of nitrogen	$qN, X_{\text{min}}$	0.010	$\text{g}\cdot\text{g}^{-1}$
Cell quota of nitrogen of inocula	$qN, X_0$	0.060	$\text{g}\cdot\text{g}^{-1}$
Half saturation constant for nitrogen uptake	$K_N$	0.005	$\text{g}\cdot\text{L}^{-1}$
Maximum specific uptake rate of nitrogen	$rN_{\text{max}}$	$1.5\cdot 10^{-6}$	$\text{g}\cdot\text{g}^{-1}\cdot\text{h}^{-1}$
Maximum photosynthetic rate	$P_{c,\text{max}}$	$3.6\cdot 10^{-2}$	$\text{h}^{-1}$
Photon efficiency	$\phi_m$	$6.5\cdot 10^{-7}$	$\text{g}\cdot(\mu\text{mol photons})^{-1}$
Nitrogen respiration rate	$rR_N$	0	$\text{h}^{-1}$

#### **4.2.2.1 Light saturation level**

Researchers have shown that the light saturation of green microalgae typically occurs at 10% of full sunlight. Fabregaz et al. (2004) grew *Nannochloropsis sp.* under diverse light intensities in a 12 hour light, 12 hour dark cycle determining a light saturation level of  $220 \mu\text{mol m}^{-2} \text{s}^{-1}$ . Gentile and Blanch (2001) determined a light saturation of  $180 \mu\text{mol}\cdot\text{m}^{-2}\cdot\text{s}^{-1}$  for *Nannochloropsis gaditana*. Lower values of the light saturation ( $74 \mu\text{mol}\cdot\text{m}^{-2}\cdot\text{s}^{-1}$ ) have been reported, however those cultures were cultivated under constant light conditions (Fang et al., 2004). Considering the mixing level, density operated, diurnal light characteristics, along with the most relevant experimental data, a light saturation of  $200 \mu\text{mol}\cdot\text{m}^{-2}\cdot\text{s}^{-1}$  is assumed. It is important to note that the nutrient levels can affect the light saturation value because nutrient depletion reduces the chlorophyll content of the microalgae. This effect is accounted for in this model through the efficiency factors associated with nitrogen uptake (Flynn et al., 1993).

#### **4.2.2.2 Absorption coefficient**

The absorption coefficient was determined experimentally for *Nannochloropsis*,  $0.0752 \text{ m}^2\cdot\text{g}^{-1}$  (Gentile and Blanch, 2001). The absorption coefficient of microalgae will vary over the course of a batch; however the variance is not significant in this application.

#### **4.2.2.3 Maximum growth rate**

The maximum cell-specific growth rate represents the highest growth rate attainable in the exponential growth phase. The maximum cell-specific growth rate

under nutrient rich conditions for this modeling effort is  $2.5 \cdot 10^{-2} \text{ h}^{-1}$  (Flynn et al., 1993; Gentile and Blanch, 2001).

#### ***4.2.2.4 Maintenance respiration rate***

A linear relationship between the maximum photosynthetic rate and the maximum growth rate has been observed (Geider and Osborne, 1992). This observation coupled with (4) shows that the respiration rate and the maintenance respiration rate can be defined as a percentage of the maximum photosynthetic rate. For this model, a respiration rate of 2% is selected to match experimental data.

#### ***4.2.2.5 Biosynthetic efficiency***

Energy is required for the reduction of nitrate to ammonium, incorporation of ammonium into amino acids, and polymerization of amino acids into proteins. This energy is accounted for through biosynthesis efficiency,  $\zeta$ , set at 4 g biomass per g nitrogen assimilated (Geider et al., 1998). Details on the maximum and minimum nitrogen to carbon ratios are presented in 2.2.8 and 2.2.9.

#### ***4.2.2.6 Optimum temperature***

A literature review indicates the optimum temperature of *Nannochloropsis oculata* is between 21 and 24 °C (Spolaore et al., 2006). For this modeling effort an optimum temperature of 23 °C is selected.

#### ***4.2.2.7 Activation energy***

The activation energy for this model is based on the energy required for activity of the Rubisco enzyme. Light-saturated photosynthesis and the carboxylase activity of

Rubisco are characterized by an activation energy of 54-72 kJ·mol<sup>-1</sup> (Geider and Osborne, 1992). A value of 63 kJ·mol<sup>-1</sup> has been selected for this model.

#### ***4.2.2.8 Maximum cell quota of nitrogen***

The maximum cell quota of nitrogen is the maximum amount of nitrogen that can be contained in the cell. Analysis of the biomass produced in the Solix photobioreactor yields a maximum cell quota of 0.15 g nitrogen per g biomass and selected for this modeling effort. For comparison, Hu and Gao (2003) determined that the protein content of *Nannochloropsis sp.* ranges between 34-41%. This converts to a maximum cell quota of 0.07-0.09 g nitrogen per g biomass. Flynn et al. (1993) found a lower maximum cell quota of 0.2 g nitrogen per g biomass.

#### ***4.2.2.9 Minimum cell quota of nitrogen***

Flynn et al. (1993) found a maximum carbon-nitrogen ratio of 28, corresponding to a cell quota of 0.036 g nitrogen per g biomass. Ambrose (2006) uses a smaller number, 0.0072 g nitrogen per g biomass, therefore, for this study the minimum cell quota is assumed to be between the two literature values, 0.010 g nitrogen per g biomass.

#### ***4.2.2.10 Cell quota of nitrogen in inocula***

Inocula are obtained from a sample of a mature, harvested culture. An analysis of the biomass composition of harvested microalgae showed a protein content of 29%. Using a nitrogen-to-protein conversion factor of 4.78, the nitrogen content for inocula is set at 0.060 g nitrogen per g biomass.

Biomass cultivated in the growth system detailed was analyzed for content by Diagnostic Center for Population and Animal Health at Michigan State University (MSU) and Dairyland Laboratories Inc, Table 11 (Dairyland Laboratories Inc., 2008; Diagnostic Center for Population and Animal Health Michigan State University, 2008). Results from this analysis were used in determining some model parameters.

Table 11 is supported by the research of Reboloso-Fuentes (2001), in which an average protein content of 28.8% was found for *Nannochloropsis* sp. (Reboloso-Fuentes et al., 2001). A conversion factor applied to the amount of protein in the cell to determine nitrogen content has been proposed in literature and used for conversion, 4.78 (Lourenco et al., 2004). These results are utilized in characterizing the nitrogen content in the biomass at inoculation.

#### ***4.2.2.11 Half Saturation constant for nitrogen uptake***

The half saturation constant for nitrogen uptake determines the rate at which the specific uptake rate of nitrogen declines when nitrogen concentration in the medium decreases. A value of  $0.005 \text{ g}\cdot\text{L}^{-1}$  will be assumed for this model (Ambrose, 2006).

#### ***4.2.2.12 Maximum specific uptake rate of nitrogen***

The maximum specific uptake rate of nitrogen is a function of the maximum photosynthetic rate with units of g nitrogen per g biomass per hour:

$$rN_{max} = P_{cmax} \cdot qN, X_{max} \quad (16)$$

From (16) the maximum specific uptake rate of nitrogen is  $1.5 \cdot 10^{-6} \text{ g}\cdot\text{g}^{-1}\cdot\text{h}^{-1}$ .

**Table 11. Summary of analysis of *Nannochloropsis oculata* cultivated Solix photobioreactor analyzed by MSU and Dairyland. Data used with published literature data for model input parameters.**

<i>Nannochloropsis oculata</i> Composition		
	MSU	Dairyland
% Moisture	36.5	39.32
% Dry Matter	63.5	60.68
% Crude Protein	18.42	17.41
% Lignin	0.95	0.01
% Crude Fat	8.26	0.6
% Ash	4.98	5.08
% Calcium	0.14	0.14
% Phosphorus	0.46	0.39
% Magnesium	0.25	0.23
% Potassium	0.71	0.66
% Sodium	0.89	0.74
% Sulfur	0.33	0.34
ppm Copper	11	16
ppm Iron	100	168
ppm Zinc	105	144
ppm Manganese	12	18

#### **4.2.2.13 Maximum photosynthetic rate**

The maximum specific carbon photosynthetic rate is linked to the maximum growth rate and can be calculated by combining (5), (12), and (16):

$$P_{c\_max} = \frac{\mu_{max} + R_c}{1 - \zeta \cdot q N_{X_{max}}} \quad (17)$$

Based on these relations,  $P_{c\_max}$  is calculated as  $3.6 \cdot 10^{-2} \text{ h}^{-1}$ .

#### **4.2.2.14 Photon efficiency**

The photon efficiency in this model is a set value, because the maximum photosynthetic rate, the absorption coefficient, and the saturation parameter are set and the following identity is assumed valid:

$$E_k = \frac{P_{cmax}}{\alpha \cdot \phi_m} \quad (18)$$

The bulk growth model, as illustrated by (18), assumes a minimum quantum requirement of approximately 46 photons, equal to a photon efficiency of 0.0217 or  $6.5 \cdot 10^{-7} \text{ g CH}_2\text{O} \cdot (\mu\text{mol photons})^{-1}$ . According to the Z-scheme of photosynthesis,  $E_k$  is 0.125 (8 mol of photons needed for production of one mole of  $\text{CH}_2\text{O}$ ), representing an idealized number of photons, which is not attainable in non-idealized systems. To model realistic systems, there are other metabolic processes that must be considered, including photorespiration and losses (Geider and Osborne, 1992). These two effects significantly lower the photon efficiency below its theoretical limit. Energy required for nitrogen absorption is incorporated into the biosynthetic efficiency term not the photon efficiency term.

### **4.2.3 Experimental Materials and Methods**

The model presented above was validated using weather and outdoor growth data from the Solix research and development facility located at Colorado State University. The following section details the cultivation system, operation, and monitoring for data collected and used in model validation.

#### ***4.2.3.1 Organism, culture media, and inoculation***

The culture *Nannochloropsis oculata* obtained from the Provasoli-Guillard National Center for Culture of Marine Phytoplankton was cultivated in batch mode starting at  $1 \text{ g}\cdot\text{L}^{-1}$  in modified f/2-20  $\text{g}\cdot\text{L}^{-1}$  media ( $0.425 \text{ g}\cdot\text{L}^{-1}$  sodium nitrate,  $0.005 \text{ g}\cdot\text{L}^{-1}$  potassium phosphate,  $1 \text{ mL}\cdot\text{L}^{-1}$  Guillard trace metals). The microalgae was initially cultivated in flasks under 24 hour low light ( $200 \mu\text{mole}\cdot\text{m}^{-2}\cdot\text{s}^{-1}$ ) until  $160 \text{ g}$  were obtained to populate one large outdoor photobioreactors at  $1 \text{ g}\cdot\text{L}^{-1}$ . All media are prepared and pushed through a 0.2 micron absolute filter into a tank with the required inocula where it is mixed to ensure homogeneity prior to inoculation.

#### ***4.2.3.2 Outdoor culture system***

The reactor system modelled for this effort is based on the Solix Generation 3 photobioreactor. The thickness of an individual reactor is 0.05 m with reactors spaced at approximately 0.15 meters. The growth system comprises 16 reactors constructed out of 0.12 mm polyethylene and structurally supported in a thermal basin. Mixing is provided through sparge air that is operated continuously at 2.5 litres per minute of sparge per litre of culture (VVM).  $\text{CO}_2$  is supplied into the sparge air and delivered to

the system with a duty cycle determined by pH feedback control (pH maintained at 7.3 +/- 0.1). The reactors are operated in repeated batch mode, growing from the inoculation density of  $1 \text{ g}\cdot\text{L}^{-1}$  to a harvest density of  $3 \text{ g}\cdot\text{L}^{-1}$ . Part of the mature culture is harvested and then fresh filtered nutrient media are added such that the reactors are re-inoculated at  $1 \text{ g}\cdot\text{L}^{-1}$ .

Model validation was done utilizing data from Solix photobioreactors. A schematic of the overall geometry is presented in Figure 14. The Solix reactor test bed is located in Fort Collins, Colorado adjacent to the Engines and Energy Conversion laboratory at Colorado State University. The basin measures 3 meters by 18 meters and has sixteen reactors with dimensions detailed in Figure 14. The outer most reactors receive more light and grow at a slightly elevated rate and were not included in the data set used for validation. The system was operated in two groups of 8 reactors. Growth was monitored continuously in one of the eight reactors as previously detailed with manual samples taken from all reactors to verify uniform growth.

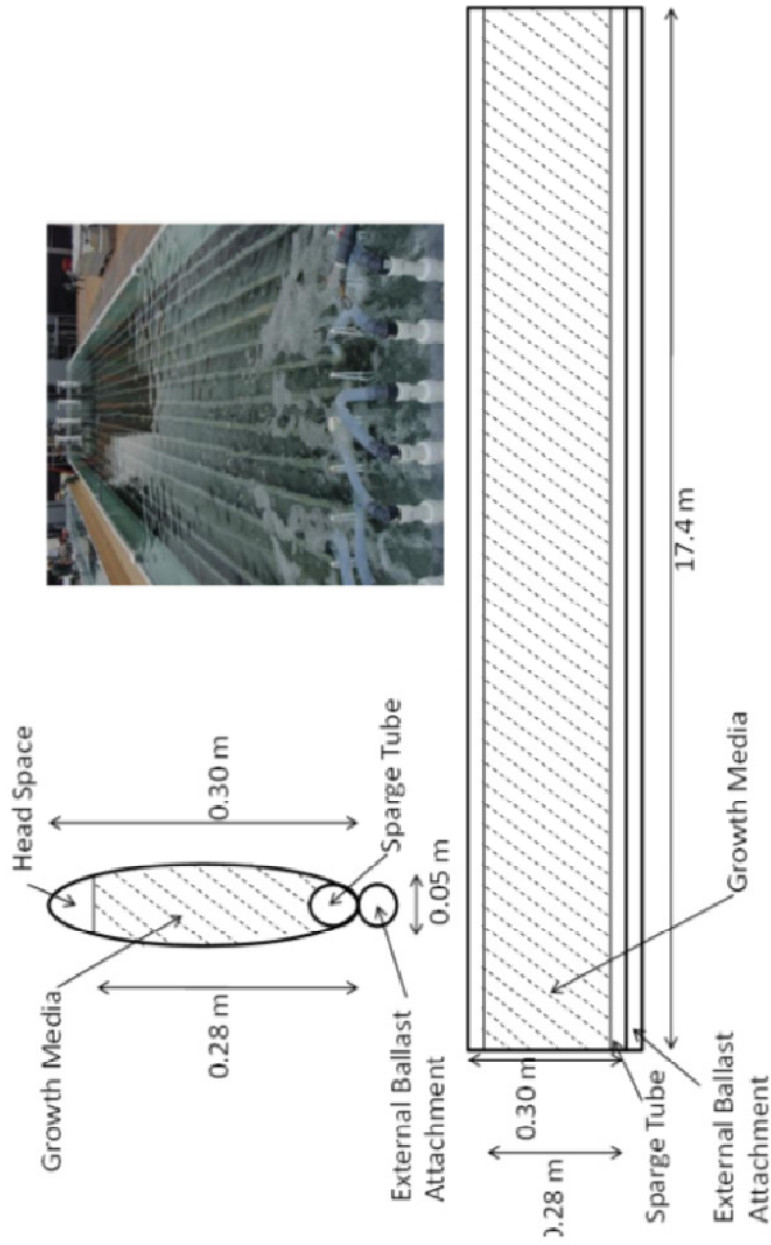


**Figure 14. Diagram and Photograph of the generation 3 Solix photobioreactor used to validate bulk growth model. Reactors are evenly spaced in a structural/thermal water basin in Fort Collins, Colorado, USA.**

Reactors were harvested as a group. All of the culture was removed from the reactors, mixed for homogeneity and the required inocula were removed. The remainder of the culture was harvested by centrifugation. New nutrient rich media was prepared, filtered, and added to the inocula. It is noted that media recycling (centrate from the centrifuge) could be done but was not standard practice. The required culture volume was then re-injected into the reactors to complete the inoculation process.

The temperature of the culture is maintained by the thermal mass of water basin which also supplies the structural support for the reactors. The temperature was continuously monitored and maintained between 19 and 26 °C via a Marley evaporative cooling system with a capacity at the location of 270,000 BTU or Jandy Lite2 pool heater with a capacity of 325,000 BTU.

#### ***4.2.3.3 Growth monitoring***

Two independent techniques were used for monitoring the growth of the culture. Optical density was monitored continuously using an Optech model ASD19-N absorption probe connected to a Fermenter Control Hardware A1. Data were logged on a minute time scale and converted to dry mass using a calibration factor. The sensor was monitored for bio-fouling and periodically cleaned.

Manual samples of the culture were taken daily to monitor growth, nutrient content, and salinity. Samples were drawn using a 10 ml syringe through sample lines attached to sample ports at the head of the reactors. Samples were then prepared for an optical density reading using the following technique: 980 µL of 0.2 micron filtered 20 g·L<sup>-1</sup> salt water was pipetted into 1.5 ml 10mm optical path length cuvette. Depending

on the dilution required, 20-40  $\mu\text{L}$  of sample was added to the cuvette and mixed using a 1000  $\mu\text{L}$  pipette. Samples were diluted such that the measured optical density was in a range of 0.1 to 0.3 such that a previously determined conversion of optical density to dry mass could be applied. Manual optical density measurements at 750 nm were performed on a Hach DR5000 spectrophotometer. Previous sampling experimentation showed that sampling location does not affect experimental results due to the homogeneity of the culture.

#### ***4.2.3.4 Lipid assay***

Lipid fractions were determined using an in-situ transesterification. The following procedure was performed based on the methods of Gonzalez et al. (1998): 5 mg of microalgae sample was spun down at 4000 relative centrifugal force (RCF) for 5 minutes followed by the removal of the supernatant. An auto-pipette was used to dispense 2.5 mL of 0.2 N KOH in methanol onto the 5 mg microalgae pellet. Samples were pipette mixed and transferred to a glass test tube previously washed in 1% HCl acid. An additional 2.5 mL of 0.2 N KOH in methanol was added and pipette mixed. Samples were then aggressively mixed using a VWR Analog Vortex Mixer on a speed setting of 10 (scale of 1 to 10) for 20 seconds followed by heating to 37  $^{\circ}\text{C}$  for 30 minutes. 1 mL of acetic acid and 2 mL of HPLC grade heptane were then added and the samples were aggressively mixed by using a VWR Analog Vortex Mixer on a speed setting of 10 (scale of 1 to 10) for 20 seconds and then centrifuged at 2000 RCF for 5 min. The organic layer was then removed and processed in a gas chromatograph (GC) to determine lipid content and composition.

Tranzesterified samples were prepared for GC analysis by first diluting the sample 1:10 with heptane. An internal standard (23:0) obtained from NU-CHEK PREP, Inc is added to the sample and the head space is then filled with nitrogen. Samples were analyzed with an Agilent Technologies 7890A GC machine utilizing a 30m x 0.32mm x 0.25um Restek FAMEWAX column. A spit-less injection is used requiring 1  $\mu\text{L}$  of sample. Helium at 1.5  $\text{mL}\cdot\text{min}^{-1}$  is used as the carrier gas. The oven is operated at 90  $^{\circ}\text{C}$  for 0.5 minutes and then ramped to 208  $^{\circ}\text{C}$  at 70  $^{\circ}\text{C}\cdot\text{min}^{-1}$ , then ramped to 230  $^{\circ}\text{C}$  at 3  $^{\circ}\text{C}\cdot\text{min}^{-1}$ , and finally to 240  $^{\circ}\text{C}$  ramped at 2  $^{\circ}\text{C}\cdot\text{min}^{-1}$  and held for 1 minute. Prior to running samples a bank is run followed by the generation of a 4 pt standard curve using a GLC-461 standard obtained from NU-CHEK PREP, Inc

## **4.3. Results and Discussion**

### ***4.3.1 Sample Growth Results***

The model is used to simulate microalgae growth for the ideal summer (June-solid blue line) and ideal winter (January-dashed black line) conditions based on cloud free, clear-sky solar irradiance for Fort Collins, Colorado based on the REST2 solar model,

(Gueymard, 2008).

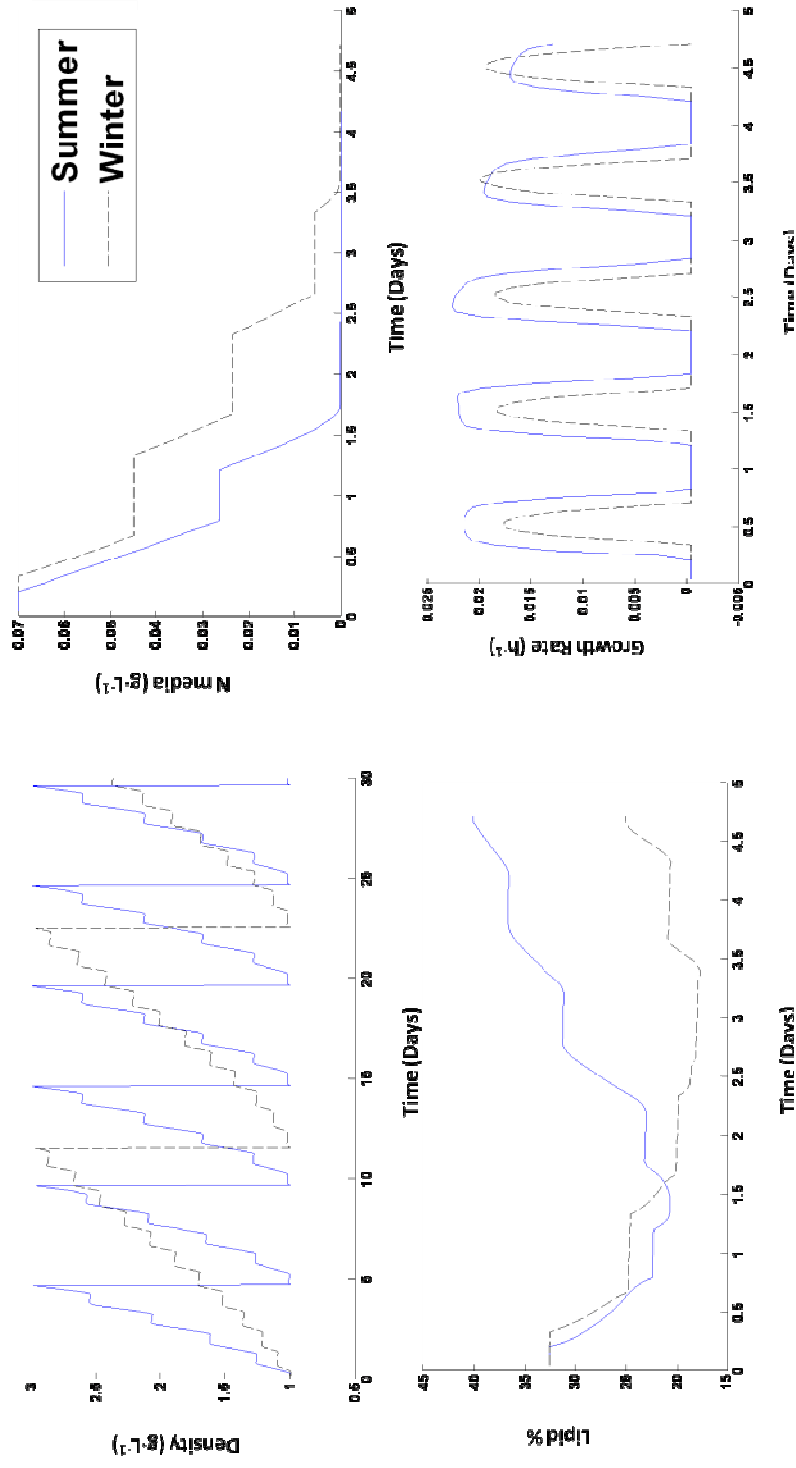


Figure 15. Solid blue line represents results from summer-time simulation and dashed black line represents winter-time simulation. All simulations assumed ideal basin temperatures and clear sky ideal light conditions based on a geographical location of Fort Collins, Colorado using the Rest2 solar model. Top Left: Model prediction of overall culture density with harvesting at 3 g-L-1 over a 30 day period. Top Right: Model results for bio-available nitrogen in media over a 5 day growth period. Bottom Left: Model results for lipid accumulation over a 5 day growth period. Bottom Right: Model results for growth rate for a 5 day growth period.

There are several notable characteristics in

. The culture is cultivated from 1 to 3 g·L<sup>-1</sup> for both summer-time and winter-time simulations. Nitrogen uptake is a direct function of light, thus in the winter the uptake of the bioavailable nitrogen from the media takes significantly longer. The overall growth in the winter is significantly lower than summer due to lower light intensity and shorter days. The specific growth rate during the dark period is negative due to respiration effects for both cases. The results presented in

are typical of the function of growth observed at the Solix research and development facility.

### ***4.3.2 Growth Model Validation***

Validation of the bulk growth model was performed by quantitatively and qualitatively comparing modeled results with real world growth results. Validation of the model is based on the American Institute of Aeronautics and Astronautics definition of model validation with the intended use of the model presented is to accurately capture the bulk growth and lipid production of an outdoor scalable photobioreactor system (Aiaa, 1998).

The model was validated using data collected at Solix Biofuels in the Summer and Fall of 2008. Two panels (A&B) were monitored during peak summer-time (high-light data); panel A for approximately three weeks followed by panel B for an additional three. The reactors were continuously monitored using insitu sensors and sampled every day manually as detailed in the main document. The primary inputs to the model are PAR and basin temperature measured at the Solix facility. The PAR was measured using a Spectrum Technologies, Inc. Quantum Light Sensor and the temperature was measured using a standard thermocouple (Spectrum Technologies Inc, 2003). All data was collected and logged using National Instruments Compact Field Point data acquisition system. An example of typical raw PAR and temperature data can be found in Figure 16.

As illustrated in Figure 16, the validation data was for a variety of real weather conditions. The first two days of summertime data presented were relatively clear free days while the next three days had afternoon partly cloudy skies decreasing the

intensity of the light. The thermal basin was maintained in such a way to keep temperature within the accepted growth range of 19-26 °C.

Winter-time (low-light data) was also collected for approximately three weeks in November and December to complete the data set. Reactor configuration, light, and temperature data from the location of the outdoor photobioreactor installation was used as primary inputs to the model with 1 week of summer-time (high-light data) and 1 week of winter-time (low-light data) model productivity results plotted against real time growth data and manual OD 750 samples, Figure 17.

As shown in Figure 17, the model qualitatively captures the growth trends from day to day including respiration during the dark period. A more quantitative comparison of the modeled growth versus actual growth on a minute time scale is presented in Figure 18 for summer-time (high-light data) and winter-time (low-light data).

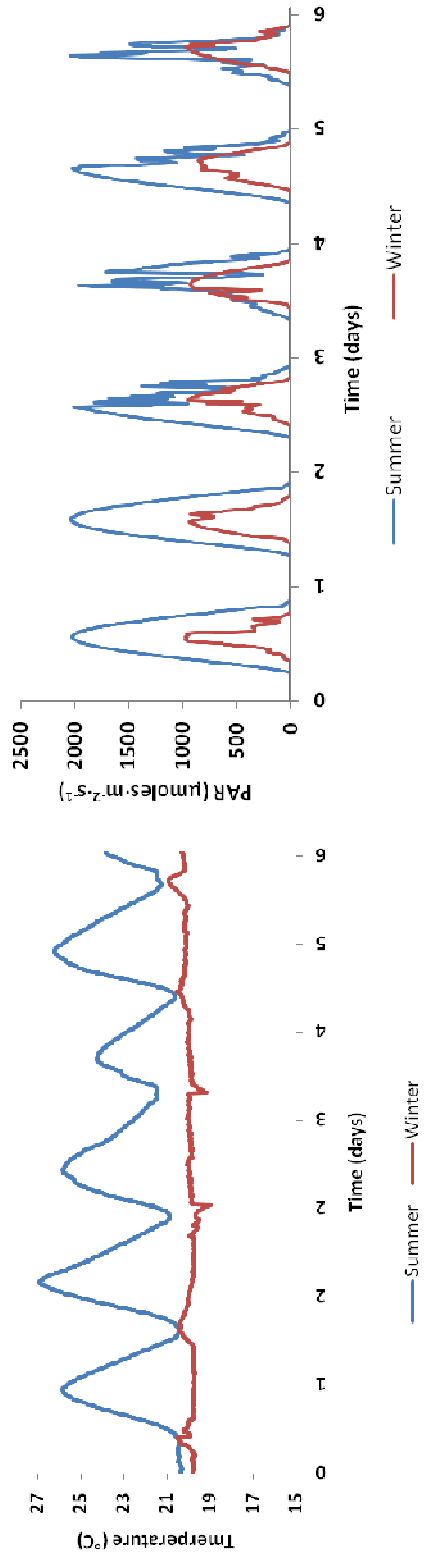


**Figure 16. Approximately one week of raw summer (blue) and winter (red) time PAR data (top) used as primary input for validation of model. Approximately one week of raw thermal basin temperature data used as primary input for model validation (bottom).**

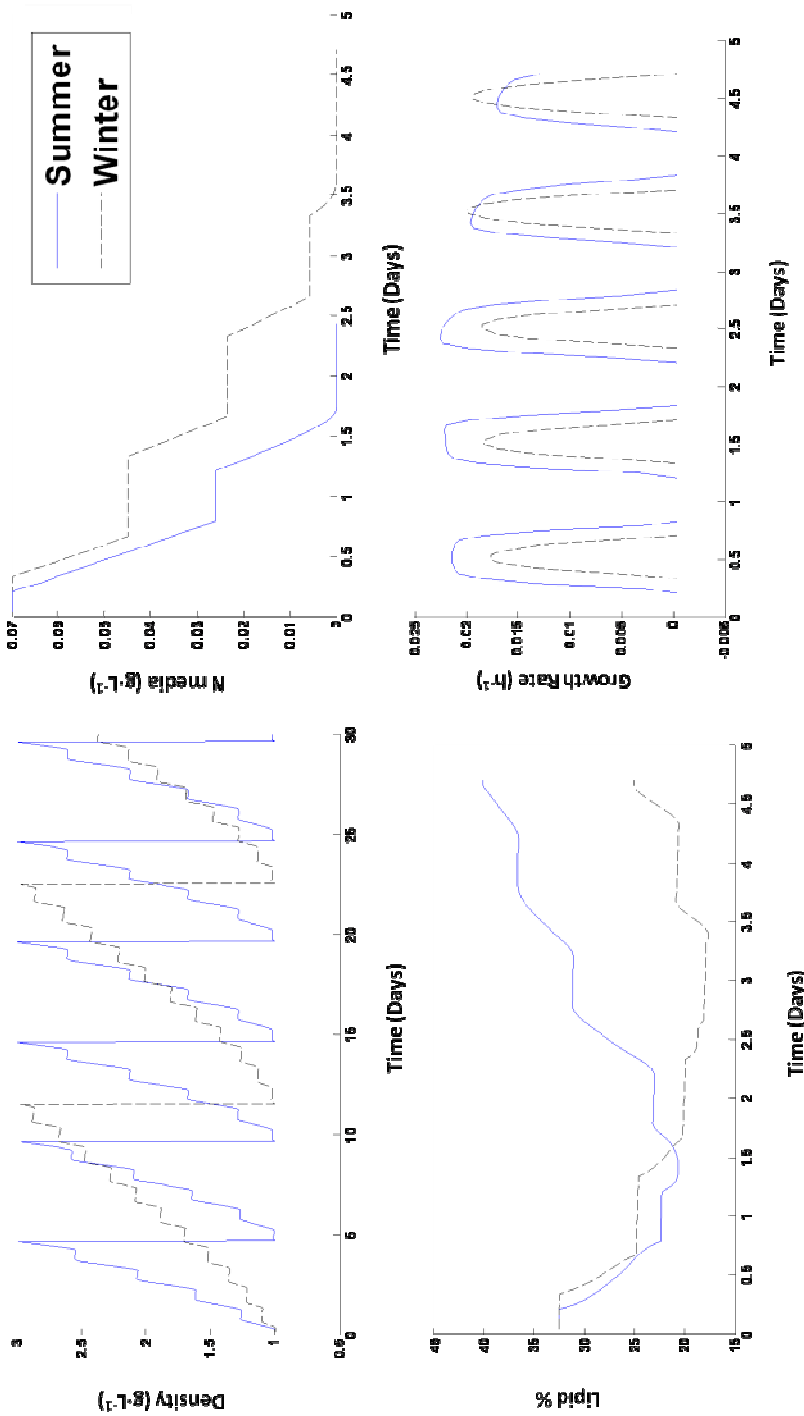
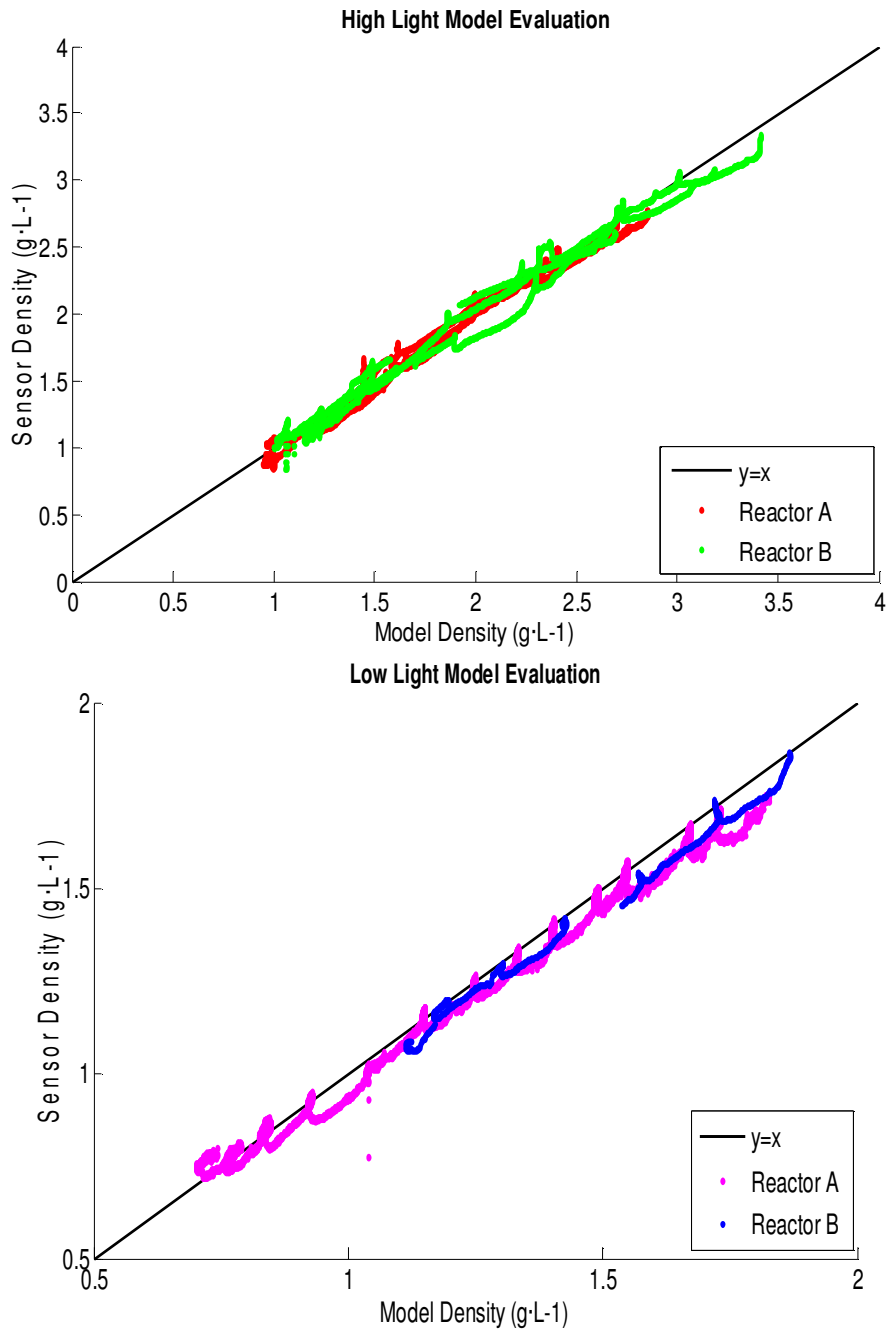


Figure 17. Plot of model output (Model), institute OD sensor (Sensor), and manual samples performed daily (Manual Sample) for two reactors A and B are presented. Approximately one week of high light (June 13-18) for reactor A and approximately one week of low light (November 11- 16) for reactor B raw growth data from the sensor and manual OD and model simulated growth are presented.



**Figure 18. Plot of predicted versus actual daily change in density on a minute time scale for 6 weeks of growth during high light conditions, summer (top) and 3 weeks of growth during low light conditions, winter (bottom).**

The maximum deviations over the 9 weeks worth of data presented in predicted biomass versus measured biomass are  $0.26 \text{ g}\cdot\text{L}^{-1}$  and  $-0.23 \text{ g}\cdot\text{L}^{-1}$  respectively. Analysis of the difference between the measured biomass density and the predicted biomass density on a minute time scale shows a mean of  $-0.00339 \text{ g}\cdot\text{L}^{-1}$  with a standard deviation of  $0.0678 \text{ g}\cdot\text{L}^{-1}$  ( $n=70,224$ ), indicating the model accurately captures the bulk growth of the system however, slightly overestimates the growth. The model is shown to be robust up to 160 hours under real diurnal light of varying intensity with a maximum overestimation of  $0.15 \text{ g}\cdot\text{L}^{-1}$  (9.2%) and under estimation of  $0.06 \text{ g}\cdot\text{L}^{-1}$  (-2.8%) and average over prediction of 3% for the 8 batches modeled, Table 12.

**Table 12. Summary of total change in biomass as predicted by the model and measured by the sensor for 8 batches, (6 high light and 2 low light) including total time of the batch.**

Reactor	Model ( $\Delta\text{g}\cdot\text{L}^{-1}$ )	Actual ( $\Delta\text{g}\cdot\text{L}^{-1}$ )	Batch Length (hr)
A-high light	1.89	1.82	135
A-high light	1.77	1.62	157
A-high light	1.56	1.54	167
A-low light	1.08	0.99	199
B-high light	2.08	2.14	147
B-high light	2.27	2.20	168
B-high light	1.68	1.60	166
B-low light	0.74	0.78	301

The validated biomass model incorporates real diurnal light and meteorological effects to accurately capturing the bulk biomass growth of the scalable outdoor photobioreactor system modeled. For the purposes of predicting bulk biomass growth

under instantaneous and batch operation for real-world climactic and thermal conditions, the model is considered validated to within the accuracies described above.

### ***4.3.3 Lipid Model Validation***

Lipid accumulation in microalgae can be triggered by a variety of variables including but not limited to nutrients, pH, salinity, temperature, and light (Fabregas et al., 2004; Fang et al., 2004; Hu and Gao, 2006; Richmond, 2004; Suen et al., 1987). The system being modeled here enters a nutrient depleted stress mode. Lipid levels as predicted by the model to reach a maximum of 44%. Lipid percentages in literature for *Nannochloropsis oculata* grown in batch mode have been reported to vary with a maximum of 55% (Suen et al., 1987). Lipid percentage of the biomass was monitored on a regular basis for three weeks of operation and is presented along with lipid percentage as predicted by the model in Figure 19.

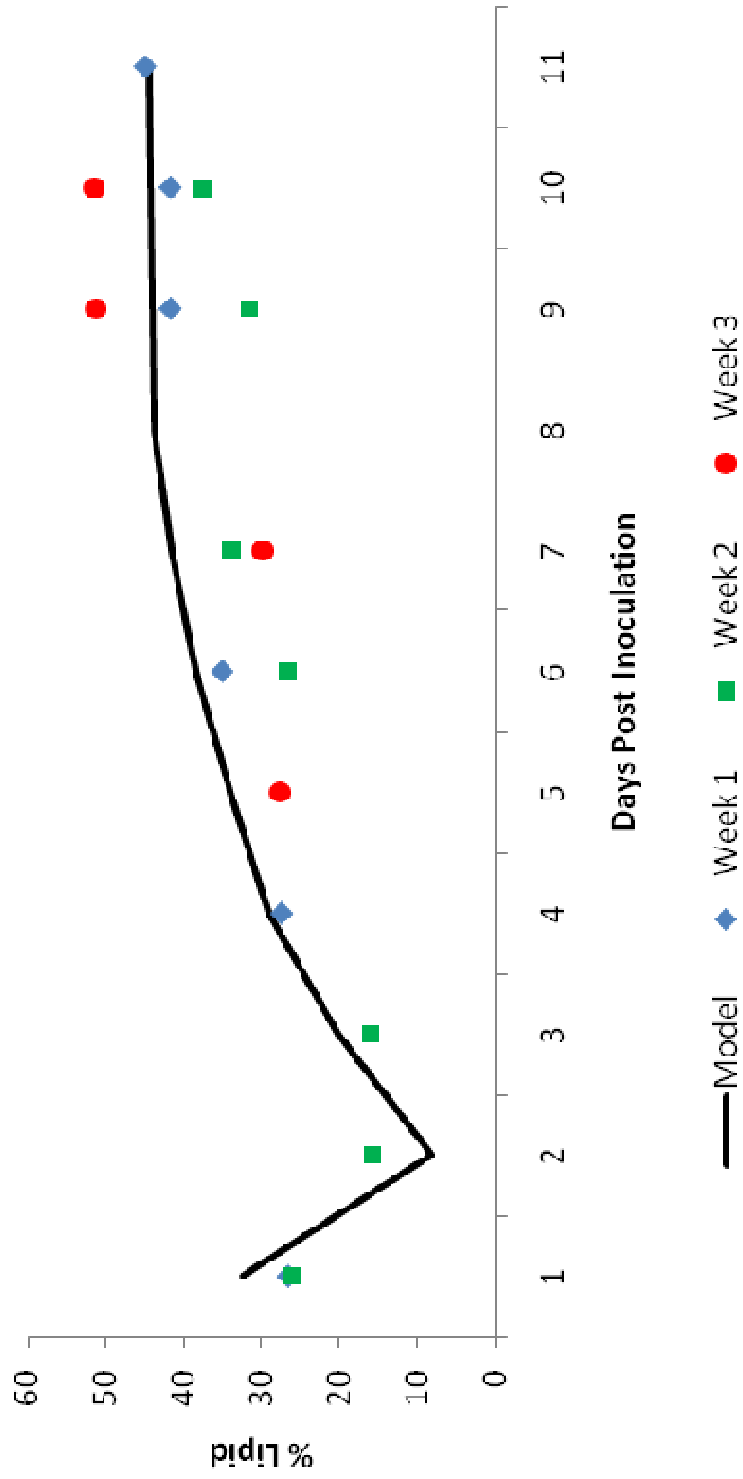


Figure 19. Plot of lipid percentage in biomass for 3 weeks of continual monitoring over 11 day period overlaid on top of predicted lipid percentage from model.

The model accurately captures the trend of the lipid content. The reactors modeled did achieve a maximum lipid percentage of 51% nine days after inoculation during normal operation, which is slightly higher than the model. Biologically, cultures grown in batch mode will transition from linear growth into stationary growth depending on nutrient availability and other factors. A different physiological model representing growth and lipid accumulation for the stationary phase is required to accurately represent growth and composition of the microalgae. In stationary growth, energy dedicated to lipid accumulation would need to be considered in more detail.

For the purposes of predicting biomass lipid content under batch operation for real-world climactic and thermal conditions, the model is considered validated with a standard deviation of error of 8.8% lipid by mass.

#### ***4.3.4 Sensitivity Analysis***

The sensitivity analysis performed on the model involved altering fundamental model inputs by +/- 20% and looking at the biomass output at 100 hr. The baseline scenario involved optimum constant temperature and cloud free clear sky solar radiation as predicted by the REST2 model for the month of June for Fort Collins, Colorado (Gueymard, 2008). An illustration of the biomass growth for the variance of the maximum photosynthetic rate is presented in Figure 20.

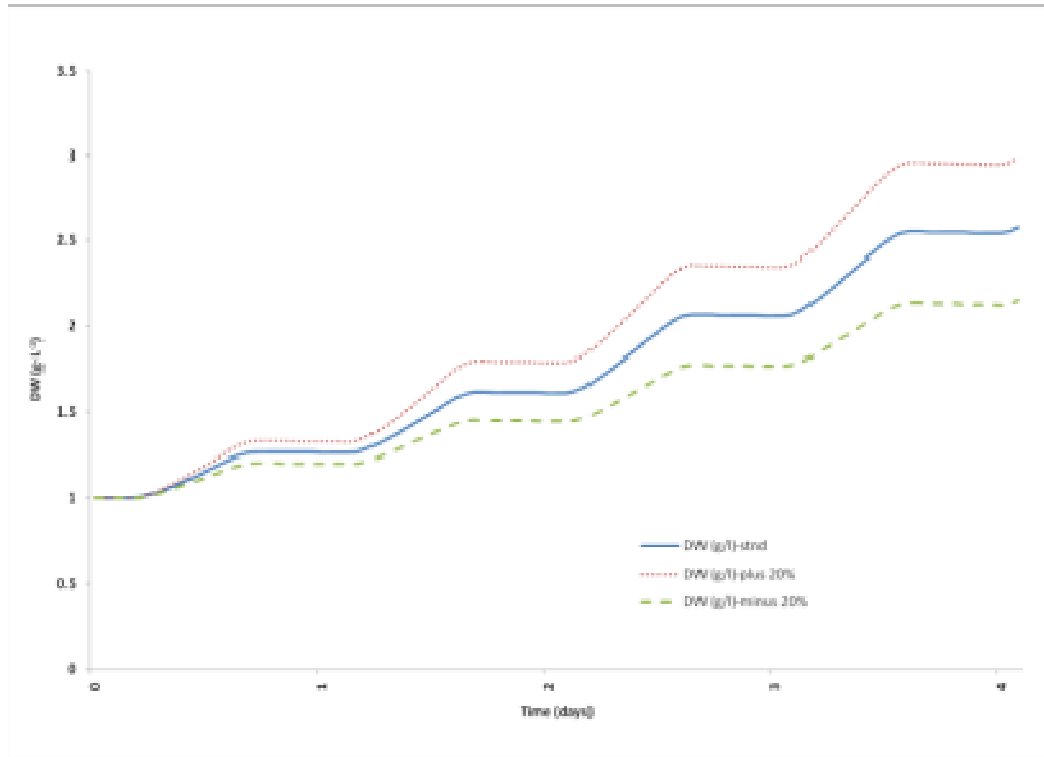


**Figure 20. Growth of baseline bulk model with the max photosynthetic rate increased and decreased by 20% for sensitivity analysis.**

The raw growth data for increasing and decreasing input parameters by 20 percent is presented in Table 13.

Table 13 illustrates that increasing some parameters by 20 percent has an increase on the overall biological output while others have a negative impact on overall output. This data shows the overall impact of the individual model inputs on a biomass productivity matrix.

Statistical analysis of variance was used to estimate t-ratios for each input parameter. Results are presented in Figure 21.

**Table 13. Summary of biomass output of model for increasing and decreasing input parameters by 20%. The baseline model density at 100 hr is 2.54 g·L<sup>-1</sup> under cloud free irradiation with optimum thermal basin component.**

Model Input	Biomass (g·L <sup>-1</sup> ) at 100 hr	
	plus 20%	minus 20%
Max Growth Rate	2.95	2.15
Max Photosynthetic Rate	2.95	2.13
Light	2.74	2.31
Max Nitrogen Cell Quota	2.73	2.37
Photon Efficiency	2.73	2.30
Biosynthetic Efficiency	2.69	2.41
Cell quota for Nitrogen	2.55	2.51
Molecular Weight	2.54	2.54
Max Nitrogen Uptake Rate	2.53	2.53
Activation Energy	2.53	2.53
Half Saturation constant-Nitrogen Uptake	2.53	2.53
Maintenance Respiration rate	2.52	2.54
Min Nitrogen Cell Quota	2.50	2.56
Optimum Temperature	2.45	2.45
Absorption Coefficient	2.36	2.78
Light Saturation	2.35	2.78

As illustrated in Figure 21, variables associated with growth parameters, light modeling, and nitrogen factors have the largest effect on the biomass productivity. The model is insensitive to variations in some parameters such as molecular weight of the microalgae.

Results from this sensitivity analysis are important to consider when adapting the model to other microalgae species. Factors with a t-ratio greater than the t-ratio at

the 95% confidence interval have a large effect on the models output thus need to be known to higher degree of certainty than characteristics inside this interval.

The validated model presented in this study provides a more detailed representation of industrial scale microalgae growth facilities to more accurately represent the true current microalgae growth potential. To understand the effects that this more detailed model will have on these scalability assessments, the model will be used to simulate a year of growth for a proposed high productivity location.

The southwestern US is primarily where deployment of first generation, large-scale microalgae facilities has been proposed. Historical weather data from Yuma, Arizona were input to the model because Yuma has the most cloud free days in the US (242 days) with 90% of annual sunlight hours being cloud free. This location assumption assumes that water and CO<sub>2</sub> are readily available and that optimum thermal conditions exist in the thermal basin.

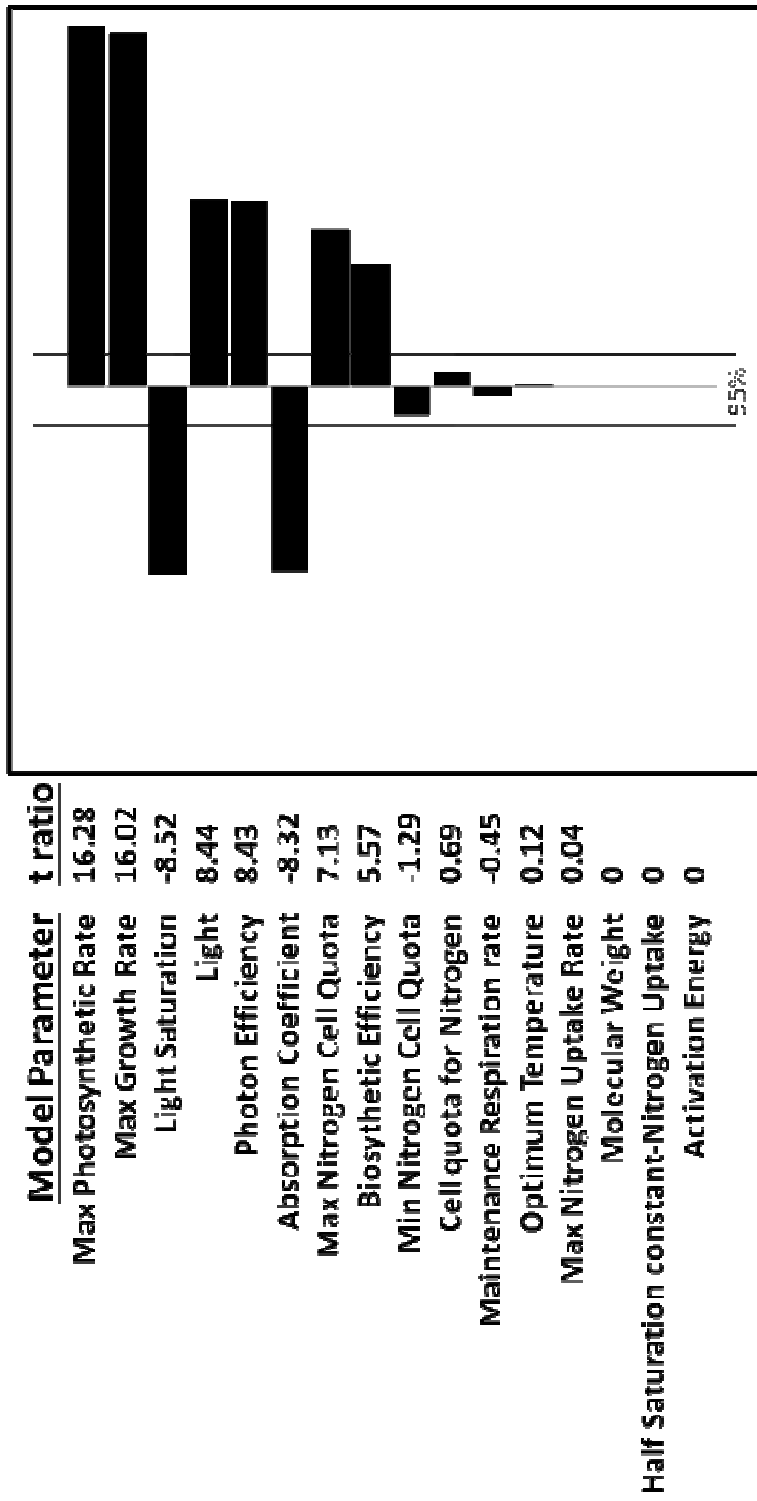


Figure 21. Sensitivity of model inputs presented in tornado plot format. Model inputs were altered by +/- 20% with total predicted biomass production after 100 hours compared to baseline scenario. Vertical lines represent 95% confidence interval.

Two different harvesting schemes were simulated: “time harvest”, where harvest of the culture occurs at 160 hr or  $3 \text{ g}\cdot\text{L}^{-1}$  (whichever occurs first), which is more representative of the function of the research and development facility used in model validation, and “density harvest”, where culture is harvested at  $3 \text{ g}\cdot\text{L}^{-1}$  regardless of elapsed time.

These results represent current maximum yields which might be achievable in the continental US due to the ideal thermal conditions and ideal geographic location selected. The time harvest simulation results in a productivity of  $5.72\cdot 10^4 \text{ kg}\cdot\text{ha}^{-1}\cdot\text{yr}^{-1}$  of biomass or  $26.452 \text{ m}^3\cdot\text{ha}^{-1}\cdot\text{yr}^{-1}$  of oil. For the density harvest, the simulation results in a productivity of  $5.79\cdot 10^4 \text{ kg}\cdot\text{ha}^{-1}\cdot\text{yr}^{-1}$  of biomass or  $28.744 \text{ m}^3\cdot\text{ha}^{-1}\cdot\text{yr}^{-1}$  of oil. The time harvest scheme represents a -1.1% difference in biomass but a -8.7% difference in oil production, relative to the density harvest scheme. Culture growth in the high-light, long days of summer facilitates the growth of the culture to  $3\text{g}\cdot\text{L}^{-1}$  in a short period of time. In the winter, the lower light intensities and shorter days mean  $3 \text{ g}\cdot\text{L}^{-1}$  is not achievable in a 160 hour time period, thus the microalgae is harvested before reaching maximal lipid content.

The validated model predicts a realistic annual productivity potential that is 7 times lower than the highest value reported in the literature surveyed, and is significantly lower than the median productivity reported in literature as shown in Table 14.

The reduced productivity can be attributed to a variety of effects that are present in this model but are not present in other models. The development of the more detailed bulk growth and lipid productivity model allows for the consideration of the effects of facility scale, harvesting strategies, meteorological effects, seasonal effects, and more. Although the resulting productivity of  $26.5 \text{ m}^3 \cdot \text{ha}^{-1} \cdot \text{yr}^{-1}$  of oil may still represent an optimistic estimation of the annual production of oil at a large-scale photobioreactor facility, this result represents the most realistic industrial scale productivity value to date.

#### ***4.3.6 Life Cycle Assessment (LCA) Modeling***

LCA is a fundamental tool that has been used to evaluate the sustainability of biofuels. The results from LCA are highly sensitive to engineering model assumptions, definitions of system boundaries, life-cycle inventories, process efficiencies, and functional units. Increasing interest in microalgae as a secondary feedstock for transportation fuels has led to multiple LCA studies. Inherent in these studies is an engineering model of the microalgae to biofuels process that incorporates a growth model.

**Table 14. Table comparing reported productivity potentials (some calculations performed for comparison purposes) from various sources. Some authors reported a range of productivity potential, consequently the high (††) and low (†) values are repeated.**

Source	Oil ( $\text{m}^3 \cdot \text{ha}^{-1} \cdot \text{yr}^{-1}$ )	Notes
Schenk et al. 2008†	12	30% <sup>a</sup>
Chisti, 2008b†	20.7	20% <sup>a</sup> , $\rho_{\text{oil}}=880 \text{ kg} \cdot \text{m}^{-3}$
<b>Bulk model, this study</b>	<b>26.5</b>	<b>Idealized, Time Harvest, Yuma, AZ</b>
Huntley and Redalje, 2007†	30.7	40% <sup>a</sup> , $\rho_{\text{oil}}=880 \text{ kg} \cdot \text{m}^{-3}$ 50% <sup>a</sup> , 3% solar conversion efficiency
Wijffels and Barbosa, 2010	40	
Yeang, 2008†	46	
Hirano et al. 1998	49.8	40% <sup>a</sup> , $\rho_{\text{oil}}=880 \text{ kg} \cdot \text{m}^{-3}$
Lardon et al. 2009	51.4	50% <sup>a</sup> , $\rho_{\text{oil}}=880 \text{ kg} \cdot \text{m}^{-3}$
Chisti, 2008b††	51.8	50% <sup>a</sup> , $\rho_{\text{oil}}=880 \text{ kg} \cdot \text{m}^{-3}$
Batan et al. 2010 <sup>3</sup> †	51.8	50% <sup>a</sup> , $\rho_{\text{oil}}=880 \text{ kg} \cdot \text{m}^{-3}$
Chisti, 2007†	58.7	30% <sup>a</sup>
Sheehan et al. 1998†	62.2	50% <sup>a</sup> , $\rho_{\text{oil}}=880 \text{ kg} \cdot \text{m}^{-3}$
Campbell et al. 2010	62.3	50% <sup>a</sup> , $\rho_{\text{oil}}=880 \text{ kg} \cdot \text{m}^{-3}$
Schenk et al. 2008††	98.5	50% <sup>a</sup>
Huntley and Redalje, 2007††	99.5	40% <sup>a</sup> , $\rho_{\text{oil}}=880 \text{ kg} \cdot \text{m}^{-3}$
Batan et al. 2010 <sup>2</sup> ††	103.8	50% <sup>a</sup> , $\rho_{\text{oil}}=880 \text{ kg} \cdot \text{m}^{-3}$
Sheehan et al. 1998††	124.4	50% <sup>a</sup> , $\rho_{\text{oil}}=880 \text{ kg} \cdot \text{m}^{-3}$
Chisti, 2007††	136.9	30% <sup>a</sup>
Yeang, 2008††	184	

<sup>a</sup>oil content in biomass

The majority of the microalgae LCA published to date use a simplistic growth model based on a daily productivity number obtained from a small scale laboratory growth facility. Large scale productivity over an entire year is then calculated based on this laboratory number. Batan et al. (2010)<sup>4</sup>, Lardon et al. (2009), Hirano et al. (1998),

<sup>3</sup> Co-authored, Batan and Quinn

and Campbell et al. (2010) all use a fixed growth rate between  $10\text{-}30\text{ g}\cdot\text{m}^{-2}\cdot\text{d}^{-1}$  ( $3.6\cdot 10^4\text{-}11.0\cdot 10^4\text{ kg}\cdot\text{ha}^{-1}\cdot\text{yr}^{-1}$ ) in their growth models. Due to the lack of published data on realistic, large-scale productivities, three of the studies discussed above run multiple scenarios using a range of fixed growth rates in modeling the productivity of large-scale facilities (Batan et al., 2010; Campbell et al., 2010; Lardon et al., 2009). This is indicative of the sensitivity of LCA analysis to the growth models implemented in the process model.

This study presents a validated, large-scale growth model that accurately captures diurnal and annual weather impacts on microalgae growth. The model can be integrated with historical weather data and can be used to more accurately represent the growth of microalgae at specific geographical locations. The majority of the geographic locations of the LCA studies surveyed are warm coastal regions. Meteorological data for the coastal location of San Diego, California were used to illustrate realistic biomass productivity and compare results to the LCA studies discussed. The thermal basin temperature was assumed to be regulated for optimum growth and the time harvest strategy was used, resulting in a productivity of  $5.42\cdot 10^4\text{ kg}\cdot\text{ha}^{-1}\cdot\text{yr}^{-1}$  of biomass or  $15\text{ g}\cdot\text{m}^{-2}\cdot\text{d}^{-1}$ . This analysis shows that the current realizable productivity of microalgae is less than the median of the typical growth rates used in the LCA models surveyed.

To enable more accurate environmental assessments of biofuel from microalgae, LCA studies need to use more accurate growth models. To date, LCA studies have made

geographic location assumptions based on material availability and nearness to markets, but have not included the effect of geographic location on growth. The model developed for this study will enable a more accurate representation of feasible large-scale production, thus improving the environmental assessment of the microalgae to biofuels process.

#### **4.4. Conclusion**

A literature-based bulk growth and lipid production model was constructed incorporating 16 species-specific variables, using light and temperature as primary inputs. Validation of this model was done utilizing 9 weeks of stochastic weather and growth data from a large scalable outdoor photobioreactor cultivating *Nannochloropsis oculata*. Historical weather data for the idealized solar location of Yuma, Arizona was used to illustrate the current productivity potential of  $5.72 \cdot 10^4 \text{ kg} \cdot \text{ha}^{-1} \cdot \text{yr}^{-1}$  of biomass or  $26.4 \text{ m}^3 \cdot \text{ha}^{-1} \cdot \text{yr}^{-1}$  of oil given optimum thermal conditions. The model was also used to illustrate the requirement for more in-depth and accurate growth modeling for LCA analysis.

## **Chapter 5- Current US Biofuel Potential from Microalgae Cultivated in Large-Scale Photobioreactors**

### **5. Abstract**

The scalability of microalgae growth systems is a primary research topic in anticipation of the commercialization of microalgae-based biofuels. Current calculations for the large-scale productivity potential of microalgae are based on growth data from small-scale non-industrially representative systems. To accurately assess the near-term large-scale microalgae potential a thermal basin model is presented and combined with a bulk growth model previously validated with industrial-scale outdoor photobioreactor growth data. The combined models are used with 15 years of hourly historical weather data from 864 locations in the US to accurately assess the current productivity potential of microalgae. Geospatial information system (GIS) land availability and slope data are used to generate a dynamic map of the current feasible locations and productivity potential of microalgae in the US. The discussion focuses on a comparison of model results with productivity potentials currently reported in literature illustrating the need for more realistic assessment of the current near-term realizable productivity potential of microalgae at industrial scale.

## 5.1 Introduction

Analyses that have attempted to model the productivity, economics, and lifecycle environmental impacts of the latest generation of microalgae cultivation systems at industrial scale have relied on the scale-up of laboratory data to model microalgae growth. The scaling of laboratory data has been justified due to the immaturity of the microalgae-to-biofuels process and lack of peer reviewed, published, scalable growth data. It is well-understood that these laboratory-scale processes do not accurately represent industrial-scale facilities (Chisti, 2007; Wijffels and Barbosa, 2010). To more accurately understand and represent the productivity potential of microalgae-based biofuels, microalgae growth and lipid accumulation models validated with industrial scale outdoor growth data must be used that incorporate real locational characteristics (James and Boriah, 2010; Quinn et al., 2011).

Previous GIS studies have generated maps highlighting feasible cultivation sights for large-scale microalgae based on land availability and slope, but fail to incorporate detailed growth models for accurate prediction of microalgae potential (Magnuson, 2010). The majority of the geographical evaluation of productivity potential has been based on a conversion of solar irradiance to biomass potential based on photosynthetic efficiency, which does not accurately represent the current large scale growth potential (Maxwell et al., 1985).

This study presents the integration of a thermal basin model with a validated industrially representative growth and lipid accumulation model to investigate the near-term realizable productivity potential of microalgae in locations that meet the land

availability and slope criteria as set forth by the DOE algae roadmap. In an effort to accurately represent the current US biomass and lipid production as a function of geographical location in the US, the models were run with 15 years of hourly meteorological data collected from 864 US locations. These results were averaged on an annual basis and overlaid with GIS land availability and slope data to produce a dynamic map of the feasible large-scale microalgae production locations in the US including productivity potential. The discussion focuses on a comparison of the modeled productivity results to current values reported in literature with an evaluation of the current total productivity potential.

## **5.2 Materials and Methods**

The following section details the thermal basin model and the meteorological weather data required for model operation, a basic overview of the validated bulk growth model, and the data and criteria for the GIS filters based on slope and land availability. The bulk model equations and thermal basin models are coded in MatLab<sup>®</sup> with GIS data reduction done using ArcGIS.

### ***5.2.1 Validated bulk growth model***

A bulk growth model previously presented and validated in chapter 4 was adapted to this study. The model accurately captures the biomass and lipid production of *Nannochloropsis oculata* cultivated in Solix Generation 3 photobioreactors requiring primary inputs of basin temperature and solar photosynthetic active radiation (PAR).

The photobioreactors modeled are structurally and thermally supported by a water basin as illustrated in Figure 22.

The bulk growth model incorporates 21 species and reactor specific characteristics to accurately depict batch biomass growth and lipid accumulation based on real-world climactic and thermal conditions. For the purposes of predicting bulk biomass growth, the model is considered validated to within the accuracies described by Quinn et al. (2011).



**Figure 22. Image of cultivation system modeled courtesy of Solix Biosystems. Photobioreactors are structurally and thermally supported in a water basin.**

The model was operated for this study with a “time harvest”, where harvest of the culture occurs at 160 hr or  $3 \text{ g}\cdot\text{L}^{-1}$  (whichever occurs first), which is more representative of the function of the research and development facility used in model

validation. Complete details on the model equations and validation can be found in Quinn et al. (2011).

### ***5.2.2 Thermal basin model***

To accurately incorporate geographical temperature effects on growth, a heat-balance model incorporating radiative, conduction, convection, and evaporative heat balance based on meteorological effects is used. The model is structured to accurately represent the temperature of the water basin pictured in Figure 22. It is assumed for this effort that the temperature of the basin and the microalgae are equivalent.

The model was adapted from the methods of Weyer-Geigel (2008). For this modeling effort, the water in the basin was represented by 16 equally spaced vertical nodes in order to capture temperature gradients. Typical thermal models for swimming pools use a single node for thermal calculations assuming no temperature gradients due to continuous circulation and a low surface to volume ratio (Molineaux et al., 1994; Szeicz and Mcmonagle, 1983). The system modeled here does not implore continuous circulation for energetic reasons and has the potential to have thermal gradients thus multiple nodes. A resistance thermal model between the nodes and the ambient are solved incrementally at each time step to accurately predict the heat-flux between nodes. Similar to solar heated hot water tanks, when an inverted temperature gradient occurs it is assumed that due to a density gradient the two adjacent nodes will mix (Duffie and Beckman, 2006). It is assumed that all nodes receive solar energy with a distribution based on the absorption characteristics of water incorporating losses at the

air water interface based on Snell's Law and solar incident angles. Heat loss with the ground and the walls is assumed to be through conduction with a heat transfer coefficient of  $10 \text{ W}\cdot\text{m}^2$  based on soil characteristics (Molineaux et al., 1994). The Sartori equation was used for evaporative loss calculations instead of a pan evaporative model based on the assumption of a large scale facility (Sartori, 2000).

The thermal basin incorporates solar radiation, dry-bulb temperature, dew-point temperature, wind speed, wind direction, cloud cover, and atmospheric pressure to calculate the heat balance and temperature of the basin. The model was developed to accurately represent the temperature of the water basin used in the Solix Generation 3 photobioreactor technology. It is interesting to note that the thermal basin model would approximate the thermal profile of an open raceway pond that operated at a depth of 60 cm.

### ***5.2.3 Geospatial information system (GIS)***

The debate of fuel versus food currently has not been applied to microalgae based biofuels due to the ability to cultivate microalgae on low quality land (U.S. Doe, 2010). An evaluation of the current locations for microalgae cultivation and the productivity potential of these locations can be done by incorporating GIS land availability and slope data with the growth model presented.

The National Land Cover Database (NLCD) 2001 assembled by the Multi-Resolution Land Characteristics Consortium to accurately represent the land cover of the United States, Alaska, Hawaii, and Puerto Rico on a 30 meter cell resolution was

used to illustrate the current feasible location of microalgae production based on land classifications. The following NLCD land cover classifications were considered as available land for cultivation for the baseline scenario: Barren, Scrubland, Shrubland, and Grassland/Herbaceous (Maxwell et al., 1985; U.S. Geological Survey, 2001). A minimum continuous land parcel of 20 hectares was also assumed based on economics of large-scale processing of harvested biomass.

Slope data with a resolution of 90 m was used to refine the current feasible microalgae cultivation locations (Arcgis, 2010). A survey of the literature illustrates there is a debate on the acceptable degree of slope. Benemann et al. 1982 (1982), Lansford et al. 1990 (1990) and Muhs et al. 2009 (2009) define a requirement for the slope to be 2% or less for economic reasons considering the construction of open raceway ponds with the DOE algae road map (2010) defining an acceptable slope of 5% or less. A 5% slope is assumed based on the DOE algae road map and the flexibility of the photobioreactor modeled to be adapted to reference the top water surface thus requiring a lower tolerance for land grading.

#### ***5.2.4 Historical weather data***

The bulk growth model and the thermal basin model both require meteorological weather data as primary inputs. Hourly weather data from 1991 to 2005 from 864 US locations was obtained and used as primary inputs to the thermal basin model and the bulk growth model (Wilcox, 2007). The thermal basin model output evaporation and basin temperature that were then input into the growth model with

solar characteristics to accurately predict biomass and lipid yields on an hourly basis over the 15 years simulated. The biomass and lipid yields were then averaged on an annual time scale.

## 5.3 Results

The results from this work are divided into two sections, the first being a map illustrating the current near term realizable productivity potential of microalgae in the US and the second effort integrating the productivity results with GIS land availability and slope criteria

### *5.3.1 Dynamic map*

The models presented were used to simulate biomass and lipid production in the US based on 15 years of hourly historical meteorological data and then averaged on an annual basis, **Error! Reference source not found..**

The microalgae productivity results were then filtered with GIS slope and land availability data as detailed above to generate the dynamic maps presented in Figure 24.

The results presented in Figure 24 represent the current near-term realistic microalgae productivity potential. It is important to note that the productivity potentials presented are on a per photosynthetic area basis and do not include land required for large scale cultivation infrastructure. The lipid potentials reported are lipids produced and do not include potential losses from extraction or tranzesterification which would be expected to affect results by less than 5%. For comparison a slope restriction of 2% was used to generate the dynamic map presented in Figure 25. For

comparison a slope restriction of 2% was used to generate the dynamic map presented in Figure 26.

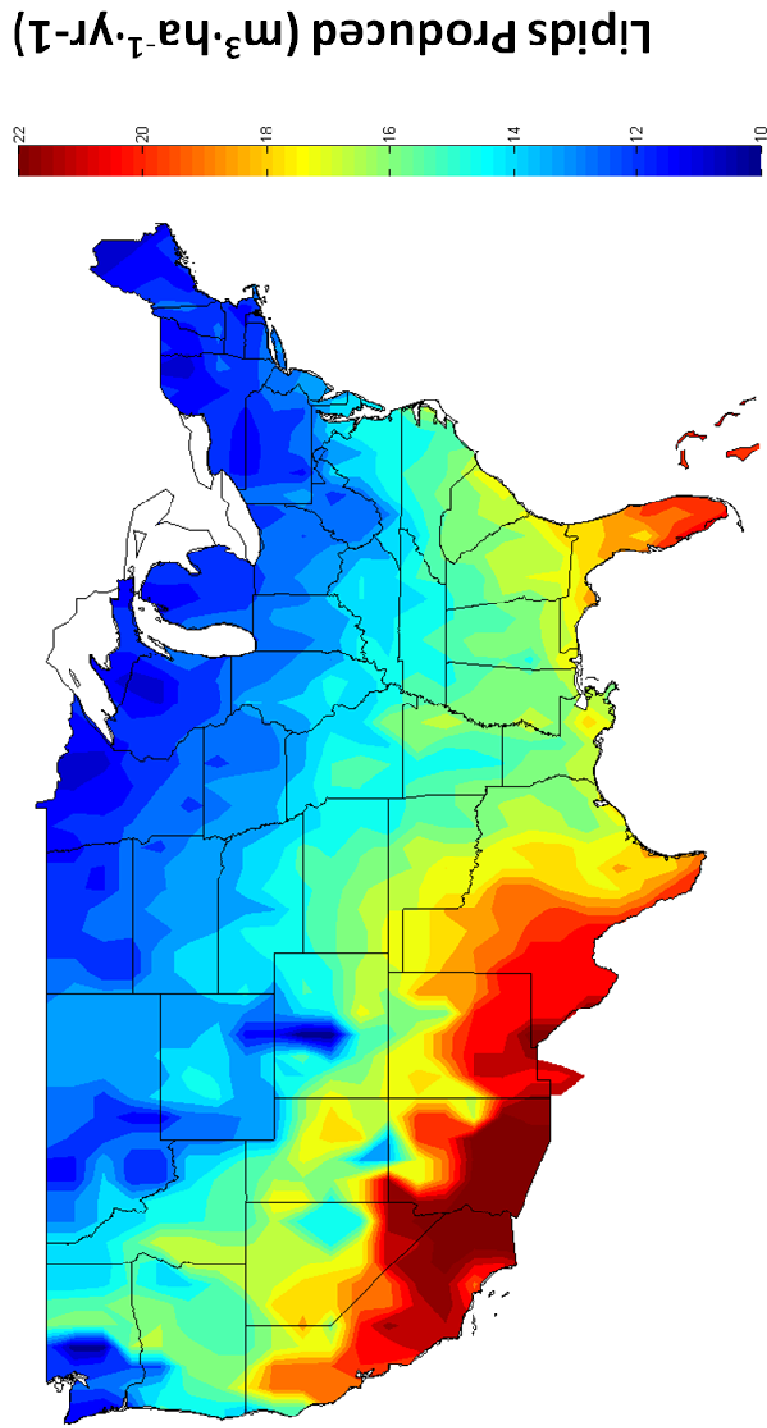
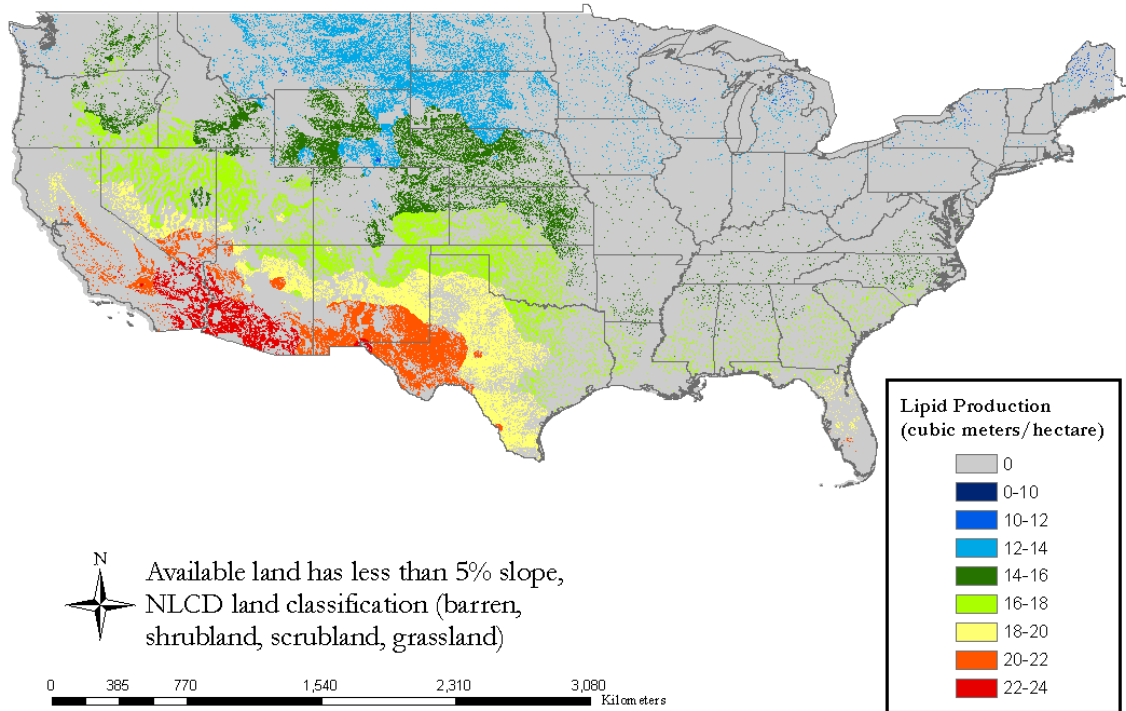


Figure 23. Lipid productivity Potential of microalgae in the US based on 15 years of hourly meteorological data.

## US Bioalgae Productivity Potential



**Figure 24. Dynamic map of near-term realizable large scale microalgae oil production in  $\text{m}^3 \cdot \text{ha}^{-1} \cdot \text{yr}^{-1}$ . Areas that do not meet the land availability and slope criteria defined for the baseline scenario have been grayed out.**

## US Bioalgae Productivity Potential

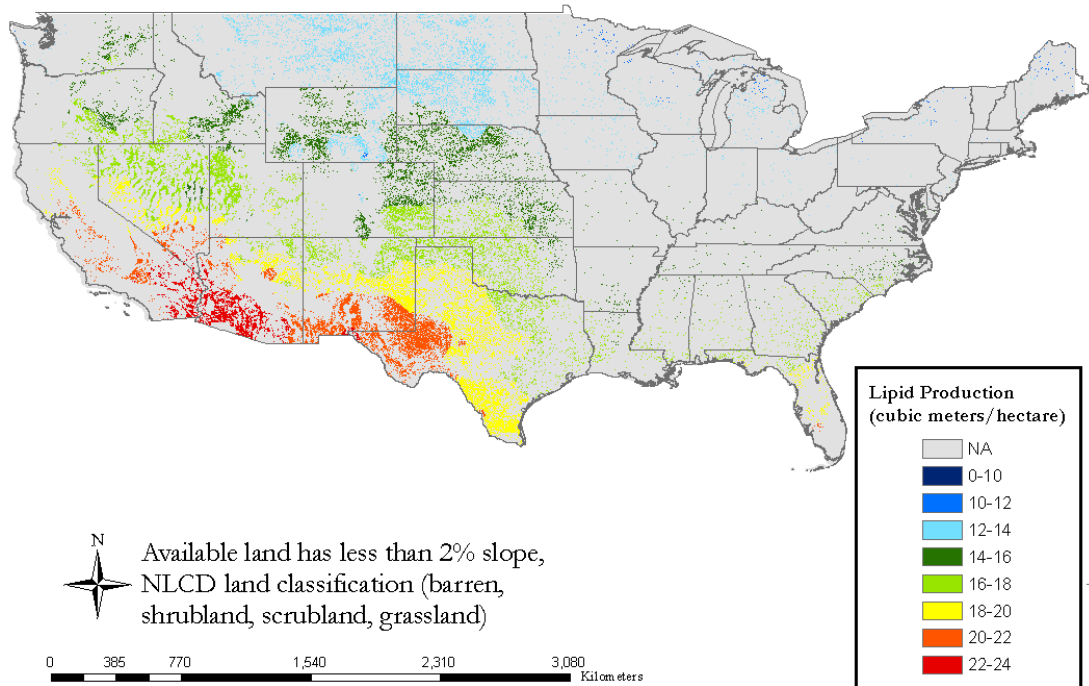


**Figure 25. Dynamic map of near-term realizable large scale microalgae oil production in  $\text{m}^3 \cdot \text{ha}^{-1} \cdot \text{yr}^{-1}$ . Areas that do not meet the land availability and 2% slope criteria have been grayed out.**

## US Bioalgae Productivity Potential

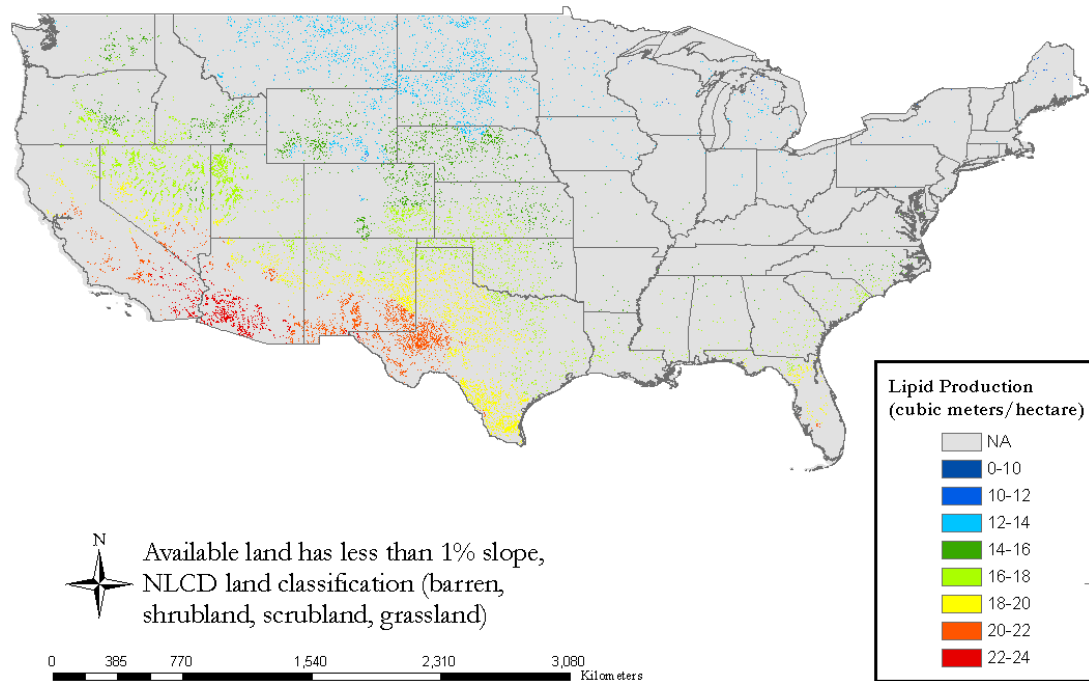


**Figure 26 Dynamic map of near-term realizable large scale microalgae oil production in  $\text{m}^3 \cdot \text{ha}^{-1} \cdot \text{yr}^{-1}$ . Areas that do not meet the land availability and 1% slope criteria have been grayed out.**

Based on the cultivation of microalgae, a packing factor of 0.8, and looking at high productivity zones (corresponding to greater than  $18 \text{ m}^3 \cdot \text{hectare}^{-1} \cdot \text{yr}^{-1}$ ), 13.1 million hectares of land would be required to meet the DOE 2030 alternative transportation fuel goal of 1 billion barrels of fuel (Batan et al., 2010; Department of Energy, 2007). The results from this study show based on the productivity, land, and slope criteria there are 146 million hectares that can produce 20.8 billion barrels of oil. This corresponds to 20.8 times the DOE 2030 alternative transportation fuel goal. A

comparison of the land slope and the total production potential is presented in Table 15.

**Table 15. Table of the land availability and total US production for slope criteria of 1%, 2%, and 5%.**

Slope	Area (ha)	Production (m <sup>3</sup> )
<1%	29,716,881	514,838,322
<2%	72,472,045	1,249,345,933
<5%	146,313,014	2,475,830,752

The 1% slope criteria represent 4.2 times the DOE 2030 alternative fuel initiative.

## 5.4 Discussion

### *5.4.1 Current practical production potential of microalgae compared to literature*

Hype around microalgae based biofuels is typically supported with productivity potentials that are orders of magnitude higher than traditional terrestrial crops (Chisti, 2007; Mata et al., 2010; Scott et al., 2010). The productivity potentials reported are typically calculated by the linear scaling of small-scale laboratory based growth and lipid data, which is far from representative of the true current productivity potential. The simplistic scaling of small-scale laboratory based data and the application to growth modeling quickly leads to erroneous assumptions about industrial growth facility function, and a large uncertainty in the productivity potential of microalgae. The true large-scale production potential of microalgae is currently unrecognizable due to the vast range of values being reported. The acceptance of this type of scaling for

productivity potentials in review articles has lead to similar analysis applied to growth models used in economic and LCA modeling that are in turn unrealistically evaluating microalgae biofuels.

Values reported in literature surveyed range from 8.2  $\text{m}^3 \cdot \text{ha}^{-1} \cdot \text{yr}^{-1}$  reported by Scott et al. 2010 (2010) to 184.0  $\text{m}^3 \cdot \text{ha}^{-1} \cdot \text{yr}^{-1}$  reported by Yeang 2008 (2008) with Clarens et al. 2010 (2010), Schenk et al. 2008 (2008), Lardon et al. 2009 (2009), Campbell et al. 2010 (2010), Sheehan et al. 1998 (1998), Huntley and Redalje 2007 (2007), Chisti et al. 2007, 2008a, 2008b (2007; 2008; 2008), Rodolfi et al. 2009 (2009), Hirano et al. 1998 (1998), Wijffels and Barbosa 2010 (2010), Williams and Laurens et al. 2010 (2010), Sawayama et al. 1999 (1999), Batan et al. 2010 (2010), and Mata et al. 2010 (2010) reporting values between these extremes, Table 16.

**Table 16. Table comparing reported productivity potentials (some calculations performed for comparison purposes) from various sources. Some authors reported a range of productivity potential, consequently the high (++) and low (†) values are repeated.**

Source	Oil Yield ( $\text{m}^3 \cdot \text{ha}^{-1} \cdot \text{yr}^{-1}$ )	Article Type	Purpose of Scaling	Notes
Scott et al. 2010 (2010) †	8.2	Review	Microalgae Potential	46% oil
Clarens et al. 2010 (2010) †	11.8	Research-Model	LCA-Modeling Effort	9.45
Schenk et al. 2008 (2008) †	12.0	Review	Microalgae Potential	10 g/m <sup>2</sup> /d,
Clarens et al. 2010 (2010) ++	16.1	Research-Model	Economic-Modeling	12.9
Lardon et al. 2009 (2009) †	18.0	Research-Model	LCA-Modeling Effort	24.75
Campbell et al. 2010 (2010) †	18.7	Research-Model	LCA-Modeling Effort	15 g/m <sup>2</sup> /d,
Sheehan et al. 1998 (1998) †	21.2	Research-Model	Economic-Modeling	17 g/m <sup>2</sup> /d,
Huntley and Redalje et al.	30.7	Research-Model	Economic-Modeling	18.5g/m <sup>2</sup> /d
Lardon et al. 2009 (2009) ++	30.8	Research-Model	LCA-Modeling Effort	19.25

Chisti et al. 2008 (2008) †	31.1	Letter Response	Microalgae Potential	25g/m2/d
Rodolfi et al. 2009 (2009)	34.1	Research-Model	Economic-Modeling	location
Campbell et al. 2010 (2010)	37.3	Research-Model	LCA-Modeling Effort	30 g/m2/d,
Hirano et al. 1998 (1998)	37.4	Research-Model	NER-Modeling Effort	30 g/m2/d,
Wijffels and Barbosa et al.	40.0	Perspective	Microalgae Potential	3% solar
Scott et al. 2010 (2010) ††	40.0	Review	Microalgae Potential	50% oil
Williams and Laurens et al.	40.7	Review	Economic-Modeling	28 g/m2/d,
Yeang et al. 2008 (2008) †	46.0	Opinion	Microalgae Potential	
Chisti et al. 2008 (2008) ††	51.9	Letter Response	Microalgae Potential	25g/m2/d
Sawayama et al. 1999 (1999)	51.9	Research-Model	Modeling Effort	15g/m2/d
Batan et al. 2010 (2010)	51.9	Research-Model	LCA-Modeling Effort	25 g/m2/d,
Chisti et al. 2007 (2007) †	58.7	Review	Microalgae Potential	30% oil,
Mata et al. 2010 (2010) †	58.7	Review	Microalgae Potential	30% oil
Sheehan et al. 1998 (1998)	74.7	Research-Model	Economic-Modeling	60 g/m2/d,
Chisti et al. 2008 (2008)	98.4	Opinion	Microalgae Potential	1.535
<hr/>				
Schenk et al. 2008 (2008) ††	98.5	Review	Microalgae Potential	50 g/m2/d,
Huntley and Redalje et	99.6	Research-Model	Economic-Modeling	60g/m2/d,
Chisti et al. 2007 (2007) ††	136.9	Review	Microalgae Potential	70% oil
Mata et al. 2010 (2010) ††	136.9	Review	Microalgae Potential	70% oil
Yeang et al.2008 (2008) ††	184.0	Opinion	Microalgae Potential	

In evaluating the productivity potentials reported in literature compared to this study, the peak annual productivity potential in the southwestern US (defined here as the continental US land area below a latitude of 37° and between a longitude of -120° and -100°) which includes southern California, southern Nevada, Arizona, New Mexico, and western Texas is 7.6 times lower than the highest value reported in the literature surveyed, and is lower than the median productivity reported in literature by 2.3 times. The reduced productivity can be attributed to a variety of effects that are present in this model but are not present in other models. The development, validation, and implementation of the more detailed bulk growth and lipid productivity model allows for the consideration of the effects of facility scale, harvesting strategies, meteorological effects, seasonal effects, and more. The results presented here represent the current realistic estimation of the annual production of oil at a large-scale based on a photobioreactor facility.

## **5.5 Conclusion**

The model presented in this study provides a more detailed representation of industrial scale microalgae growth potential by incorporating hourly meteorological effects. The results presented represent the geographically specific current near-term microalgae potential based on a photobioreactor achievable. Results from this study are compared to current large scale productivity potentials reported in literature showing the majority of the studies surveyed over estimate the current near term realizable productivity potential. The productivity results are combined with GIS slope

and land availability data to generate a dynamic map illustrates the current locations for large scale production. Results show the southwestern US including western Texas as prime areas for large scale microalgae cultivation based on productivity potential.

## Chapter 6- Scale-Up of Flat Plate Photobioreactors Considering Diffuse and Direct Light Characteristics<sup>5</sup>

### Abstract

This study investigates the scale up of photobioreactors based on the productivity of *Nannochloropsis salina* as a function of direct and diffuse light. The scale up and optimization of photobioreactors was analyzed by determining the growth response of a small scale system designed to represent a core sample of a large scale photobioreactor. The small scale test apparatus was operated at a variety of light intensities on a batch time scale to generate a photosynthetic-irradiance (PI) growth data set with the data collected was used to inform a PI growth model. The scalability of the PI growth model to predict productivity in large scale systems was evaluated by comparison with experimental growth data collected from two geometrically different large-scale photobioreactors operated at a variety of light intensities. For direct comparison, the small and large scale experimental systems presented were operated similarly and in such a way to incorporate large scale relevant time scales, light intensities, mixing, and nutrient loads. Validation of the scalability of the PI growth model enables the comparisons of different photobioreactor geometries and design

---

<sup>5</sup> The work presented in this chapter is based on the publication Quinn, J, Turner, C, Bradley, T, in review. Scale-up of flat plate photobioreactor considering diffuse and direct light characteristics. *Appl. Microbiol. Biotechnol.*

optimization incorporating growth effects from diffuse and direct light. Discussion focuses on the application of the PI growth model to assess the effect of diffuse light growth compared to direct light growth for the evaluation of photobioreactor geometries followed by the use of the model for photobioreactor geometry optimization based on areal productivity.

## 6.1 Introduction

Microalgae have several sustainability, economic, and environmental impact benefits, when compared to first-generation biofuel feedstocks (Batan et al., 2010). Microalgae are characterized by higher solar energy yield, year-round cultivation, the use of lower quality or brackish water, and the use of less- and lower-quality land (Brown and Zeiler, 1993; Dismukes et al., 2008; Li et al., 2008; Posten and Schaub, 2009; Raja et al., 2008; Wijffels and Barbosa, 2010; Williams et al., 2009). Of the thousands of species of microalgae a select few are currently being considered for the commercial cultivation for the production of biofuel. Under conditions typical of commercial scale reactor systems, *Nannochloropsis salina* can achieve a lipid content of 50% by weight (Emdadi and Berland, 1989; Fabregas et al., 2004; Suen et al., 1987), and an average annual growth rate of  $25 \text{ g m}^{-2} \text{ day}^{-1}$  (Boussiba et al., 1987; Gudín and Chaumont, 1991; Suen et al., 1987). In laboratory conditions, *Nannochloropsis* can attain lipid percentages of 60% by weight and growth rates of  $260 \text{ mg L}^{-1} \text{ hr}^{-1}$  or  $150 \text{ g m}^{-2} \text{ day}^{-1}$  (Richmond et al., 2003; Rodolfi et al., 2009). These characteristically high productivities are primary reasons this species is being investigated for cultivation at large scale.

Previous research studies have characterized some microalgae species for photosynthetic behavior and applied this data to modeling efforts, but these studies have unresolved problems. The majority of photosynthetic-irradiance (PI) curves generated use second time scales, which is not applicable to large scale systems where growth rates must be characterized in significantly longer time scales (Ihnken et al., 2010). Studies have shown time of day and photon flux density history can affect the initial slope of the PI curve in phytoplankton thus short-time scale PI curves do not capture all relevant growth behavior (Furuya et al., 1998; Harding et al., 1982; Henley, 1993). PI curves have been generated for some microalgae species, *Chlorella*, *Scenedesmus*, *Chlamydomonas*, and *Chaetoceros* on one day time scales, however inconsistencies in light levels and exposure time make the application of data to large scale modeling and reactor evaluation difficult (Ihnken et al., 2010; Sorokin, 1957). Geider and Osborne (1986) generated a PI curve for *Nannochloris atomus* on a longer time scale, however did not measure growth at light intensities greater than  $200 \mu\text{mol m}^{-2} \text{s}^{-1}$  which are required for application to outdoor systems. To date there is a lack of growth data characterizing the growth of *Nannochloropsis salina* at variable light intensity on long time scales that is applicable to large-scale, outdoor reactor modeling and design optimization and evaluation.

Previous modeling efforts have looked into the scale-up of microbiological systems, however inconsistent assumptions and arbitrary scaling factors limit the application of previous studies to large scale reactor design. Janssen et al. (2003) evaluate the feasibility of the scalability of a variety of photobioreactor geometries, but

do not support their conclusions with calculations or data. Others have focused effort on conceptualizing the scale up of photobioreactors but again fail to incorporate any real data (Perner-Nochta and Posten, 2007; Sastre et al., 2007). Some modeling efforts have successfully scaled small systems, however the utilization of arbitrary scaling factors limit the application of the work (Molina et al., 2000). There is a current need for transparent, scalable growth modeling techniques with applications to large scale reactor design optimization and evaluation.

This article presents experimental results that address the problems present in previous studies and the application of data to modeling and reactor evaluation and optimization efforts at large scale. Two systems were constructed, a small scale test reactor system and a large scale photobioreactor system. For the purpose of scalability, the small scale system was designed and built to represent a core sample of the large scale reactors. The small scale system was operated at a variety of light intensities on a batch time scale with the data collected used to generate a PI growth model that incorporates diffuse and direct light growth characteristics. The large-scale photobioreactor test system was constructed and used to generate growth data from two geometrically different photobioreactors under a variety of light intensities for the evaluation of scalability of the PI growth model. Results show the small scale PI growth model accurately predicts growth in the large scale system at a variety of light intensities validating the core sample technique. The discussion presents an evaluation of photobioreactors based on diffuse versus direct light growth and a geometric

optimization based on the PI growth model of a flat plate photobioreactor on the metric of areal productivity.

## **6.2 Experimental Materials and Methods**

The following section details the small scale and large scale test reactor configurations, operation of the test reactors, culture and media, and measurement techniques used for data collection. The small scale test apparatus was constructed to mimic the large scale system through a core sample technique. The core sample technique is based on describing the growth in the large photobioreactor based on multiple small core samples, Figure 27.

The productivity characterization of the small scale reactors as a function of light intensity on a batch time scale was done with results used to generate a logarithmic PI growth model based on light intensity. The model generated from the data collected in the small scale system is then used to predict the large scale photobioreactor productivity. Correlation illustrates the effectiveness of the core sample technique for capturing productivity at large scale without arbitrary scaling factors.

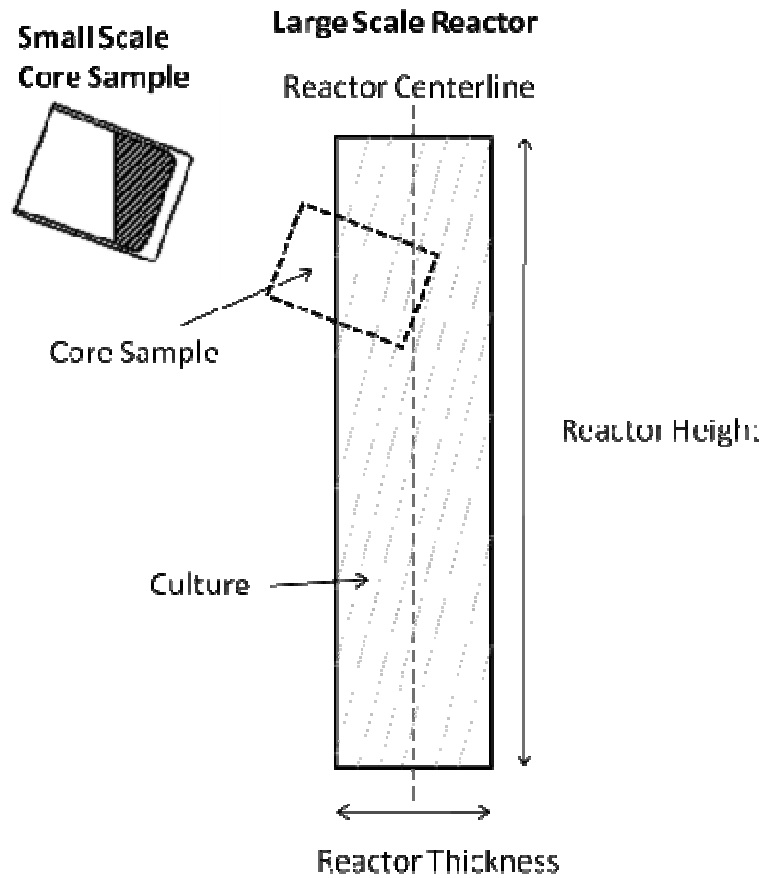


**Figure 27 Schematic of core sample technique relating the geometry of the small scale system to the large scale system.**

### ***6.2.1 Small Scale System***

#### **6.2.1.1 Reactor geometry, illumination, and operation**

For small scale reactor data collection, two identical test apparatuses were constructed. Each test apparatus consisted of 6 cylindrical glass reactor vessels, 8.9 cm deep and 7.7 cm in diameter. Two culture volumes based on inherent variability in thickness of the large scale system were tested in the small scale experimentation: 1) the high volume scenario with 150 mL of culture corresponding to a depth of 0.036 m,

and 2) the low volume scenario with 75 mL of culture corresponding to a depth of 0.018 m. The outer surface of each reactor was coated with an opaque material, making the top surface the only illuminated surface. All reactors shared a common polycarbonate headspace which was continually purged with filtered (0.2 micron) humidified air at a rate of  $0.28 \text{ m}^3 \text{ hr}^{-1}$  (10 SCFH) during photoactive periods, Figure 28. The pH of the reactors was monitored and controlled by introducing 2%  $\text{CO}_2$  ( $5.7 \cdot 10^{-3} \text{ m}^3 \text{ hr}^{-1}$ ) into the humidified air to ensure a pH range of  $7.5 \pm 0.3$  during photoactive periods.

The polycarbonate structure was manufactured to integrate with a Polyscience 28 L shaking thermal water bath system. The shaker was operated 24 hours a day at a rotational speed of 140 revolutions per minute at an eccentricity setting of 9 with the thermal basin set at  $23^\circ\text{C}$ .

Illumination of the system was done using a Sun Systems Yield Master II Classic with a 1000 watt daylight metal halide grow lamp selected for its accurate representation of solar photosynthetic active radiation (PAR). The illumination system was operated on a 16 hour light, 8 hour dark period. A variety of light intensities were tested with the desired light intensity achieved in two ways, 1) by varying the height of the artificial lights and 2) by applying screens to the top of the polycarbonate structure. The system was operated in biological triplicate for each of the light intensities tested. A labeled schematic of the test reactor systems is presented in Figure 29.

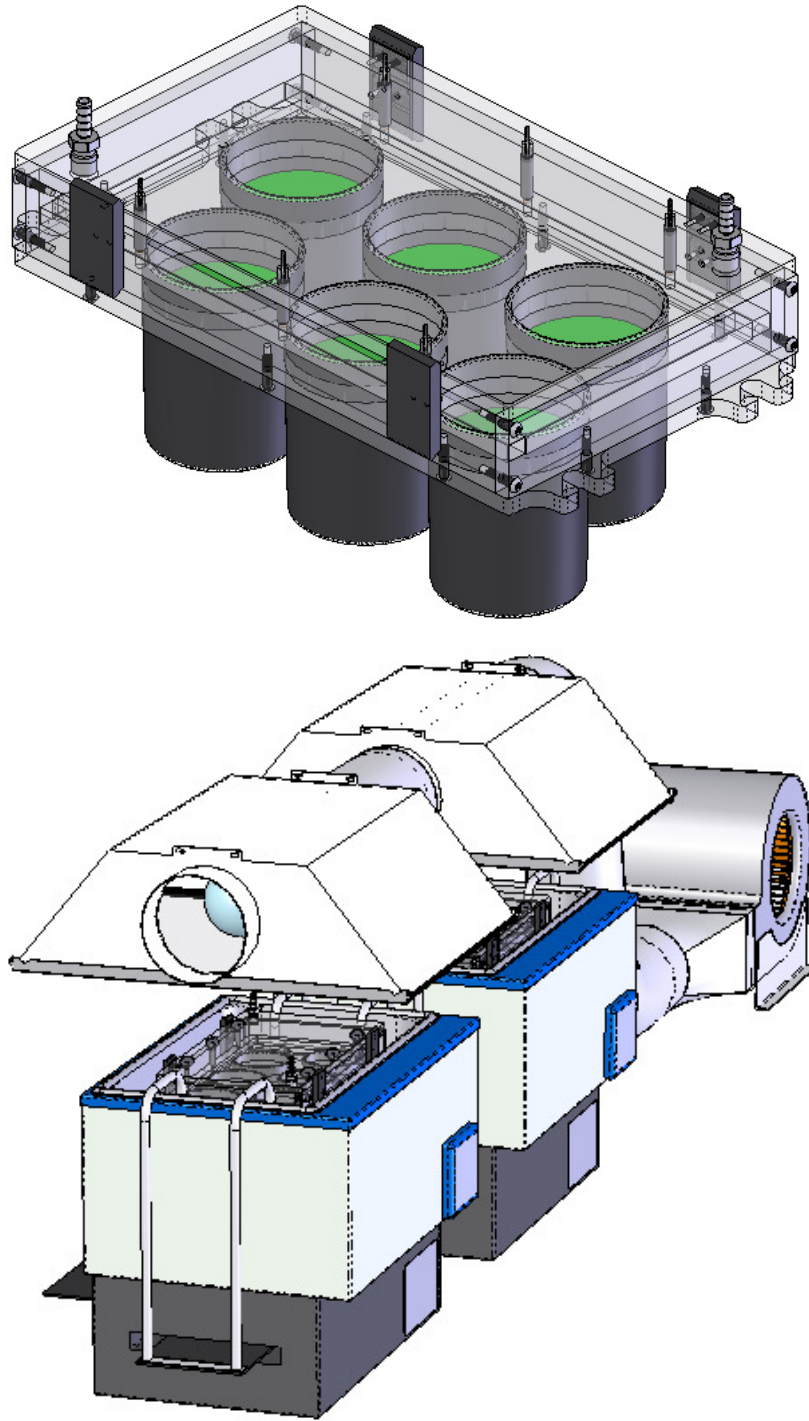


**Figure 28 CAD representation of one test apparatus consisting of 6 test reactors (left). Two of the apparatus (left) were constructed with each one attached to a Polyscience 28 L shaking thermal basin and illuminated with a Sun Systems, Yield Master II classic with a 1000 watt metal halide grow lamp (right).**

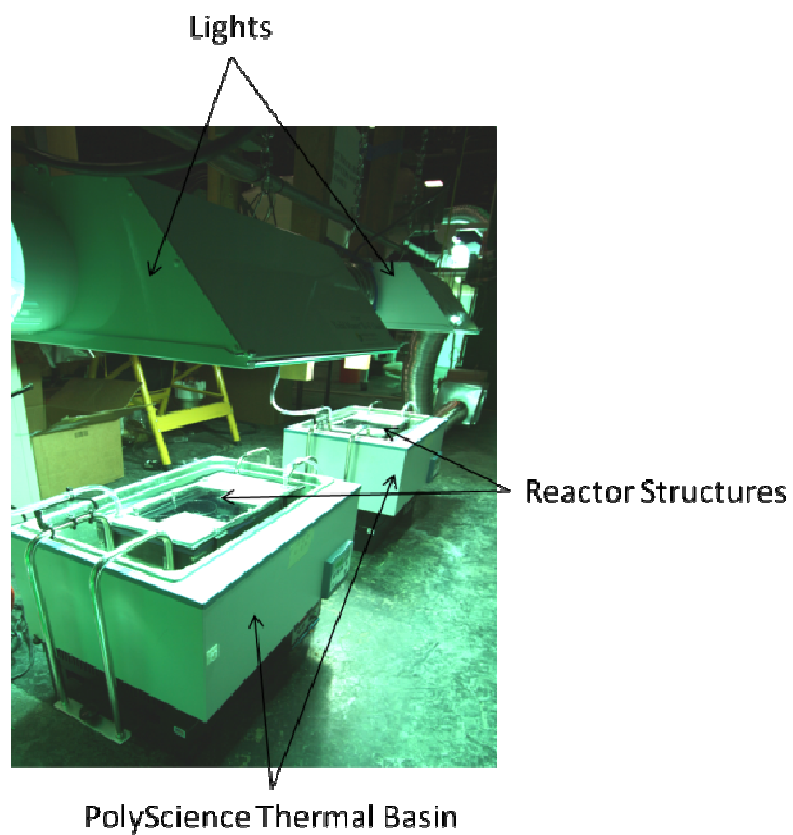
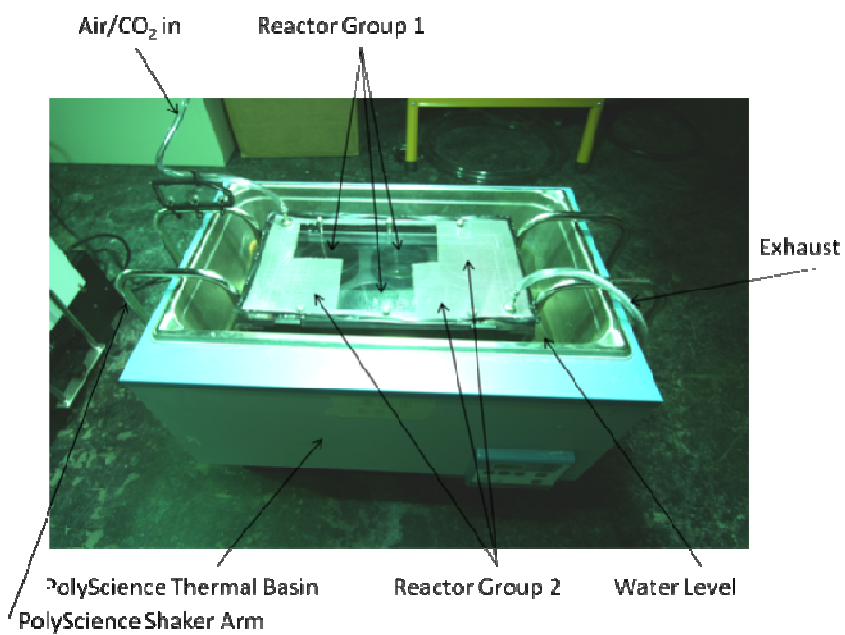


**Figure 29. Picture of one of two small scale units used for data collection (left). Picture of two test apparatuses (right).**

The reactors were grouped according to the measured light intensities such that the three reactors grouped all have similar light intensities. The desired light intensity was achieved through raising and lowering the light source and by shading the system with standard metal window screen with a screen mesh of 18 wires per inch by 14 wires per inch.

#### 6.2.1.2 Growth monitoring equipment and technique

Growth monitoring was performed daily, at the beginning of the light cycle. Prior to sampling, the volume of each reactor was checked and 0.2 micron filtered de-ionized water was added to restore the reactors to the original inoculation volume. Optical density (OD) measurements at 750 nanometres were performed on a Hach DR5000 spectrophotometer. Samples were prepared for an optical density reading using the following technique: Depending on the dilution required, 80-160  $\mu\text{L}$  of sample was added to a 3 mL-10 mm optical path length cuvette using a 200  $\mu\text{L}$  pipette. 1840-1960  $\mu\text{L}$  (depending on dilution) of 0.2 micron filtered 20  $\text{g}\cdot\text{L}^{-1}$  salt water was pipetted into the cuvette followed by pipette mixing. Samples were diluted such that the measured optical density was in a range of 0.1 to 0.3 such that a previously determined conversion of optical density to dry mass could be applied. Conversion of OD to dry mass was done using a previously determined correlation factor. Previous sampling experimentation showed that sampling location and depth did not appreciably affect experimental results.

### 6.2.1.3 Photo-adaptation and data collection batches

For each of the light intensities tested, a photo-adaptation batch was cultivated for a minimum of 4 light cycles. The photo-adaptation cycles were not used in data processing. After photo-adaptation, two data acquisition batches (4 light cycles) were run. Inoculation for the data acquisition batches involved the mixing of the three biological triplicate cultures, combining the required inocula with nutrient rich media (detailed below) and re-inoculating the reactors at  $1.1 \text{ g L}^{-1}$  with a  $\sigma = 0.087$  (n=114).

## **6.2.2 Large Scale System**

### 6.2.2.1 Reactor geometry, illumination, and operation

The large indoor cultivation system was modeled after the Solix AGS generation 3 photobioreactor. The cultivation system comprised 16 reactors divided into two groups of 8 with the geometries of one reactor from each group detailed in Figure 30 (support structure not depicted).

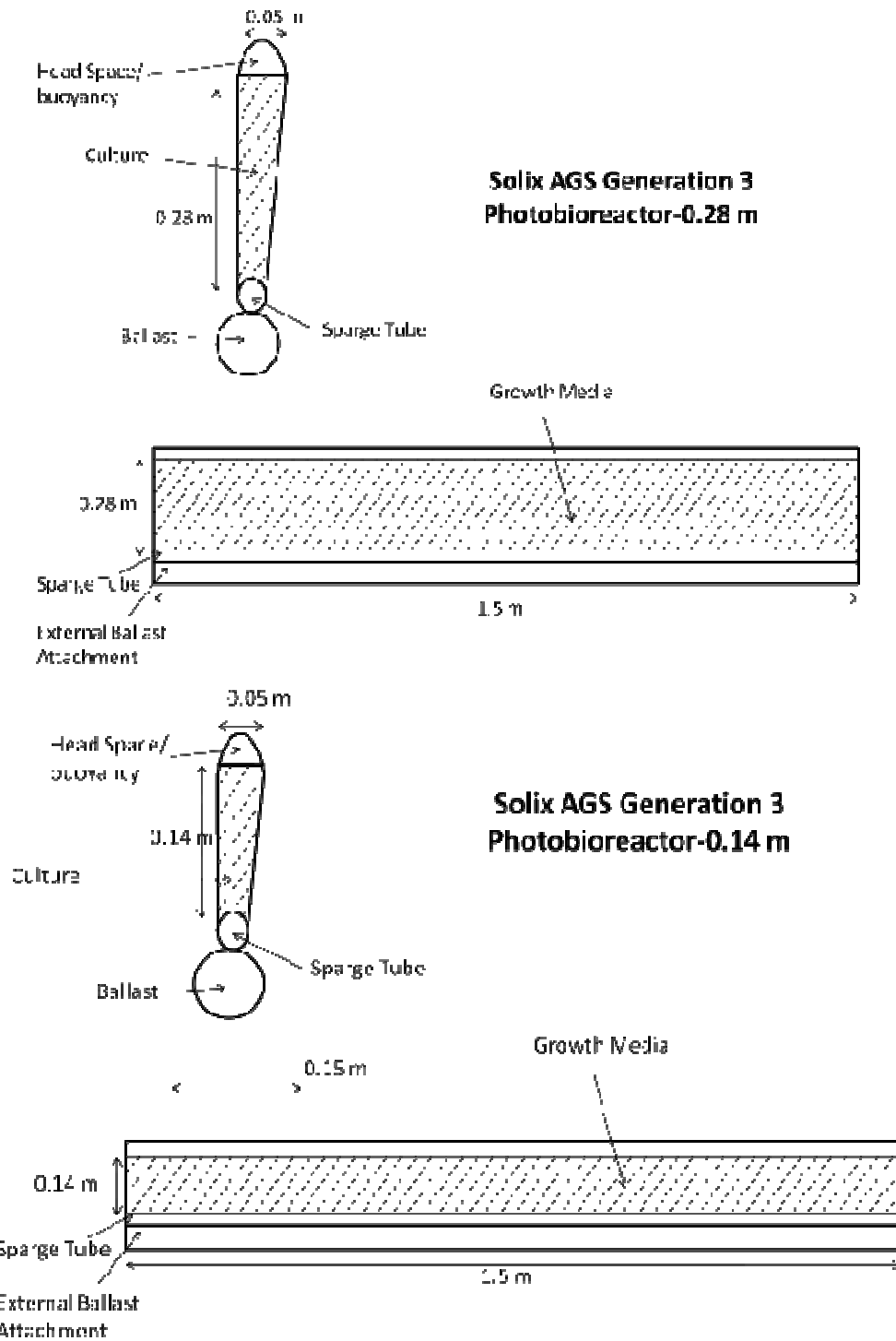


**Figure 30 Geometry of large scale photobioreactors based on Solix generation 3 technology, 0.28m deep reactors-left and 0.14 m deep reactors-right. The primary difference between the two geometries is the culture height and volume is halved. Support structure is not detailed.**

The large indoor photobioreactor test bed, based on the geometry of the Solix generation 3 photobioreactor technology, was constructed such that the reactor depth could be varied discretely. Experimentation involved the construction of four different reactor depths, two for growth data collection and model validation and two additional reactor configurations for light characterization. The growth reactor geometries differ in depth by a factor of 2: one having a culture depth of 0.28 m and the second geometry having a depth of 0.14 m. For light characterization two more reactors were constructed with depths of 0.56 m and 0.84 m. The photobioreactors were constructed out of 0.12 mm polyethylene and structurally and thermally supported by a water basin measuring 3 m x 1.2 m x 1.5 m. Temperature in the basin was maintained at 23°C +/- 2°C using a pool heater. The thickness of an individual photobioreactor is approximately 0.05 m but varies due to the flexible structure by approximately 0.01 m. The reactors were spaced at 0.15 m. Mixing was provided by filtered sparge air 24 hours a day at a rate of 0.34 m<sup>3</sup> hr<sup>-1</sup> per reactor. The pH of the system was maintained with CO<sub>2</sub> mixed with the sparge air during photo-active (light) periods to maintain a pH of 7.5 +/- 0.3.

The system was illuminated using 10 lamps (Sun Systems Yield Master II Classic) with 1000 watt daylight metal halide grow lamps mounted on a light rack above the thermal basin. Two light regimes were simulated with the system: 1) a high light scenario-which involved 10 lights angled at 5°, and 2) a low light scenario-which involved 5 lights angled at 35° with two additional low light T5 fluorescent banks mounted towards the rear of the basin. The addition of the low light fluorescent banks

was to improve the uniformity of the light in the low light scenario. The illumination system for both the high and low light scenarios were operated on a 16 hour light, 8 hour dark cycle.

Detailed images of the large scale system are presented in Figure 31. Data collected from the reactors closest to the front and back walls was not used due to increased light intensity from reflection off the thermal basin walls.

The light rack which supported the 10 lights used could be pulled back for harvest and re-inoculation. Two large squirrel cages were ducted to the light banks to provide the required cooling air to the illumination system.

8-0.28 m deep reactors

Exhaust Tubes

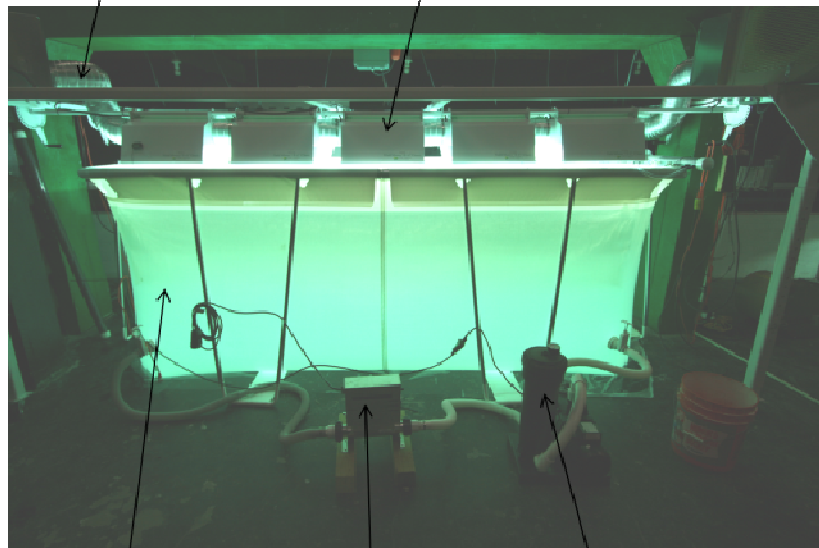


Thermal Basin

8-0.14 m deep reactors

Cooling Air for Lights

Front Row of Light Bank



Thermal Basin

Pool Heater

Pool Filter

**Figure 31. Photograph with light bank removed of large scale reactors (left). Photograph of large scale growth system with lights turned on (right).**

### 6.2.2.2 Growth monitoring equipment and technique

Manual samples of the culture to monitor growth were taken daily at the beginning of the light cycle. Samples were drawn using a 10 mL syringe through sample lines attached to the reactors. Previous sampling experimentation showed that sampling location does not affect experimental results. OD measurements at 750 nm were performed on a Hach DR5000 spectrophotometer with dry mass calculated by a previously determined correlation constant. Samples were prepared for an optical density reading using the following technique: Depending on the dilution required, 80-160  $\mu\text{L}$  of sample was added to a 3 mL-10 mm optical path length cuvette using a 200  $\mu\text{L}$  pipette. 1840-1960  $\mu\text{L}$  (depending on dilution) of 0.2 micron filtered 20  $\text{g}\cdot\text{L}^{-1}$  salt water was pipetted into the cuvette followed by pipette mixing. Samples were diluted such that the measured optical density was in a range of 0.1 to 0.3 such that a previously determined conversion of optical density to dry mass could be applied. The effects of evaporative losses on OD measurements were corrected for by measuring the volume of the reactors at both inoculation and at harvest.

### 6.2.2.3 Photo-adaptation and data collection batches

Inocula were obtained from Solix with flow cytometry performed to verify a contamination level of less than 1% by count. Prior to inoculation in the experimental reactors, the culture obtained from Solix was cultivated in the indoor system in one, 0.28 m deep reactor to a density of 3  $\text{g}\cdot\text{L}^{-1}$ . The culture was then harvested, mixed with nutrient rich media (detailed below), and injected into three, 0.28 m deep reactors and

cultivated to  $3 \text{ g L}^{-1}$ . The 16 reactor system was then inoculated from this culture at  $1 \text{ g L}^{-1}$ .

So as to simulate the growth behavior of a large-scale PBR system, data was collected from only the middle six of the eight reactors in each experimental set. The two exterior reactors were excluded from data analysis because of reactor edge effects including reflection of light from the sides of the thermal basin.

### ***6.2.3 Culture and Growth Media***

*Nannochloropsis salina* 1776 was originally obtained by Solix Biofuels from the Provasoli-Guillard National Center for Culture of Marine Phytoplankton. The nutrient rich growth media was made by modifying f/2 growth media to a salinity of  $20 \text{ g L}^{-1}$ , adding  $10 \text{ mM NO}_3^- \text{ L}^{-1}$ ,  $7.9 \text{ mM PO}_4^- \text{ L}^{-1}$  and  $1 \text{ mL L}^{-1}$  Guillard trace metals. All growth media was filtered using a 0.2 micron absolute filter.

### ***6.2.4 Light Measurement Device and Technique***

Light intensity was measured using a Heinz Walz US-SQS/L spherical PAR sensor connector to a LI-COR L1-250A light meter. For measuring the light in the small scale system, a light measuring reactor was constructed to mimic the biological reactors. For accuracy, the light was measured at the four extremes (north, east, south, and west) of the shaker motion and averaged.

The light intensity on the surface of the reactors in the large scale system were measured at 0.025 m intervals.

### ***6.2.5 Comparison of Small Scale and Large Scale Growth Systems***

The two systems presented are very different in shape and physical operation. The two systems utilize different mixing regimes. Mixing will have an impact on the growth if the system is mixed on a time scale where algae is receiving light on a time scale similar to the time required to activate the photosynthesis system. This type of mixing represents a turbulent fluid system and requires a large amount of energy. The fluid dynamics of both the small scale and large scale systems presented operate in a regime where mixing does not play a critical role on the growth (Qiang and Richmond, 1996). Increasing the mixing to a level that will have an effect is not commercially feasible for microalgae biofuels.

In all other logistic operations the two systems were operated similarly, harvest and inoculations were performed during the dark period, the culture cultivated went through photo-adaptation periods prior to data collection, sampling was performed on both systems at the beginning of the light cycle, and both systems operated on a 16/8 light/dark cycle. These similarities enable the comparison of the two data sets.

## **6.3 Results**

This section details the productivity results of the small scale system, PI growth model based on the growth data collected in the small scale reactors, the large scale reactor data, and the evaluation of scaling of the small scale PI growth model to predict the growth in the large scale system.

### 6.3.1 Small Scale Reactor Growth Data

The 150 mL scenario experimentation consisted of the testing of 73 light intensities ranging from 72 to 1471  $\mu\text{moles m}^{-2} \text{s}^{-1}$ . The 75 mL scenario consisted of the testing of 40 light intensities with light ranging from 119 to 1477  $\mu\text{moles m}^{-2} \text{s}^{-1}$ . Raw growth data collected for 4 different light intensities is presented in Figure 32.

The productivity data collected over a 4 day batch was averaged and plotted in Figure 33 with a logarithmic curve fit performed.

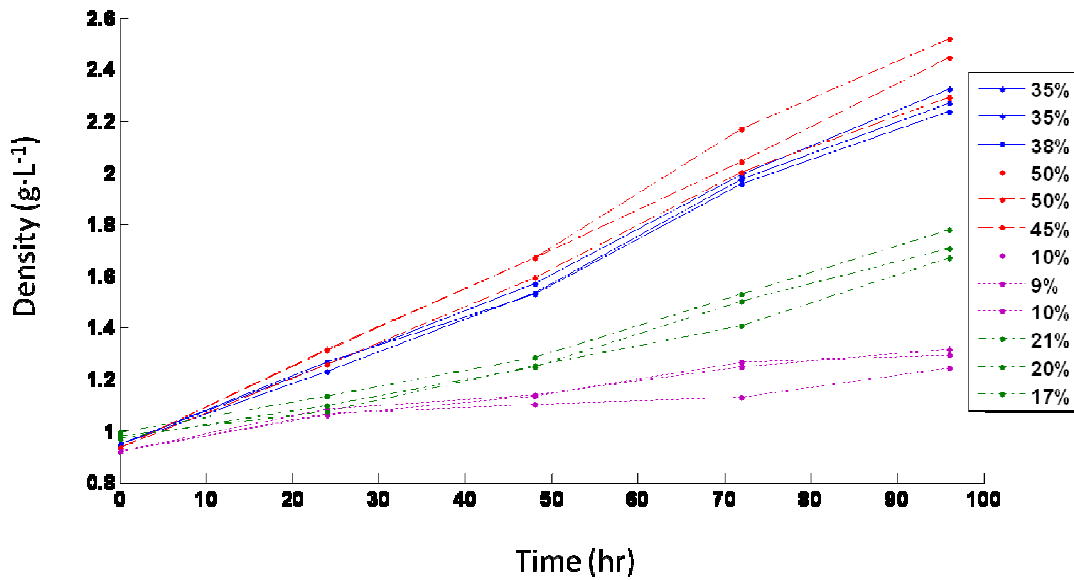
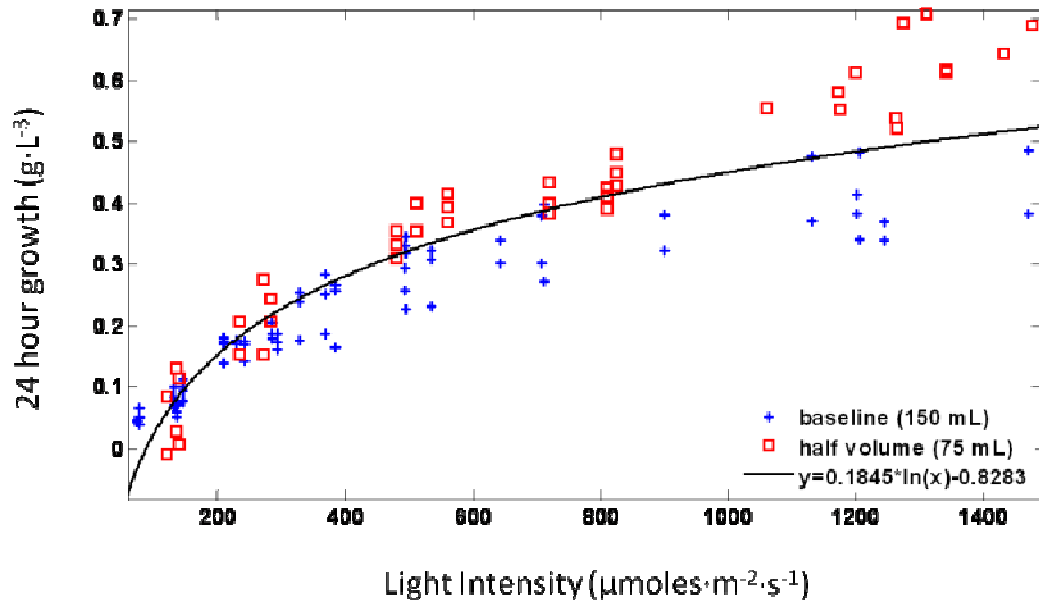


Figure 32. Raw growth data collected for 4 different light intensities. The percentages reported in the figure are light intensity with respect to 1500  $\mu\text{moles}\cdot\text{m}^{-2}\cdot\text{s}^{-1}$ .



**Figure 33 Batch averaged growth data from small scale test reactor. Growth reported in average 24 hour productivity in grams per liter of culture based on a 4 day batch versus light intensity for the two volumes tested, 150 mL and 75 mL.**

The data presented in Figure 33 has the same typical shape and characteristics of traditional PI curves. Equations to model PI data have been presented in the literature. The following section uses literature-based models to statistically evaluate the PI data collected from the small scale system used in this study. The PI models of Smith(1936) (1) and Webb et al. (1974) (2) were selected and fit to the baseline data ( $\alpha = 0.933 \text{ g}\cdot\text{s}\cdot\text{m}^{-2}\cdot\mu\text{mol}^{-1}$ ,  $P_m = 0.70 \text{ g}\cdot\text{L}^{-1}$ ,  $R_d = -0.05 \text{ g}\cdot\text{L}^{-1}$ ).

$$P = P_m \frac{\alpha I}{\sqrt{P_m^2 + (\alpha I)^2}} + R_d \quad (1)$$

$$P = P_m \left( 1 - e^{\frac{-\alpha I}{P_m}} \right) + R_d \quad (2)$$

Qualitatively results from this analysis show the data is of the expected shape. For a more quantitative analysis, the data was compared to the two PI models and the natural logarithmic curve fit previously presented. The absolute average difference and standard deviation (n=114) for the two literature models and the natural logarithmic curve fit are: Smith (1936)  $|\bar{x}|=0.0527 \text{ g}\cdot\text{L}^{-1}$  and  $\sigma=.0419$ , Webb et al. (1974)  $|\bar{x}|= -0.131\text{g}\cdot\text{L}^{-1}$  and  $\sigma=0.0430$ , and ln curve fit  $|\bar{x}| = 0.0484\text{g}\cdot\text{L}^{-1}$  and  $\sigma =0.0455$ . This analysis illustrates that both models accurately capture the data with Smith (1936) slightly over predicting growth, Webb et al. (1974) slightly under predicting growth, and the natural logarithmic curve representing the most accurate model. Thus the natural logarithmic curve was used for predicting the growth of the large scale system presented in the results section of the main document.

A statistical analysis presented of the three models, Smith(1936), Webb et al. (1974), and the logarithmic curve fit, the logarithmic curve fit most accurately describes the data with a coefficient of determination of 0.8519, an absolute average difference of  $|\bar{x}| = 0.0484\text{g L}^{-1}$ , and a standard deviation of  $\sigma =0.0455$ . This represents a strong correlation considering the variability inherent in biological systems.

### ***6.3.2 Large Scale Reactor Growth Data***

Daily productivity data was collected from six-0.28 m deep and six-0.14 m deep reactors over the course of 6 four day batches (three high light and three low light growth scenarios) with productivity data presented in Table 17.

**Table 17. 24 hr average productivity of three 4 day batches is presented for the 0.28 m deep and 0.14 m deep reactors for the two different light intensities tested.**

Reactor Dev (n=18)	High Light (3 batches)		Low Light (3 batches)	
	Average 24 hr Growth (g L <sup>-1</sup> )	Std Dev (n=18)	Average 24 hr Growth (g L <sup>-1</sup> )	Std
0.14 m	0.686	0.069	0.331	0.051
0.28 m	0.472	0.032	0.276	0.057

The productivity per unit area of the system detailed increases by 66% with the doubling of the depth of the reactors (doubling the volume). A Student's t-test with 99% confidence interval was used to show the doubling of the depth of a reactor from 0.14 m to 0.28 m has a significant impact on the productivity.

### ***6.3.3 Modeling- Large Scale Growth Based on Small Scale PI Data***

The data collected in the small scale system was used to inform a PI growth model based on a core sample technique. The small scale data was used to generate a PI growth model as a function of light intensity based on a natural logarithmic curve fit, eqn. 1, with  $A=0.1845$  and  $B=-0.8283$ .

$$G(I) = A \ln(I) + B \quad (1)$$

To evaluate the core sample technique, the PI growth model, eqn 1, was used to predicting the productivity ( $P_{\text{total}}$ ) of the large scale system using light measurements collected on the surface of the large scale reactor,  $I(x)$ , as the primary input (2).

It was assumed for the high light scenario when all 10 lights where being used at an angle of 5 degrees that the light intensity on all of the reactors was the same. The light measurements for the high light scenario for the 0.28 m and 0.14 m deep reactors are presented in Figure 34. The light intensity on the reactors for the low light scenario was not uniform as presented in Figure 35.

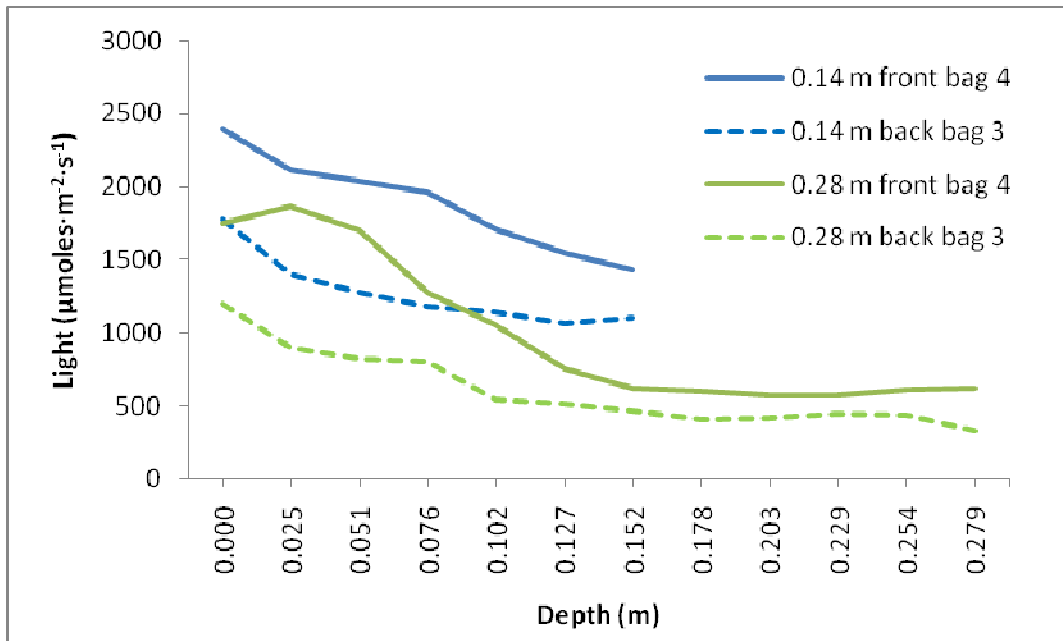


**Figure 34. Light measurements for the high light scenario for the 0.28 m and 0.14 m deep reactors with the water surface being zero and down into the basin being positive.**

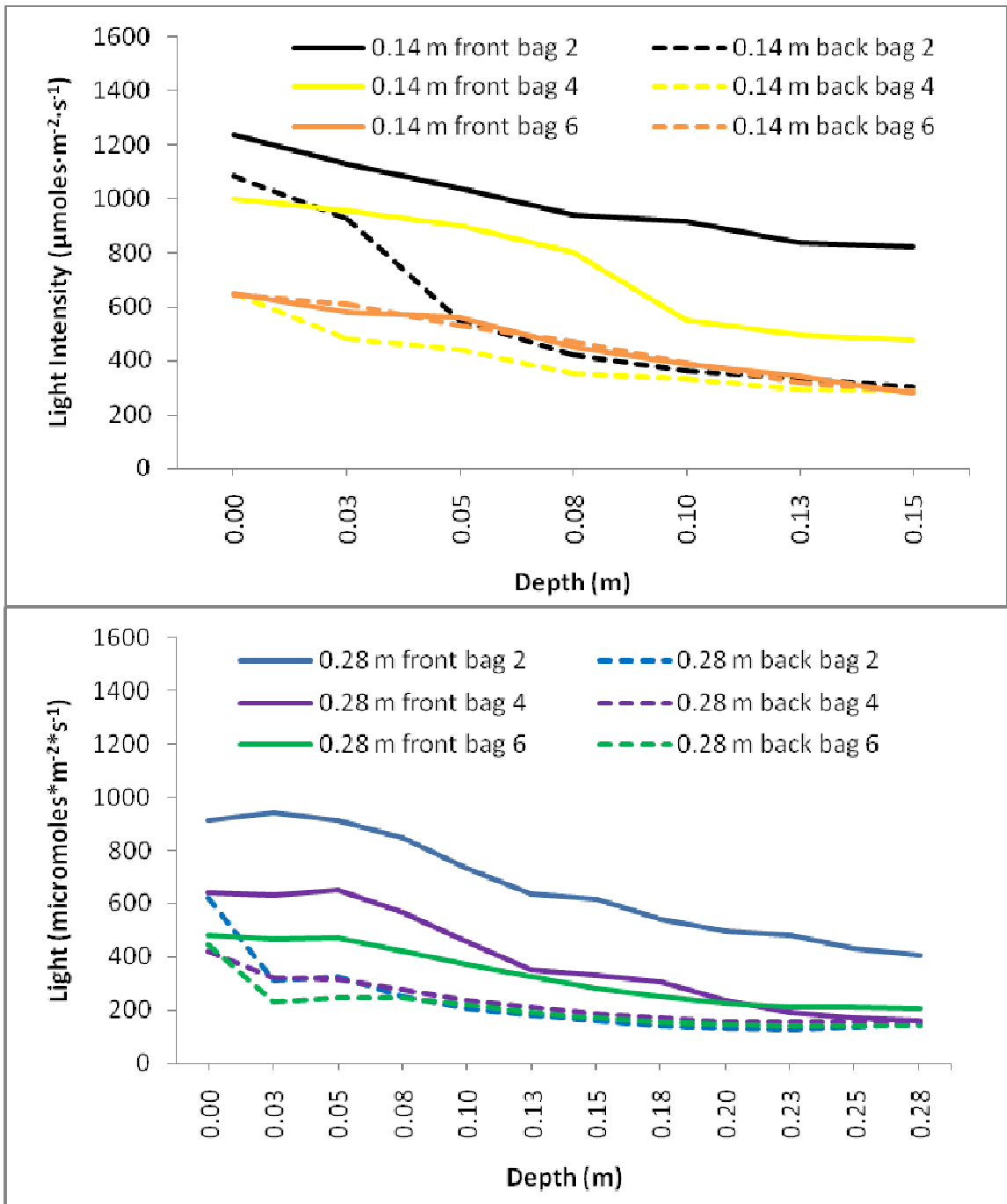
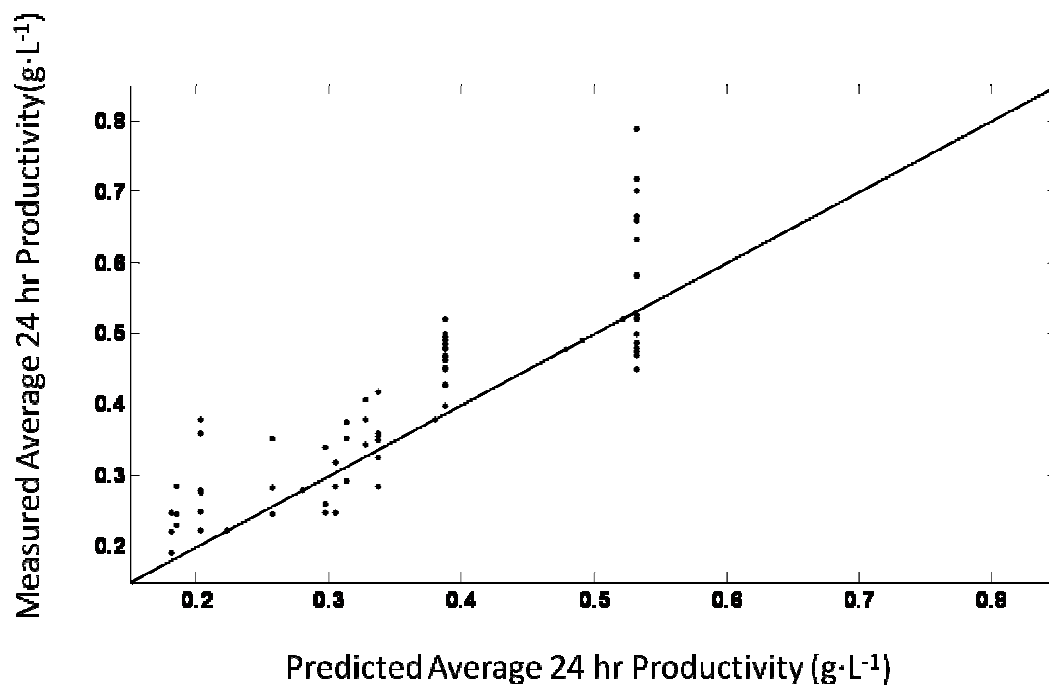


Figure 35. Light intensity on the 0.14 m deep reactors (left) and the 0.28 m reactors (right) for the low light scenario.

The light intensity on reactors 3 and 5 were not directly measured but assumed to be the average of the surrounding reactors.

$$P_{total} = \sum_{area} G(I(x)) = \sum_{area} A \ln(I(x)) + B \quad (2)$$

The resulting predicted productivity of the large scale system based on the small scale PI model was compared to the measured productivity for the evaluation of the scalability of the core sample modeling technique Figure 36.



**Figure 36 Predicted 24 hour productivity in large reactors by PI growth model based small scale data versus measured 24 hour productivity in large scale reactors.**

The absolute average deviation of the 24 hour predicted productivity compared to the actual 24 hour productivity is  $|\bar{x}| = 0.060 \text{ g L}^{-1}$ . The application of the small scale PI

growth model to accurately predict the large scale system under a variety of light intensities is validated to this uncertainty.

## **6.4 Discussion**

Previous characterization of microalgae has focused on the evaluation of productivity potential as a function of light intensity in systems that are not representative of large scale reactors. The small scale data collected in this study was used to inform a PI growth model that accurately predicts the productivity in a large scale system without arbitrary scaling factors, illustrating the effectiveness of the core sample technique in capturing productivity at scale. The following section details the application of the data and model generated in this study to reactor design based on diffuse versus direct light utilization, and presents a geometric optimization analysis of the photobioreactor geometry presented.

### ***6.4.1 Application of Data to Modeling and Evaluation of Photobioreactors***

Photobioreactors have many advantages over open raceway ponds, one being the ability to capture both direct and diffuse light (Li et al., 2008; Pulz, 2001; Richmond, 2004). Hu et al. (1996) illustrates the importance of considering diffuse light in outdoor photobioreactor systems, however previous modeling efforts of photobioreactors typically have not directly accounted for growth from diffuse light (Mairet et al., 2011; Packer et al., 2010; Quinn et al., 2011). This study incorporates the effects of diffuse light for future systems level modeling, design optimization, and evaluation efforts by

collecting reactor relevant growth data at applicable outdoor diffuse and direct light intensities.

#### 6.4.1.1 Diffuse versus direct light growth

In comparison to open raceway ponds that collect strictly high light intensities, a photobioreactor has a percentage of area that receives high light but a second area that collects diffuse light (Hu et al., 1996; Qiang and Richmond, 1994). Diffuse light represents an important component when considering the design and modeling of photobioreactors due to the extended surface area inherent in their design. The data presented can be used to make a high level assessment of extended surface area growth in photobioreactors.

Direct sunlight at noon on a summer day is  $2000 \mu\text{mol m}^{-2} \text{s}^{-1}$ . By making the assumption that diffuse light is 10% the intensity of direct sunlight (Gueymard, 2008), the growth on a square meter of diffusely illuminated area compared to the same area directly lit is 3.8 times less based on the data presented. Thus, in order to justify the increased capital and operating costs of a photobioreactor based on productivity increases from diffuse light collection, there must be significant area dedicated to diffuse light capture.

The redistribution of high light to the low light portions of the reactor through reflection or diffusion could have an impact on productivity by increasing the photosynthetic efficiency of the system. Analysis of the data presented in Figure 33 shows that there is a significant increase in growth when light intensity is increased to a

level of  $500 \mu\text{mol m}^{-2} \text{s}^{-1}$  with further increases in light intensity having diminished returns in terms of productivity. The photosynthetic efficiency in the high light portion of the reactor is low due to light saturated photosynthesis while the growth in the diffusely illuminated portions are light limited with a high photosynthetic efficiency. An increase in the light intensity in the diffusely illuminated portion of the reactor from the redistribution of high light will result in an overall increase in productivity based on the logarithmic relationship between light and growth presented.

Redistribution of light in the 0.28 m deep reactors based on simulation could increase the overall productivity to  $33.9 \text{ g m}^{-2} \text{ d}^{-1}$  (an increase of 19.6%). Redistribution of light in the 0.14 m deep reactors would have minimal impact on the overall productivity due to the already high intensity of light incident on both the front and back surfaces. Analysis was performed for the redistribution of light based on conservation of light and maximal productivity to show a depth of 0.51 m yields a maximum productivity of  $35 \text{ g m}^{-2} \text{ d}^{-1}$ . The potential to increase productivity combined with other photobioreactor advantages make the redistribution of light in photobioreactor architecture an area of increasing research and development.

#### 6.4.1.2 Photobioreactor design evaluation and optimization

Utilizing the data presented, the question of what is the optimal depth for the photobioreactor presented can be answered. For large scale application, typical growth productivities are reported in the metric of grams per square meter per day. The growth data collected in the large scale reactors was reduced to this metric for

discussion purposes. In order to evaluate an optimum photobioreactor depth, photobioreactors were constructed with a 0.56 m and 0.84 m depth and inoculated for the purpose of measuring the light intensity on the surface of the reactors for the highlight condition (see supplementary online material for light measurement data). The growth in the deeper reactors can be predicting using the PI growth model coupled with these light measurements and used to evaluate optimum reactor depth based on a  $\text{g m}^{-2} \text{d}^{-1}$  metric, Figure 37.

Increasing the reactor depth (diffusely illuminated portion) of the photobioreactor indicates a global maximum based on the metric of total areal productivity ( $\text{g m}^{-2} \text{d}^{-1}$ ). The growth data presented shows that increasing the reactor depth and volume by a factor of 2, going from the 0.14 m to 0.28 m, yields an overall increase in areal productivity of 66%. Increasing the depth and volume by a factor of 2 again, going from a depth of 0.28 m to 0.56 m, increases productivity by 6% on a  $\text{g m}^{-2} \text{d}^{-1}$  metric. In evaluating this on a process level, the energy required for dewater linearly scales with the volume processed based on centrifugation, thus the optimization of photobioreactor geometry cannot be limited strictly to areal productivity but must be integrated into a process level analysis for optimization on a systems level.

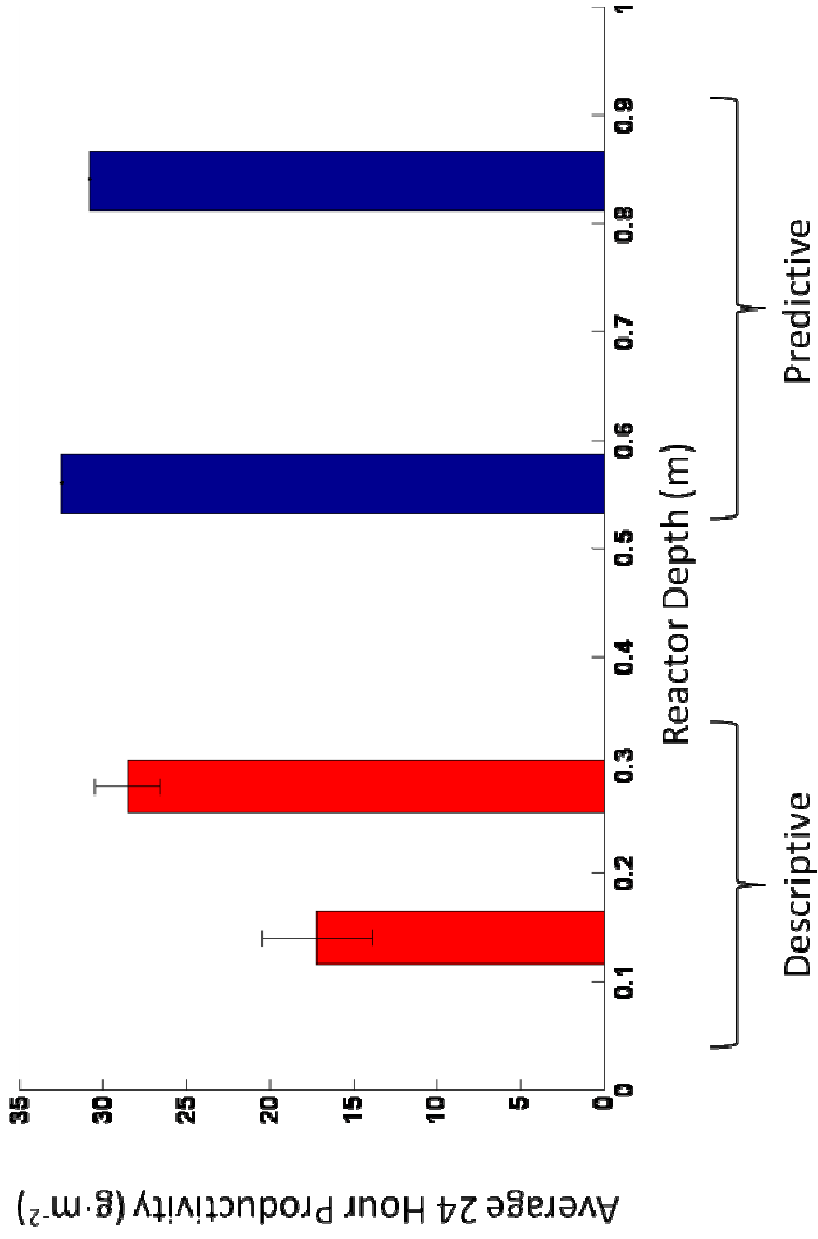


Figure 37 Measured average 24 hour productivity in grams per square meter for the 0.14 m and 0.28 m deep reactors compared to the predicted productivity for 0.56 m and 0.84 m reactors based on the PI growth model presented

An optimization analysis based on a maximal areal productivity was performed based on the data presented in Figure 37 to determine an optimum reactor depth. Results of the analysis illustrate an optimum reactor depth of 0.55 m corresponding to an areal productivity of  $33.0 \text{ g m}^{-2} \text{ d}^{-1}$ . This optimization does not consider the redistribution of light on the photobioreactor surface.

In comparing the growth in  $\text{g L}^{-1} \text{ d}^{-1}$  as a function of increasing depth an exponential decrease is observed. The 0.14 m deep reactors average productivity on a  $\text{g L}^{-1} \text{ d}^{-1}$  basis is 17.4% higher than the 0.28 m deep reactors, 56.2% higher than the 0.56 m deep reactors, and 70.2% higher than the 0.84 m deep reactors. This increased productivity rate could be important to consider in contexts of the robustness of a culture to native invasive species.

#### ***6.4.2 Photic Reduction***

In reactors that operate at relatively high density, the culture can be divided into two different zones, the illuminated “photic” zone and the “dark” zone. For data reduction it is then assumed that all growth can be attributed to the photic zone. The photic zone is defined for this study by the penetration depth of the light based on a cutoff light intensity of  $15 \text{ } \mu\text{mole}\cdot\text{m}^{-2}\cdot\text{s}^{-1}$ .

Previous modeling efforts have presented analysis and scale up of reactor data based on the concept of a photic-volume (Molina et al., 2000). In an effort to evaluate the scale up of the photic-volume concept the data presented in this study was reducing

using similar techniques presented by Molina et al. (2000). To determine the photic-volume the penetration depth must be determined.

It is well accepted that light modeling in algal cultures increases in complexity with increasing densities due to the potential effects of light scattering. A variety of modeling efforts have made different assumptions regarding the overall impact of scattering (Fernández et al., 1997; Gitelson et al., 1996; Janssen et al., 2003; Kim et al., 2002; Packer et al., 2010). A survey of the literature indicates ideal Lambert-Beer assumptions will lead to erroneous conclusions at the culture densities studies. There currently lacks sufficient data for light penetration effects at the densities studied for *Nannochloropsis salina*. The modeling effort presented in this work directly measured the light attenuation characteristics of *Nannochloropsis salina* cultures and used these results to determine the penetration depth and in turn the photic-volume.

To determine the light penetration depth experimental data was collected at three different densities and in three different sized culture vessels. Experimental setup and results for determining the light penetration depth is presented in the supplementary material. It is interesting to note that the results from this experimentation show that Lambert-Beer assumptions do not apply which is supported by literature (Fernández et al., 1997).

#### 6.4.2.1 Penetration Depth

As illustrated in the literature Lambert-Beer law is not applicable for modeling local light intensities in high density cultures (Fernández et al., 1997). Due to a lack in

published data the attenuation characteristics of high density *Nannochloropsis salina* was determined experimentally.

#### 6.4.2.1.1 *Materials and Methods*

In order to evaluate the attenuation characteristics of *Nannochloropsis salina*, an experiment was conducted measuring the light intensity that passes through a known culture depth. The depth of the culture was continually increased with light measurements taken at each depth increase. This process was done in three different sized beakers, 200 mL, 100 mL, and 80 mL with three different densities tested, 2.07 g·L<sup>-1</sup>, 3.28 g·L<sup>-1</sup>, and 4.87 g·L<sup>-1</sup>. A schematic of the experimental setup is presented in Figure 38.

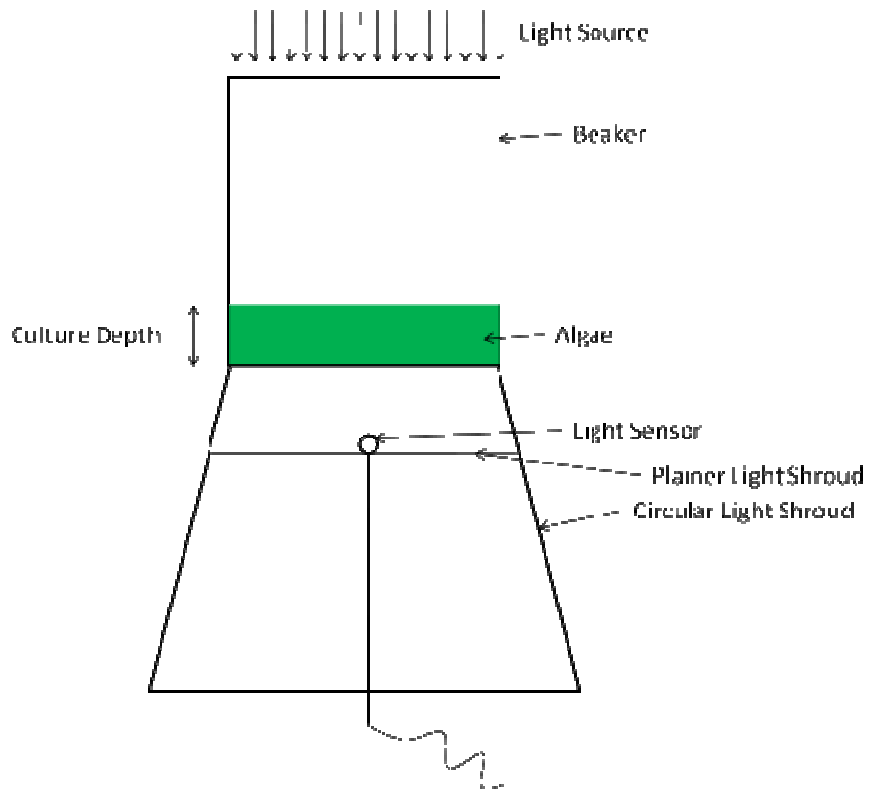


**Figure 38. Schematic for attenuation experimentation.**

The light was measured using a Heinz Walz US-SQS/L spherical PAR sensor (Effeltrich, Germany) connector to a LI-COR L1-250A light meter (Lincoln, NE). Illumination of the system was done using a Sun Systems Yield Master II Classic (Denver, CO) with a 1000 watt Hortilux-Blue daylight metal halide grow lamp (Mentor, OH).

## Results

### *6.4.2.1.2 Results*

Preliminary data reduction illustrated a logarithmic relationship in light attenuation, however not linear as Lambert-Beer would predict. In the reduction of the data each beaker had a different “dark” light measurement due to the geometry of the lip of the beakers. This offset was subtracted from the measured values. The depth of

the culture was determined in technical triplicate with calipers. The data was reduced and fit with a quadratic curve fit, Figure 39.

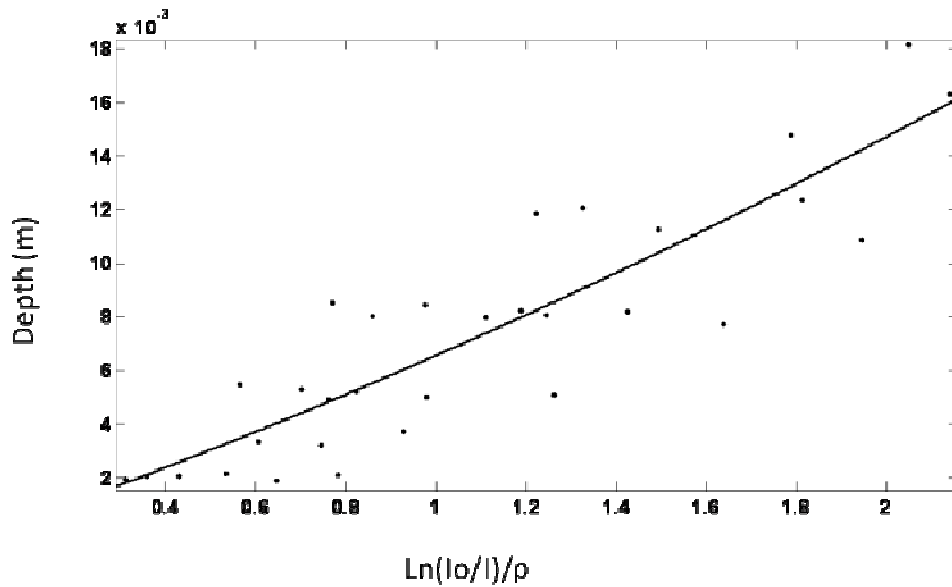


**Figure 39. Results from absorption characterization experimentation. Data is from three densities all tested in three different beaker sizes.**

A quadratic curve fit was used to more accurately represent the data. The reduction of the data presented in the main document on the metric of photic volume was done based on the results of this experimentation with a surface area of  $0.0047 \text{ m}^2$ . The surface area was calculated based on the fluid geometry of the reactors in motion.

Assuming that all of the growth in the small scale reactors is attributed to a photic-volume (defined by the illuminated surface area of the microalgae and the penetration depth), results for the baseline and half volume data is presented in Figure 40.

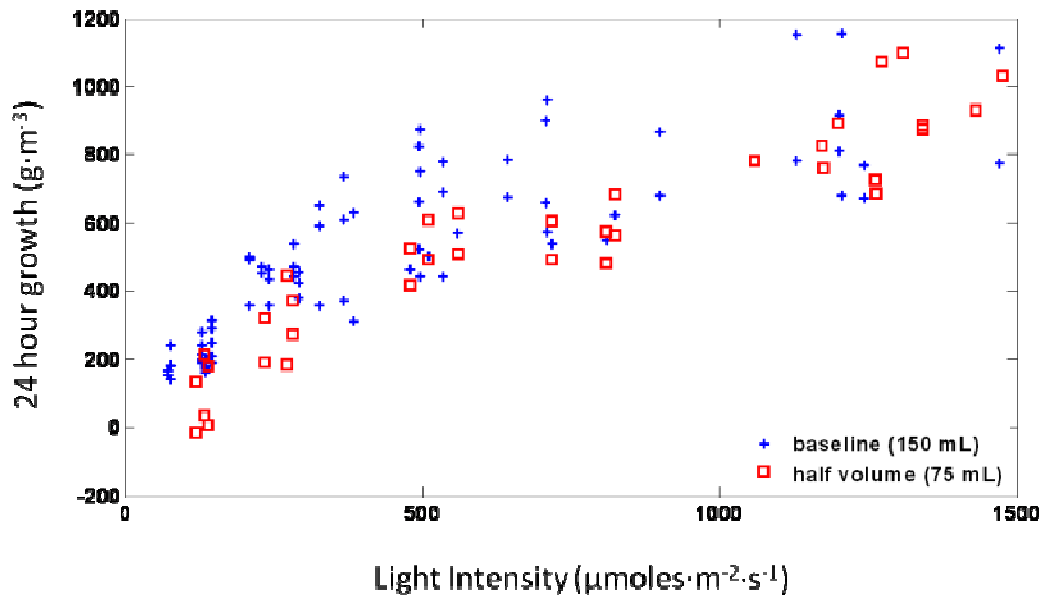


**Figure 40. Plot of baseline (150 mL) and half volume (75 mL) small scale growth data reduced based on attributing the growth to a photic-volume defined by the surface area of the reactors and a light penetration depth. The average productivity based on a 4 day batch is presented in grams of microalgae per cubic meter of photic-volume.**

The data presented in Figure 40 shows that on a small scale photic-volume growth can be used to accurately predict the growth in a slightly larger reactor. To further investigate the scaling of the concept of photic-volume growth data, the large scale growth data previously presented was similarly reduced using the concept of photic-volume growth.

A growth model based on the small scale data presented in Figure 40 was used to predict the growth in the large scale system. To accurately represent the small scale system a natural logarithmic curve was fit with a coefficient of determination of 0.768. This model with the measured light intensities of the large scale system was used to predict the growth of the large scale system. The results of the predicted versus measured growth are presented in Figure 41.

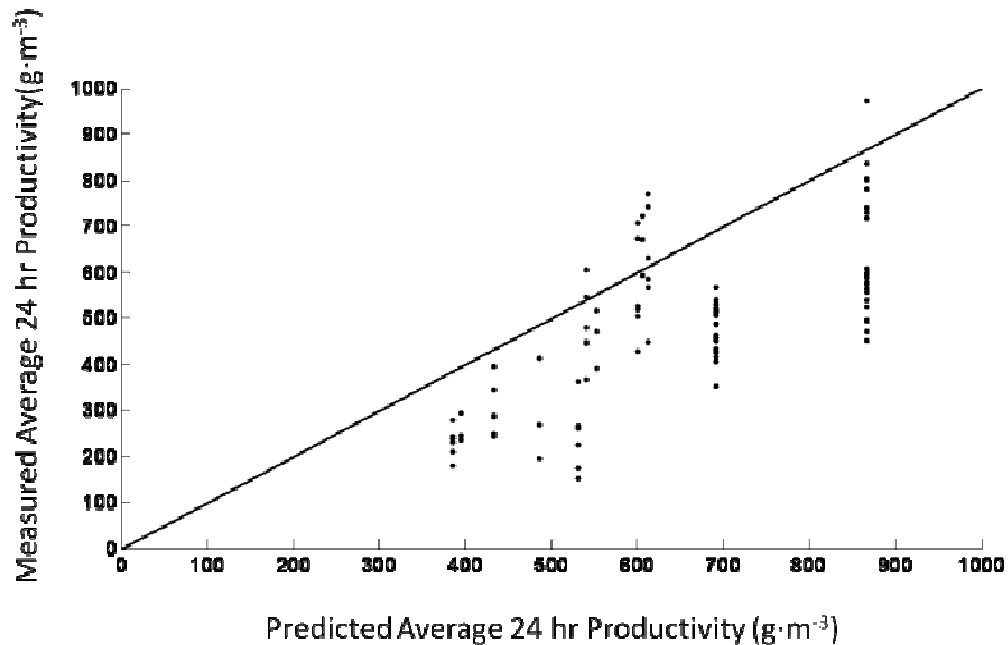


**Figure 41. Predicted 24 hour productivity in large scale reactors based on natural logarithmic model of small scale growth data (Figure 40) versus measured 24 hour productivity in large scale.**

Analysis of the error involved in photic-volume modeling of the growth in the large scale reactors based on the small scale data is 46.4%. This shows that scaling the small scale data to predict the large scale growth based on photic-volume significantly overestimates the large scale growth.

An analysis was performed to evaluate the scaling of the ½x reactor data to predict the growth in the 1x reactors. A natural logarithmic curve was fit to the ½x reactor growth data reduced using the concept of photic-volume growth and used to predict the growth in the 1x reactors. An analysis of the error involved with this type of scaled modeling showed an absolute average over prediction of 22.7% (see supplementary material for figures). This combined with the results presented in Figure 41 illustrates the limited application of the scaling of photic-volume growth data.

## 6.4.2.2 1/2x reactor predicting 1x reactor growth

### 6.4.2.2.1 photic data reduction

A similar analysis was performed as previously detailed to look at the accuracy of the 1/2x reactor data reduced using the concept of photic-volume to predict the growth in the 1x reactors. The 1/2x reactor growth data was reduced using the previously detailed photic-volume concept with a natural logarithmic curve fit, Figure 42.

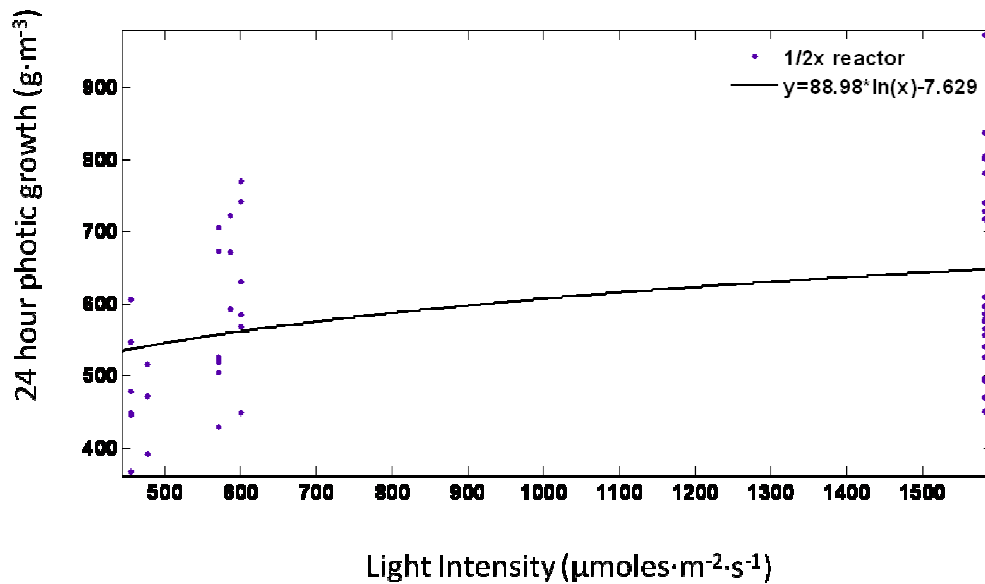


**Figure 42. . 1/2x reactor photic growth data with a natural logarithmic curve fit. Photic growth data is 24 hr batch averaged growth based on a 4 day batch plotted against average light intensity on the surface of the reactors.**

The natural logarithmic curve fit has a coefficient of determination of 0.138. The measured light on the surface of the 1x reactors was input into the curve to predict the growth. The predicted versus actual 24 hour batch average photic growth based on a 4 day batch is presented in .

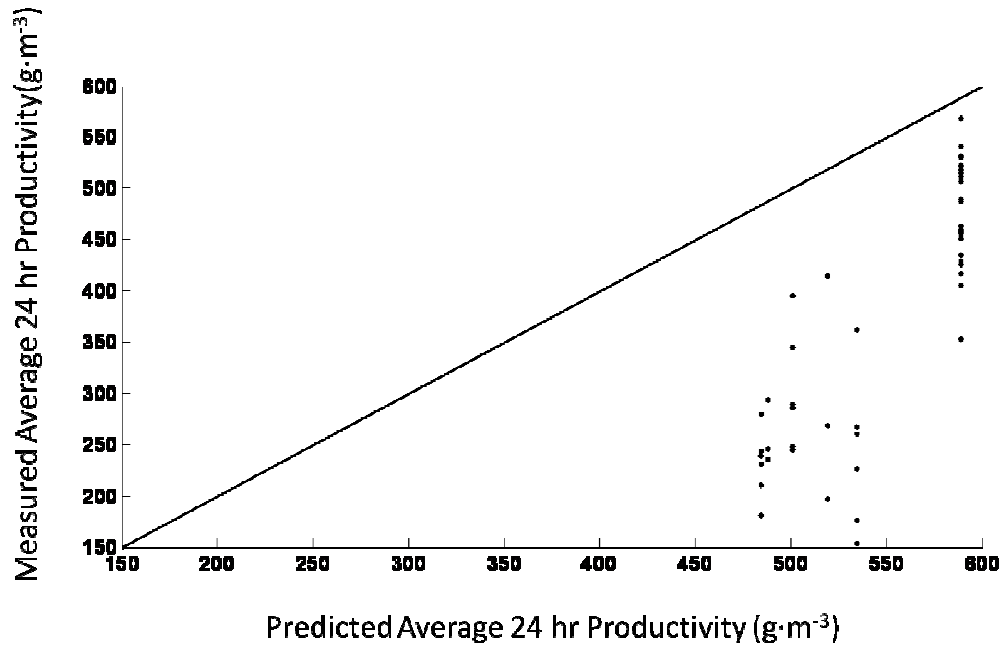


**Figure 43. Predicted 24 hour photic growth in 1x reactors by ½x photic data versus measured 24 hour photic growth in 1x reactors.**

An analysis of the absolute error is scaling the ½ x reactor data to predict the 1x reactor growth is an absolute average under prediction by 64.4%.

#### *6.4.2.2.2 g·L<sup>-1</sup> data reduction*

As previously detailed the scaling of the ½x reactor data to predict the 1x reactor data was evaluated. A natural logarithmic curve was fit to the ½x reactor data Figure 44.

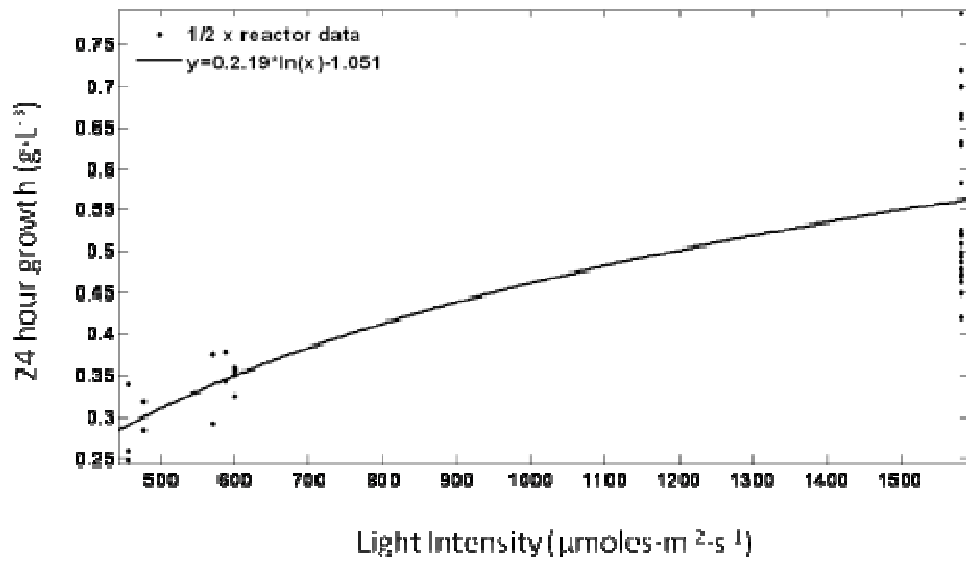


**Figure 44. ½x reactor growth data with a natural logarithmic curve fit. Growth data is 24 hr batch averaged growth based on a 4 day batch plotted against average light intensity on the surface of the reactors.**

The natural logarithmic curve fit has a coefficient of determination of 0.661. The measured light on the surface of the 1x reactors was input into the curve to predict the growth. The predicted versus actual 24 hour batch average growth based on a 4 day batch is presented in Figure 45.

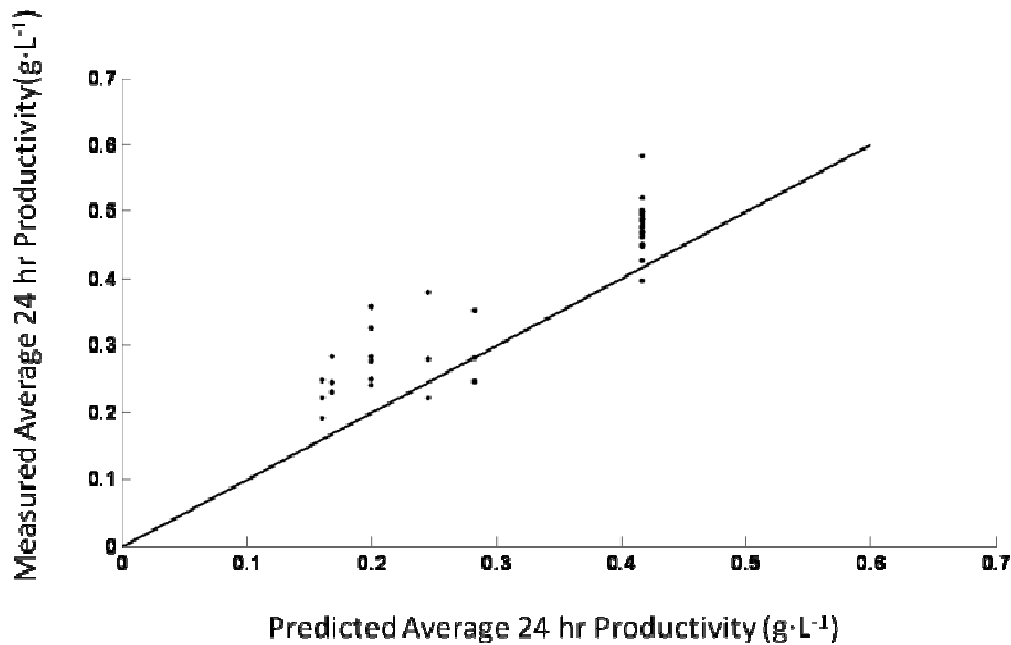


**Figure 45. Predicted 24 hour productivity in 1x reactors by ½x data versus measured 24 hour productivity in 1x reactors.**

The scaling of the ½x reactor data to predict the productivity in the 1x reactors is accurate with an error absolute average error  $|\bar{x}|=0.067 \text{ g}\cdot\text{L}^{-1}$ .

## 6.5 Conclusions

For the purpose of photobioreactor evaluation and design optimization at large scale, this study presents the experimental results from two growth platforms and the resulting validated large scale growth model incorporating diffuse and direct light characterization for *Nannochloropsis salina*. The data collected from the small scale test reactors, designed to represent a core sample of a large scale photobioreactor, is used to generate a PI growth model that incorporates diffuse and direct light effects. The scalability of the PI growth model is validated with growth data from two geometrically

different large scale photobioreactors operated at a variety of light intensities. The resulting validated large scale growth model is then used for design optimization and evaluation of large scale photobioreactors. An evaluation of diffuse light growth compared to direct light growth for large scale outdoor photobioreactors based on the data collected indicates the growth in the diffuse portion of the reactor is significantly lower than that in the directly illuminated portion. Optimization of the reactor geometry based on the PI growth model show on an areal metric an optimum depth of 0.55 m corresponding to an areal productivity of  $33.0 \text{ g m}^{-2} \text{ d}^{-1}$  can be achieved for the system presented.

## **Chapter 7-Conclusions**

The renewed interest in microalgae biofuels based on energy uncertainty has lead to the need for more detailed analysis to critically evaluate the microalgae to biofuels process. This dissertation presented a literature review of the current status of life-cycle assessments and growth modeling which confirms the need for more detailed and more accurate modeling of the microalgae process for integration into system level assessments. Current large scale modeling efforts use laboratory based growth and process data to evaluate microalgae at large scale that inevitably misrepresent microalgae potential and has lead to erroneous conclusions around scalability, productivity potential, and environmental impact. The models and analysis presented in this dissertation are experimentally validated with large scale systems and used to critically evaluate the microalgae to biofuels process in more detail than any other work to date. The work presented in this dissertation can be broken down into three components, each uniquely add significant knowledge to the field of microalgae biofuels:

1. Modular engineering process model used for life-cycle assessment
2. A literature based bulk growth model used to evaluate the current productivity potential in the US

3. A detailed growth model incorporating diffuse and direct light characteristics used for design optimization and evaluation.

## **7.1 Engineering Process Model and LCA**

The LCA presented is based on an engineering model that goes into more detail than any previous work, was built modular for evaluation of alternative processes, and utilized consistent boundaries to more accurately represent the current near term realizable environmental impact of a large scale photobioreactor growth facility.

Biofuels derived from microalgae have the potential to replace petroleum fuel and first-generation biofuel, but the efficacy with which sustainability goals can be achieved is dependent on the lifecycle impacts of the microalgae-to-biofuel process. This dissertation work presents a detailed, industrial-scale engineering model for the species *Nannochloropsis* using a photobioreactor architecture constructed to accurately represent the biofuels process from growth to transportation and distribution of fuel. The purpose of the detailed engineering process model of the microalgae growth, harvest, and extraction phases is to describe the material inputs, material outputs, and types and amounts of energy consumed in the microalgae feedstock processing stages based on a large scale facility (315 hectares). The temporal unit for evaluation of the process is 1 year. The engineering model incorporates waste heat recovery, recycling of materials through out the process to accurately represent the current technologies. The engineering model is integrated with a lifecycle energy and greenhouse gas emissions analysis compatible with the methods and boundaries of the Argonne National

Laboratory GREET model, thereby ensuring comparability to preexisting fuel-cycle assessments. Results are used to evaluate the net energy ratio (NER) and net greenhouse gas emissions (GHGs) of microalgae biodiesel in comparison to petroleum diesel and soybean-based biodiesel with a boundary equivalent to “well-to-pump”. Results from this study show that microalgae biofuels outperform soy based biodiesel on the metric of NER and GHG. The scalability of the consumables and products of the proposed microalgae-to-biofuels processes are assessed in the context of 150 billion liters (40 billion gallons) of annual production showing potential problems with nitrogen consumption and glycerin production.

## **7.2 Bulk Growth Modeling**

The novelty behind the literature based bulk growth model is the detailed construction and validation using outdoor large scale growth data at a variety of light and temperatures. This validated model was then used to significantly advance the current methods for evaluating productivity potential. A dynamic map critically evaluate the geographical potential of microalgae based on real meteorological effects was generated using 15 years of hourly historical data and GIS land availability and slope representing a new frontier in evaluating large scale growth locations. The data presented from the thermal growth model when compared to current large scale productivity potentials reported in literature shows the majority of the studies surveyed over estimate the current near term realizable microalgae productivity potential.

Scalability results do show microalgae do scale to 2030 DOE alternative fuel goals with Texas having the productivity potential of Arizona, New Mexico, and Hawaii combined.

### **7.3 Diffuse Versus Direct Light Evaluation**

The diffuse versus direct light growth characterization presented is the first instance where small scale growth modeling has been used to accurately represent a large scale system without arbitrary scaling factors. This work presents a core sample technique for characterizing microalgae growth as a function of light intensity that is applicable to reactor design and evaluation. The work is novel by characterizing the growth of *Nannochloropsis sp.* based on reactor relevant growth configurations and applying that to photobioreactor optimization.

Data was collected from small scale test reactors, designed to represent a core sample of a large scale photobioreactor, used to generate a PI growth model that incorporates diffuse and direct light effects. The scalability of the PI growth model based on the small scale test configuration was validated with growth data from two geometrically different large scale photobioreactors operated at a variety of light intensities. The resulting validated large scale growth model was then used for design optimization and evaluation of large scale photobioreactors. An evaluation of diffuse light growth compared to direct light growth for large scale outdoor photobioreactors based on the data collected indicates the growth in the diffuse portion of the reactor is significantly lower than that in the directly illuminated portion. The results from this

study indicate natural diffuse light does not have the impact as previously reported in literature and adapted into PBR design.

#### **7.4 Dissertation impact**

The experimentally validated modeling efforts presented in this dissertation are designed and used to accurately represent the current near term realizable microalgae potential and environmental impact. Models are built transparently and validated to show where microalgae biofuels are today in terms of environmental impact, productivity potential, and reactor evaluation. The work presented significantly contributes to the field of microalgae biofuels by realistically evaluating growth through experimentally validated models with novel scaling techniques presented.

## **Chapter 8- Future Work in Feasibility of Large Scale Production**

To date my research has focused on the evaluation of the microalgae to biofuels process and the optimization of growth systems with published results on Life-Cycle Environmental Assessment, Growth Biology Kinetics, and Growth Systems Modeling. The following is a summary of my research experience, focus, objectives, and strategies presented in this work. The summary is followed by three future research proposals.

The research presented can be summarized with the following research charge.

***RESEARCHERS HAVE SHOWN THAT THE SYSTEM SCALE ECONOMIC AND SUSTAINABILITY PERFORMANCE OF MICROALGAE BIOFUELS IS DEPENDANT ON THE CONSUMPTIONS AND PRODUCTS OF THE MICROALGAE DURING THE FEEDSTOCK STAGES. IN ORDER TO QUANTIFY THE SENSITIVITY OF MICROALGAE FEEDSTOCK GROWTH AND PROCESSING ON SYSTEM-SCALE PERFORMANCE METRICS WE MUST CONNECT HIGH-LEVEL MODELS OF MICROALGAE GROWTH (VALIDATED THROUGH EXPERIMENTAL GROWTH DATA) AND PROCESSING TO THESE SYSTEM-SCALE PERFORMANCE METRICS.***

This charge breaks down into the following three primary research topics. Each topic details the research work done, currently being undertaken, and future efforts.

## **8.1 The Potential Productivity and Feasibility of Large Scale Microalgae**

### **Production in the US**

Evaluation and feasibility of mass production of second generation biomass feedstocks for the production of non-petroleum based fuels is a key component to the current R&D path set forward by DOE. Current microalgae productivity reported in literature range from  $12 \text{ m}^3 \cdot \text{ha}^{-1} \cdot \text{yr}^{-1}$  reported by Schenk et al. to  $184.0 \text{ m}^3 \cdot \text{ha}^{-1} \cdot \text{yr}^{-1}$  reported by Yeang (Schenk et al., 2008; Yeang, 2008). Gouveia and Oliveira, Huntley and Redalje, Rodolfi et al., Sheehan et al., Wijffels and Barbosa, Clarens et al., and Chisti report values between these extremes (Chisti, 2007; Chisti, 2008; Chisti, 2008; Clarens et al., 2010; Huntley and Redalje, 2007; Sheehan et al., July 1998; Wijffels and Barbosa, 2010). The majority of the productivity potentials reported are based on small scale laboratory data which do not relate to large scale or, more importantly, incorporate meteorological or season effects on microalgae productivity.

I developed and validated a bulk growth model that enabled the generation of a dynamic map for the realistic near term production potential of microalgae in the US, Figure 47. The map was constructed utilizing a validated bulk growth model. The bulk growth model is founded in literature and incorporates 16 species specific characteristics and a reactor configuration that utilizes light and temperature as primary inputs. The model was then validated with experimental data, utilizing 9 weeks worth of light, temperature, and growth data from a large scale outdoor photobioreactor operated in batch mode, Figure 46.

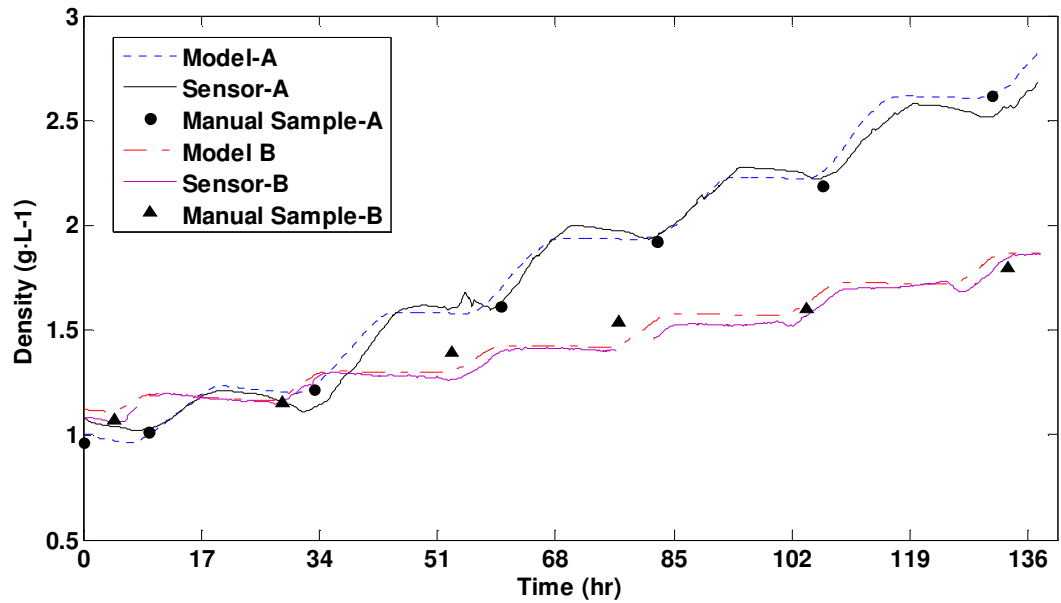


**Figure 46. Plot of model output (Model), institute OD sensor (Sensor), and manual sample performed daily (Manual Sample) in reactor A at high light (June 13-18) and in reactor B at low light (November 11- 16). Some sensor data has been removed due to sensor maintenance.**

The integration of this model with a thermal basin model and historical weather data from various locations across the US was used to generate a dynamic map illustrating current the biomass and lipid productivity potential (Quinn et al., 2010).

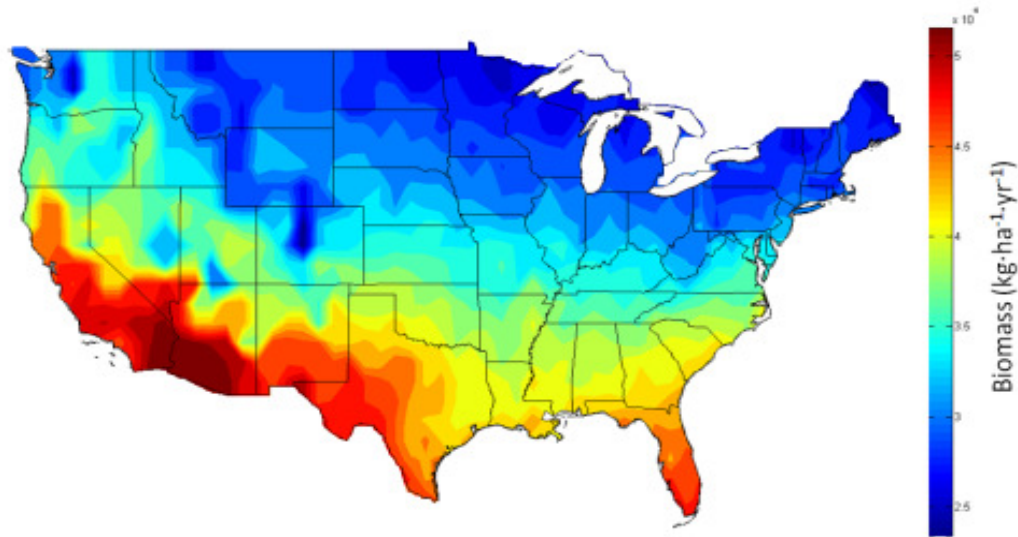


**Figure 47. Biomass productivity potential of the US generated using validated bulk growth model including thermal effects. Plot generated using 15 years of historical weather information from 788 Continental US location.**

My current research effort is dedicated to using the growth model to evaluate day to day logistic operations of a large scale microalgae facility. Multiple factors will affect the operations of large scale facilities including but not limited to microclimates, geographical location, diurnal variation, meteorological phenomenon, harvesting scheme, and species contamination. Evaluation of these factors can be done computationally utilizing this bulk growth model. The bulk growth model incorporates the effects of light, temperature, and species specific characteristics to accurately predict microalgae biomass growth and lipid accumulation. Incorporating this model with a systems level process flow model will enable the evaluation of current and proposed processing technologies on a large scale.

In an effort to continue to evaluate the scalability and footprint of large scale production, I am proposing a future research project to evaluate the integration of waste water streams with microalgae cultivation.. Researchers have shown that, on a small scale, microalgae have the potential to have a major impact as a second generation biofuel, however there are key roadblocks, a major one being scalability. My scalability analysis of an engineering growth model shows that at large scale the nutrient requirements are astronomically high and will require the utilization of waste streams (Batan et al., 2010).

Currently, few commercial facilities are utilizing commercial nitrogen or CO<sub>2</sub> waste streams. It is imperative to establish if there is a detrimental effect on microalgae growth from commercial waste nitrogen or CO<sub>2</sub> exhaust. This study proposes the use of a variety of nitrogen and CO<sub>2</sub> sources, including coal fired power plant exhaust, CO<sub>2</sub> from amine plant, CO<sub>2</sub> from the brewing of beer, nitrogen from extracted biomass, nitrogen from secondary treated wastewater, etc.

The results from this experiment will be incorporated into a modeling effort that will enable a more realistic evaluation of the commercial production of microalgae from commercial nitrogen and CO<sub>2</sub> waste sources. A full proposal of this work is presented at the end of this summary.

## **8.2 Net Energy and Greenhouse Gas Emissions Evaluation of Biodiesel Derived from Microalgae**

Microalgae Biofuels have the potential to replace petroleum fuels and first-generation biofuels, but the efficacy with which sustainability goals can be achieved is dependent on the lifecycle impacts of the microalgae-to-biofuel process (Chisti, 2007; Wijffels and Barbosa, 2010). One charge of my research has focused on the environmental assessment of the microalgae to biofuel process as compared to conventional diesel sources through Life Cycle Assessment. In order to describe the environmental impact (net energy and green house gas impacts) of microalgae biodiesel, a I have constructed a valid, extensible, and internally consistent model of the materials inputs, energy use, and products for the process. The three primary components of this model are: a detailed engineering process simulation of microalgae from growth through extraction, a more generalized model of microalgae from conversion to end use, and an integrated calculation of net energy and greenhouse gas (GHG) emissions due to impacts from the inputs, outputs, processes, and co-product allocation for the microalgae biodiesel production. This study was built on academic literature, industrial consultation, and pilot plant experience of microalgae feedstock processing to generate a model of net energy and GHG emissions of the microalgae-to-biofuel process.

Maintaining a consistent LCA boundary, the microalgae to biofuel process was compared to soy based biofuels as well as conventional diesel in terms of net energy ratio (NER) and GHG emissions . The fundamental results of the study show microalgae

have a NER of 0.93 MJ/MJ compared to soy at 1.64 MJ/MJ and on a GHG basis microalgae realize a  $-75.29 \text{ gCO}_{2\text{-eq}}\cdot\text{MJ}^{-1}$  reduction with soy at  $-71.73 \text{ gCO}_{2\text{-eq}}\cdot\text{MJ}^{-1}$ . A sensitivity analysis highlighted the importance of understanding the kinetics of microalgae growth, nutrient, and water consumption (Batan et al., 2010).

This analysis illustrated the need for the evaluation of direct Nitrous Oxide ( $\text{N}_2\text{O}$ ) emissions from microalgae. I am currently involved in the design and implementation of an experiment to evaluate  $\text{N}_2\text{O}$  emissions from microalgae. These emissions are yet unknown and could represent a major environmental impact due to the amount of fertilizer required for growth coupled with the high (299  $\text{CO}_2\text{eq}$ ) global warming potential of  $\text{N}_2\text{O}$ . Previous LCA studies have ignored or assumed  $\text{N}_2\text{O}$  emissions to be negligible (Aresta et al., 2005; Batan et al., 2010; Campbell et al., 2010; Clarens et al., 2010; Lardon et al., 2009; Stephenson et al., 2010). The experiment being conducted cultivates microalgae in 2 L Erlenmeyer flasks intended to simulate the cultivation conditions in a large scale closed photobioreactor. Theoretical calculations using the Intergovernmental Panel on Climate Change (IPCC) standards for terrestrial crops (1% of available nitrogen is converted into  $\text{N}_2\text{O}$ ) suggest that  $\text{N}_2\text{O}$  concentrations of up to 120 ppm would be expected. Initial results show  $\text{N}_2\text{O}$  concentration accumulated in the headspace over an 8 hour period on the order of  $60\pm.2\text{ppm}$  above atmospheric  $\text{N}_2\text{O}$  levels, indicating that under normal growing conditions, microalgae do produce the same level of  $\text{N}_2\text{O}$  as terrestrial plants. Further experimentation is being conducted to determine the cultivation conditions under which  $\text{N}_2\text{O}$  emissions might be elevated or suppressed.

I am proposing a more detailed LCA project that incorporates these experimental results and utilizes the validated bulk growth model presented above. This project would more accurately represent the growth potential based on geographical location by adapting the already validated bulk growth model instead of scaling single laboratory based growth data as previous studies have done (Aresta et al., 2005; Batan et al., 2010; Campbell et al., 2010; Clarens et al., 2010; Hirano et al., 1998; Lardon et al., 2009). The bulk growth model presented will be integrated into a systems level model of the microalgae to biofuel process and capture growth, lipid, protein, and carbohydrate composition of the biomass produced. The bulk growth model integrated with historical weather data will enable a realistic realizable location specific annual evaluation that incorporates variability of microalgae composition and its effects on product and co-product allocation inherent in a LCA. This study also proposes the use of recent N<sub>2</sub>O experimental data to more accurately represent the evaluation of the energy burden required for the suppression of N<sub>2</sub>O, and the environmental impact comparison of photobioreactors and open raceway ponds.

A full proposal of this work is presented at the end of this summary.

### **8.3 Direct versus Diffuse Light Utilization-Design Optimization through Experimentally Validated Models**

Previous research efforts developed models of microalgae growth that use a 1<sup>st</sup> order model of light absorption within the algae reactor. This has limitations in terms of the understanding that can be gained and also in terms of the applicability of these

models to the engineering challenges that are in reactor design today. I have undertaken three primary tasks to look at the design optimization of light utilization in photobioreactors. The first task was the generation of photosynthetic irradiation (PI) data curves of *Nannochloropsis salina* based on a photic volume growth metric, Figure 48 (Quinn et al., 2010). Researchers have developed PI curves for various species, however the time scales the collected data do not facilitate accurate growth modeling or application to large scale outdoor systems (Coutinho and Yoneshigue, 1988; Furuya et al., 1998; Lizotte and Sullivan, 1991; Macintyre et al., 2002; Sorokin, 1957; Williams and Laurens, 2010). The data presented in Figure 48 was generated by designing, building, and monitoring a small scale growth system that was representative of a large outdoor system.

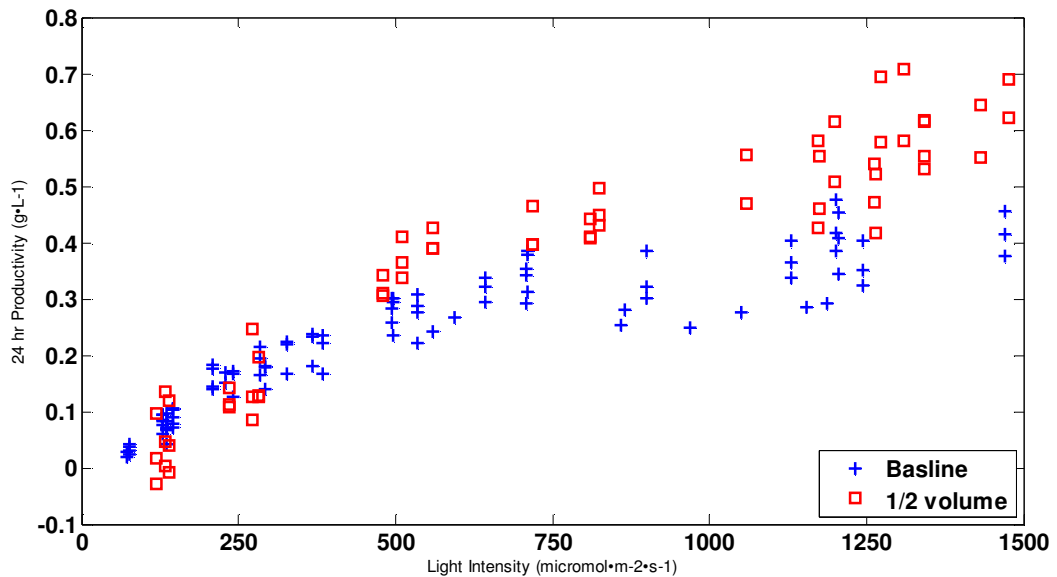


**Figure 48. Experimental growth data at two different culture volumes normalized to active photic volume and logarithmically curve fit. Data presented is batch averaged growth collected over a 5 day period in biological triplicate.**

The second task is the integration of the PI data with growth and geometry modeling. Using the concept of an active photic volume, I compared, head to head, different growth architectures. Finally, this model was validated utilizing data attained from a secondary experimental apparatus designed to directly evaluate growth as a function of reactor geometry.

The initial modeling and data presented illustrates the potential impact of improving light utilization through altering the distribution of high intensity natural light to diffusely lit portions of photobioreactors. My recent publication of productivity in an outdoor scalable photobioreactor shows that current productivity is well below the mean of theoretical potential (Quinn et al., 2010). For microalgae to be achieving expected theoretical productivities, the light utilization must be improved through innovation. The research I propose here would be an initial step towards improving the light utilization thus improving the productivity of microalgae.

My proposed research would utilize preexisting growth concepts to directly improve the overall productivity of photobioreactor cultivated microalgae. The core concept of is the redistribution of high intensity light such that the reactor operates at a higher overall efficiency. Wasted light impingent on the directly illuminated portion of the photobioreactor can be reflected onto the diffusely illuminated portion of the photobioreactor adjacent. The increased light intensity with dramatically improve the overall productivity of the diffusely illuminated portion of the reactor with the directly illuminated portion of the reactor taking a minor hit in productivity, Figure 48.

This research would build on fundamental growth concepts previously detailed in literature. The project would enable the initial evaluation of advance light altering photobioreactors prior to intensive capital investment in materials research. A full proposal of this work is presented at the end of this summary.

## **8.4 Research Proposal-Integration of Microalgae Growth Utilizing Commercial CO<sub>2</sub> and Nutrient Sources**

### ***8.4.1 Background***

Microalgae have several environmental , sustainability, and economic benefits, when compared to first-generation biofuel feedstocks (Batan et al., 2010). Microalgae are characterized by higher solar energy yield, year-round cultivation, the use of lower quality or brackish water, and the use of less- and lower-quality land (Brown and Zeiler, 1993; Dismukes et al., 2008; Li et al., 2008; Posten and Schaub, 2009; Raja et al., 2008; Williams et al., 2009). The theoretical maximum production of oil from algae has been shown to be 354,000 L·ha<sup>-1</sup>·year<sup>-1</sup> (38,000 gal·ac<sup>-1</sup>·year<sup>-1</sup>) (Weyer, 2009). Pilot plant facilities and scalable experimental data have shown a near term realizable production of 46,000 liters/(hectare\*yr) (5000 gal/(acre\*yr)), compared to 2,533 liters/(hectare\*yr) (271 gal/(acre\*yr)) of ethanol from corn or 584 liters/hectare/yr (62.5 gal/(acre\*yr)) of biodiesel from soybeans (Ahmed et al., 1994; Chisti, 2007; Pimentel, 2005; Pradhan et al., 2008; Weyer, 2009; Yeang, 2008).

A detailed industrial-scale engineering model for the growth of the species *Nannochloropsis* using a photobioreactor architecture has been built. The engineering

model builds on academic literature, industrial consultation, and pilot plant experience of microalgae feedstock processing to generate a model

Thus the model produced is valid, extensible, and internally consistent. The primary output of the model is the material inputs and material outputs from the microalgae growth process.

#### ***8.4.2 Engineering Growth Model***

The baseline model of microalgae to biodiesel process is based on a 315 hectares (776 acres) facility, which includes photosynthetically active and built areas. The temporal unit for evaluation of the process is 1 year.

Two primary architectures for mass-culture of microalgae have been proposed: open raceway ponds (ORP) and photobioreactors (PBR). PBR cultivation has advantages over ORP in they can achieve higher microalgae densities, higher productivity, and mitigate contamination. Current technological advances have reduced the capital and operating costs of PBRs making them more appealing as a commercially viable system (Richmond, 2004).

The microalgae strain *Nannochloropsis salina* was selected and modeled because of its high lipid content and high growth rate. Under the conditions of the Colorado State University pilot plant scale reactor system, *Nannochloropsis salina* can achieve a lipid content of 50% by weight (Emdadi and Berland, 1989; Fabregas et al., 2004; Suen et al., 1987), and an average annual growth rate of  $25 \text{ g}\cdot\text{m}^{-2}\cdot\text{day}^{-1}$  (Boussiba et al., 1987; Gudin and Chaumont, 1991; Suen et al., 1987). The use of these validated data for this

study is conservative and proper, considering that under laboratory conditions, *Nannochloropsis* can attain lipid percentages of 60% by weight and growth rates of 260  $\text{mg}\cdot\text{L}^{-1}\cdot\text{hr}^{-1}$  or 150  $\text{g}\cdot\text{m}^{-2}\cdot\text{day}^{-1}$  extrapolated to the system modeled (Richmond et al., 2003; Rodolfi et al., 2009). The nitrogen and phosphate content of the microalgae are defined as 15% and 2% by mass according to biological growth requirements and lipid productivity research (Arrigo, 2005; Redfield, 1958; Rodolfi et al., 2009). The salinity of the system is set at 20  $\text{g}\cdot\text{L}^{-1}$  (Abu-Rezq et al., 1999).  $\text{CO}_2$  enriched air (2%  $\text{CO}_2$ ) is sparged through the bioreactor to provide carbon and active mixing of the culture. The difference between precipitation and evaporation results in water losses of 2.5  $\text{cm}\cdot\text{day}^{-1}$  (1  $\text{in}\cdot\text{day}^{-1}$ ) from the water bath that supports the reactors (Smith et al., 1994). The polyethylene PBR bags are replaced at 5 year intervals. Diesel is used to fuel transportation on the facility for maintenance and inspection. The material inputs, and material outputs for the growth model are detailed in Table 1.

**Table 18. Summary material and energy inputs and outputs for the baseline microalgae growth process for a period of 1 year**

<b>STAGE/Inputs</b>	<b>VALUE</b>	<b>UNITS</b>
<b>GROWTH STAGE</b>		
Photosynthetic area per facility area	0.80	ha·ha <sup>-1</sup>
Salt consumption	134	g·(kg dry algae) <sup>-1</sup>
Nitrogen fertilizer consumption	147	g·(kg dry algae) <sup>-1</sup>
Phosphorus fertilizer consumption	20	g·(kg dry algae) <sup>-1</sup>
Polyethylene consumption	1.17	m <sup>3</sup> ·ha <sup>-1</sup>
Diesel fuel consumption	10	L·ha <sup>-1</sup>
Electricity consumption	41,404	kWh·ha <sup>-1</sup>
Microalgae biomass yield	91,000	kg·ha <sup>-1</sup>

The Energy Policy Act of 1992 directed the US Department of Energy to evaluate the goal of replacing 30% (~150 billion liters) of the transportation fuel consumed in the US by 2010 with replacement fuels. In March of 2007 this goal was deemed unreachable and the deadline for fuel replacement was changed to 2030 (Department of Energy, 2007). Algae-based biofuels are purported to be the most scalable of the biofuel processes currently available (Chisti, 2007). The baseline growth model was scaled assuming realistic extraction efficiencies to determine the feasibility of producing on a large scale.

Table 4 illustrates the need for the evaluation of the cultivation of microalgae utilizing CO<sub>2</sub> from commercial facilities and need for the evaluation of alternative nitrogen sources. Alternative sources of nitrogen and water, including wastewater (Yun et al., 1997) or anaerobic digestion for nitrogen recovery from the extracted biomass (Chisti, 2008) have been proposed but there lacks physical growth evidence to the effect of such changes on microalgae.

#### ***8.4.3 Research Question***

Based on the preliminary results, a primary research question can be posed:  
How does the integration of commercial CO<sub>2</sub> exhaust gases and nitrogen from wastewater treatment plants effect the overall design and performance of a microalgae growth system?

**Table 19. Scalability metrics derived from the baseline microalgae to biofuels process model scaled to a production of 40 billion gallons per year of microalgae biodiesel**

Scalability Metric	Value	Notes
Land Required	4.41x10 <sup>6</sup> hectares (1.09x10 <sup>7</sup> acres)	16% of Colorado Land Area (0.45% of US Land Area) (U.S. Census Bureau, 2009)
CO <sub>2</sub> Consumption	8.17 x10 <sup>11</sup> kg·a <sup>-1</sup>	32% of CO <sub>2</sub> from US power generation (Energy Information Administration, 2007)
Water Consumption	5.07 x10 <sup>12</sup> L·a <sup>-1</sup> (1.34 x10 <sup>12</sup> gal·a <sup>-1</sup> )	27% of Colorado river annual flow (Reisner, 1993)
Nitrogen Consumption	4.71 x10 <sup>10</sup> kg·a <sup>-1</sup>	1900% of US urea production (U.S. Census Bureau, 2009)
Algae Biodiesel Production	150 x10 <sup>9</sup> L·a <sup>-1</sup> (40 x10 <sup>9</sup> gal·a <sup>-1</sup> )	18% of US Transportation Energy Sector (Energy Information Administration, 2009)

#### **8.4.4 Research Tasks**

The research can be broken down into four primary tasks, (1) design and optimization of a growth system for integration of alternative CO<sub>2</sub> and nutrient sources,

(2) modeling of gas absorption kinetics, (3) Environmental assessment of alternative nitrogen sources, (4) optimization of the system to maximize CO<sub>2</sub> utilization.

#### ***8.4.5 Research Impact***

Evaluation and feasibility of mass production of second generation biomass feedstocks for the production of non-petroleum based fuels is a key component to the current R&D path set forward by DOE. Researchers have shown on small scale microalgae have the potential to have a major impact on as a second generation feedstock, however there are key roadblocks to commercialization, including scalability. Currently few commercial facilities are utilizing commercial CO<sub>2</sub> exhaust. It is imperative to establish if there is a detrimental effect on microalgae growth from commercial CO<sub>2</sub> exhaust. This study proposes the use of a variety of CO<sub>2</sub> sources, including coal fired power plant exhaust, CO<sub>2</sub> from the brewing of beer, CO<sub>2</sub> from amine plant, etc. A kinetics model of the interactions from other gases present in exhaust gases will help to pinpoint any build up of potential toxins in the growth media. The results from this experiment and modeling effort will enable a more realistic evaluation of the commercial production of microalgae from commercial CO<sub>2</sub> sources. The utilization of CO<sub>2</sub> would also be evaluated. The Aquatic Species Program attained a CO<sub>2</sub> utilization of greater than 90%, however it represented an energy intensive process. The recycling of headspace gasses in closed photobioreactors represents a more economically appealing solution. This study would look into the feasibility of obtaining low cost high CO<sub>2</sub> utilization.

The integration of non-traditional nutrient sources is a key milestone to the success of microalgae at large scale. Currently, microalgae biomass is produced in the laboratory or pilot plant facility so the nutrient load is not significant. As illustrated in the scalability of the engineering growth model, at large scale the nutrient requirements are astronomically high. The integration of wastewater nutrients with microalgae have been done previously, however not for the end goal of biofuel. A primary focus of this study is to actually integrate the utilization of nutrients from wastewater in the growth of microalgae currently being researched for cultivation for the production of biofuels. This study would aim to then evaluate the ease of integration at scale.

This study would also generate a preliminary model to evaluate the environmental impact of recovery of nitrogen from extracted biomass. The recycling of nitrogen from extracted biomass could represent a more energy intensive process than the direct manufacturing of fertilizer on a life-cycle assessment metric. The development of a detailed engineering model capturing the materials and energy required for the recycling of internal nitrogen in the biomass would enable the environmental evaluation of the process.

#### ***8.4.6 Summary***

Microalgae cultivation is the subject of research funding from DOE, DOD, NSF, C2B2, and others. The integration of commercial CO<sub>2</sub> exhaust and alternative nutrient sources is a new frontier and represents a key hurdle in the large scale commercialization of microalgae to biofuel.

## **8.5 Research Proposal-Net Energy and Life Cycle Assessment of Current Microalgae Cultivation Systems**

### ***8.5.1 Background***

The next generation of biofuel feedstocks must be critically analyzed to determine their energetic and greenhouse gas (GHG) emissions impact while considering scalability to a significant level of production. Compared to first-generation biofuel feedstocks, microalgae are characterized by higher solar energy yield, year-round cultivation, the use of lower quality or brackish water, and the use of less- and lower-quality land (Brown and Zeiler, 1993; Dismukes et al., 2008; Li et al., 2008; Posten and Schaub, 2009; Raja et al., 2008; Williams et al., 2009). Researchers have shown that microalgae feedstock cultivation can be coupled with combustion power plants or other CO<sub>2</sub> sources to sequester GHG emissions and has the potential to utilize nutrients from wastewater treatment plants (Li et al., 2008). The theoretical maximum production of oil from microalgae has been calculated at 354,000 L·ha<sup>-1</sup>·a<sup>-1</sup> (38,000 gal·acre<sup>-1</sup>·a<sup>-1</sup>) (Weyer et al., 2009), but pilot plant facilities and scalable experimental data have shown a near term realizable production of 46,000 liters·hectare<sup>-1</sup>·a<sup>-1</sup> (5000 gal·acre<sup>-1</sup>·a<sup>-1</sup>), compared to 2,533 liters·hectare<sup>-1</sup>·a<sup>-1</sup> (271 gal·acre<sup>-1</sup>·a<sup>-1</sup>) of ethanol from corn or 584 liters·hectare<sup>-1</sup>·a<sup>-1</sup> (62.5 gal·acre<sup>-1</sup>·a<sup>-1</sup>) of biodiesel from soybeans (Ahmed et al., 1994; Chisti, 2007; Pimentel, 2005; Pradhan et al., 2008; Yeang, 2008).

Life cycle assessment (LCA) is the fundamental tool that has been used to evaluate the sustainability of biofuels. Although LCA is a well recognized method,

published standards are incomplete and are not widely adhered to (Delucchi, 2004). The LCA literature makes use of the metrics of net energy ratio (NER, defined here as the ratio of energy consumed to fuel energy produced) and GHG emissions per unit of energy produced as the functional units for comparison purposes. The results from LCA are highly sensitive to definitions of system boundaries, life-cycle inventories, process efficiencies, and functional units (Farrell et al., 2006; Hill et al., 2006; Pimentel, 2005). LCA studies often include various NER definitions, key parameter values, sources of fossil energy, and co-product allocation and displacement methods, complicating comparisons among studies and policy synthesis (Davis et al., 2009; Farrell et al., 2006; Hill et al., 2006; Kim and Dale, 2002; Pimentel, 2005; Sheehan et al., 1998).

#### Current Life-cycle Assessment Modeling

LCA is a fundamental tool that has been used to evaluate the sustainability of biofuels. The results from LCA are highly sensitive to engineering model assumptions, definitions of system boundaries, life-cycle inventories, process efficiencies, and functional units. Increasing interest in microalgae as a secondary feedstock for transportation fuels has led to multiple LCA studies. Inherent in these studies is an engineering model of the microalgae to biofuels process which incorporates a growth model.

The majority of the microalgae LCA published to date utilize a simplistic growth model based on a daily productivity number obtained from a small scale laboratory growth facility. Large scale productivity over an entire year is then calculated based on this laboratory based number. Batan et al. 2010, Lardon et al. 2009, Hirano et al. 1998,

and Campbell et al. 2010 all use a fixed growth rate between  $10\text{-}30\text{ g}\cdot\text{m}^{-2}\cdot\text{d}^{-1}$  ( $3.6\cdot 10^4\text{-}11.0\cdot 10^4\text{ kg}\cdot\text{ha}^{-1}\cdot\text{yr}^{-1}$ ) in their growth models (Batan et al., 2010; Campbell et al., 2010; Hirano et al., 1998; Lardon et al., 2009). Clarens et al. 2010 scaled productivity data collected in open raceway ponds which was normalized to incident PAR on a monthly time scale. This approach does a better job of modeling growth than previous studies, however inconsistencies in the growth data as a function of light intensity lead to potential errors when scaled to other geographical locations (Clarens et al., 2010). Due to the lack of published data on realistic large scale productivities, three of the studies discussed above run multiple scenarios using a range of fixed growth rates in modeling the productivity of large scale facilities (Batan et al., 2010; Campbell et al., 2010; Lardon et al., 2009). This is indicative of the sensitivity of LCA analysis to the growth models implemented in the process model.

This study proposes the use of a validated large scale growth model that accurately captures diurnal and annual weather impacts on microalgae growth (Quinn et al., 2010). The model presented can be integrated with historical weather data and can be used to more accurately represent the growth of microalgae at specific geographical locations. The majority of the geographic locations of the LCA studies presented are warm coastal regions. Meteorological data for the coastal location of San Diego, California was used to illustrate realistic biomass productivity and compare results to the LCA studies discussed. The thermal basin temperature was assumed to be regulated for optimum growth and time harvest logic was used, resulting in  $5.42\cdot 10^4\text{ kg}\cdot\text{ha}^{-1}\cdot\text{yr}^{-1}$  of biomass produced or  $15\text{ g}\cdot\text{m}^{-2}\cdot\text{d}^{-1}$ . This analysis shows that the current

realizable productivity of microalgae is less than the median of the typical growth rates used in the LCA models surveyed.

### ***8.5.2 Research Question***

Based on the preliminary results a primary research question can be posed: How does the integration of a more detailed growth model effect current NER and GHG emissions of a microalgae to biofuels process?

### ***8.5.3 Research Tasks***

The research can be broken down into two primary tasks, (1) integrate a detailed validated growth model with engineering process model of the microalgae to biofuel, (2) utilize GREET to evaluate and compare NER and GHG of conventional biofuels and microalgae, (3) perform a sensitivity analysis based on growth scheme and geographical location.

### ***8.5.4 Research Impact***

Evaluation and feasibility of mass production of second generation biomass feedstocks for the production of non-petroleum based fuels is a key component to the current R&D path set forward by DOE. Researchers have shown on small scale that microalgae have the potential to have a major impact on biofuel production as a second generation feedstock, however there are key roadblocks including accurately representing the annual productivity potential of microalgae. Current environmental assessments rely on the scaling of laboratory based data for growth modeling. This

project would more accurately represent the growth potential based on geographical location by adapting a validated bulk growth model. The growth model will be used to evaluate on a NER and GHG basis of alternative growth schemes.

The growth model presented for integration into a systems level model of the microalgae to biofuel process and captures growth and lipid, protein, and carbohydrate composition of the biomass produced. The system level model incorporating this level of composition detail will enable the evaluation of operations on a more systems level metric. The bulk growth mode integrated with historical weather will enable a statistically significant annual evaluation that incorporates variability of microalgae composition and its effects on product and co-product allocation inherent in a LCA.

This study proposes the use of recent N<sub>2</sub>O experimental data to more accurately represent the evaluation of the energy burden required for the suppression of N<sub>2</sub>O. The systems level model will be expanded to include the evaluation of open raceway ponds (ORP) and photobioreactors (PBR) in order to directly compare the GHG emissions of systems capable of suppressing N<sub>2</sub>O (PBR) and systems that cannot (ORP).

### ***8.5.5 Summary***

Microalgae biofuels is the subject of research funding from DOE, DOD, NSF, C2B2, and others. The integration of current realistic growth modeling with systems level modeling is a new frontier and represents a key hurdle in environmental assessment of microalgae to biofuel.

## **8.6 Research Proposal-Optimization of Light Utilization in Outdoor**

### **Photobioreactors**

#### ***8.6.1 Background***

Microalgae-based biofuels have several sustainability, economic, and environmental impacts benefits (Batan et al., 2010). When compared to first-generation biofuel feedstocks, microalgae are characterized by higher solar energy yield, year-round cultivation, the use of lower quality or brackish water, and the use of less- and lower-quality land. Microalgae feedstock cultivation can be coupled with combustion power plants or other CO<sub>2</sub> sources to sequester green house gas (GHG) emissions and has the potential to utilize nutrients from wastewater treatment plants (Chisti, 2008; Schenk et al., 2008; Wijffels and Barbosa, 2010). The theoretical maximum production of oil from microalgae has been calculated at 354,000 L·ha<sup>-1</sup>·a<sup>-1</sup> (38,000 gal·acre<sup>-1</sup>·a<sup>-1</sup>) (Weyer et al., 2009), but pilot plant facilities and scalable experimental data have shown a near term realizable production of 46,000 liters·hectare<sup>-1</sup>·a<sup>-1</sup> (5000 gal·acre<sup>-1</sup>·a<sup>-1</sup>), compared to 2,533 liters·hectare<sup>-1</sup>·a<sup>-1</sup> (271 gal·acre<sup>-1</sup>·a<sup>-1</sup>) of ethanol from corn or 584 liters·hectare<sup>-1</sup>·a<sup>-1</sup> (62.5 gal·acre<sup>-1</sup>·a<sup>-1</sup>) of biodiesel from soybeans (Ahmed et al., 1994; Chisti, 2007; Pimentel, 2005; Pradhan et al., 2008; Yeang, 2008). These advantages have led to an increased interest in microalgae as a second generation feedstock for biofuels.

Two primary architectures for mass-culture of microalgae have been proposed: open raceway ponds (ORP) and photobioreactors (PBR). PBR cultivation has advantages

over ORP in they can achieve higher microalgae densities, higher productivity, and mitigate contamination. Current technological advances have reduced the capital and operating costs of PBRs making them more appealing as a commercially viable system (Richmond, 2004).

### ***8.6.2 Diffuse versus Direct Light Utilization***

There is limited data on the growth of microalgae at light levels that are consistent with diffuse light levels in outdoor photobioreactors. A model was constructed to estimate the effect of diffuse light on the overall productivity of a photobioreactor. Data from Qiang and Richmond 1994 was used to estimate the impact of diffuse light (Qiang and Richmond, 1994). The model was constructed to simulate the overall productivity of a photobioreactor incorporating direct and diffuse light regions. The reactor geometry that was simulated was a photobioreactor with an optical path of 0.05 meters with reactor spacing of 0.15 meters. The overall productivity was calculated by first determining the light intensity on a photobioreactor on an hourly basis and mapping this light intensity with growth data from Qiang and Richmond 1994 to calculate the productivity. Results from the modeling effort are presented in Figure 49.

The data used for simulation was generated at a range of densities. For this modeling effort all of the densities where simulated.

The model was used to evaluate the effect of diffuse light in two different reactor configurations, 1x which corresponds to a photobioreactor that is 0.3 meters deep and 2x which corresponds to a photobioreactor that is 0.6 meters deep. As illustrated in Figure 49, the diffuse light constitutes between 11% and 54% of the overall annual productivity. Increasing the depth of the system by a factor of 2 approximately doubles the diffuse light of the system; however the overall productivity due to the diffusely lit portion of the system only increases by 60%.

Preliminary literature data supports that above a certain light intensity microalgae are very inefficient. Photosynthesis-irradiation (PI) curves have been generated for a variety of microalgae species with data collected for *Nannochloropsis salina* and fit with the Smith, Webb et al., and a natural logarithmic curve presented in Figure 50 (Smith, 1936; Webb et al., 1974).

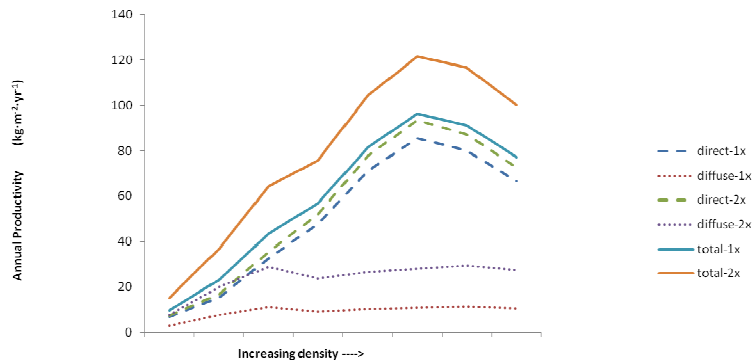


**Figure 49. Modeling results of direct, diffuse and total productivity in a photobioreactor. Two geometries are presented, 1x, photobioreactor depth of 0.3 m and 2x, photobioreactor depth of 0.6 m**

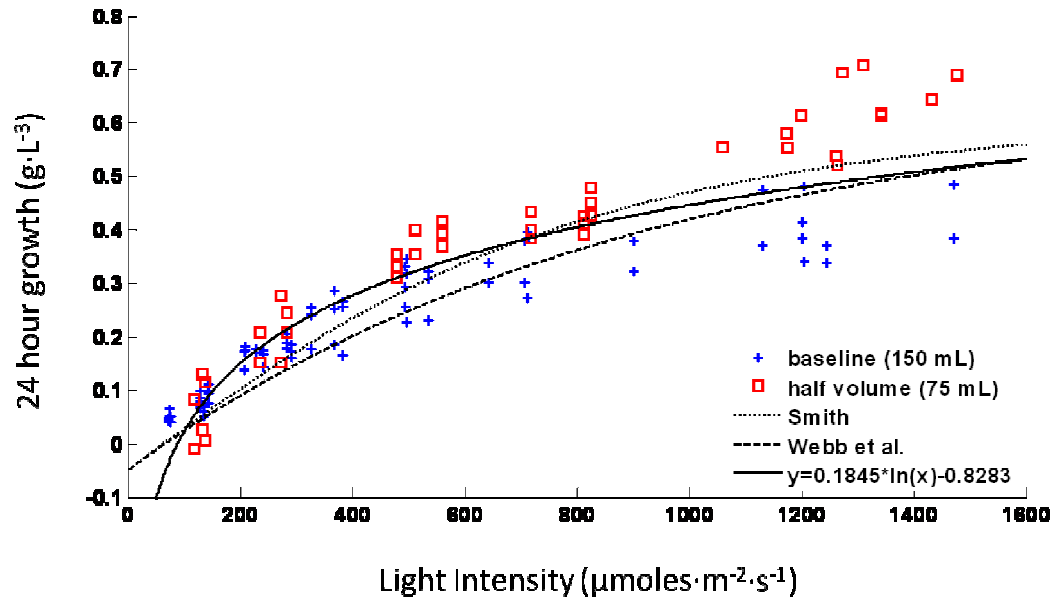


**Figure 50.** PI curve for *Nannochloropsis Salina* cultivated in a 5 day batch fit with Smith model using  $\alpha = 0.778 \text{ g}\cdot\text{s}\cdot\text{m}^{-2}\cdot\mu\text{mol}^{-1}$ ,  $P_m = 0.50 \text{ g}\cdot\text{L}^{-1}$ ,  $R_d = -0.05 \text{ g}\cdot\text{L}^{-1}$ .

PI curves are used for species characterization (Furuya et al., 1998; Harding et al., 1982; Henley, 1993; Ihnken et al., 2010; Sorokin, 1957). As illustrated in Figure 50, for light intensities above  $500 \mu\text{mol}^{-1}\cdot\text{m}^{-2}\cdot\text{s}^{-1}$  there is not a significant increase in productivity. At low light intensities the growth is typically 4-5 times lower than at the higher light intensities.

### **8.6.3 Research Question**

Based on the preliminary results presented above, a primary research question can be posed: Can the incident light be more efficiently utilized to increase the productivity of the photobioreactor geometry?

#### ***8.6.4 Research Tasks***

The research can be broken down into four primary tasks, (1) development of a test bed for the development of the implementation of growth experimentation, (2) develop a baseline growth scenario involving traditional PBR geometry and illumination, (3) develop an advanced light distribution PBR system, (4) Evaluate commercial feasibility of advanced PBR.

#### ***8.6.5 Research Impact***

Current microalgae productivity reported in literature range from  $12 \text{ m}^3 \cdot \text{ha}^{-1} \cdot \text{yr}^{-1}$  reported by Schenk et al. to  $184.0 \text{ m}^3 \cdot \text{ha}^{-1} \cdot \text{yr}^{-1}$  reported by Yeang (Schenk et al., 2008; Yeang, 2008). Gouveia and Oliveira, Huntley and Redalje, Rodolfi et al., Sheehan et al., Wijffels and Barbosa, Clarens et al., and Chisti report values between these extremes (Chisti, 2007; Chisti, 2008; Chisti, 2008; Clarens et al., 2010; Huntley and Redalje, 2007; Sheehan et al., July 1998; Wijffels and Barbosa, 2010). Recent publication of productivity in an outdoor scalable photobioreactor shows the current productivity below the mean of these reported values. For microalgae to be achieving expected theoretical productivities, the light utilization must be improved through innovation. The research proposed here would be an initial step towards improving the light utilization and therefore significantly improving the productivity of microalgae.

The initial modeling and data presented in the background illustrates the potential impact of the proposed research. The proposed research would utilize preexisting growth concepts to directly improve the overall productivity of

photobioreactor cultivated microalgae. The core concept of the research is redistributing the light such that the reactor operates at a higher overall efficiency. Wasted light impinging on the directly illuminated portion of the photobioreactor can be reflected onto the diffusely illuminated portion of the photobioreactor adjacent. The increased light intensity would dramatically improve the overall productivity of the diffusely illuminated portion of the reactor with the directly illuminated portion of the reactor taking only a minor hit in productivity.

The research proposed builds on fundamental growth concepts previously detailed in literature. The project would enable the initial evaluation of advanced light altering photobioreactors. The initial proof of principle evaluation is required prior to the capital-intensive materials research.

### ***8.6.6 Summary***

Microalgae biofuels is the subject of research funding from DOE, DOD, NSF, C2B2, and others. The integration of current realistic growth modeling with growth experimentation is a new frontier and represents a key hurdle in achieving productivity potential expected from microalgae.

## References

- Abu-Rezq, T S, Al-Musallam, L, Al-Shimmari, J, Dias, P, 1999. Optimum production conditions for different high-quality marine algae. *Hydrobiologia*, 403, 97-107.
- Adams, F G, Shachmurove, Y, 2008. Modeling and forecasting energy consumption in china: Implications for chinese energy demand and imports in 2020. *Energy Economics*, 30, 1263-1278.
- Adler, P R, Del Grosso, S J, Parton, W J, 2007. Life-cycle assessment of net greenhouse-gas flux for bioenergy cropping systems. *Ecol. Appl.*, 17, 675-691.
- Ahmed, I, Morris, D, Decker, J, 1994. How much energy does it take to make a gallon of soydiesel? Inst. for Local Self-Reliance, Washington, DC.
- Aiaa, 1998. Guide for the verification and validation of computational fluid dynamics simulations American Institute of Aeronautics and Astronautics, Reston, VA.
- Alexandrov, G A, Yamagata, Y, 2007. A peaked function for modeling temperature dependence of plant productivity. *Ecol. Model.*, 200, 189-192.
- Ambrose, R B, 2006. Wasp7 benthic algae-model theory and users guide. U.S. EPA, Office of Research and Development, Athens, Georgia.
- Arcgis, 2010. World topographic map.
- Aresta, M, Dibenedetto, A, Barberio, G, 2005. Utilization of macro-algae for enhanced co<sub>2</sub> fixation and biofuels production: Development of a computing software for an lca study, pp. 1679-1693.

- Arrigo, K R, 2005. Marine microorganisms and global nutrient cycles (vol 437, pg 349, 2005).  
*Nature*, 438, 122-122.
- Barbosa, M J, Janssen, M, Ham, N, Tramper, J, Wijffels, R H, 2003. Microalgae cultivation in air-lift reactors: Modeling biomass yield and growth rate as a function of mixing frequency.  
*Biotechnol. Bioeng.*, 82, 170-179.
- Batan, L, Quinn, J, Willson, B, Bradley, T, 2010. Net energy and greenhouse gas emission evaluation of biodiesel derived from microalgae. *Environ. Sci. Technol.*, 44, 7975-7980.
- Beer, L L, Boyd, E S, Peters, J W, Posewitz, M C, 2009. Engineering algae for biohydrogen and biofuel production. *Curr. Opin. Biotechnol.*, 20, 264-271.
- Benemann, J R, Goebel, R P, Weissman, J C, Augenstein, D C, 1982. Microalgae as a source of liquid fuels. *Final Technical Report, US Department of Energy, Office of Research*, DOE/ER/30014-TR.
- Benson, B C, Gutierrez-Wing, M T, Rusch, K A, 2007. The development of a mechanistic model to investigate the impacts of the light dynamics on algal productivity in a hydraulically integrated serial turbidostat algal reactor (histar). *Aquac. Eng.*, 36, 198-211.
- Bothe, H, 2007. Biology of the nitrogen cycle. 1 ed. Elsevier, Amsterdam, Netherlands.
- Boussiba, S, Vonshak, A, Cohen, Z, Avissar, Y, Richmond, A, 1987. Lipid and biomass production by the halotolerant microalga *nannochloropsis-salina*. *Biomass*, 12, 37-47.
- Brown, L M, Zeiler, K G, 1993. Aquatic biomass and carbon-dioxide trapping. Pergamon-Elsevier Science Ltd, pp. 1005-1013.
- Brown, L M, Zeiler, K G, 1993. Aquatic biomass and carbon-dioxide trapping. *Energy Conversion and Management*, 34, 1005-1013.
- Campbell, P K, Beer, T, Batten, D, 2010. Life cycle assessment of biodiesel production from microalgae in ponds Bioresour. Technol.

- Campbell, P K, Beer, T, Batten, D, 2010. Life cycle assessment of biodiesel production from microalgae in ponds. *Bioresour. Technol.*, 102, 50-56.
- Campbell, P K, Beer, T, Batten, D, 2011. Life cycle assessment of biodiesel production from microalgae in ponds. *Bioresour. Technol.*, 102, 50-56.
- Carraretto, C, Macor, A, Mirandola, A, Stoppato, A, Tonon, S, 2004. Biodiesel as alternative fuel: Experimental analysis and energetic evaluations. *Energy*, 29, 2195-2211.
- Chisti, Y, 1998 Pneumatically agitated bioreactors in industrial and environmental bioprocessing: Hydrodynamics, hydraulics, and transport phenomena. *Appl Mech Rev*, 51, 33-111.
- Chisti, Y, 2007. Biodiesel from microalgae. *Biotechnol. Adv.*, 25, 294-306.
- Chisti, Y, 2008. Biodiesel from microalgae beats bioethanol. *Trends Biotechnol.*, 26, 126-131.
- Chisti, Y, 2008. Response to reijnders: Do biofuels from microalgae beat biofuels from terrestrial plants? *Trends Biotechnol.*, 26, 351-352.
- Clarens, a F, Resurreccion, E P, White, M A, Colosi, L M, 2010. Environmental life cycle comparison of algae to other bioenergy feedstocks. *Environ. Sci. Technol.*, 44, 1813-1819.
- Conkerton, E J, Wan, P J, Richard, O A, 1995. Hexane and heptane as extraction solvents for cottonseed - a laboratory-scale study. *J. Am. Oil Chem. Soc.*, 72, 963-965.
- Cornet, J F, Dussap, C G, Dubertret, G, 1992. A structured model for simulation of cultures of the cyanobacterium *spirulina-platensis* in photobioreactors .1. Coupling between light transfer and growth-kinetics. *Biotechnol. Bioeng.*, 40, 817-825.
- Coutinho, R, Yoneshigue, Y, 1988. Diurnal-variation in photosynthesis vs irradiance curves from sun and shade plants of pterocladia-capillacea (gmelin) bornet et thuret (gelidiaciaceae, rhodophyta) from cabo-frio, rio-de-janeiro, brazil. *J. Exp. Mar. Biol. Ecol.*, 118, 217-228.
- Dailyland Laboratories Inc., 2008. Feed and forage report sample number 006604, Arcedia, WI.

- Davis, S C, Anderson-Teixeira, K J, Delucia, E H, 2009. Life-cycle analysis and the ecology of biofuels. *Trends Plant Sci.*, 14, 140-146.
- De Pauw, N, Morales, J, Persoone, G, 1984. Mass culture of microalgae in aquaculture systems: Progress and constraints. *Hydrobiologia*, 116, 121-134.
- Delucchi, M A, 2004. Conceptual and methodological issues in lifecycle analyses of transportation fuels. U.S. Environmental Protection Agency, Davis, CA.
- Delwiche, C C, 1981. Denitrification, nitrification, and atmospheric nitrous oxide. John Wiley & Sons, New York.
- Department of Energy, 2007. Alternative fuel transportation program; replacement fuel goal modification Office of Energy Efficiency and Renewable Energy. Department of Energy, Diagnostic Center for Population and Animal Health Michigan State University, 2008. Report of laboraotory examination #000578305. Michigan State University, Lansing, MI.
- Dismukes, G C, Carrieri, D, Bennette, N, Ananyev, G M, Posewitz, M C, 2008. Aquatic phototrophs: Efficient alternatives to land-based crops for biofuels. *Curr. Opin. Biotechnol.*, 19, 235-240.
- Dominguez, H, Nunez, M J, Lema, J M, 1995. Enzyme-assisted hexane extraction of soya bean oil. *Food Chem.*, 54, 223-231.
- Doney, S C, 2011. The growing human footprint on coastal and open-ocean biogeochemistry. *Science*, 328, 1512-1516.
- Duffie, J A, Beckman, W A, 2006. Solar engineering of thermal processes. Wiley, Hoboken, N.J.
- Emdadi, D, Berland, B, 1989. Variation in lipid class composition during batch growth of nanochloropsis-salina and pavlova-lutheri. *Mar. Chem.*, 26, 215-225.

- Energy Information Administration, 2007. Emissions from energy consumption at conventional power plants and combined-heat-and-power plants  
<http://www.eia.doe.gov/cneaf/electricity/epa/epat5p1.html>. December 2009
- Energy Information Administration, 2007. Supply and disposition of electricity  
<http://www.eia.doe.gov/cneaf/electricity/epa/epates2.html>. December 2009
- Energy Information Administration, 2009. U.S. Natural gas gross withdrawals (million cubic feet). <http://tonto.eia.doe.gov/dnav/ng/hist/n9010us2m.htm>. November 2009
- Energy Information Administration, 2010. World crude oil prices.  
[http://tonto.eia.doe.gov/dnav/pet/pet\\_pri\\_wco\\_k\\_w.htm](http://tonto.eia.doe.gov/dnav/pet/pet_pri_wco_k_w.htm). 2010
- Fabregas, J, Maseda, A, Dominguez, A, Otero, A, 2004. The cell composition of *nannochloropsis* sp changes under different irradiances in semicontinuous culture. *World J. Microbiol. Biotechnol.*, 20, 31-35.
- Fang, X, Wei, C, Cai, Z L, Fan, O, 2004. Effects of organic carbon sources on cell growth and eicosapentaenoic acid content of *nannochloropsis* sp. *J. Appl. Phycol.*, 16, 499-503.
- Farrell, a E, Plevin, R J, Turner, B T, Jones, a D, O'hare, M, Kammen, D M, 2006. Ethanol can contribute to energy and environmental goals. *Science*, 311, 506-508.
- Fernandez, F G A, Camacho, F G, Perez, J a S, Sevilla, J M F, Grima, E M, 1998. Modeling of biomass productivity in tubular photobioreactors for microalgal cultures: Effects of dilution rate, tube diameter, and solar irradiance. *Biotechnol. Bioeng.*, 58, 605-616.
- Fernández, F G A, Camacho, F G, Pérez, J a S, Sevilla, J M F, Grima, E M, 1997. A model for light distribution and average solar irradiance inside outdoor tubular photobioreactors for the microalgal mass culture. *Biotechnol. Bioeng.*, 55, 701-714.

- Flynn, K J, Davidson, K, Leftley, J W, 1993. Carbon-nitrogen relations during batch growth of *nannochloropsis oculata* (eustigmatophyceae) under alternating light and dark. *J. Appl. Phycol.*, 5, 465-475.
- Forster, P, Ramaswamy, V. , Artaxo, P., Berntsen, T., Betts, R., Fahey, D.W., Haywood, J., Lean, J., Lowe, D.C., Myhre, G., Nganga, J., Prinn, R., Raga, G., Schulz, M., Van Dorland, R., 2007. 2007: Changes in atmospheric constituents and in radiative forcing. *Climate Change 2007: The Physical Science Basis. Contribution of Working Group I to the Fourth Assessment Report of the Intergovernmental Panel on Climate Change.*
- Fuentes, M M R, Sanchez, J L G, Sevilla, J M F, Fernandez, F G A, Perez, J a S, Grima, E M, 1999. Outdoor continuous culture of porphyridium cruentum in a tubular photobioreactor: Quantitative analysis of the daily cyclic variation of culture parameters, pp. 271-288.
- Furuya, K, Hasegawa, O, Yoshikawa, T, Taguchi, S, 1998. Photosynthesis-irradiance relationship of phytoplankton and primary production in the vicinity of kuroshio warm core ring in spring. *Journal of Oceanography*, 54, 545-552.
- Gandhi, a P, Joshi, K C, Jha, K, Parihar, V S, Srivastav, D C, Raghunadh, P, Kawalkar, J, Jain, S K, Tripathi, R N, 2003. Studies on alternative solvents for the extraction of oil-i soybean. *International Journal of Food Science and Technology*, 38, 369-375.
- Geider, R J, Macintyre, H L, Kana, T M, 1997. Dynamic model of phytoplankton growth and acclimation: Responses of the balanced growth rate and the chlorophyll a:Carbon ratio to light, nutrient-limitation and temperature. *Marine Ecology-Progress Series*, 148, 187-200.
- Geider, R J, Macintyre, H L, Kana, T M, 1998. A dynamic regulatory model of phytoplanktonic acclimation to light, nutrients, and temperature. *Limnol. Oceanogr.*, 43, 679-694.

- Geider, R J, Osborne, B A, 1986. Light-absorption, photosynthesis and growth of *nannochloris-atomus* in nutrient-saturated cultures. *Marine Biology*, 93, 351-360.
- Geider, R J, Osborne, B A, 1992. Algal photosynthesis. Chapman and Hall, New York.
- Gentile, M P, Blanch, H W, 2001. Physiology and xanthophyll cycle activity of *nannochloropsis gaditana*. *Biotechnol. Bioeng.*, 75, 1-12.
- Ghirardi, M L, Zhang, J P, Lee, J W, Flynn, T, Seibert, M, Greenbaum, E, Melis, A, 2000. Microalgae: A green source of renewable h-2. *Trends Biotechnol.*, 18, 506-511.
- Gillenwater, M, 2008. Forgotten carbon: Indirect co2 in greenhouse gas emission inventories. *Environmental Science & Policy*, 11, 195-203.
- Gitelson, A, Qiuang, H, Richmond, A, 1996. Photic volume in photobioreactors supporting ultrahigh population densities of the photoautotroph *spirulina platensis*. *Appl. Environ. Microbiol.*, 62, 1570-1573.
- Glover, T, **2000**. Pocket ref. Sequoia Publishing, Inc., Littleton, CO.
- Goldman, J C, 1979. Outdoor algal mass-cultures .2. Photosynthetic yield limitations. *Water Res.*, 13, 119-136.
- Golterman, H, 1985. Denitrification in the nitrogen cycle. Plenum Press, New York, New York.
- Gonzalez, M J I, Medina, a R, Grima, E M, Gimenez, a G, Carstens, M, Cerdan, L E, 1998. Optimization of fatty acid extraction from *phaeodactylum tricornutum* utex 640 biomass. *J. Am. Oil Chem. Soc.*, 75, 1735-1740.
- Grima, E M, Belarbi, E H, Fernandez, F G A, Medina, a R, Chisti, Y, 2003. Recovery of microalgal biomass and metabolites: Process options and economics. *Biotechnol. Adv.*, 20, 491-515.
- Gudin, C, Chaumont, D, 1991. Cell fragility - the key problem of microalgae mass-production in closed photobioreactors. *Bioresour. Technol.*, 38, 145-151.

- Gueymard, C A, 2008. Rest2: High-performance solar radiation model for cloudless-sky irradiance, illuminance, and photosynthetically active radiation - validation with a benchmark dataset. *Solar Energy*, 82, 272-285.
- Hang, L, Tu, M, 2007. The impacts of energy prices on energy intensity: Evidence from china. *Energy Policy*, 35, 2978-2988.
- Harding, L W, Prezelin, B B, Sweeney, B M, Cox, J L, 1982. Diel oscillations of the photosynthesis-irradiance (p-i) relationship in natural assemblages of phytoplankton. *Marine Biology*, 67, 167-178.
- Harwood, J L, Guschina, I A, 2009. The versatility of algae and their lipid metabolism. *Biochimie*, 91, 679-684.
- Henley, W J, 1993. Measurement and interpretation of photosynthetic light-response curves in algae in the context of photoinhibition and diel changes. *J. Phycol.*, 29, 729-739.
- Herum, 1960. Performance of auger conveyors for farm feed materials. University of Illinois Agricultural Experiment Station.
- Hill, J, Nelson, E, Tilman, D, Polasky, S, Tiffany, D, 2006. Environmental, economic, and energetic costs and benefits of biodiesel and ethanol biofuels. *Proc. Natl. Acad. Sci. U. S. A.*, 103, 11206-11210.
- Hirano, A, Hon-Nami, K, Kunito, S, Hada, M, Ogushi, Y, 1998. Temperature effect on continuous gasification of microalgal biomass: Theoretical yield of methanol production and its energy balance. *Catalysis Today*, 45, 399-404.
- Hossain, S, Salle, A, Boyce, a N, Chowdhury, P, Naquiuddin, M, 2008. Biodiesel fuel production from algae as renewable energy. *American Journal of Biochemistry and Biotechnology*, 4, 250-254.

- Hu, H H, Gao, K S, 2003. Optimization of growth and fatty acid composition of a unicellular marine picoplankton, *nannochloropsis sp.*, with enriched carbon sources. *Biotechnol. Lett.*, 25, 421-425.
- Hu, H H, Gao, K S, 2006. Response of growth and fatty acid compositions of *nannochloropsis sp* to environmental factors under elevated CO<sub>2</sub> concentration. *Biotechnol. Lett.*, 28, 987-992.
- Hu, Q, Guterman, H, Richmond, A, 1996. A flat inclined modular photobioreactor for outdoor mass cultivation of photoautotrophs. *Biotechnol. Bioeng.*, 51, 51-60.
- Hu, Q, Sommerfeld, M, Jarvis, E, Ghirardi, M, Posewitz, M, Seibert, M, Darzins, A, 2008. Microalgal triacylglycerols as feedstocks for biofuel production: Perspectives and advances. *Plant Journal*, 54, 621-639.
- Huntley, M E, Redalje, D G, 2007. CO<sub>2</sub> mitigation and renewable oil from photosynthetic microbes: A new appraisal. *Mitigation and Adaptation Strategies for Global Change.*, 12, 573-608.
- Huo, H, Wang, M, Bloyd, C, Putsche, V, 2009. Life-cycle assessment of energy use and greenhouse gas emissions of soybean-derived biodiesel and renewable fuels. *Environ. Sci. Technol.*, 43, 750-756.
- Ihnken, S, Eggert, A, Beardall, J, 2010. Exposure times in rapid light curves affect photosynthetic parameters in algae. *Aquat. Bot.*, 93, 185-194.
- Ippc, 2006. 2006 ipcc guidelines for national greenhouse gas inventories. National Greenhouse Gas Inventories Programme, Japan.
- James, S C, Boriah, V, 2010. Modeling algae growth in an open-channel raceway. *J. Comput. Biol.*, 17, 895-906.

- Jannasch, H W, 1960. Denitrification as influenced by photosynthetic oxygen production. *J. Gen. Microbiol.*, 23, 55-63.
- Janssen, M, Tramper, J, Mur, L R, Wijffels, R H, 2003. Enclosed outdoor photobioreactors: Light regime, photosynthetic efficiency, scale-up, and future prospects. *Biotechnol. Bioeng.*, 81, 193-210.
- Jorquera, O, Kiperstok, A, Sales, E A, Embirucu, M, Ghirardi, M L, 2010. Comparative energy life-cycle analyses of microalgal biomass production in open ponds and photobioreactors. *Bioresour. Technol.*, 101, 1406-1413.
- Kadam, K L, 2002. Environmental implications of power generation via coal-microalgae cofiring. *Energy*, 27, 905-922.
- Kerr, R A, Kintisch, E, 2010. Climate change nrc reports strongly advocate action on global warming. *Science*, 328, 1085-1085.
- Keystone\_Division, 2002. Polypropylene filter cartridges.
- Kim, J D, Kaushik, S J, 1992. Contribution of digestible energy from carbohydrates and estimation of protein-energy requirements for growth of rainbow-trout (*oncorhynchus-mykiss*). *Aquaculture*, 106, 161-169.
- Kim, N J, Suh, I S, Hur, B K, Lee, C G, 2002. Simple monodimensional model for linear growth rate of photosynthetic microorganisms in flat-plate photobioreactors. *J. Microbiol. Biotechnol.*, 12, 962-971.
- Kim, S, Dale, B E, 2002. Allocation procedure in ethanol production system from corn grain - i. System expansion. *Int. J. Life Cycle Assess.*, 7, 237-243.
- Kost, W, 2010. Bio vita starter-a premium starter feed for freshwater fishery applications in: J Quinn (Ed.). Bio-Oregon, Longview Washington.

- Lansford, R, Hernandez, J, Enis, P, Truby, D, Mapel, C, 1990. Evaluation of available saline water resources in new mexico for the production of microalgae. *Solar Energy Research Institute, SERI/TR-232-3597*.
- Lardon, L, Helias, A, Sialve, B, Stayer, J P, Bernard, O, 2009. Life-cycle assessment of biodiesel production from microalgae. *Environ. Sci. Technol.*, 43, 6475-6481.
- Legovic, T, Cruzado, A, 1997. A model of phytoplankton growth on multiple nutrients based on the michaelis-menten-monod uptake, droop's growth and liebigs law. *Ecol. Model.*, 99, 19-31.
- Lehr, F, Posten, C, 2009. Closed photo-bioreactors as tools for biofuel production. *Curr. Opin. Biotechnol.*, 20, 280-285.
- Lemesle, V, Mailleret, L, 2008. A mechanistic investigation of the algae growth "Droop" Model. *Acta Biotheor.*, 56, 87-102.
- Li, Q, Du, W, Liu, D H, 2008. Perspectives of microbial oils for biodiesel production. *Appl. Microbiol. Biotechnol.*, 80, 749-756.
- Li, Y, Horsman, M, Wu, N, Lan, C Q, Dubois-Calero, N, 2008. Biofuels from microalgae. *Biotechnol. Prog.*, 24, 815-820.
- Lizotte, M P, Sullivan, C W, 1991. Photosynthesis-irradiance relationships in microalgae associated with antarctic pack ice - evidence for insitu activity. *Marine Ecology-Progress Series*, 71, 175-184.
- Lourenco, S O, Barbarino, E, Lavin, P L, Marque, U M L, Aidar, E, 2004. Distribution of intracellular nitrogen in marine microalgae: Calculation of new nitrogen-to-protein conversion factors. *Eur. J. Phycol.*, 39, 17-32.

- Lubzens, E, Gibson, O, Zmora, O, Sukenik, A, 1995. Potential advantages of frozen algae (nannochloropsis sp) for rotifer (brachionus-plicatilis) culture. *Aquaculture*, 133, 295-309.
- Lutz, C, Meyer, B, Wolter, M I, 2010. The global multisector/multicountry 3-e model ginfors. A description of the model and a baseline forecast for global energy demand and co2 emissions. *International Journal of Global Environmental Issues*, 10, 25-45.
- Macintyre, H L, Kana, T M, Anning, T, Geider, R J, 2002. Photoacclimation of photosynthesis irradiance response curves and photosynthetic pigments in microalgae and cyanobacteria. *J. Phycol.*, 38, 17-38.
- Magnuson, J, 2010. Algal biofuels Washington State Bioenergy Research Symposium. Washington State's Resource Agencies & Research Institutions, Seattle, WA.
- Mairet, F, Bernard, O, Masci, P, Lacour, T, Sciandra, A, 2011. Modelling neutral lipid production by the microalga *isochrysis aff. Galbana* under nitrogen limitation. *Bioresour. Technol.*, 102, 142-149.
- Markovits, A, Conejeros, R, Lopez, L, Lutz, M, 1992. Evaluation of marine microalga nannochloropsis sp as a potential dietary-supplement - chemical, nutritional and short-term toxicological evaluation in rats. *Nutr. Res.*, 12, 1273-1284.
- Mata, T M, Martins, a A, Caetano, N S, 2010. Microalgae for biodiesel production and other applications: A review. *Renewable and Sustainable Energy Reviews*, 14, 217-232.
- Maxwell, E L, Folger, a G, Hogg, S E, 1985. Resource evaluation and site selection for microalgae production systems. *Solar Energy Research Institute, SERI/TR-215-2484*.
- Metting, F B, 1996. Biodiversity and application of microalgae. *J. Ind. Microbiol. Biotechnol.*, 17, 477-489.

- Minowa, T, Sawayama, S, 1999. A novel microalgal system for energy production with nitrogen cycling. *Fuel*, 78, 1213-1215.
- Molina, E M, Fernandez, F G, Camacho, F G, Rubio, F C, Chisti, Y, 2000. Scale-up of tubular photobioreactors. *J. Appl. Phycol.*, 12, 355-368.
- Molineaux, B, Lachal, B, Guisan, O, 1994. Thermal analysis of five outdoor swimming pools heated by unglazed solar collectors. *Solar Energy*, 53, 21-26.
- Muhs, J, Viamajala, S, Heydorn, B, Edwards, M, Hu, Q, Hobbs, R, Allen, M, Barton, D, Fenk, T, Bayless, D, Cooksey, K, Kuritz, T, Crocker, M, Morton, S, Sears, J, Daggett, D, Hazlebeck, D, Hassenia, J, 2009. A summary of opportunities, challenges, and research needs: Algae biofuels & carbon recycling. [www.utah.gov/ustar/documents/63.pdf](http://www.utah.gov/ustar/documents/63.pdf). 28 Jan 2011
- Nash, a M, Frankel, E N, 1986. Limited extraction of soybeans with hexane. *J. Am. Oil Chem. Soc.*, 63, 244-246.
- Packer, A, Li, Y, Andersen, T, Hu, Q, Kuang, Y, Sommerfeld, M, 2010. Growth and neutral lipid synthesis in green microalgae: A mathematical model. *Bioresour. Technol.*, 102, 111-117.
- Perner-Nochta, I, Posten, C, 2007. Simulations of light intensity variation in photobioreactors. *J. Biotechnol.*, 131, 276-285.
- Pimentel, D, Patzek, T W, 2005. Ethanol production using corn, switchgrass, and wood; biodiesel production using soybean and sunflower  
*Natural Resources Research*, 14, 65-76.
- Pimentel, D, Patzek, T W, 2005. Ethanol production using corn, switchgrass, and wood; biodiesel production using soybean and sunflower. *Natural Resources Research*, 14, 65-76.

- Pimentel, D, Patzek, T.W., 2005. Ethanol production using corn, switchgrass, and wood; biodiesel production using soybean and sunflower. *Natural Resources Research*, 14, 65-76.
- Posten, C, 2009. Design principles of photo-bioreactors for cultivation of microalgae. *Eng. Life Sci.*, 9, 165-177.
- Posten, C, Schaub, G, 2009. Microalgae and terrestrial biomass as source for fuels-a process view, pp. 64-69.
- Posten, C, Schaub, G, 2009. Microalgae and terrestrial biomass as source for fuels-a process view. *J. Biotechnol.*, 142, 64-69.
- Pradhan, A, Shrestha, D S, Van Gerpen, J, Duffield, J, 2008. The energy balance of soybean oil biodiesel production: A review of past studies. *Transactions of the Asabe*, 51, 185-194.
- Pulz, O, 2001. Photobioreactors: Production systems for phototrophic microorganisms. *Appl. Microbiol. Biotechnol.*, 57, 287-293.
- Pulz, O, Gross, W, 2004. Valuable products from biotechnology of microalgae. *Appl. Microbiol. Biotechnol.*, 65, 635-648.
- Qiang, H, Faiman, D, Richmond, A, 1998. Optimal tilt angles of enclosed reactors for growing photoautotrophic microorganisms outdoors. *Journal of Fermentation and Bioengineering*, 85, 230-236.
- Qiang, H, Richmond, A, 1994. Optimizing the population-density in *isochrysis-galbana* grown outdoors in a glass column photobioreactor. *J. Appl. Phycol.*, 6, 391-396.
- Qiang, H, Richmond, A, 1996. Productivity and photosynthetic efficiency of *spirulina platensis* as affected by light intensity, algal density and rate of mixing in a flat plate photobioreactor. *J. Appl. Phycol.*, 8, 139-145.

- Qiang, H, Zarmi, Y, Richmond, A, 1998. Combined effects of light intensity, light-path and culture density on output rate of spirulina platensis (cyanobacteria). *Eur. J. Phycol.*, 33, 165-171.
- Quinn, J, De Winter, L, Bradley, T, 2010. Microalgae bulk growth model with application to industrial scale systems. *Bioresource Technology*, in review.
- Quinn, J, De Winter, L, Bradley, T, 2011. Microalgae bulk growth model with application to industrial scale systems. *Bioresour. Technol.*, 102, 5083-5092.
- Quinn, J, Dewinter, L, Bradley, T, 2011. Microalgae bulk growth model with application to industrial scale systems *Bioresour. Technol.*
- Quinn, J, Dewinter, L, Bradley, T, 2011. Microalgae bulk growth model with application to industrial scale systems *Bioresour. Technol.*
- Quinn, J, Turner, C, Bradley, T, 2010. Photosynthesis irradiance relationship for nanochloropsis salina on a batch time scale. *J. Phycol.*, in review.
- Quinn, J, Turner, C, Bradley, T, in review. Scale-up of flat plate photobioreactor considering diffuse and direct light characteristics. *Appl. Microbiol. Biotechnol.*
- Raja, R, Hemaiswarya, S, Kumar, N A, Sridhar, S, Rengasamy, R, 2008. A perspective on the biotechnological potential of microalgae. *Crit. Rev. Microbiol.*, 34, 77-88.
- Reboloso-Fuentes, M M, Navarro-Perez, A, Garcia-Camacho, F, Ramos-Miras, J J, Guil-Guerrero, J L, 2001. Biomass nutrient profiles of the microalga nanochloropsis. *J. Agric. Food Chem.*, 49, 2966-2972.
- Redfield, a C, 1958. The biological control of chemical factors in the environment. *Am. Sci.*, 46, 205-221.
- Reijnders, L, 2008. Do biofuels from microalgae beat biofuels from terrestrial plants? *Trends Biotechnol.*, 26, 349-350.

- Reisner, M, 1993. Cadillac desert: The american west and its disappearing water. Penguin Books, New York.
- Renaud, S M, Parry, D L, Thinh, L V, Kuo, C, Padovan, A, Sammy, N, 1991. Effect of light-intensity on the proximate biochemical and fatty-acid composition of *isochrysis* sp and *nannochloropsis-oculata* for use in tropical aquaculture. *J. Appl. Phycol.*, 3, 43-53.
- Reske, J, Siebrecht, J, Hazebroek, J, 1997. Triacylglycerol composition and structure in genetically modified sunflower and soybean oils. *J. Am. Oil Chem. Soc.*, 74, 989-998.
- Richmond, A, 2000. Microalgal biotechnology at the turn of the millennium: A personal view. Kluwer Academic Publ, pp. 441-451.
- Richmond, A, 2004. Handbook of microalgal culture biotechnology and applied phycology. Blackwell Science, Oxford, UK.
- Richmond, A, Zhang, C W, Zarmi, Y, 2003. Efficient use of strong light for high photosynthetic productivity: Interrelationships between the optical path, the optimal population density and cell-growth inhibition. *Biomol. Eng.*, 20, 229-236.
- Rodolfi, L, Zittelli, G C, Bassi, N, Padovani, G, Biondi, N, Bonini, G, Tredici, M R, 2009. Microalgae for oil: Strain selection, induction of lipid synthesis and outdoor mass cultivation in a low-cost photobioreactor. *Biotechnol. Bioeng.*, 102, 100-112.
- Rosenberg, J N, Oyler, G A, Wilkinson, L, Betenbaugh, M J, 2008. A green light for engineered algae: Redirecting metabolism to fuel a biotechnology revolution. *Curr. Opin. Biotechnol.*, 19, 430-436.
- Rossignol, N, Lebeau, T, Jaouen, P, Robert, J M, 2000. Comparison of two membrane - photobioreactors, with free or immobilized cells, for the production of pigments by a marine diatom. *Bioprocess Engineering*, 23, 495-501.

- Sacks, L E, Barker, H A, 1949. The influence of oxygen on nitrate and nitrite reduction. *J. Bacteriol.*, 58, 11-22.
- Sartori, E, 2000. A critical review on equations employed for the calculation of the evaporation rate from free water surfaces. *Solar Energy*, 68, 77-89.
- Sastre, R R, Coesgoer, Z, Perner-Nochta, I, Fleck-Schneider, P, Posten, C, 2007. Scale-down of microalgae cultivations in tubular photo-bioreactors - a conceptual approach. *J. Biotechnol.*, 132, 127-133.
- Sawayama, S, Minowa, T, Yokoyama, S Y, 1999. Possibility of renewable energy production and co2 mitigation by thermochemical liquefaction of microalgae. *Biomass Bioenergy*, 17, 33-39.
- Schenk, P M, Thomas-Hall, S R, Stephens, E, Marx, U C, Mussgnug, J H, Posten, C, Kruse, O, Hankamer, B, 2008. Second generation biofuels: High-efficiency microalgae for biodiesel production. *BioEnergy Research*, 1, 20-43.
- Scott, S A, Davey, M P, Dennis, J S, Horst, I, Howe, C J, Lea-Smith, D J, Smith, a G, 2010. Biodiesel from algae: Challenges and prospects. *Curr. Opin. Biotechnol.*, 21, 277-286.
- Seinfeld, J H, Pandis, S N-, 1998. Atmospheric chemistry and physics from air pollution to climate change. Wiley, New York.
- Shah, R, 2003. Fundamentals of heat exchanger design. John Wiley & Sons, Hoboken, NJ.
- Sheehan, J, Camobreco, V, Duffield, J, Graboski, M A, Shapouri, H, 1998. An overview of biodiesel and petroleum diesel life cycles. National Renewable Energy Laboratory, Golden, CO.
- Sheehan, J, Dunahay, T, Benemann, J, Roessler, P, 1998. A look back at the us department of energy's aquatic species program: Biodiesel from algae. *NREL report*, TP-580-24190.

- Sheehan, J, Dunahay, T, Benemann, J, Roessler, P, July 1998. A look back at the us department of energy's aquatic species program: Biodiesel from algae.
- Skerman, V B D, Macrae, I C, 1957. The influence of oxygen availability on the degree of nitrate reduction by pseudomonas-denitrificans. *Can. J. Microbiol.*, 3, 505-530.
- Skerman, V B D, Macrae, I C, 1957. The influence of oxygen on the reduction of nitrate by adapted cells of pseudomonas denitrificans. *Can. J. Microbiol.*, 3, 215-230.
- Smith, C C, Lof, G, Jones, R, 1994. Measurement and analysis of evaporation from in inactive outdoor swimming pool. *Solar Energy*, 53, 3-7.
- Smith, E L, 1936. Photosynthesis in relation to light and carbon dioxide. *Proc. Natl. Acad. Sci. U. S. A.*, 22, 504-511.
- Sorokin, C, 1957. The effects of light intensity on the growth rates of green algae. *Maryland Agricultural Experiment Station, Scientific Article A 650*.
- Spectrum Technologies Inc, 2003. Measuring light. in: S T Inc (Ed.). Spectrum Technologies Inc, Plainfield, Illinois.
- Spolaore, P, Joannis-Cassan, C, Duran, E, Isambert, A, 2006. Optimization of *nannochloropsis oculata* growth using the response surface method. *J. Chem. Technol. Biotechnol.*, 81, 1049-1056.
- Stephenson, a L, Kazamia, E, Dennis, J S, Howe, C J, Scott, S A, Smith, a G, 2010. Life-cycle assessment of potential algal biodiesel production in the united kingdom: A comparison of raceways and air-lift tubular bioreactors. *Energy & Fuels*, 24, 4062-4077.
- Suen, Y, Hubbard, J S, Holzer, G, Tornabene, T G, 1987. Total lipid production of the green-alga *nannochloropsis sp qii* under different nitrogen regimes. *J. Phycol.*, 23, 289-296.

- Sukenik, A, Zmora, O, Carmeli, Y, 1993. Biochemical quality of marine unicellular algae with special emphasis on lipid-composition .2. *Nannochloropsis* sp. *Aquaculture*, 117, 313-326.
- Szeicz, G, Mcmonagle, R C, 1983. The heat balance of urban swimming pools. *Solar Energy*, 30, 247-259.
- Takagi, M, Watanabe, K, Yamaberi, K, Yoshida, T, 2000. Limited feeding of potassium nitrate for intracellular lipid and triglyceride accumulation of *nannochloris* sp utex Ib1999. *Appl. Microbiol. Biotechnol.*, 54, 112-117.
- Tonon, T, Harvey, D, Larson, T R, Graham, I A, 2002. Long chain polyunsaturated fatty acid production and partitioning to triacylglycerols in four microalgae. *Phytochemistry*, 61, 15-24.
- Trenberth, K E, 2010. The climate fix what scientists and politicians won't tell you about global warming. *Science*, 330, 1178-1179.
- Tsukahara, K, Sawayama, S, 2005. Liquid fuel production using microalgae. *Journal of the Japan Petroleum Institute*, 48, 251-259.
- U. S. Department of Commerce, 2009. Aquaculture in the united states.  
<http://aquaculture.noaa.gov/us/welcome.html>. December 1, 2009
- U.S. Census Bureau, 2009. Mq325b - fertilizers and related chemicals.  
[http://www.census.gov/manufacturing/cir/historical\\_data/mq325b/index.html](http://www.census.gov/manufacturing/cir/historical_data/mq325b/index.html).  
October 22, 2009
- U.S. Census Bureau, 2009. State & county quickfacts.  
<http://quickfacts.census.gov/qfd/index.html>. December 2009
- U.S. Doe, 2010. National algal biofuels technology roadmap. in: U.S. Department of Energy (Ed.).
- U.S. Geological Survey, 2001. National land cover database (nlcd 2001).

Wang, 2008. Estimation of energy efficiencies of us petroleum refineries.

[http://www.transportation.anl.gov/modeling\\_simulation/GREET/publications.html](http://www.transportation.anl.gov/modeling_simulation/GREET/publications.html).

December 2009

Wang, M, and Elgowainy, A., 2005. Operating manual for greet: Version 1.7. Center for Transportation Research, Energy Systems Division, Argonne National Laboratory.

Webb, W L, Newton, M, Starr, D, 1974. Carbon-dioxide exchange of alnus-rubra - mathematical-model. *Oecologia*, 17, 281-291.

Weissman, J C, Goebel, R P, Benemann, J R, 1988. Photobioreactor design - mixing, carbon utilization, and oxygen accumulation. *Biotechnol. Bioeng.*, 31, 336-344.

Weyer-Geigel, K M, 2008. Heat-balance model and thermal analysis of an algae growth system for biofuel. Colorado State University.

Weyer, K, **2009**. Theoretical maximum algal oil production  
BioEnergy Research.

Weyer, K, 2009. Theoretical maximum algal oil production BioEnergy Research.

Weyer, K M, Bush, D R, Darzins, A, Willson, B D, 2009. Theoretical maximum algal oil production.  
*BioEnergy Research*, 3, 204-213.

White, F, **1999**. Fluid mechanics. McGraw-Hill, Boston, MA.

Wijffels, R H, Barbosa, M J, 2010. An outlook on microalgal biofuels. *Science*, 329, 796-799.

Wilcox, S, 2007. 1991-2005 national solar radiation database Related Information: National Renewable Energy Laboratory (NREL) (Fact Sheet), pp. Medium: ED; Size: 2 pp.

Williams, P J, Thomas, D N, Reynolds, C S, 2002. Phytoplankton productivity: Carbon assimilation in marine and freshwater ecosystems. Blackwell Science, Oxford, UK.

- Williams, P J L, Laurens, L M L, 2010. Microalgae as biodiesel & biomass feedstocks: Review & analysis of the biochemistry, energetics & economics. *Energy & Environmental Science*, 3, 554-590.
- Williams, P R D, Inman, D, Aden, A, Heath, G A, 2009. Environmental and sustainability factors associated with next-generation biofuels in the us: What do we really know? *Environ. Sci. Technol.*, 43, 4763-4775.
- Yamaberi, K, Takagi, M, Yoshida, T, 1998. Nitrogen depletion for intracellular triglyceride accumulation to enhance liquefaction yield of marine microalgal cells into a fuel oil. *Journal of Marine Biotechnology*, 6, 44-48.
- Yanovsky, V, **2009**. Westfalia separator food tec. in: V Yanovsky (Ed.). GEA, Oelde, Germany.
- Yazdani, S S, Gonzalez, R, 2007. Anaerobic fermentation of glycerol: A path to economic viability for the biofuels industry. *Current Opinion in Biotechnology*, 18, 213-219.
- Yeang, K, 2008. Biofuel from algae. *Architectural Design*, 78, 118-119.
- Yun, Y S, Lee, S B, Park, J M, Lee, C I, Yang, J W, 1997. Carbon dioxide fixation by algal cultivation using wastewater nutrients. *Journal of Chemical Technology and Biotechnology*, 69, 451-455.
- Zhang, W N, Liu, D C, 2005. A new process for preparation of soybean protein concentrate with hexane-aqueous ethanol mixed solvents. *J. AOAC Int.*, 88, 1217-1222.